

NASA/TM-2016-218976



Initial Evaluation of Acoustic Emission SHM of PRSEUS Multi-Bay Box Tests

Michael R. Horne
National Institute of Aerospace, Hampton, Virginia

Eric I. Madaras
Langley Research Center, Hampton, Virginia

August 2016

NASA STI Program . . . in Profile

Since its founding, NASA has been dedicated to the advancement of aeronautics and space science. The NASA scientific and technical information (STI) program plays a key part in helping NASA maintain this important role.

The NASA STI program operates under the auspices of the Agency Chief Information Officer. It collects, organizes, provides for archiving, and disseminates NASA's STI. The NASA STI program provides access to the NTRS Registered and its public interface, the NASA Technical Reports Server, thus providing one of the largest collections of aeronautical and space science STI in the world. Results are published in both non-NASA channels and by NASA in the NASA STI Report Series, which includes the following report types:

- **TECHNICAL PUBLICATION.** Reports of completed research or a major significant phase of research that present the results of NASA Programs and include extensive data or theoretical analysis. Includes compilations of significant scientific and technical data and information deemed to be of continuing reference value. NASA counter-part of peer-reviewed formal professional papers but has less stringent limitations on manuscript length and extent of graphic presentations.
- **TECHNICAL MEMORANDUM.** Scientific and technical findings that are preliminary or of specialized interest, e.g., quick release reports, working papers, and bibliographies that contain minimal annotation. Does not contain extensive analysis.
- **CONTRACTOR REPORT.** Scientific and technical findings by NASA-sponsored contractors and grantees.

- **CONFERENCE PUBLICATION.** Collected papers from scientific and technical conferences, symposia, seminars, or other meetings sponsored or co-sponsored by NASA.
- **SPECIAL PUBLICATION.** Scientific, technical, or historical information from NASA programs, projects, and missions, often concerned with subjects having substantial public interest.
- **TECHNICAL TRANSLATION.** English-language translations of foreign scientific and technical material pertinent to NASA's mission.

Specialized services also include organizing and publishing research results, distributing specialized research announcements and feeds, providing information desk and personal search support, and enabling data exchange services.

For more information about the NASA STI program, see the following:

- Access the NASA STI program home page at <http://www.sti.nasa.gov>
- E-mail your question to help@sti.nasa.gov
- Phone the NASA STI Information Desk at 757-864-9658
- Write to:
NASA STI Information Desk
Mail Stop 148
NASA Langley Research Center
Hampton, VA 23681-2199

NASA/TM-2016-218976



Initial Evaluation of Acoustic Emission SHM of PRSEUS Multi-Bay Box Tests

Michael R. Horne
National Institute of Aerospace, Hampton, Virginia

Eric I. Madaras
Langley Research Center, Hampton, Virginia

National Aeronautics and
Space Administration

Langley Research Center
Hampton, Virginia 23681-2199

August 2016

The use of trademarks or names of manufacturers in this report is for accurate reporting and does not constitute an official endorsement, either expressed or implied, of such products or manufacturers by the National Aeronautics and Space Administration.

Available from:

NASA STI Program / Mail Stop 148
NASA Langley Research Center
Hampton, VA 23681-2199
Fax: 757-864-6500

Table of Contents

Table of Contents	i
Table of Figures	iii
Table of Tables	iii
Abstract	1
1.0 Introduction	1
2.0 Acoustic Emission Collection Test Configuration	3
3.0 AE Metrics	7
4.0 Analysis	7
4.1 Phase I Checkout Tests	9
4.1.1 Leak Test and System Check	9
4.1.2 Down-bending 31.8 kips (-0.5g)	11
4.1.3 Up-bending 79.5 kips (1.25g)	13
4.1.4 Down-bending 31.8 kips and Pressure 4.6 psi (-0.5g + 0.5P)	15
4.1.5 Up-bending 79.5 kips and Pressure 4.6 psi (1.25g + 0.5P)	17
4.2 Phase II DLL Tests	19
4.2.1 Pressure 12.2 psi (1.33P)	19
4.2.2 Down-bending 63.6 kips (-1.0g)	21
4.2.3 Down-bending 63.6 kips and Pressure 9.2 psi (-1.0g + 1.0P)	23
4.2.4 Up-bending 159 kips (2.5g)	25
4.2.5 Up-bending 159 kips and Pressure 9.2 psi (2.5g + 1.0P)	27
4.3 Phase III DUL Tests	29
4.3.1 Down-bending 95.4 kips (-1.5g)	29
4.3.2 Down-bending 95.4 kips and Pressure 13.8 psi (-1.5g + 1.5P)	31
4.3.3 Up-bending 238.5 kips (3.75g) Trial 1	33
4.3.4 Up-bending 238.5 kips (3.75g) Trial 2	35
4.3.5 Up-bending 238.5 kips and Pressure 13.8 psi (3.75g + 1.5P)	37
4.3.6 Pressure 18.4 psi (2P) Trial 1	39
4.3.7 Pressure 18.4 psi (2P) Trial 2	41
4.4 Phase IV Post-Impact Checkout Tests	43
4.4.1 All tests (Nominally same loading as in Phase I)	43
4.5 Phase V Post-Impact DLL Tests	45
4.5.1 Down-bending 63.6 kips (-1.0g)	45
4.5.2 Down-bending 63.6 kips and Pressure 9.2 psi (-1.0g + 1.0P)	46
4.5.3 Pressure 12.2 psi (1.33P)	47
4.5.4 Up-bending 159 kips (2.5g)	48
4.5.5 Up-bending 159 kips and Pressure 9.2 psi (2.5g + 1.0P)	49
4.6 Phase VI Post-Impact DUL Tests	50
4.6.1 Down-bending 95.4 kips (-1.5g)	50
4.6.2 Down-bending 95.4 kips and Pressure 13.8 psi (-1.5g + 1.5P) Trial 1, 2, and 3	51
4.6.3 Down-bending 95.4 kips and Pressure 13.8 psi (-1.5g + 1.5P) Trial 4	51
4.6.4 Down-bending 95.4 kips and Pressure 13.8 psi (-1.5g + 1.5P) Trial 5	52
4.6.5 Pressure 18.4 psi (2P)	53
4.6.6 Up-bending 238.5 kips (3.75g)	54
4.7 Phase VII Post-Impact Combined Loads Failure Test	55
4.7.1 Trial 1-3	55

4.7.2 Trial 4.....	55
4.8 Phase VIII Post-Sawcut Up-bending Failure Test.....	58
4.8.1 Trial 1-3	58
4.8.2 Trial 4 Up-bending to Failure	60
5.0 Summary and Conclusions	60
6.0 References.....	61
Appendix A: Pressure Checkout and Phase 1 Checkout Tests	A1
Appendix B: Phase II Design Limit Load (DLL) Tests.....	B1
Appendix C: Phase III Design Ultimate Load (DUL) Tests	C1
Appendix D: Phase IV Post-Impact Checkout (PIC) Tests	D1
Appendix E: Phase V Post-impact DLL (PI DLL) Tests.....	E1
Appendix F: Phase VI Post-impact DUL (PI DUL) Tests.....	F1
Appendix G: Phase VII Post-impact Combined Loads (PICL) Failure Test	G1
Appendix H: Phase VIII Post-Sawcut Final Failure Test	H1
Appendix I: Test Matrix.....	I1

Table of Figures

Figure 1. Lowering the MBB into the CoLTs test area.....	iii
Figure 2. Typical AE Sensor (inset) and Pre-Amplifier (3 shown) installation on MBB.....	3
Figure 3. OML view of the AE sensor locations on Crown.....	4
Figure 4 OML view of the AE sensor locations on upper forward bulkhead. Upper aft bulkhead has sensors in corresponding locations on starboard end, (see Figure 3).....	5
Figure 5. OML view of the AE sensor locations on Keel.....	5
Figure 6. Post failure view of the forward bulkhead side of the MBB with close-up of the failure.....	6
Figure 7. Post failue view of the aft bulkhead side of the MBB with close-up of the failure.....	6
Figure 8. Cumulative Energy: close view. Pre-Phase I Checkout and Leak test by zone.....	10
Figure 9. Cumulative Energy: close view. Phase I: 31.8 kips down-bend.....	12
Figure 10. Cumulative Energy: close view. Phase I: 79.5 kips up-bend.....	14
Figure 11. Cumulative Energy: close view. Phase I: 31.8 kips down-bend + 4.6 psi.....	16
Figure 12. Cumulative Energy: close view. Phase I: 79.5 kips up-bend + 4.6 psi.....	18
Figure 13. Cumulative Energy: close view. Phase II: 12.2 psi.....	20
Figure 14. Cumulative Energy: close view. Phase II: 63.6 kips down-bend.....	22
Figure 15. Cumulative Energy: close view. Phase II: 63.6 kips down-bend + 9.2 psi.....	24
Figure 16. Cumulative Energy: close view. Phase II: 159 kips up-bend.....	26
Figure 17. Cumulative Energy: close view. Phase II: 159 kips up-bend + 9.2 psi.....	28
Figure 18. Cumulative Energy: close view. Phase III: 95.4 kips down-bend.....	30
Figure 19. Cumulative Energy: close view. Phase III: 95.4 kips down-bend + 13.8 psi.....	32
Figure 20. Cumulative Energy: close view. Phase III: 238.5 kips up-bend trial 1.....	34
Figure 21. Cumulative Energy: close view. Phase III: 238.5 kips up-bend trial 2.....	36
Figure 22. Cumulative Energy: close view. Phase III: 238.5 kips up-bend + 13.8 psi.....	38
Figure 23. Cumulative Energy: close view. Phase III: 18.4 psi trial 1.....	40
Figure 24. Cumulative Energy: close view. Phase III: 18.4 psi trial 2.....	42
Figure 25. Cumulative Energy: close view. Phase IV: 79.5 kips up-bending + 4.6 psi.....	44
Figure 26. Cumulative Energy: close view. Phase V: 63.6 kips down-bend.....	45
Figure 27. Cumulative Energy: close view. Phase V: 63.6 kips down-bend + 9.2 psi.....	46
Figure 28. Cumulative Energy: close view. Phase V: 12.2 psi.....	47
Figure 29. Cumulative Energy: close view. Phase V: 159 kips up-bend.....	48
Figure 30. Cumulative Energy: close view. Phase V: 159 kips up-bend + 9.2 psi.....	49
Figure 31. Cumulative Energy: close view. Phase VI: 95.4 kips down-bend.....	50
Figure 32. Cumulative Energy: close view. Phase VI: 95.4 kips down-bend + 13.8 psi trial 4.....	51
Figure 33. Cumulative Energy: close view. Phase VI: 95.4 kips down-bend + 13.8 psi trial 5.....	52
Figure 34. Cumulative Energy: close view. Phase VI: 18.4 psi.....	53
Figure 35. Cumulative Energy: close view. Phase VI: 238.5 kips up-bend.....	54
Figure 36. Cumulative Energy: close view. Phase VII: First load and pressure peak.....	56
Figure 37. Cumulative Energy: close view. Phase VII: Second load peak, zero pressure.....	57
Figure 38. Cumulative Energy: close view. Post-sawcut Up-bend: low energy portion of crown channels before load drop.....	58
Figure 39. Cumulative Energy: Post-sawcut Up-bend. Plot from top: Crown, Bulkheads, and Keel.....	59

Table of Tables

Table 1. Test Matrix for MBB.....	2
-----------------------------------	---

Symbols and Abbreviations

AE	Acoustic Emission
CoLTs	Combined Loads Test facility
DLL	Design Limit Load
DUL	Design Ultimate Load
g	acceleration due to gravity (resultant load for these tests = 63.6 kips)
LaRC	NASA Langley Research Center
MBB	Multibay Box
NDE	Nondestructive Evaluation
P	Operating pressure (P = 9.2 psi)
PI	Post-Impact
PIC	Post-Impact Checkout
PLB	pencil lead break
PRSEUS	Pultruded Rod Stitched Efficient Unitized Structure
SHM	Structural Health Monitoring
VIC	Visual Image Correlation

Abstract

A series of tests of the Pultruded Rod Stitched Efficient Unitized Structure (PRSEUS) HWB Multi-Bay Test Article were conducted during the second quarter of 2015 at NASA Langley Research Center (LaRC) in the Combined Loads Test facility (COLTS). This report documents the Acoustic Emission (AE) data collected during those tests along with an initial analysis of the data. A more detailed analysis will be presented in future publications.

1.0 Introduction

A MultiBay Box (MBB) test article as seen in [Figure 1](#), constructed of Pultruded Rod Stitched Efficient Unitized Structure (PRSEUS) composite panels [1, 2] was tested with various combinations of pressurization and mechanical loads at NASA Langley Research Center (LaRC). (see [Table 1](#)) This occurred in the Combined Loads Test facility (CoLTs). Two series of tests were conducted before and after intentionally induced impact damage at several locations. Each series started with checkout tests to verify the proper operation of all instrumentation and continued through limit load and ultimate load tests. Following those series were two “failure” tests. One was a schedule of combined loads which did not result in failure as planned. The final test (denoted as the “post-sawcut failure test”) consisted of up-bending until failure occurred after a section of the crown was cut out. This report documents the Acoustic Emission (AE) data collected during those tests along with an initial analysis where appropriate.

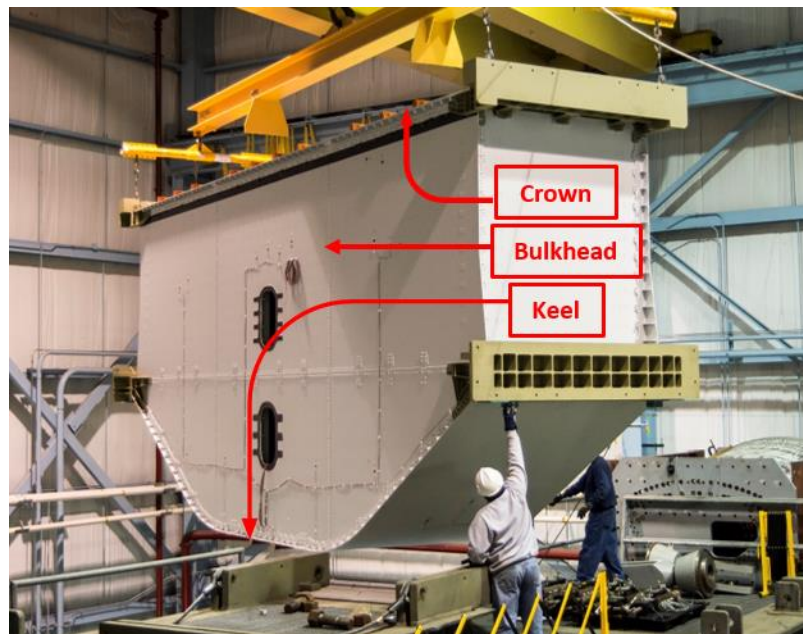


Figure 1. Lowering the MBB into the CoLTs test area.

Table 1. Test Matrix for MBB

Test Group	CoLTs run #	Test Date	Test Description and Loads
Phase I: Checkout Tests	1	2015-04-09	Pressure check 2 psi
		2015-04-13	No test, collected noise
	2	2015-04-14	31.8 kips down-bending (- 0.5g)
	3	2015-04-14	79.5 kips up-bending (1.25g)
	4	2015-04-14	31.8 kips down-bending + 4.6 psi (-0.5g + 0.5P)
	5	2015-04-14	79.5 kips up-bending + 4.6 psi (1.25g + 0.5P)
Phase II: DLL	6	2015-04-14	12.2 psi (1.33P)
	7	2015-04-15	63.6 kips down-bending (-1g)
	8	2015-04-15	63.6 kips down + 9.2 psi (-1g + 1P)
	9	2015-04-15	159 kips up-bending (2.5g)
	10	2015-04-15	159 kips up-bending + 9.2 psi (2.5g + 1P)
Phase III: DUL	11	2015-04-15	95.4 kips down-bending (-1.5g)
	12	2015-04-16	95.4 kips down-bending + 13.8 psi (-1.5g + 1.5P)
	13	2015-04-16	238.5 kips up-bending (3.75g): trial 1
	14	2015-04-16	238.5 kips up-bending (3.75g): success
	15	2015-04-16	238.5 kips up-bending + 13.8 psi (3.75g + 1.5P)
	16	2015-04-16	18.4 psi (2P): trial 1
	17	2015-04-16	18.4 psi (2P): success
Impacts		2015-04-24	Impacts: Collected AE part-time
Phase IV: Checkout	18	2015-04-30	4.6 psi (0.5P)
	19	2015-04-30	31.8 kips (-0.5g)
	20	2015-04-30	79.5 kips up-bending (1.25g)
	21	2015-04-30	31.8 kips down-bending + 4.6 psi (-0.5g + 0.5P)
	22	2015-04-30	79.5 kips up-bending + 4.6 psi (1.25g + 0.5P)
Phase V: DLL	23	2015-05-01	63.6 kips down-bending (-1g)
	24	2015-05-01	63.6 kips down-bending + 9.2 psi (-1g + 1P)
	25	2015-05-01	12.2 psi (1.33P)
	26	2015-05-01	159 kips up-bending (2.5g)
	27	2015-05-01	159 kips up-bending + 9.2 psi (2.5g + 1P)
Phase VI: DUL	28	2015-05-07	95.4 kips down-bending (-1.5g)
	29-32	2015-05-07	95.4 kips down-bending + 13.8 psi (-1.5g+1.5P): trial 1-4
	33	2015-05-07	95.4 kips down-bending + 13.8 psi (-1.5g+1.5P): success
	34	2015-05-07	18.4 psi (2P)
	35	2015-05-07	238.5 kips up-bending (3.75g)
Phase VII: Combined loads	36-38	2015-05-08	Trial 1-3
	39	2015-05-08	Trial 4: success
Post-sawcut failure	40-42	2015-06-03	Trial 1-3
	43	2015-06-03	Trial 4: success

2.0 Acoustic Emission Collection Test Configuration

Twenty-four acoustic emission sensors (Digital Wave B225.5) were mounted on the outside of the MBB test article. The AE sensors, which have a diameter of approximately 0.75 inches, were bonded with Lord 202 acrylic adhesive onto aluminum metal tape that was attached to the test article for easy removal as seen in the inset in [Figure 2](#). The sensors were connected to low noise thin coaxial sensor cables, which in turn were connected to Digital Wave PA0 preamp/line drivers, to buffer the signal back to the data acquisition system. The preamps, as seen in [Figure 2](#), were connected via thicker low noise coaxial cables to Digital Wave FM1 signal conditioning amplifiers, which were remotely located in the CoLTs control room. The FM1 amplifiers were connected to a computer containing multi-channel Digital Wave data acquisition hardware and software that recorded the data for subsequent processing. The channel identification numbers match the sensor identification numbers referred to in this report.

The transducer locations are indicated in [Figures 3, 4, and 5](#) for the crown, bulkheads, and keel, respectively. The locations for sensors 2, 8, 13, and 14 on the crown and 15 and 17 on the forward and aft bulkhead were guided by critical areas identified in a nonlinear analysis for loads beyond DUL [3]. These critical areas are illustrated in [Figures 3 and 4](#) as the red outlined regions. The remainder of the sensor locations were identified to give adequate coverage of the regions of interest (including near impact regions, see [Figure 5](#)) and were located to not intrude into central areas speckled for optical strain mapping.

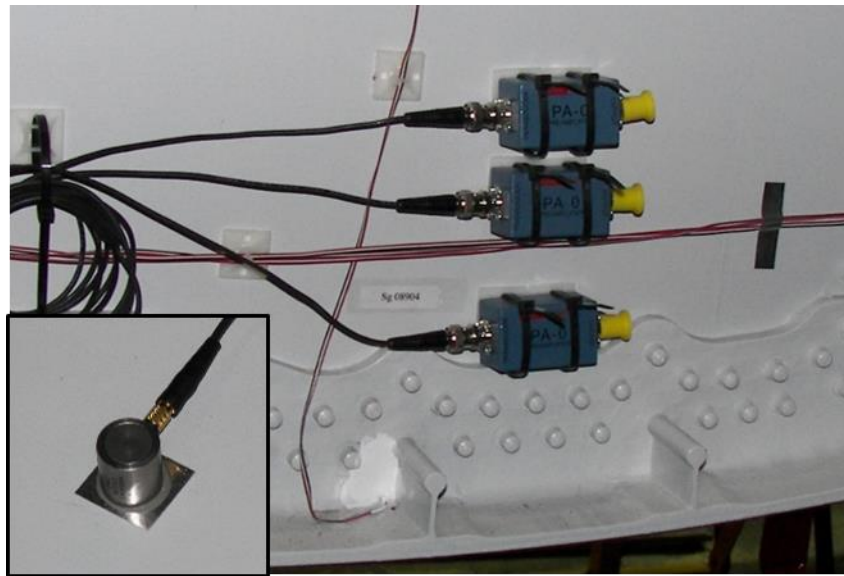


Figure 2. Typical AE Sensor (inset) and Pre-Amplifier (3 shown) installation on MBB

For future reference, **Figure 3** also shows how some of the sensor locations relate to subsequent damage regions of buckling fracture that occurred in the last test (post-sawcut). The “primary” failure mode during that test was buckling extending from the tips of the sawcut towards the crown-bulkhead edges as indicated by the blue shaded region of **Figure 3** enclosing sensors 12 and 6. The location of “secondary” buckling that also occurred in the last test is shown in **Figure 3** as the blue shaded region enclosing sensors 10, 14, and 4. In addition, **Figure 3** shows that sensors 1, 2, 7, and 8 were moved for the post-sawcut test from locations near the loading end (starboard) to locations closer to the sawcut. As seen in **Figures 6** and **7**, failure continued asymmetrically from those regions into and down the aft and forward bulkheads. On the forward bulkhead, visible failure occurred down the bulkhead centerline below sensor 6 and above the upper access hatch. On the aft bulkhead, the visible failure occurred down the bulkhead below AE sensor 10.

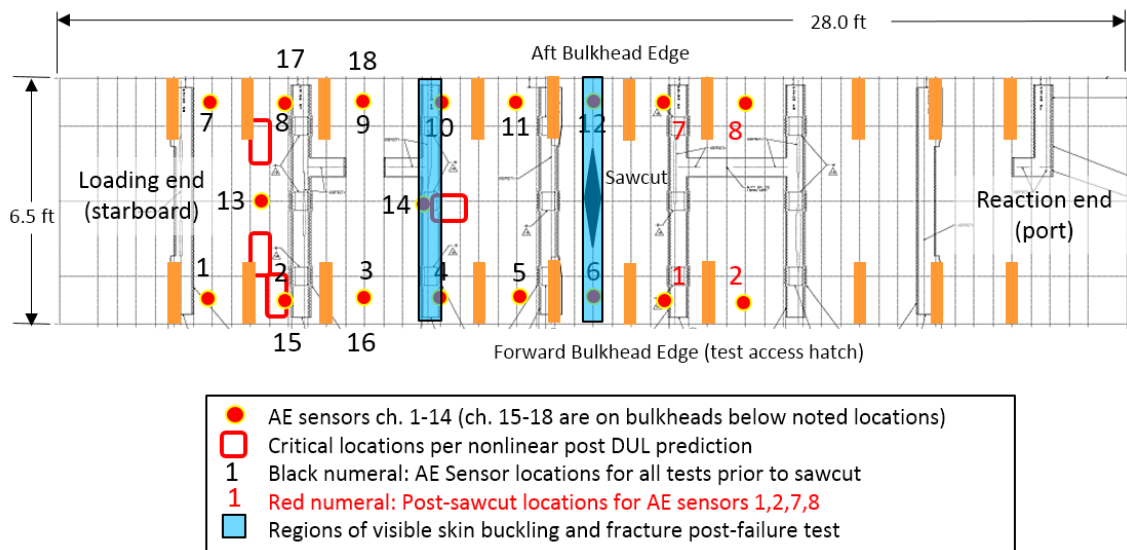


Figure 3. OML view of the AE sensor locations on Crown.

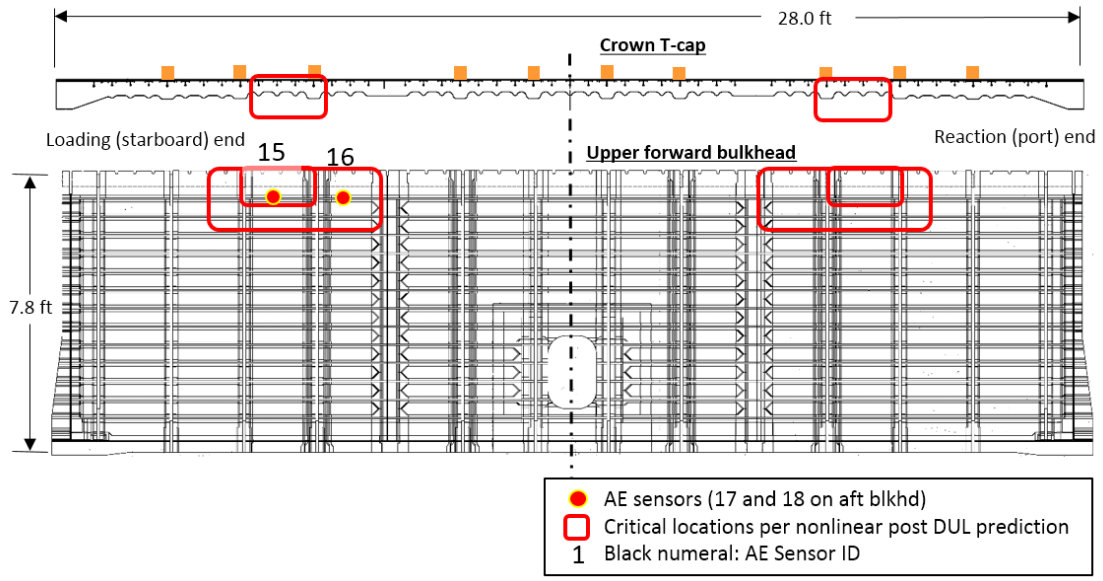


Figure 4 OML view of the AE sensor locations on upper forward bulkhead. Upper aft bulkhead has sensors in corresponding locations on starboard end, (see [Figure 3](#)).

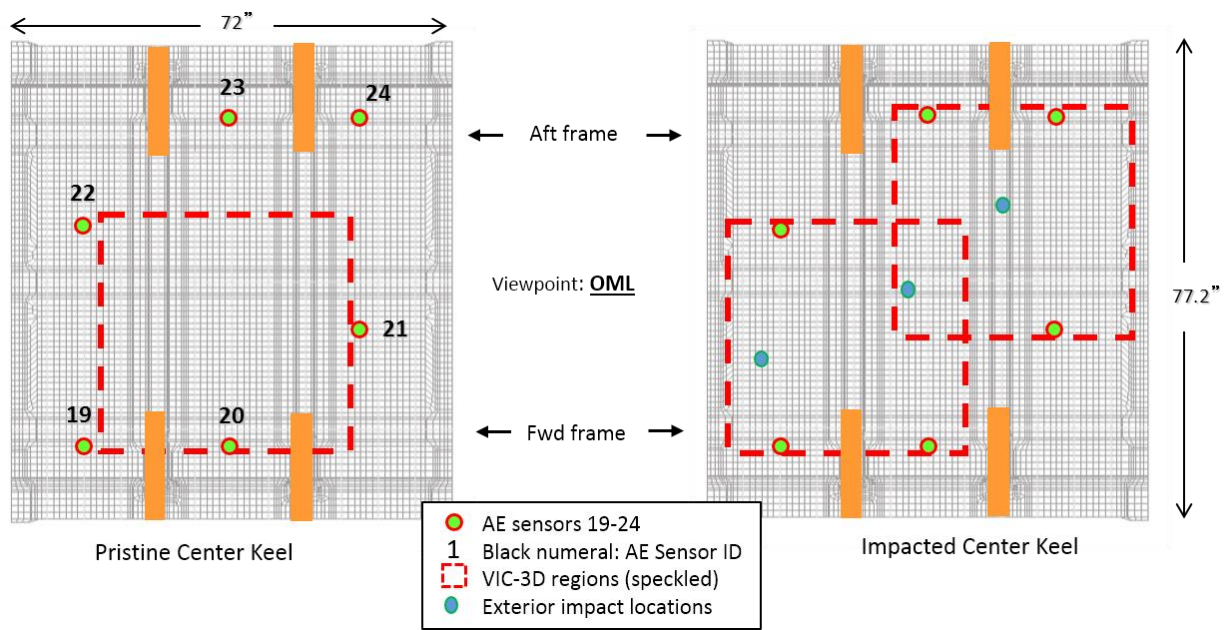


Figure 5. OML view of the AE sensor locations on Keel.

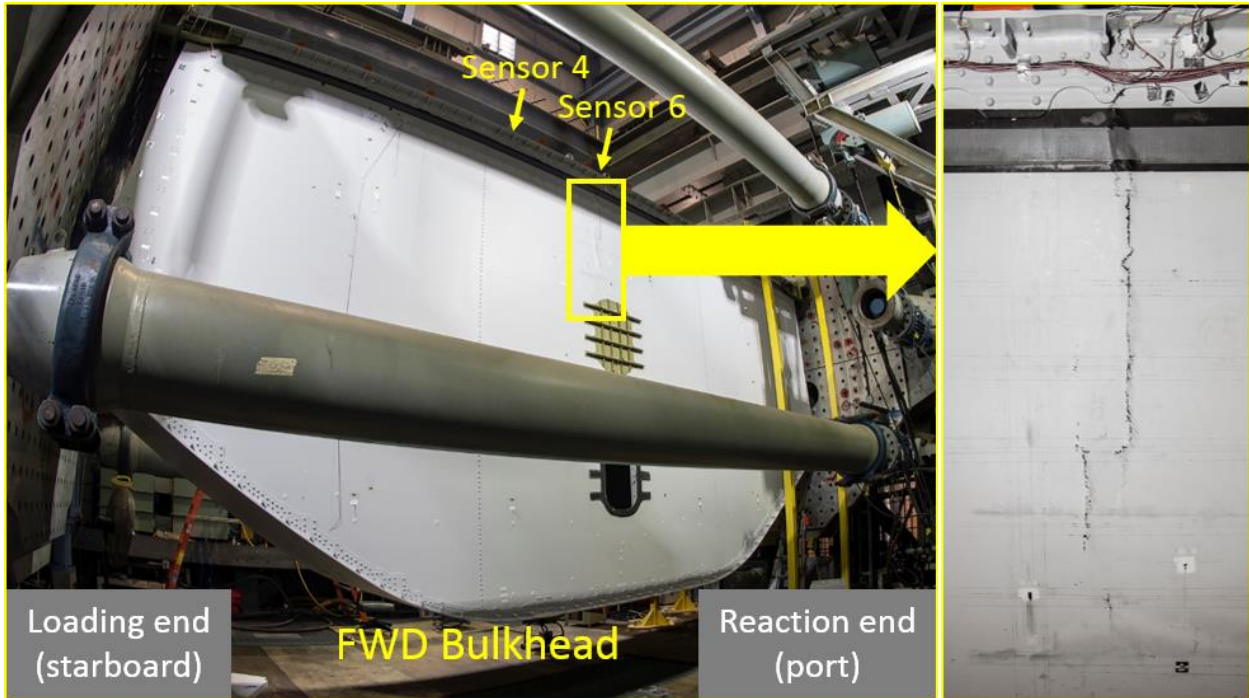


Figure 6. Post failure view of the forward bulkhead side of the MBB with close-up of the failure.

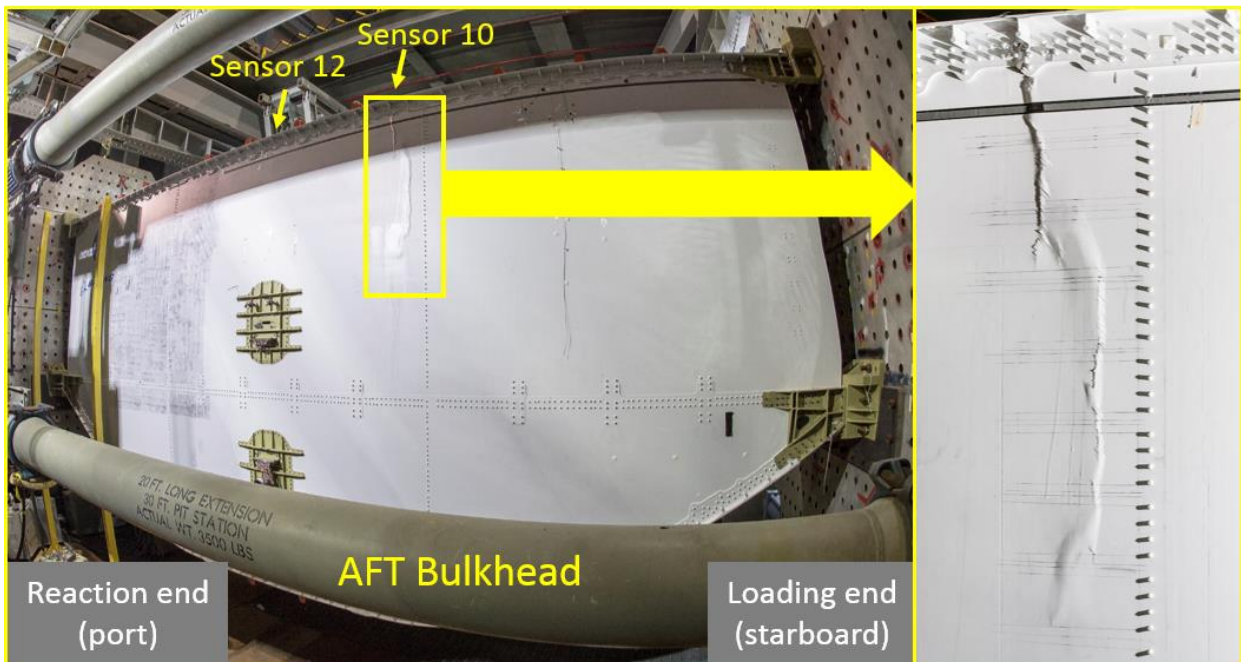


Figure 7. Post failure view of the aft bulkhead side of the MBB with close-up of the failure

3.0 AE Metrics

A discussion of the metrics is available in a previous PRSEUS NASA TM [4].

4.0 Analysis

Nearly all of the figures in this section follow a format where each contains a plot of the AE cumulative energy vs time, by channel, for each of three zones (crown, bulkhead, and keel). [4] These are typically close-up views of AE events of interest. The appendices provide separate plots of full views for each test and an expanded version of the test matrix that was shown in **Table 1**. The test matrix and plots are arranged in chronological order. The matrix includes the relevant data acquisition settings. In these tests, the gain settings were changed twice. Once at the very beginning when doing checkout testing to low loads, and later for the second test of Phase II to reduce signal amplitude saturation. The settings were not changed for the rest of the testing. Test-to-test changes in signal gain are compensated in the cumulative energy vs. time graphs by scaling all the plotted data to a zero (dB) gain thereby allowing comparisons between tests. A 16-256 kHz bandpass filter was applied to filter out DC offset and high frequency noise, which were not damage-associated-AE.

As noted, there is a detailed discussion of AE methodology elsewhere [4] but it is appropriate to note some concepts here. The AE instrumentation is “listening” to all channels continuously with the data for each channel filling its individual circular data buffer. Should any one of the 24 channels detect a signal exceeding a set threshold point, a trigger signal is sent to save all the buffers. All the channels are captured simultaneously for a short window in time regardless of the activity occurring at any particular sensor. Since the channels are continuously filling circular buffers, the saved data can cover pre- and post-trigger time as specified by the user. This data is used to calculate the cumulative signal energy used in this document at each sensor for every event [4]. Cumulative energy at each sensor is a zonal analysis because calculating AE source location by triangulation is difficult due to the sparse uneven distribution of sensors and the complexity of the composite structure [4].

For many of the tests, a sensor channel displays what we call a “nil-damage-occurring profile”. This happens when there is little in the acquired AE signals but background noise. Even though these types of signals are small, the system will calculate the sensor’s energy. Since the channel’s signal energy in those cases are small, the cumulative energy growth is slow. In addition, the noise from channel to channel may not be equivalent. These behaviors can create smoothly increasing plots of cumulative energy, with no significant “jumps” (large single event energy increase, compared to previous events), and no single sensor energy accumulating out of step with the others. This behavior of “nil-damage-occurring profiles” in the energy vs. time plots can be seen on many channels and sometimes for an entire zone.

Composites typically do not fail until damage localizes. When this occurs, the nearest sensor response increases out of step from the other sensors and disrupts the “nil-damage-profile”. However, a distinction is made between non-critical and critical damage. The “nil-damage profile” can also result from early composite damage, such as matrix hazing and cracking. This damage is not localized in a macroscopic sense because it can occur on small length scales but is distributed over larger regions and relatively long time scales. Although irreversible and therefore technically damage, it is typically considered non-critical.

Discussed elsewhere [4], the Kaiser Effect is typically interpreted in the realm of fatigue testing with repeated loadings of the same type. In the Kaiser Effect, AE occurs only under unprecedented load (a load that has not been previously applied), if no damage has occurred in the interim by *another mechanism*. In the tests there were three loading regimes (pressure, up-bending, and down-bending) and various combinations of them. Because of this complexity in the loading, a more fundamental interpretation,

elsewhere called the Kaiser Principle [5] can be used. The Kaiser Principle states that AE occurs only under unprecedented *stress*. However, stress at a point in material can be described as a tensor with six independent components that have magnitude and direction and each component has its own Kaiser Principle effect. While a detailed discussion of this concept is beyond the scope of this publication, the following discusses some pertinent information for this principle.

In a metal structure for aeronautics, in the absence of visible cracks or corrosion, the metal is considered “damage” free. Conversely, the presence of cracks and corrosion indicates a damaged state. However, in composites such as the type used for the structure in these tests, the mere existence of cracks, as noted previously, is not enough to consider that critical damage has occurred. Fractured material exhibits nonlinear behavior, so the existence of cracks, even under small deformations, has introduced nonlinearity into the material on a local scale even though the global behavior may be nearly linear. Therefore, the question to ask is; how does this nonlinearity affect the local state of stress in the region of the cracking? Is it possible for a new loading scheme with different stress tensor components, which may not be unprecedented in the region of the non-critical cracking, to develop new damage (and hence new AE)? This leads to a concept of the Felicity Ratio [4], which is a measure of the degree of apparent violation of the Kaiser Effect. The Felicity Ratio (ratio of load when AE starts over previous unprecedented load) requires tests to be repeated. In this report’s testing, there were a few select instances of consecutive cycles of the load during a single test or several tests in a row attempting to reach the same target. Those cases allow for a straightforward interpretation of the results with the Felicity Ratio. One should note that a Felicity Ratio less than 0.95 has been presented as a rejection criterion for fiber-reinforced pressure vessels in an ASTM standard practice [6] and the ASME Boiler and Pressure Vessel Code [7]. Further discussion of the Kaiser Principle and Felicity Ratio is held for future publication.

Finally, AE that occurs during unloading is also discussed. The Phase I up-bending plus pressure test discussed in section 4.1.5 is the first test that produced AE events during the stress unloading, albeit, small count and small amplitude. This typically indicates a behavior of internal friction that occurs on loading, which then exhibits emissions during unloading. This behavior is a function of the complexity of the fracture surfaces in the structure. The closer to zero load that AE continues to occur usually implies more intensive damage is present. Most of the remaining tests beyond the one mentioned show this behavior. The exceptions are typically the down-bending-only tests. Instances where other evidence contradicts this interpretation are noted.

4.1 Phase I Checkout Tests

4.1.1 Leak Test and System Check

This first test of the pristine structure, an instrument checkout and leak test to low pressure, was not officially considered part of the Phase I tests and would usually be considered irrelevant. However, it has been reported that the locations of the earliest, albeit small energy, AE may be indicative of the regions involved in the final failure [4].

Being pressure-only, this test is the most “symmetric” loading of the exterior structure. However, as seen in [Figure 8](#), the peak cumulative energy of the keel sensors (lower plot) is highest, followed by the crown sensors (top plot) and then the bulkhead sensors (middle plot).

The cumulative energy of the crown sensors 2, 6, 13, and 14 are highest during the 3-psi final peak. Of those four sensors, 14 is located in the region where the secondary buckle will occur in the post-sawcut test and is near a critical location as indicated in [Figure 3](#). Sensors 2 and 13 are also in or near a critical location.

Sensor 6 was located in the region that will become the primary shear buckle zone, during the post-sawcut test, resulting from the high stresses at the tips of the sawcut. Since the sawcut was not in place for this test, it would be inappropriate to suggest that the sensor 6 responses of this test alone foretell a major contribution to the failure in the post-sawcut test. However, cumulative energy on sensor 6 was the highest in the Phase VI up-bending test, and most of the Phase VII Combined Load test, which included up-bending. As noted in the section 4.8.2 discussion of the post-sawcut test, the response from sensor 6 was dominating toward the end of test. All of this evidence does suggest a weakness compared to the mirror location near sensor 12 at the aft bulkhead-crown edge.

At this point, it should be noted that the “failure” tests were not pressure-only and a further analysis of these early events may require comparing AE from comparable states of stress as noted previously.

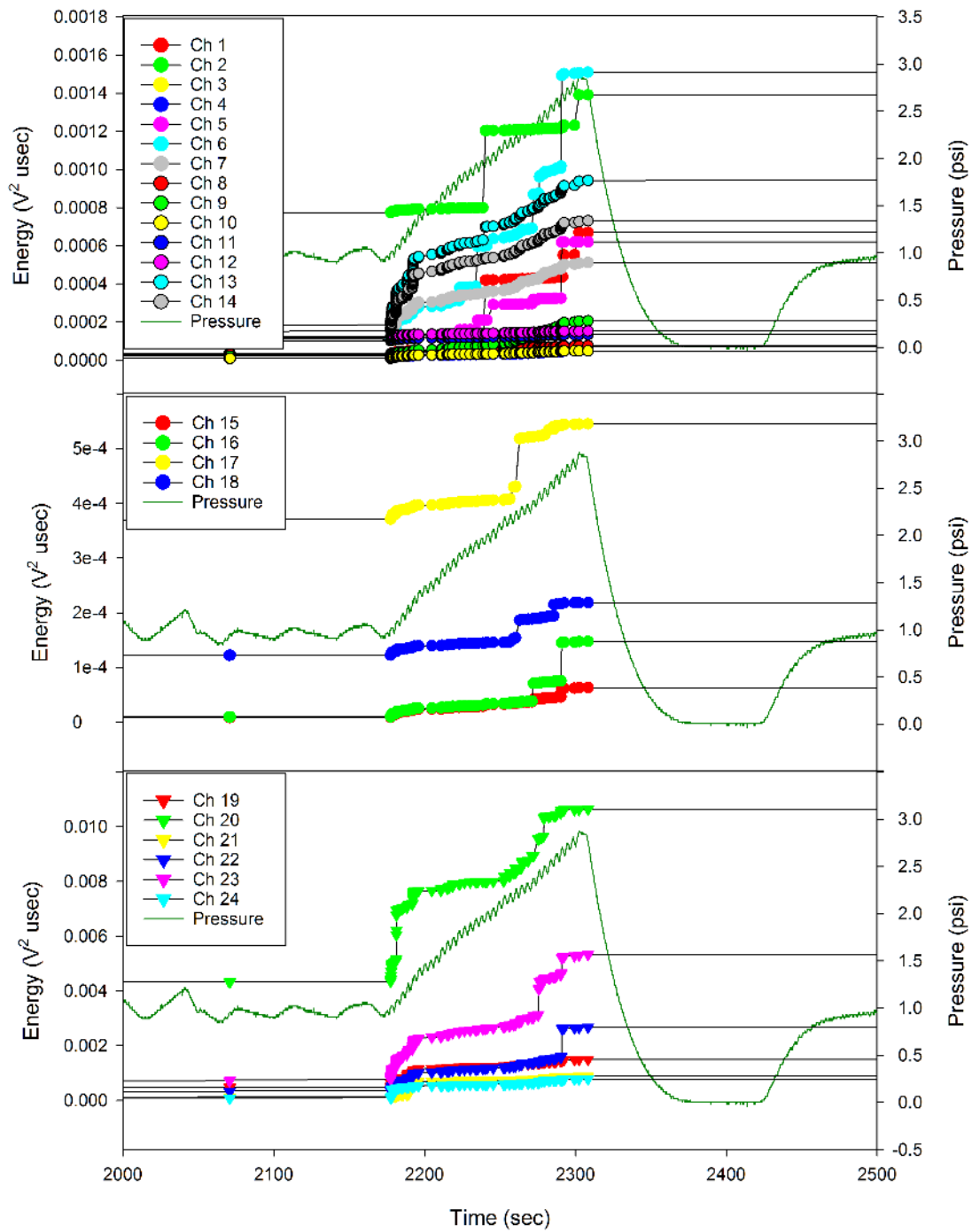


Figure 8. Cumulative Energy: close view. Pre-Phase I Checkout and Leak test by zone. Plot from top: Crown, Bulkheads, and Keel.

4.1.2 Down-bending 31.8 kips (-0.5g)

As seen in **Figure 9**, the peak cumulative energy of the crown sensors is the highest (top plot), followed by the bulkhead sensors (middle plot) and then keel sensors (lower plot). This is expected with the crown and upper portions of the bulkhead being in tension from a down-bending load. Of the crown sensors, the cumulative energies decrease in general with distance from the fixed end. This parallels the expected response to decreasing strain with distance from the fixed end. Therefore, it makes sense that 6 and 12 are highest for most of the test. On the forward side, sensor 6 shows a jump in energy around 1500 seconds (-30 kips) that must have relieved some stress because 12, 11 and 8 soon thereafter show higher cumulative energy. The bulkhead sensors, in order of decreasing energy, are 17, 18, 16, and 15. The aft bulkhead sensors are higher indicating, at least, greater “damage” initiation. The keel sensors, being the least active, are a good example of the “nil-damage-occurring” profile, discussed previously.

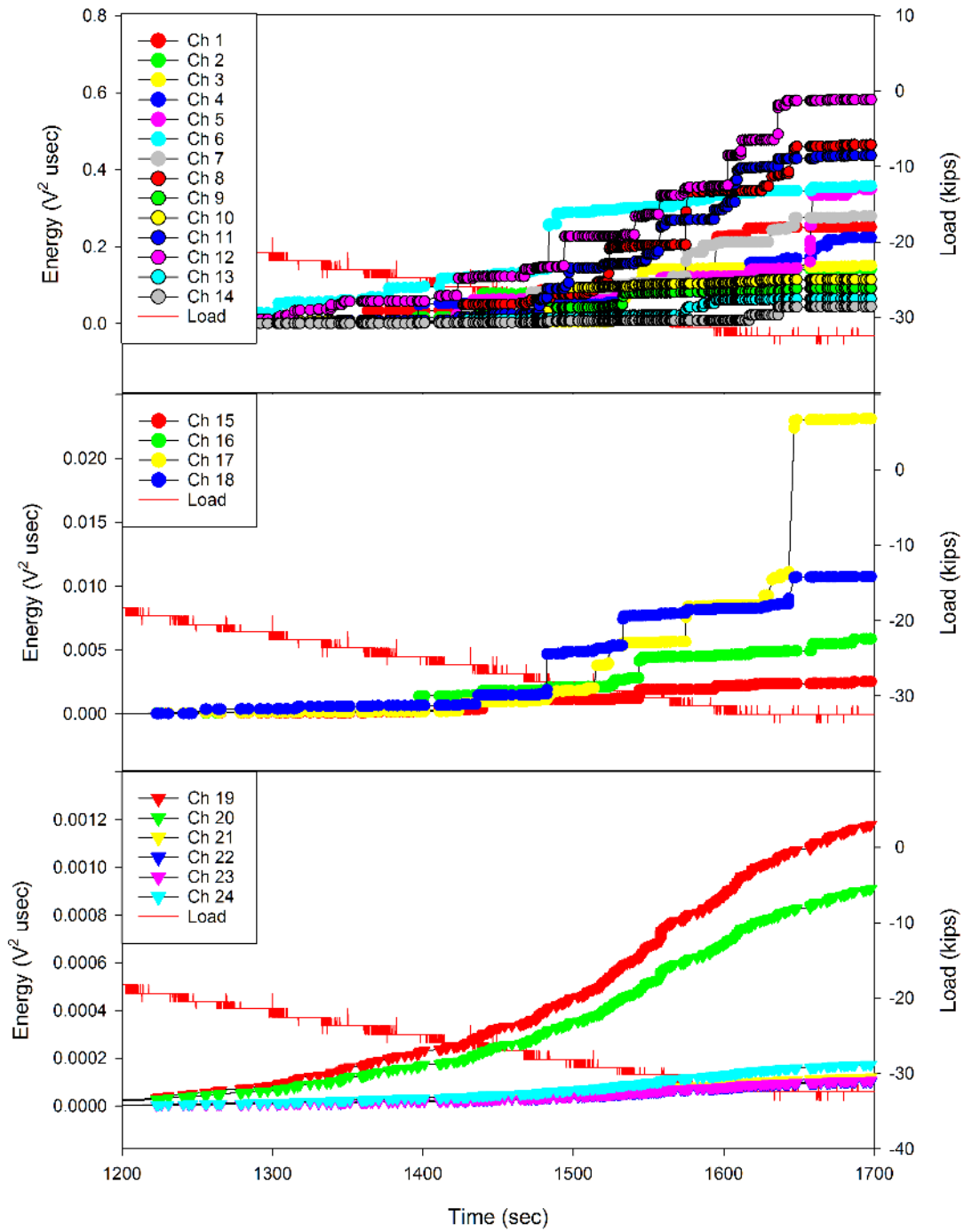


Figure 9. Cumulative Energy: close view. Phase I: 31.8 kips down-bend. Plot from top: Crown, Bulkheads, and Keel.

4.1.3 Up-bending 79.5 kips (1.25g)

As seen in **Figure 10**, the peak cumulative energy of the keel sensors is highest by two orders-of-magnitude (lower plot) over the crown sensors (top plot). The crown sensors are an order-of-magnitude greater than the bulkhead sensors (middle plot). This is the expected behavior with the keel in tension and the crown in compression from an up-bending load. Cumulative energy at keel sensors 20 and 23 is higher than the other keel sensors. However, most of the events do not show any significant energy jumps, so there is little to suggest any particular area is accumulating localized damage. In addition, the bulkhead sensors predominantly show the nil-damage-occurring profile, with a pattern of cumulative energies in decreasing order from the aft side to the forward side at sensors 18, 17, 16, and then 15. Crown sensors 4, 8, and 14 had significant events between 50 and 55 kip, in comparison to the consistently small events for the other crown sensors. Sensor 8 is near a critical area. Sensor 4 is in the region where the secondary buckle will occur in the post-sawcut test. Sensor 14 is near both a critical area and the secondary buckling region.

As seen in the appendices in **Figures A-7, A-8, and A-9**, this test had two load cycles, the first only reaching about 40 kips before unloading and reloading to the target load of 79.5 kips. One can see that for all the sensors no AE is generated in the second load cycle until reaching the peak level of the first. Considering the Kaiser Effect and a Felicity Ratio (load at current emission divided by previous peak load) of 1.0 or greater, this indicates the structure was not degrading during the first cycle of this test.

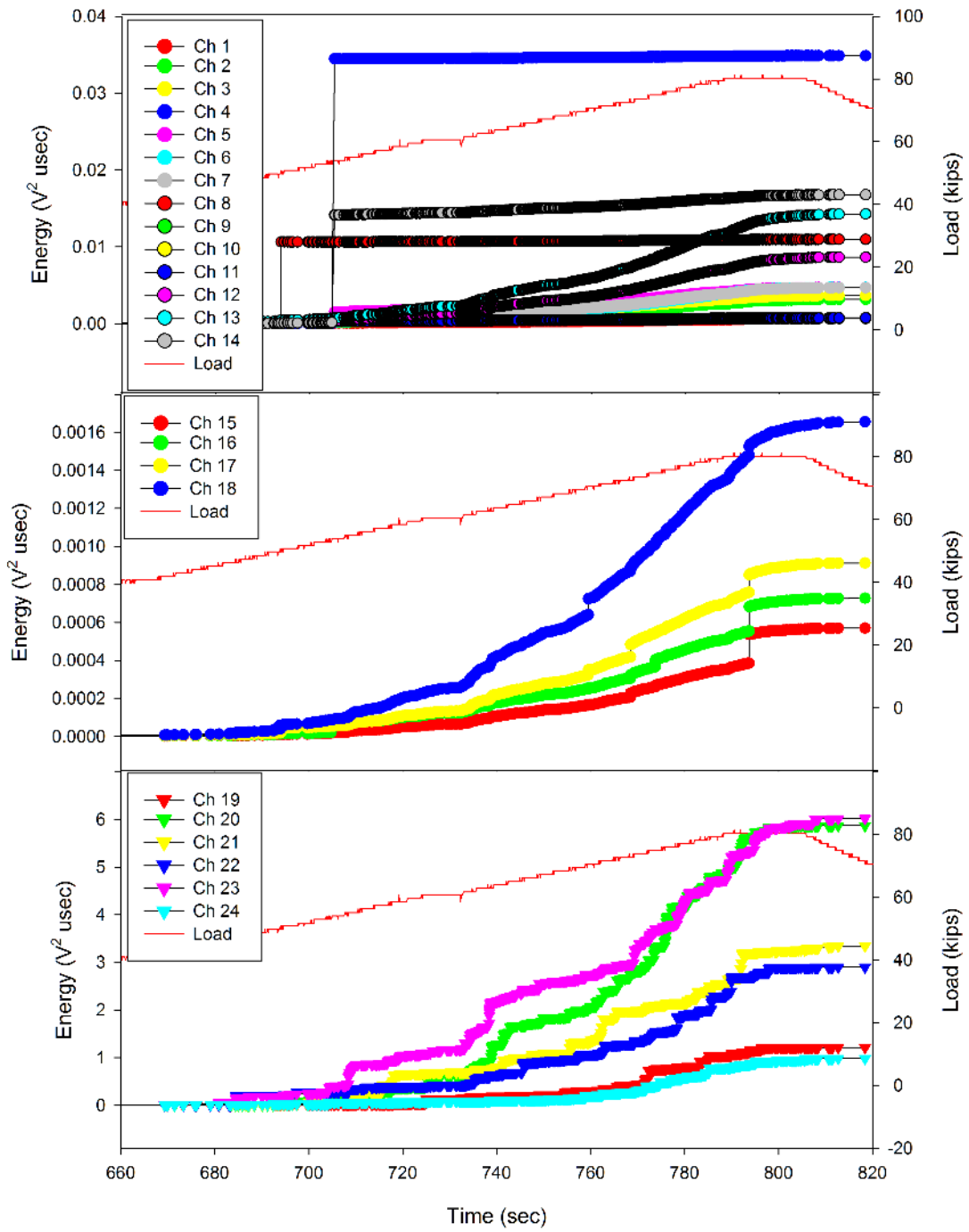


Figure 10. Cumulative Energy: close view. Phase I: 79.5 kips up-bend. Plot from top: Crown, Bulkheads, and Keel.

4.1.4 Down-bending 31.8 kips and Pressure 4.6 psi (-0.5g + 0.5P)

As seen in [Figure 11](#), the peak cumulative energy of the crown sensors is highest (top plot), followed by the bulkhead sensors (middle plot) and then keel sensors (lower plot). This is the expected behavior with the tension in the crown being additive from the down-bending and internal pressure. On the forward bulkhead edge of the crown, sensors 5 and 6 are higher early in the test. Aft edge sensors 7 and 8 overtake them via significant jumps around 2200 seconds (approximately 4 psi and 28 kips). Sensors 7 and 8 eventually are highest at the peak loads. In a pattern similar to the crown sensors, the forward bulkhead sensors 15 and 16 are higher earlier, but are lower at the peak than the aft ones, 17 and 18. The keel sensors, being the least active, are a good example of the “nil-damage-occurring” profile, discussed previously.

The combined loads for this test underwent 2 cycles, as seen in the appendices in [Figures A-10](#), [A-11](#), and [A-12](#). The load and pressure were closely controlled so that the peaks of each are nearly in phase for both cycles. No AE occurred in first cycle and did not start in the second cycle until exceeding the load peaks of the first cycle. Considering the Kaiser Effect and a Felicity Ratio (load at current emission divided by previous peak load) of 1.0 or greater, this indicates the structure was not degrading during the first cycle of this test.

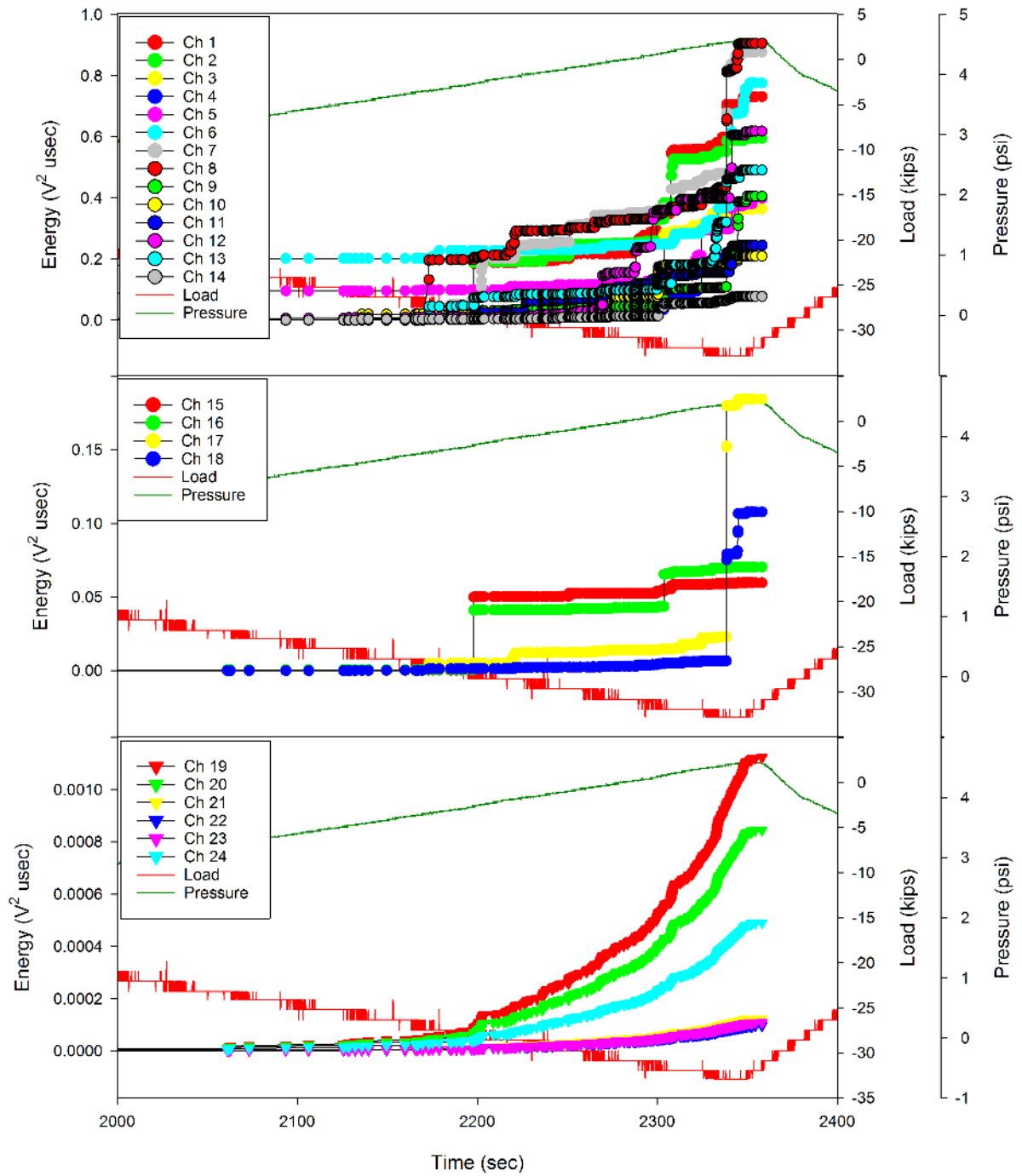


Figure 11. Cumulative Energy: close view. Phase I: 31.8 kips down-bend + 4.6 psi. Plot from top: Crown, Bulkheads, and Keel.

4.1.5 Up-bending 79.5 kips and Pressure 4.6 psi (1.25g + 0.5P)

As seen in [Figure 12](#), the peak cumulative energy of the keel sensors are highest (bottom plot) by two orders of magnitude over the crown sensors (top plot) and then the bulkhead sensors (middle plot). This is expected with the keel having additive tension from the pressure and up-bending. However, the keel shows little to distinguish it, other than sensors 20 and 23 moving up more rapidly in a manner similar to the previous up-bending only test (79.5 kips, 1.25 g). The bulkheads mostly show the smooth nil-damage-occurring profile.

However, most interesting is that the cumulative energy of sensor 4 on the crown is higher than the other crown sensors by a large margin. This is due to singular jumps early in the test, which are also exhibited by sensors 8 and 14. The pattern is nearly identical to the previous up-bending-only test (79.5 kips, 1.25g). These sensors are on patched regions of the crown, indicated by the dark gray outlines seen in [Figure 3](#). It is possible that the patches and the defects they fix are not deforming in a cohesive manner and have high internal friction at various locations.

In addition, as seen in the appendices in [Figures A-13](#), [A-14](#), and [A-15](#), this is the first test with some AE events, albeit small energy, occurring during most of unloading. The last event occurs just before a jog or hold during unload at about 20 kips. Combining this evidence with the AE noted in the previous paragraph could indicate looseness in some of the joints and structural connections, but not significant damage accumulation.

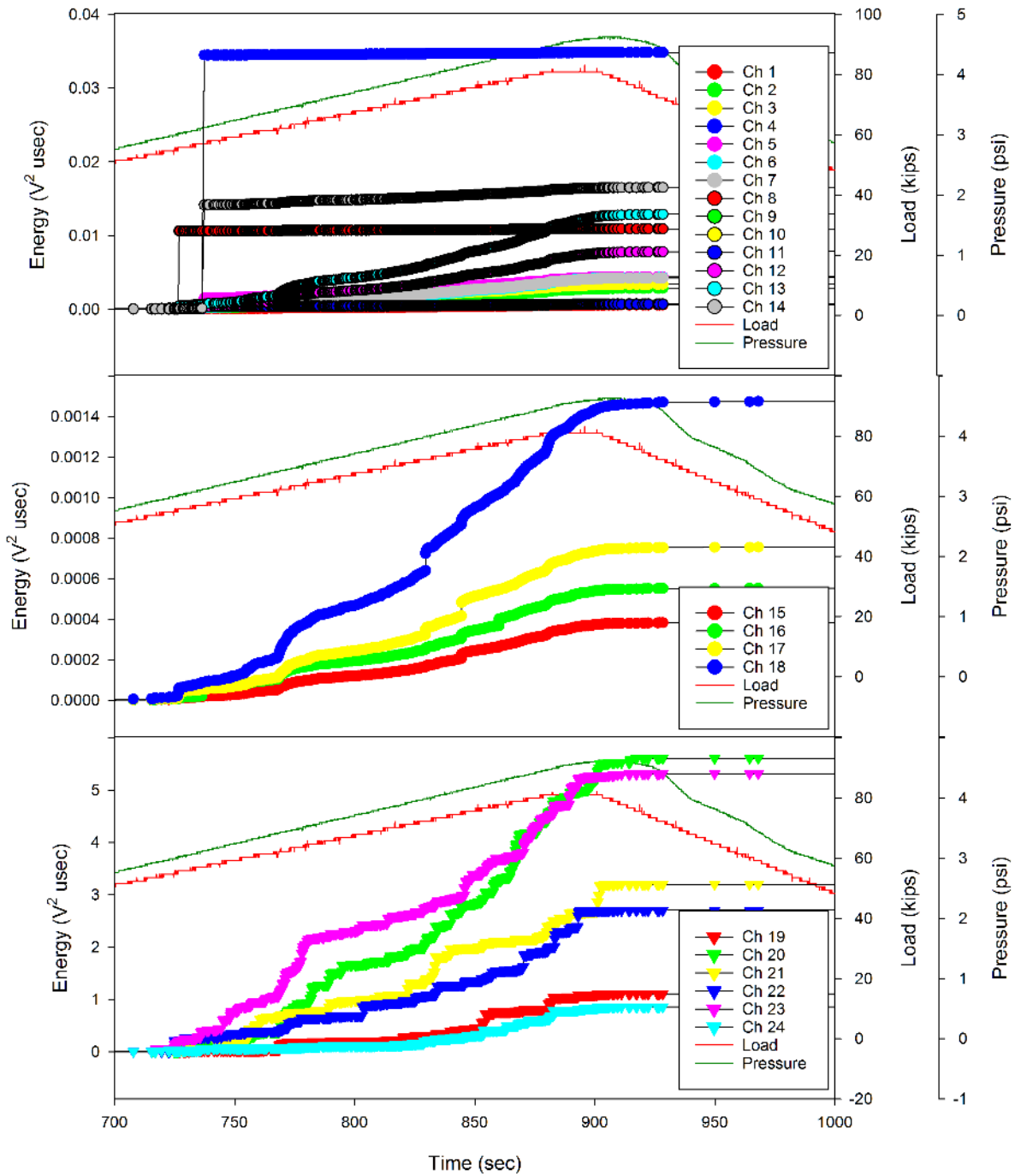


Figure 12. Cumulative Energy: close view. Phase I: 79.5 kips up-bend + 4.6 psi. Plot from top: Crown, Bulkheads, and Keel.

4.2 Phase II DLL Tests

This is the series of tests with various combinations of limit load conditions.

4.2.1 Pressure 12.2 psi (1.33P)

As seen in [Figure 13](#), the peak cumulative energies of all three zones have the same order of magnitude, which is expected with a pressure-only load creating tension in the skin. The bulkhead's cumulative energies are slightly higher than the crown, with the keel being the lowest. AE in all three zones starts at about 5 psi compared to the previous pressure-only peak pressure of 2.0 psi in Phase I. The Felicity Ratio is greater than 1.0 suggesting no significant damage occurred from the similar stress patterns created by previous pressurization or any of the intervening tests of other loading schemes.

Activity is occurring at many sensors, typically short bursts at random times, with random patterns. Only sensor 6 on the crown and sensor 23 on the keel show any indication of higher activity. Even though the bulkhead sensors cumulative energy are the highest, there are no other indications of damage localization. The bulkhead plots exhibit the nil-damage profile. This is a design-limit-load test, so, at worst; the damage would be expected to be non-critical.

As seen in the appendices in [Figures B-1](#), [B-2](#), and [B-3](#) we see small unloading events near zero, which does indicate some internal friction.

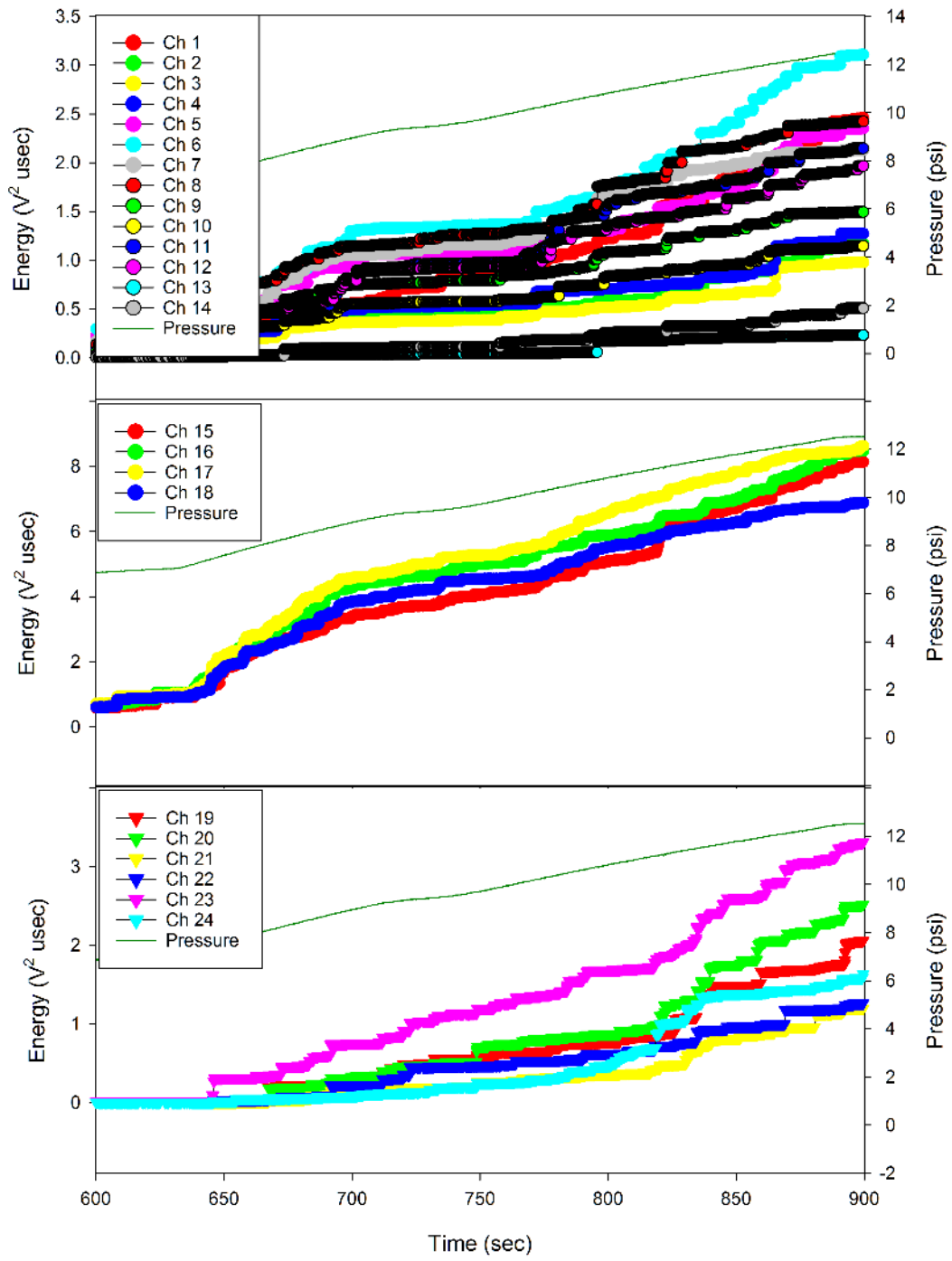


Figure 13. Cumulative Energy: close view. Phase II: 12.2 psi. Plot from top: Crown, Bulkheads, and Keel.

4.2.2 Down-bending 63.6 kips (-1.0g)

As seen in [Figure 14](#), the peak cumulative energy of the crown sensors (top plot) is highest over the bulkhead sensors (middle plot) with the keel sensors (lower plot) another two orders of magnitude lower. This is expected behavior from tension in the crown from down-bending.

The location of the crown sensor 12 on the aft edge closest to the fixed end is one of the sensors in the region of highest strain. As expected, it is higher in cumulative energy beginning at around 1150 seconds (-50 kips). However, sensors 6, 7 and 4 increase more rapidly and are highest by the end of test. Sensor 6 at a location (on the forward bulkhead edge) that mirrors the location of sensor 12 (on the aft bulkhead) should see similar strains. This change in highest cumulative energy could indicate some asymmetry in the loading or response of the structure.

Sensor 4, also on the forward edge, is in the region where secondary buckling will occur in the post-sawcut test. Sensor 7 seems to be an anomaly, not being close to any critical areas or near high strain regions.

AE, at a high rate, begins in all zones starts at about 38 kips while in previous tests the peak load in down-bending was 32 kips. The Felicity Ratio is greater than 1.0, so this could indicate that the structure was not significantly degraded during the previous tests. Technically, since there were intervening tests of different loading schemes, an evaluation of the Kaiser and Felicity effects using load as the marker could be questioned. However, this might be ignored, because there is an absence of other events that suggest damage.

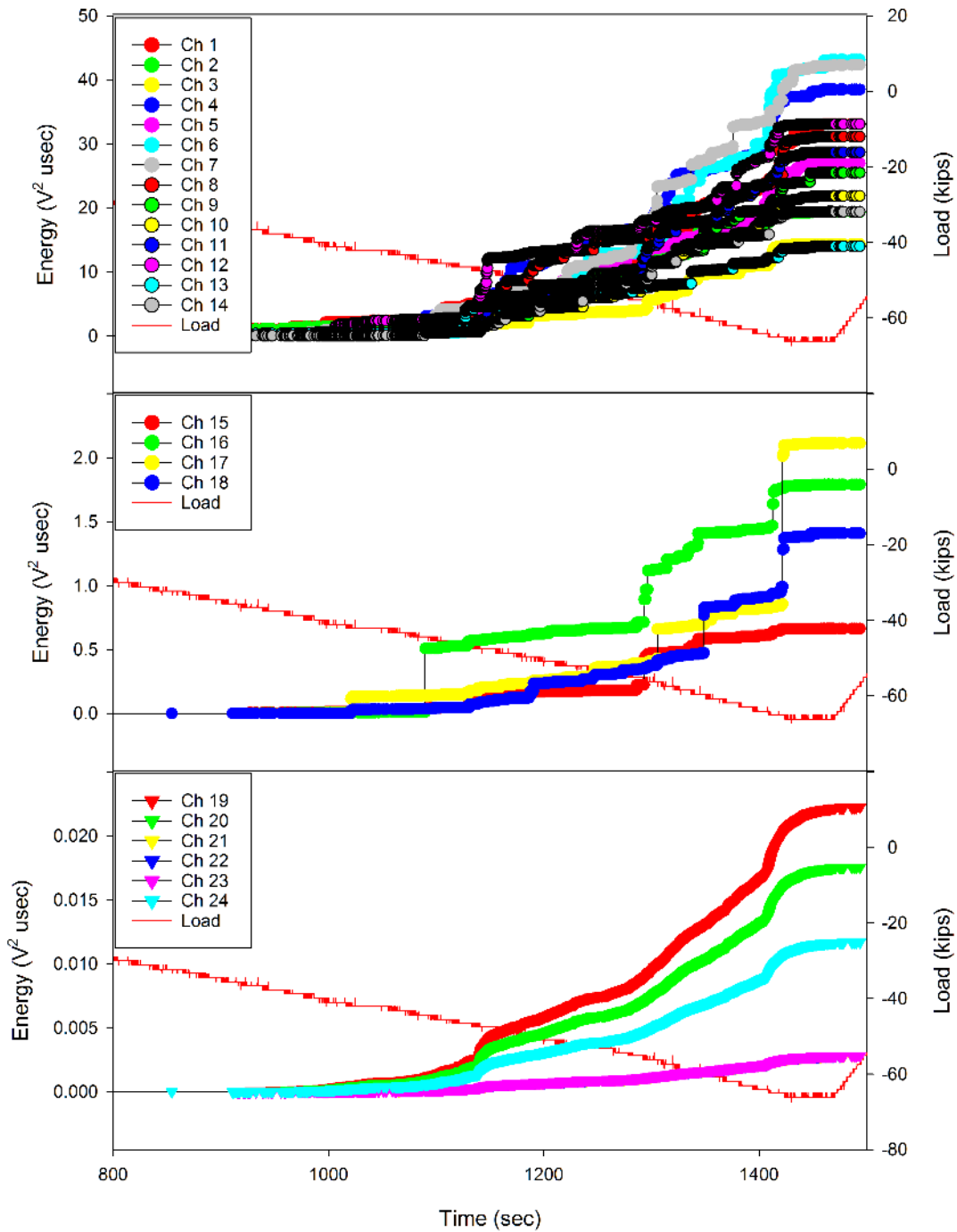


Figure 14. Cumulative Energy: close view. Phase II: 63.6 kips down-bend. Plot from top: Crown, Bulkheads, and Keel.

4.2.3 Down-bending 63.6 kips and Pressure 9.2 psi (-1.0g + 1.0P)

As seen in **Figure 15**, the peak cumulative energy of the crown sensors (top plot) is highest over the bulkhead sensors (middle plot) with the keel sensors (lower plot) another two orders of magnitude lower. This is the expected behavior with the tension in the crown being additive from the down-bending and internal pressure.

As seen in the appendices in **Figures B-7, B-8, and B-9**, this is another test with two cycles. Very little AE occurs in the first cycle which has load and pressure peaks at approximately 20 kips and 4.5 psi. AE does not restart in the second cycle until reaching about 30 kips and 4.5 psi. Close inspection of the numerical data leads to calculations of a Felicity Ratio = 1.61 for the load data and 0.98 for the pressure data. As noted earlier, there is a question about assuming that damage from loading and pressure are independent. Assuming that the ratio of load to pressure stays constant the stress tensor does not rotate. Therefore, it may be likely that one should get the same Felicity Ratio using load data or pressure data. The ratio of target load to target pressure for this test is approximately 6.9 kips/psi. However, looking at the down-bending trace and the pressure trace in **Figures B-7, B-8, and B-9** it is obvious that the ratio of load to pressure is not constant during the first cycle of this test. During a period of constant load at about 500 seconds, the ratio varies from approximately 4.4 to 8. This is beyond the scope of this document to discuss. However, this does suggest that a formulation of a Kaiser Principle using stress would yield a better evaluation.

Crown aft edge sensors 7, 8, 11 and 12 along with forward sensor 6 have the highest cumulative energy by the end of the test. The aft bulkhead sensor 18 shows a large increase just before 1800 seconds (-60 kips, 9 psi). Except for a few events in the first cycle, the keel shows the smooth nil-damage-occurring profile.

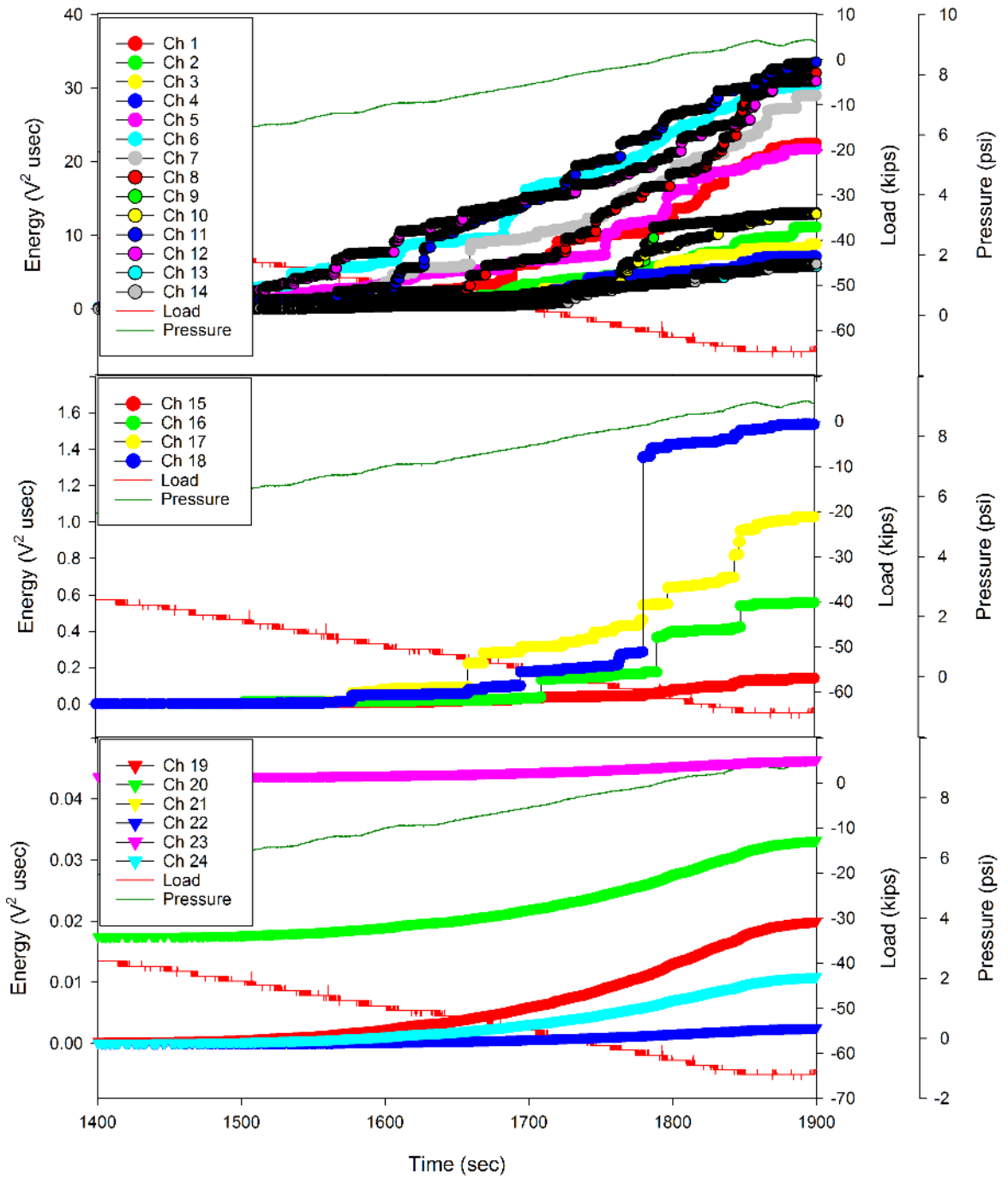


Figure 15. Cumulative Energy: close view. Phase II: 63.6 kips down-bend + 9.2 psi. Plot from top: Crown, Bulkheads, and Keel.

4.2.4 Up-bending 159 kips (2.5g)

As seen in **Figure 16**, the peak cumulative energy of the keel sensors (bottom plot) is highest, followed by the crown sensors (top plot) and then the bulkhead sensors (middle plot). This is expected with the keel being in tension from the up-bending.

As in all previous up-bending tests, even though the peak energies are highest, the keel AE does not show distinct indications of localization. However, there is an interesting pattern of energy in three groups of sensors. Sensors 20 and 23, which are on the centerline running from forward to aft, are exhibiting approximately the same cumulative energy and are higher than the other keel sensors. The pair of sensors nearest the centerline running lengthwise (sensors 21 and 22) also have approximately the same energy but at a distinctly lower level than the leaders. Sensors 19 and 24 on a keel diagonal also have similar energy, but at much lower level than the others.

Crown sensors 1 and 6 show sizable events early. However, sensor 4 on the forward edge and sensor 14 in the middle (from forward to aft) are highest on the crown by the end of the test. Both are in the region where the secondary buckle will occur during the post-sawcut test.

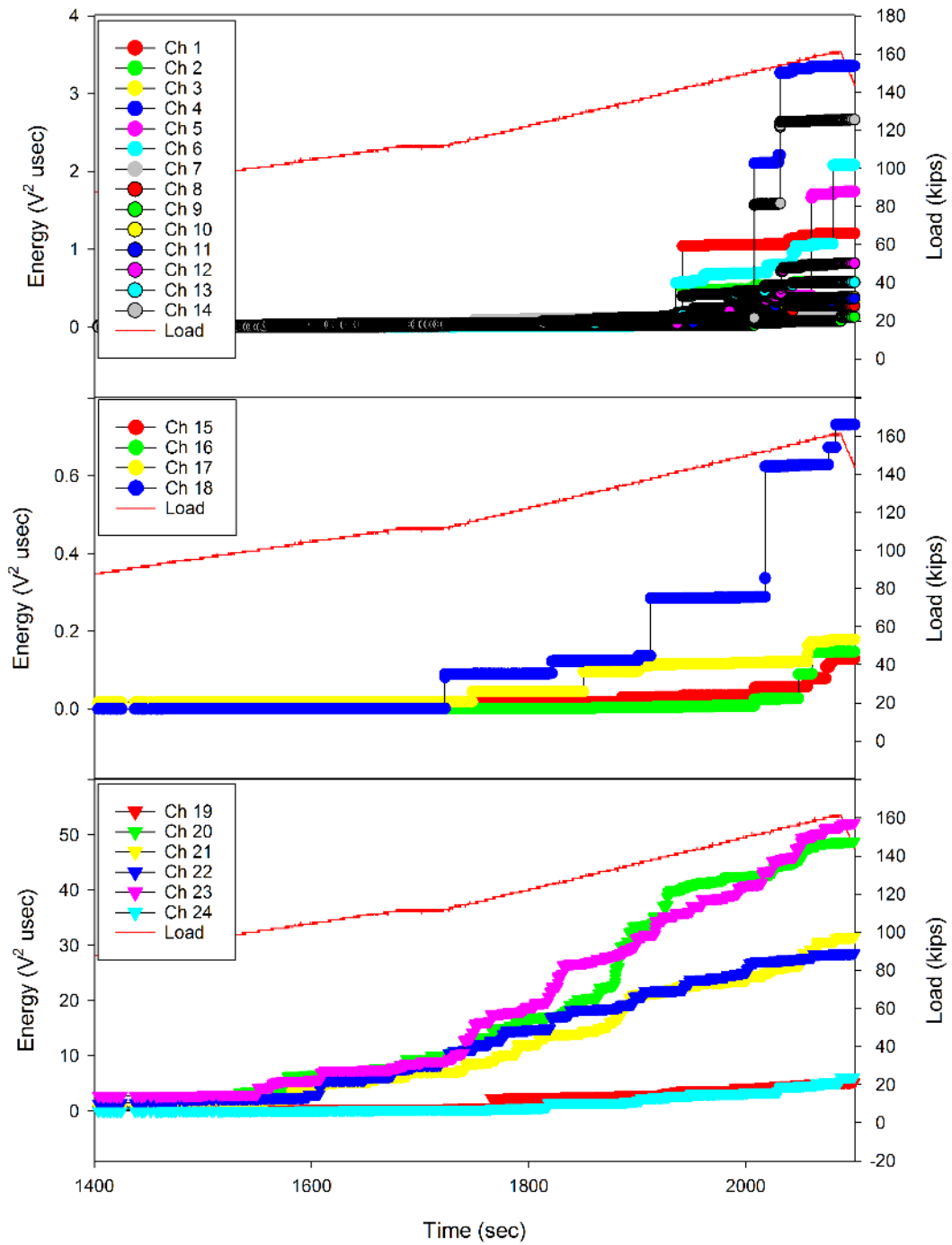


Figure 16. Cumulative Energy: close view. Phase II: 159 kips up-bend. Plot from top: Crown, Bulkheads, and Keel.

4.2.5 Up-bending 159 kips and Pressure 9.2 psi (2.5g + 1.0P)

As seen in **Figure 17**, the peak cumulative energy of the keel sensors (bottom plot) is highest, followed by the crown sensors (top plot) and then the bulkhead sensors (middle plot). This is expected with the keel having additive tension from the pressure and up-bending.

Again, even though the peak energies are highest, the keel AE does not show distinct indications of localization. However, the added pressure alters the pattern from the previous test discussed in section 4.2.4. Sensors 20 and 23 on the centerline running from forward to aft are highest but are joined by sensor 21 by the end of the test. Sensors 19, 22, and 24 are similar but lower energy than the others.

On the crown, sensor 14 is highest for most of the test. Sensors 4, 6, and 10 follow. The cumulative energy from the rest of the crown sensors lag by a significant margin approaching the load peaks. Sensors 4, 14, and 10 are the three sensors located along the secondary buckle region that occurs during the future post-sawcut test.

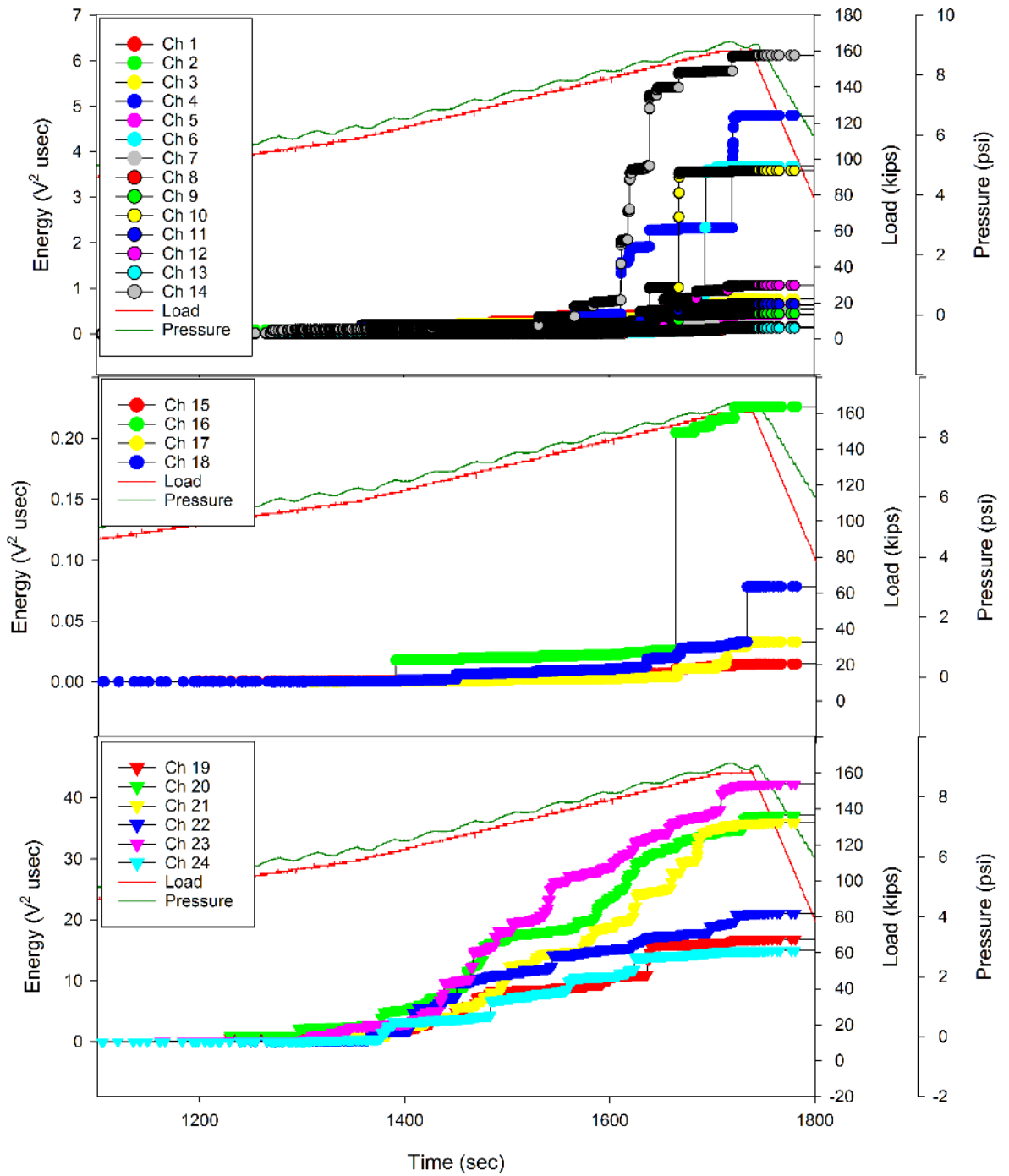


Figure 17. Cumulative Energy: close view. Phase II: 159 kips up-bend + 9.2 psi. Plot from top: Crown, Bulkheads, and Keel.

4.3 Phase III DUL Tests

This is the series of tests with various combinations of ultimate load conditions. Excluding the combined load test and post-sawcut failures, the highest target loads reached during this set are unprecedented for the remainder of the tests. As seen in the plots in Appendix C, all the tests have post-load AE occurring down to zero load (with greater number of events than in Phase II) which typically indicates significant fracture or opening of fracture surfaces during loading that creates internal friction during unloading, and contributing more damage during each test.

4.3.1 Down-bending 95.4 kips (-1.5g)

As seen in [Figure 18](#), the peak cumulative energy of the crown sensors (top plot) is highest over the bulkhead sensors (middle plot) with the keel sensors (lower plot) another two orders of magnitude lower. This is expected with tension in the crown from the down-bending.

On the crown, forward edge sensors 1 and 4 and aft sensors 7, 8, and 11 are higher by the end of the test with sensors 1 and 7 (the most starboard ones) as the highest. Forward bulkhead sensors 15 and 16 show significant jumps to become higher over the aft sensors 17 and 18.

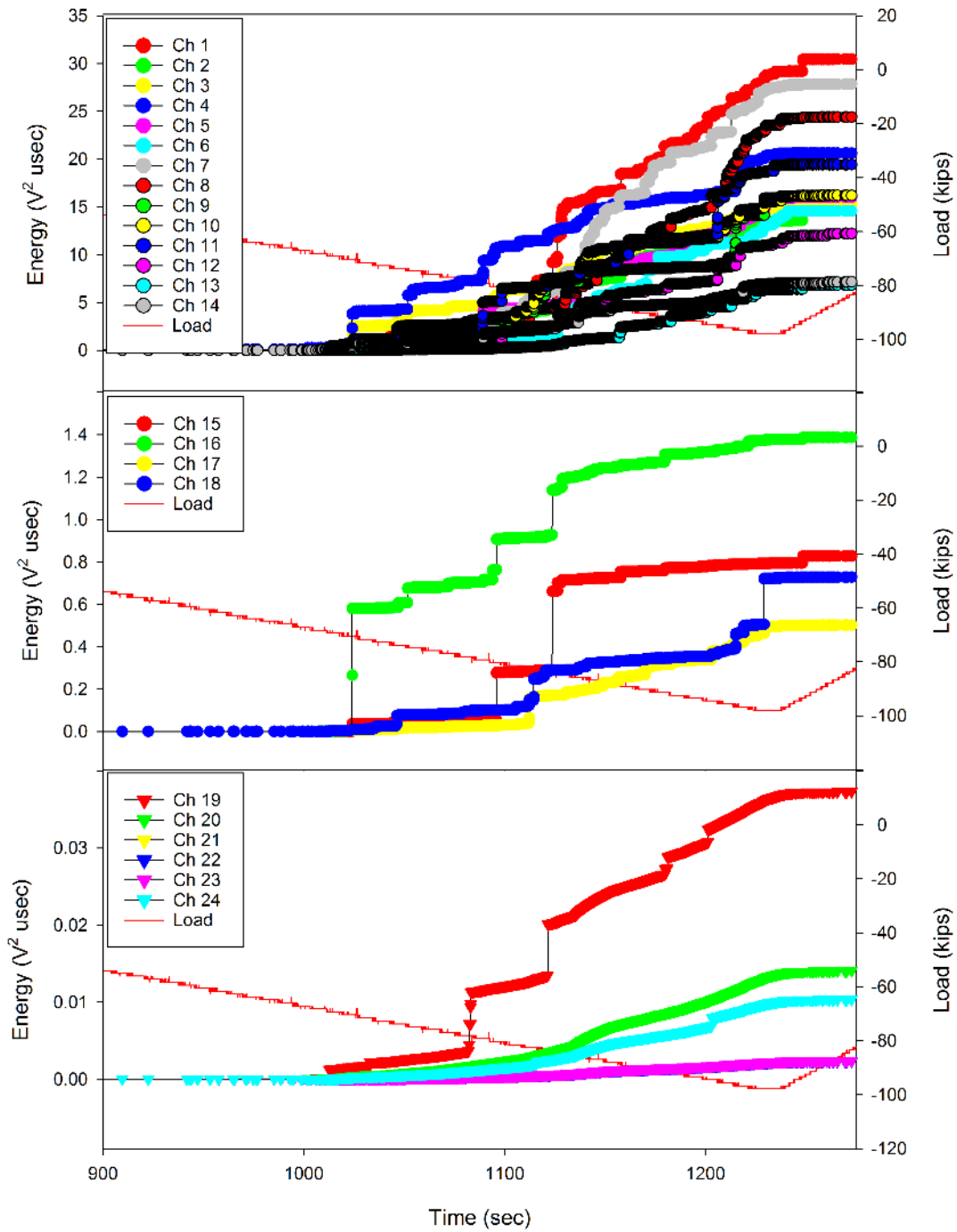


Figure 18. Cumulative Energy: close view. Phase III: 95.4 kips down-bend. Plot from top: Crown, Bulkheads, and Keel.

4.3.2 Down-bending 95.4 kips and Pressure 13.8 psi (-1.5g + 1.5P)

As seen in **Figure 19**, the peak cumulative energy of the crown sensors (top plot) is highest, followed by the bulkhead sensors (middle plot), and then the keel sensors (lower plot). This is expected with additive tension in the crown from the down-bending and pressure.

On the crown, the forward edge sensor 6 is highest for most of the test, followed by forward edge sensor 1 and aft edge sensor 8. Of the bulkhead sensors, aft sensor 17 is highest by a significant margin over the other bulkhead sensors. This test adds pressure to the scheme of the previous test discussed in section 4.3.1. This seems to accelerate preferentially the damage near the crown forward edge sensor 6. The added pressure also swaps the highest damage accumulation from the forward bulkhead sensors 15 and 16 seen during the previous test to the aft bulkhead sensors 17 and 18.

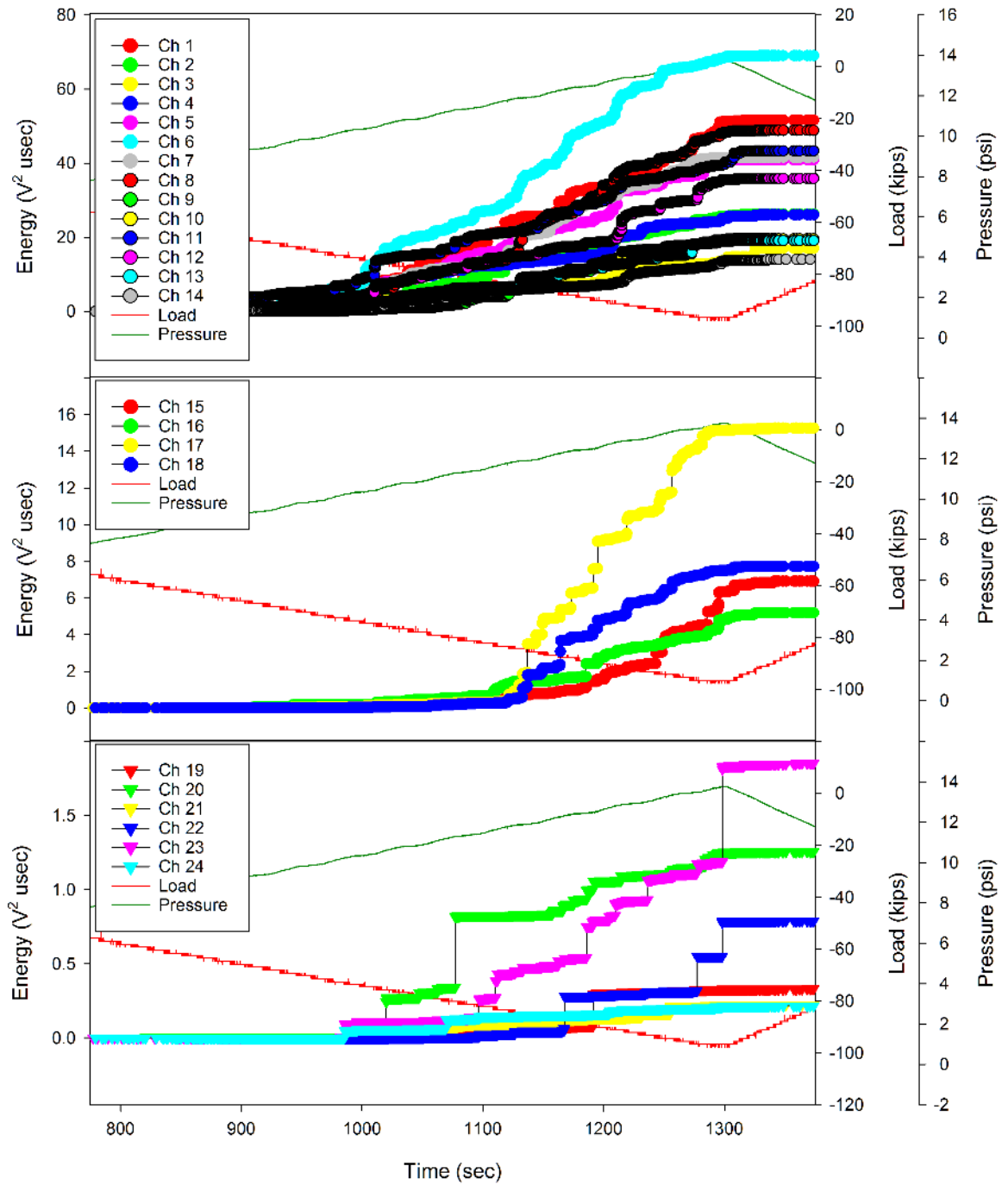


Figure 19. Cumulative Energy: close view. Phase III: 95.4 kips down-bend + 13.8 psi. Plot from top: Crown, Bulkheads, and Keel.

4.3.3 Up-bending 238.5 kips (3.75g) Trial 1

As seen in [Figure 20](#), this test only reaches approximately 170 kips. Even though this is an up-bending test and the keel is in tension, the keel is lowest in peak cumulative energy. The peak cumulative energies of the keel and the bulkheads are comparable. They are also an order of magnitude below the crown energy. However, the highest peak cumulative energy of the crown is an order of magnitude less than any previous up-bending tests. This is possibly because it has surpassed those previous loads by only 10 percent. On the crown, forward edge sensors 6 and 5, and aft edge sensor 7 are the only ones of the crown that are significantly higher approaching the peak load. Of the bulkhead sensors, the aft sensors 17 and 18 are highest at the end of test, via a few significant jumps.

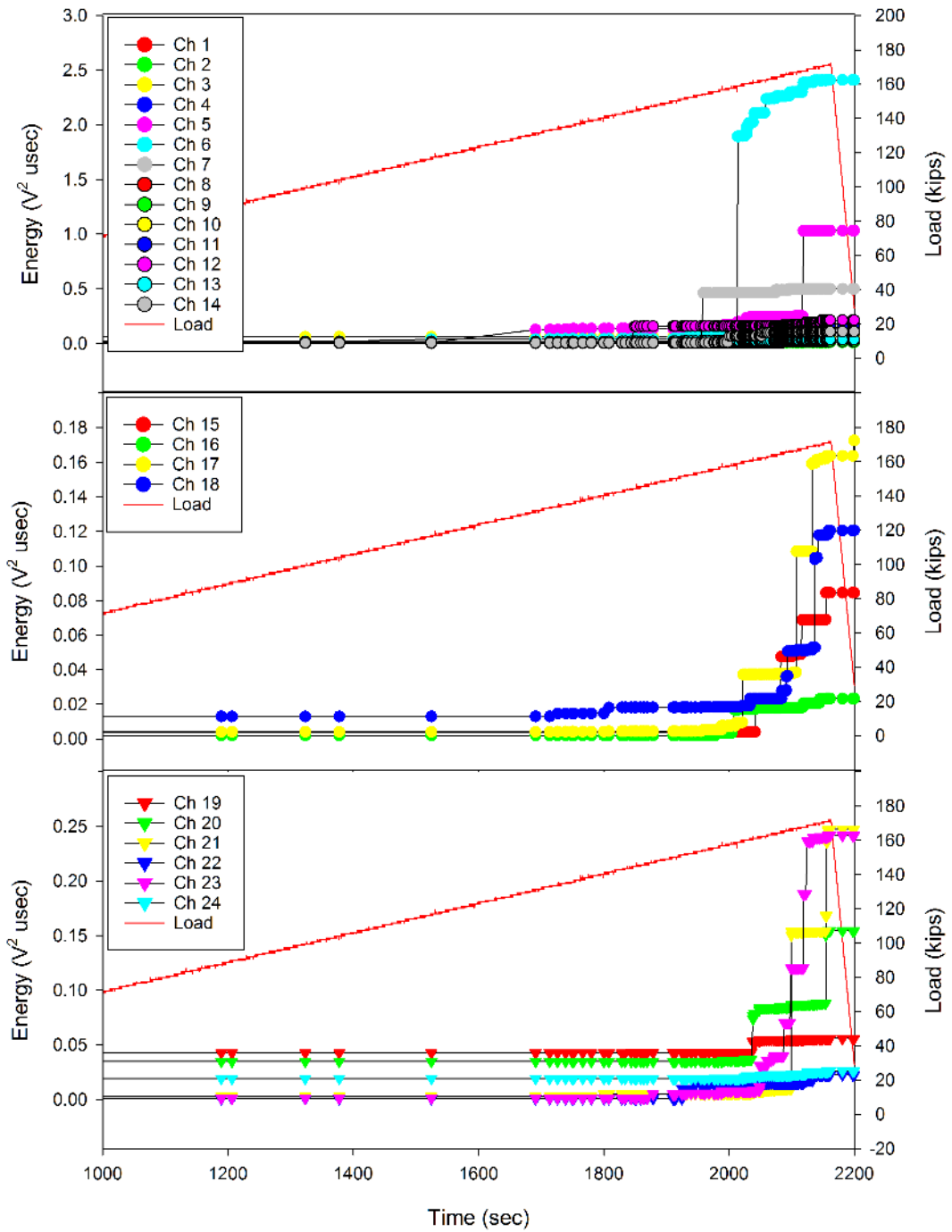


Figure 20. Cumulative Energy: close view. Phase III: 238.5 kips up-bend trial 1. Plot from top: Crown, Bulkheads, and Keel.

4.3.4 Up-bending 238.5 kips (3.75g) Trial 2

This test is the second and successful attempt to reach this particular goal load.

As seen in **Figure 21**, the majority of the sensors on the crown, keel, and bulkheads have comparable peak cumulative energy. On the crown, the highest peak cumulative energy is the forward edge sensor 6 by a significant margin, with the midline sensor 14 higher than the rest by a small margin. The bulkheads continue the trend from the previous test with the aft bulkhead sensors 17 and 18 having the highest peak cumulative energy due to large energy events.

Because the load scheme is equivalent to that of the previous test, this allows a valid Kaiser and Felicity Effect evaluation of damage development. A small cluster of events occur at approximately 120 kips (seen in **Figures C-10, C-11, and C-12**) and the steadily-increasing-energy AE starts at approximately 160 kips. In comparison with the previous test, the Felicity Ratio is approximately 0.7 using the early cluster of events. If one ignores them and calculates Felicity Ratio using the steadily-increasing-energy events, it is still below 1.0. These calculations are strong evidence of rapidly increasing damage accumulation.

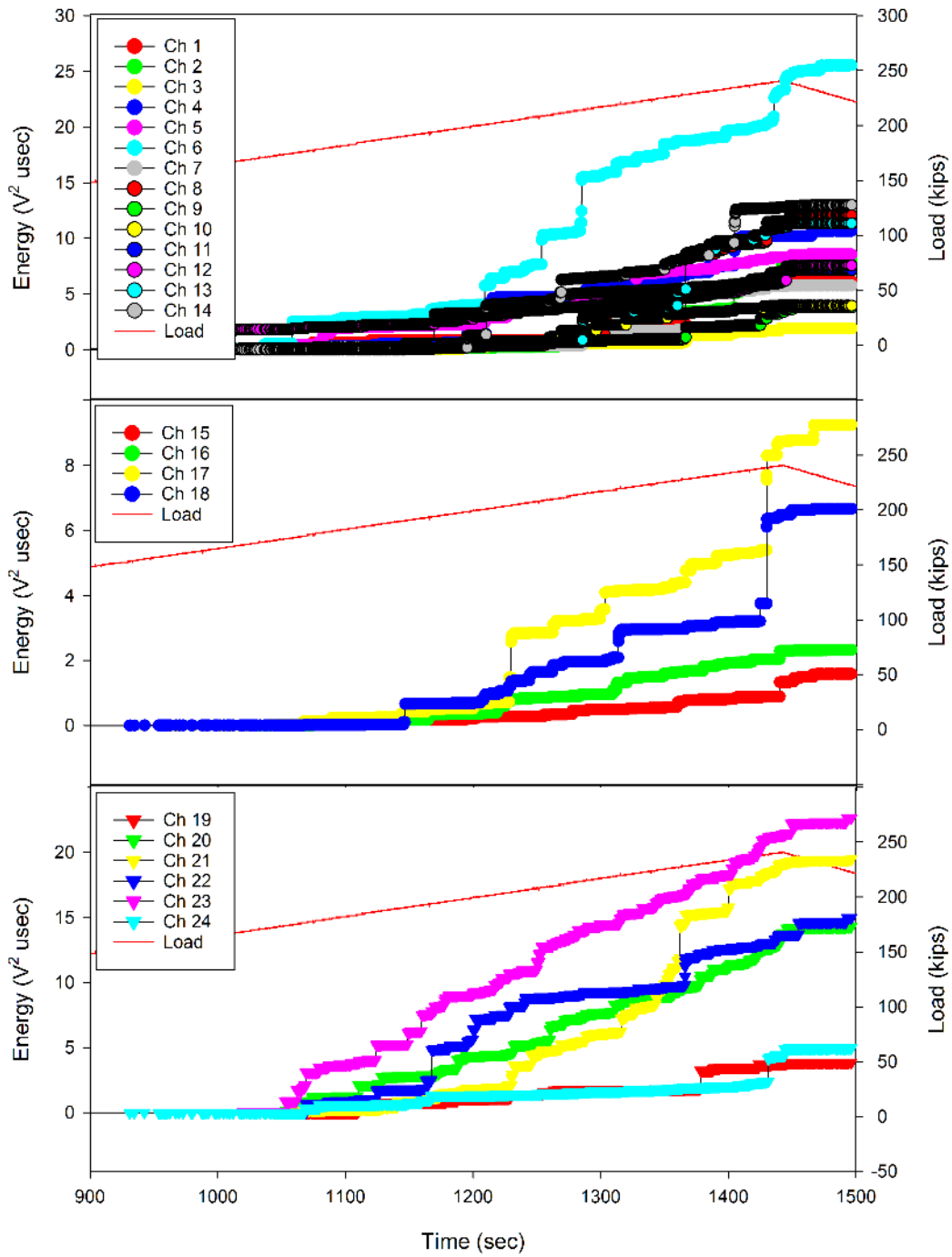


Figure 21. Cumulative Energy: close view. Phase III: 238.5 kips up-bend trial 2. Plot from top: Crown, Bulkheads, and Keel.

4.3.5 Up-bending 238.5 kips and Pressure 13.8 psi (3.75g + 1.5P)

This test adds pressure to the scheme of the previous test discussed in section 4.3.4. As seen in **Figure 22**, all three zones have peak cumulative energy of the same order of magnitude. The crown (top plot) is highest by approximately a factor of two over the keel (lower plot) and approximately a factor of seven over the bulkheads (middle plot). This shows that the additive tension in the keel from the pressure and up-bending does not supersede the damage already accumulated in the crown.

The added pressure seems to accelerate preferentially the damage in the regions of the buckles that will occur in the post-sawcut test. This is indicated by Sensors 14, 10 and 4 having the highest cumulative energy (future secondary buckle region). Next lowest are sensors 6 and 12 (future primary buckle region) and sensors 5 and 11 (next to future primary buckle region). This indicates weakening of the regions that will eventually fail.

Of the bulkheads, aft sensors 17 and 18 again have higher cumulative energy than the forward sensors.

As seen in **Figures C-13, C-14, and C-15**, AE starts at approximately 90 kips and 5 psi. In comparison to the previous unprecedented loads, which occur in this set of DUL tests, the Felicity Ratio calculated using load is approximately 0.4. The Felicity Ratio calculated using pressure is also approximately 0.4. As noted earlier, there is a question about these calculations using load and pressure independently. However, since the results are equivalent and well below 1.0, these calculations are strong evidence of rapidly increasing damage accumulation.

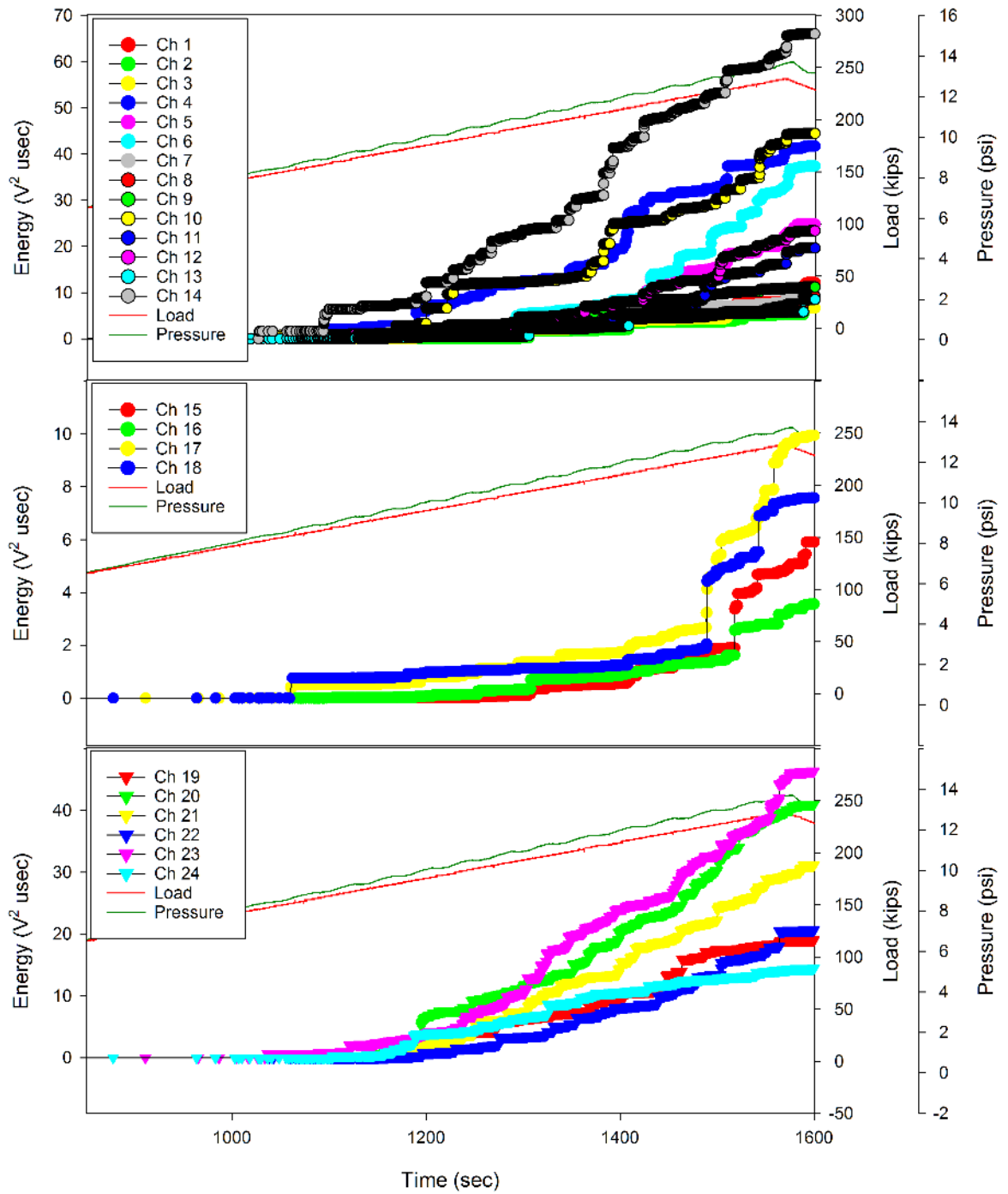


Figure 22. Cumulative Energy: close view. Phase III: 238.5 kips up-bend + 13.8 psi. Plot from top: Crown, Bulkheads, and Keel.

4.3.6 Pressure 18.4 psi (2P) Trial 1

This first trial reaches 14 psi. Again all zones have comparable cumulative energy peaks, with bulkheads higher by only a factor of two over the crown. The crown is higher by a factor of two over the keel. As seen in [Figure 23](#), of the crown, aft edge sensors 8, 10, 11, and forward edge sensor 2 have the highest cumulative energy at the end of the test. Bulkheads have significant jumps both forward and aft. Keel sensors 22 and 23 have large events at about 12 psi.

The earliest AE are bursts at approximately 7 and 9 psi with the steadily increasing energy events starting around 11 psi. In comparison to the unprecedented pressure of 13.8 psi in this set of DUL tests, and assuming the earliest burst is damage related, the Felicity Ratio is approximately 0.5. This calculation is strong evidence of rapidly increasing damage accumulation.

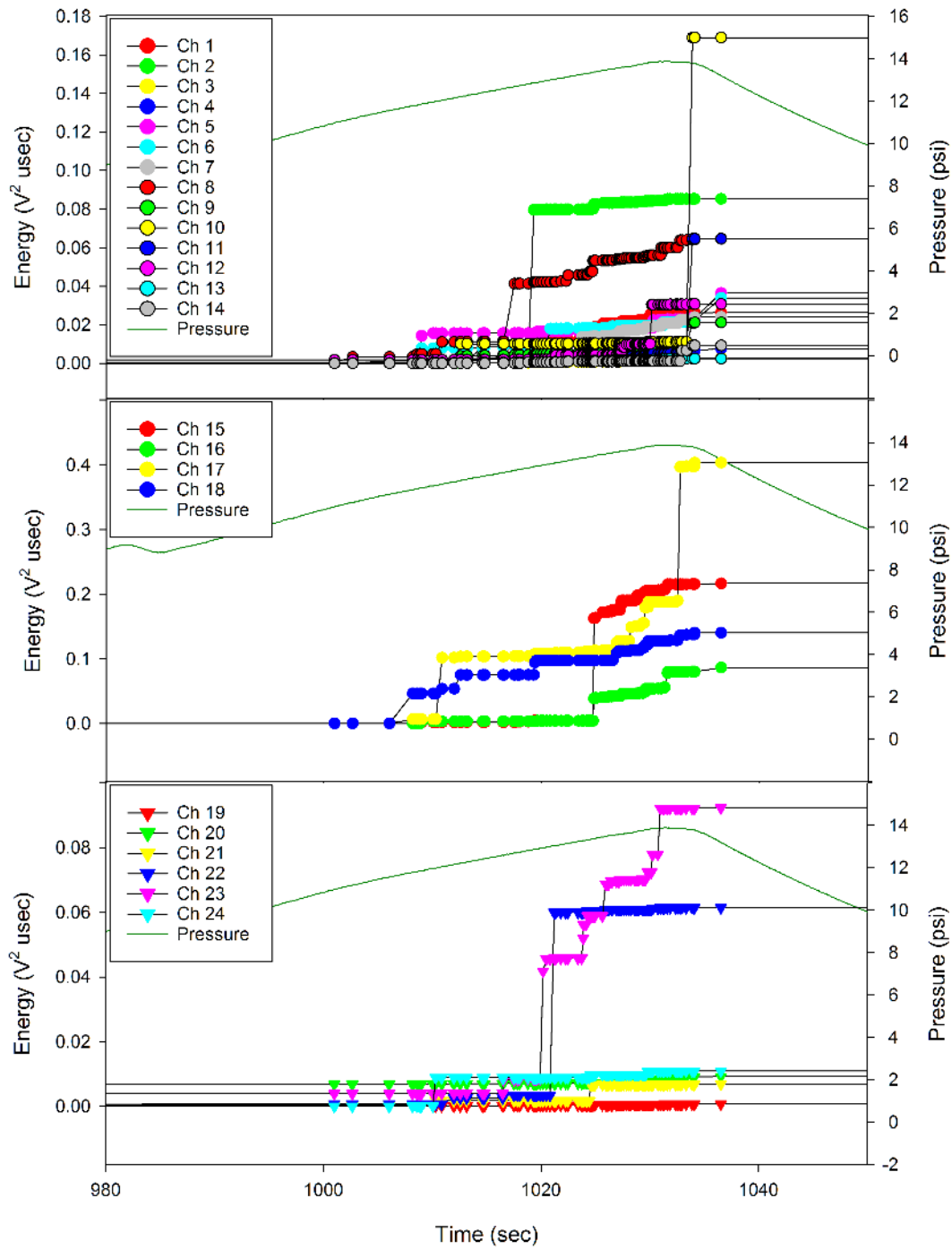


Figure 23. Cumulative Energy: close view. Phase III: 18.4 psi trial 1. Plot from top: Crown, Bulkheads, and Keel.

4.3.7 Pressure 18.4 psi (2P) Trial 2

As seen in [Figure 24](#), this second attempt is successful at reaching the target pressure. The peak cumulative energy in decreasing steps of approximately a factor-of-three are the bulkheads followed by the crown and then the keel. Of the crown, aft edge sensors 7, 8, and forward edge sensors 1 and 6 have the highest cumulative energy. A large energy event occurs near sensor 6 just after unloading starts.

The steadily-occurring AE starts around 11 psi with significant energy increases starting around 14 psi. In comparison to the unprecedented pressure of 14 psi in Trial 1 of this test scheme and using the 11 psi start pressure, the Felicity Ratio is approximately 0.8. This is evidence of increasing damage accumulation.

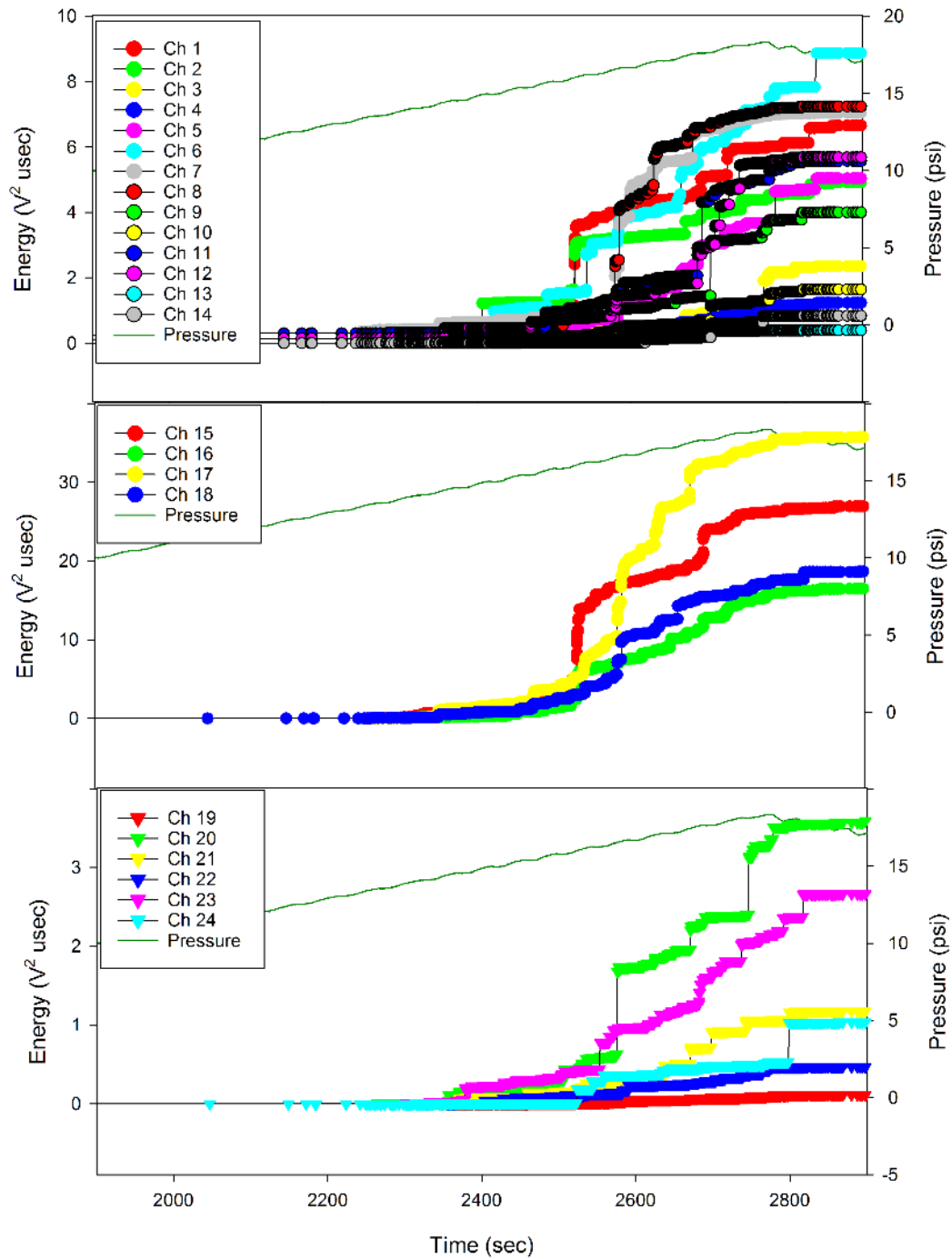


Figure 24. Cumulative Energy: close view. Phase III: 18.4 psi trial 2. Plot from top: Crown, Bulkheads, and Keel.

4.4 Phase IV Post-Impact Checkout Tests

4.4.1 All tests (Nominally same loading as in Phase I)

This is the first series of tests after the planned impacts to the keel and the bulkheads. The impact energies were sufficient to generate fractures and even penetrated the skin on the keel. Unfortunately, no sensors were located near the bulkhead impacts.

The load levels of these tests are equivalent to the first set of checkout tests and are much lower than the Phase II and III pre-impact series of tests. The AE from Phase III (DUL) indicated significant damage accumulation. With significant damage accumulation, it is possible that AE would occur at the low load levels applied in this phase, making it more difficult to distinguish test-damage AE from AE of the impact regions under load. If the impacts did affect AE generation in the global structural load carrying sense, the sensors closest to the impact locations (on the keel) would be expected to have large energy AE events. This was not the case, so the AE that occurred in this series is likely due to the damage accumulated before the impacts.

Figure 25 shows the test that is last in this series of checkout tests: 79.5 kips up-bending plus 4.6 psi. It is the test with the combination of the highest load and pressure producing the largest number of events in this checkout series. However, over this entire series, there were less than 40 events in total, so this test will be the only one presented here. The small number of events indicates that further damage accumulation at or below the peak loads in this series, would probably be very limited and slow.

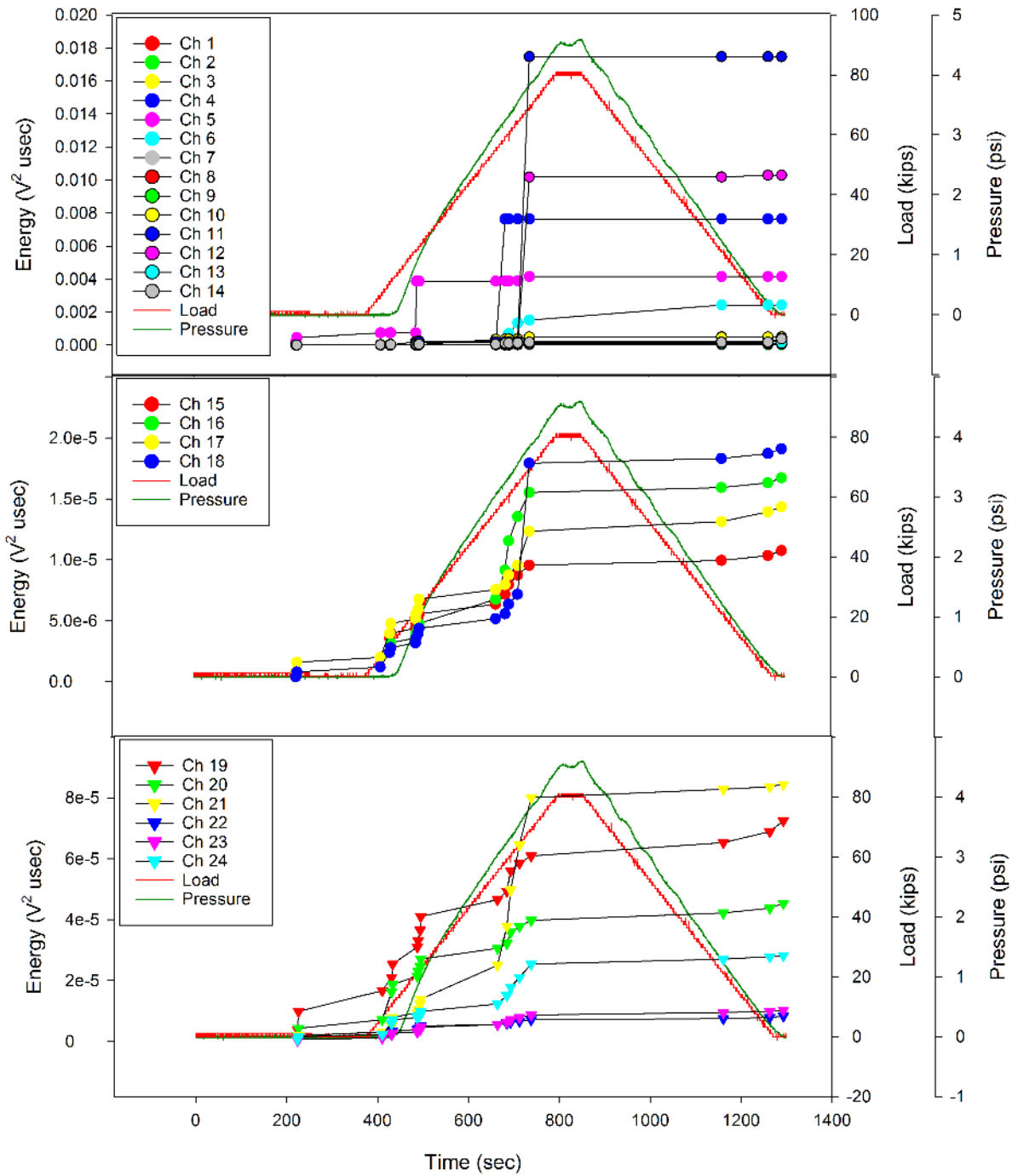


Figure 25. Cumulative Energy: close view. Phase IV: 79.5 kips up-bending + 4.6 psi. Plot from top: Crown, Bulkheads, and Keel.

4.5 Phase V Post-Impact DLL Tests

This is the series of post-impact tests with combinations of load cases similar to those in Phase II. Intervening tests went to higher loads, and the AE from them indicated that significant damage accumulation occurred, so there is limited value in discussing these tests in detail.

4.5.1 Down-bending 63.6 kips (-1.0g)

As seen in **Figure 26**, there is much less AE in this test compared to the pre-impact counterpart in Phase II. Therefore, considering the Kaiser Effect, the fact that AE exists at all, indicates damage accumulation from the previous tests. That damage was extensive since the AE started early in the loading and continues well into the unloading.

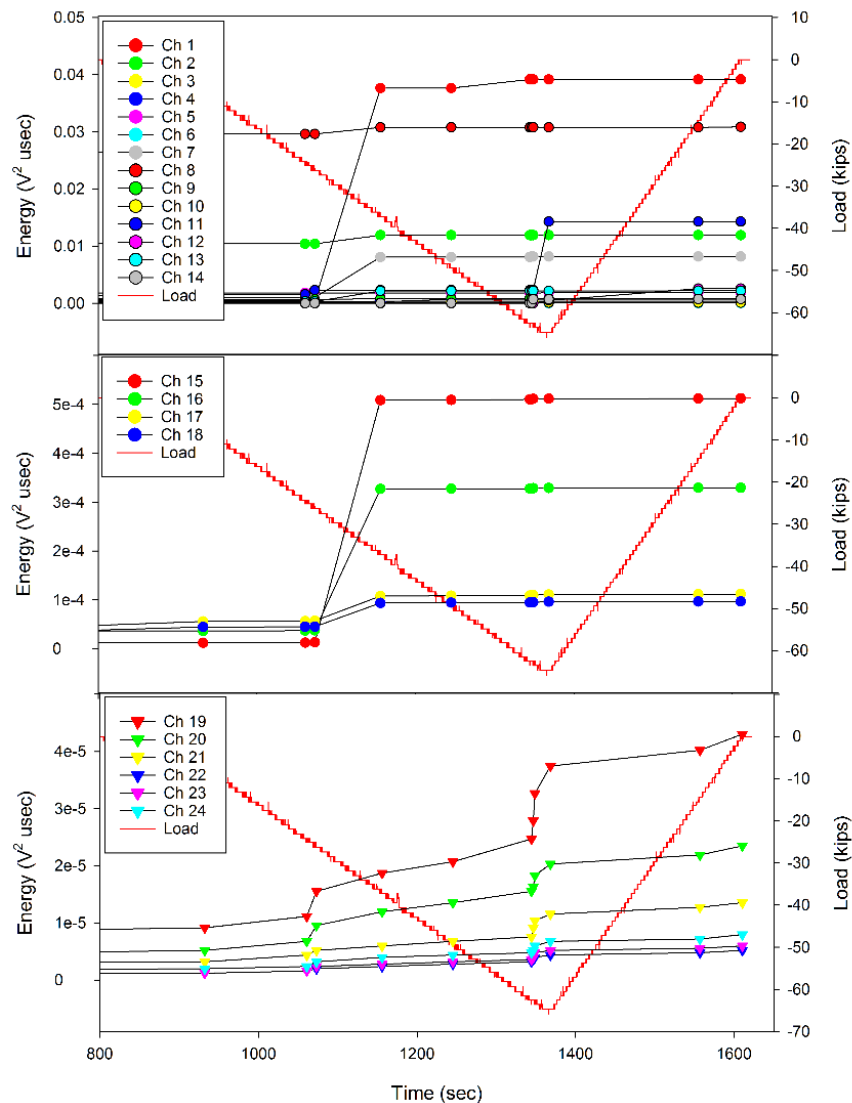


Figure 26. Cumulative Energy: close view. Phase V: 63.6 kips down-bend. Plot from top: Crown, Bulkheads, and Keel.

4.5.2 Down-bending 63.6 kips and Pressure 9.2 psi (-1.0g + 1.0P)

Again, as seen in [Figure 27](#), the fact that AE exists at all, particularly since approximately half the events occur during unloading, does indicate previous damage accumulation.

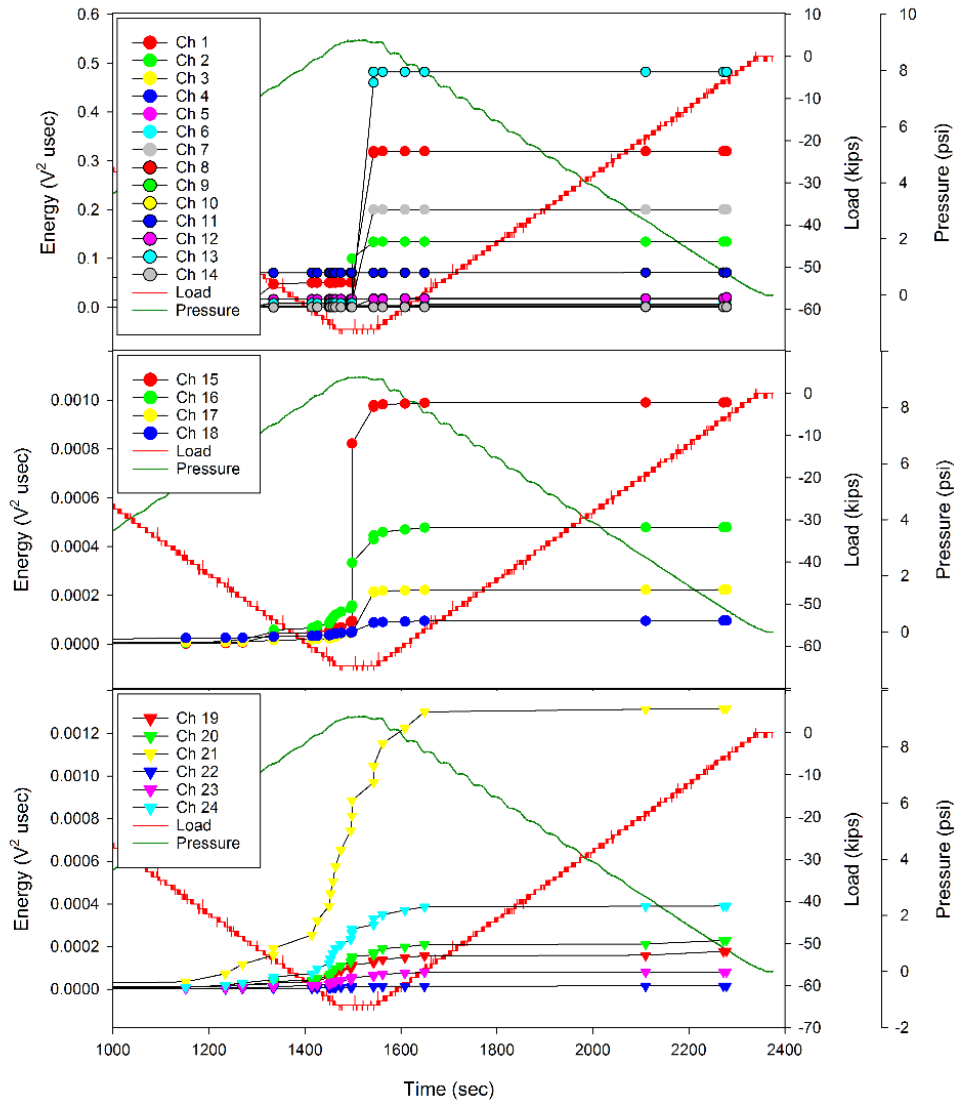


Figure 27. Cumulative Energy: close view. Phase V: 63.6 kips down-bend + 9.2 psi. Plot from top: Crown, Bulkheads, and Keel.

4.5.3 Pressure 12.2 psi (1.33P)

Again, as seen in [Figure 28](#), AE starts at low loads on loading and ends at low loads on unloading. This indicates previous significant damage accumulation.

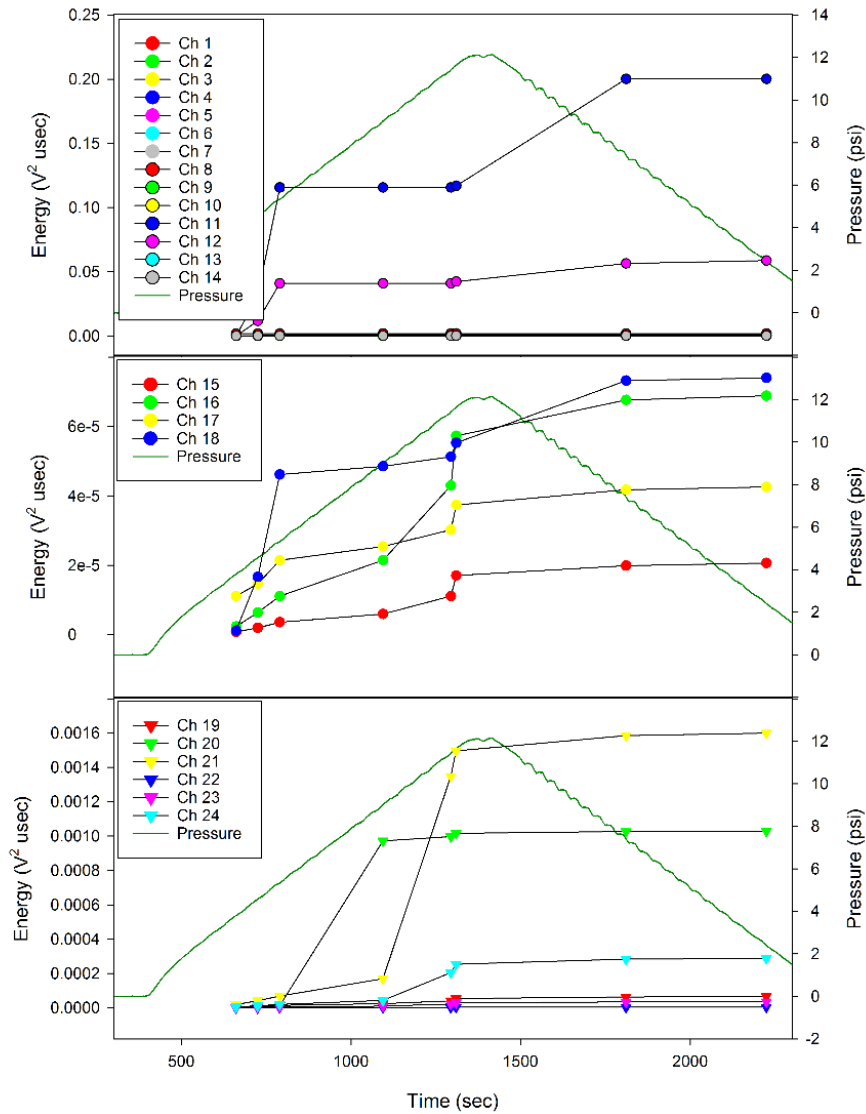


Figure 28. Cumulative Energy: close view. Phase V: 12.2 psi. Plot from top: Crown, Bulkheads, and Keel.

4.5.4 Up-bending 159 kips (2.5g)

Again, as seen in [Figure 29](#), AE starts at low loads on loading and ends at low loads on unloading. This indicates previous significant damage accumulation.

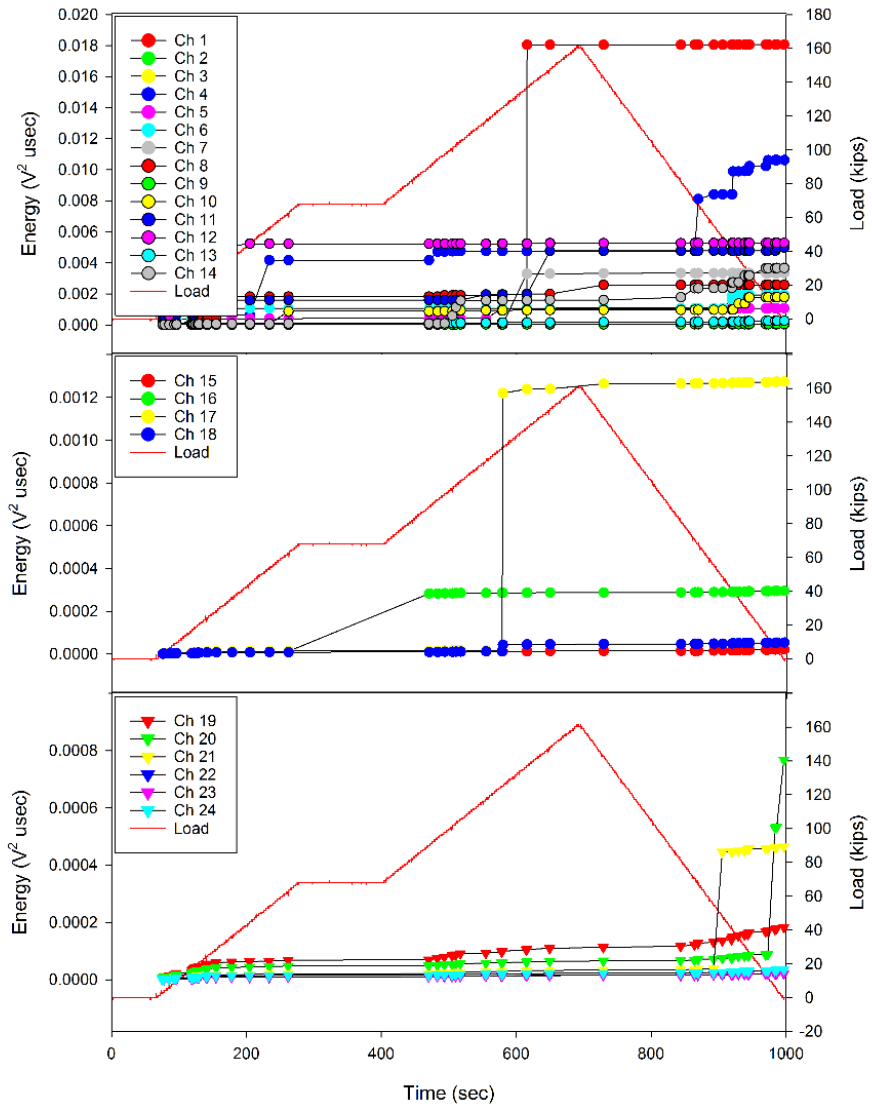


Figure 29. Cumulative Energy: close view. Phase V: 159 kips up-bend. Plot from top: Crown, Bulkheads, and Keel.

4.5.5 Up-bending 159 kips and Pressure 9.2 psi (2.5g + 1.0P)

Again, as seen in **Figure 30**, AE starts at low loads on loading and ends at low loads on unloading. This indicates previous significant damage accumulation.

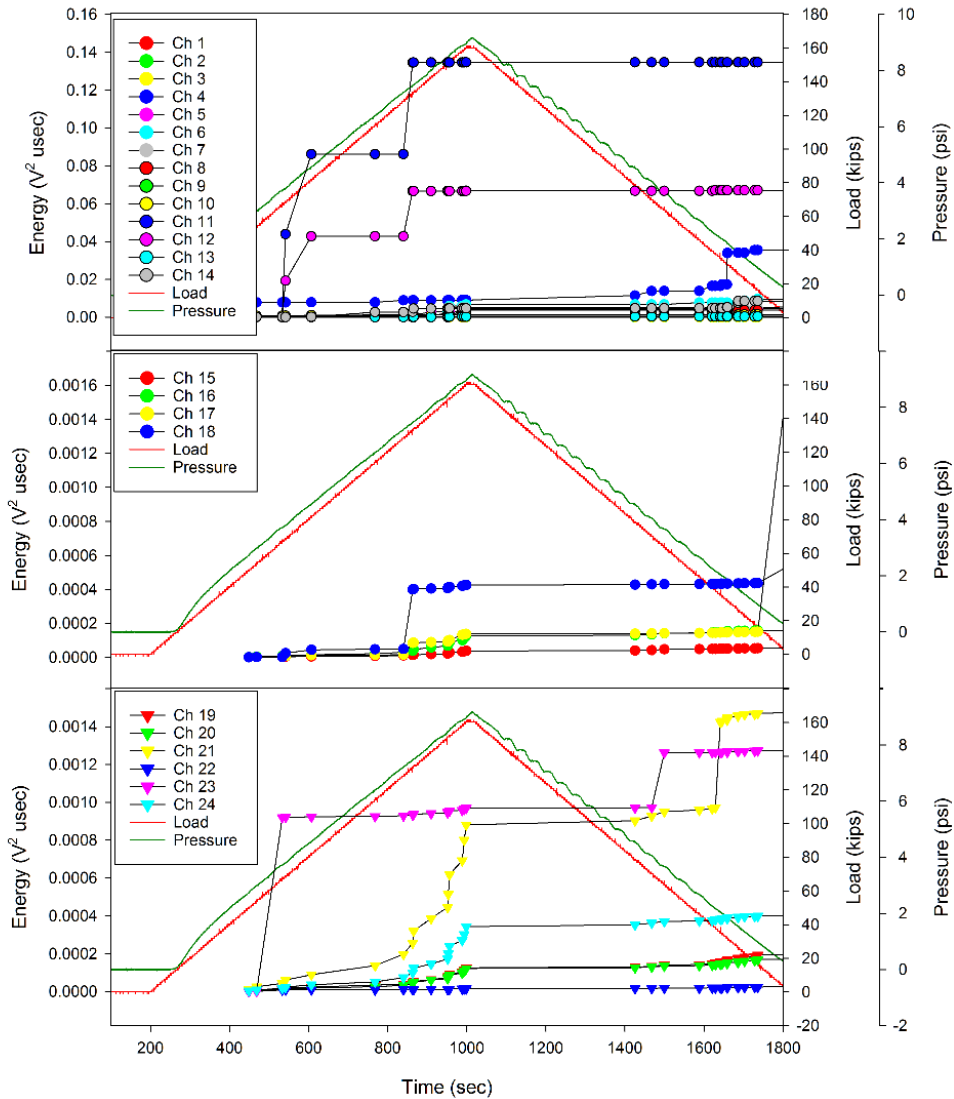


Figure 30. Cumulative Energy: close view. Phase V: 159 kips up-bend + 9.2 psi. Plot from top: Crown, Bulkheads, and Keel.

4.6 Phase VI Post-Impact DUL Tests

This is the series of post-impact tests with similar combinations of load cases to those in Phase III.

4.6.1 Down-bending 95.4 kips (-1.5g)

Again, as seen in **Figure 31**, AE starts at low loads on loading (approximately 10% of the peak) and ends at low loads on unloading. This indicates previous significant damage accumulation.

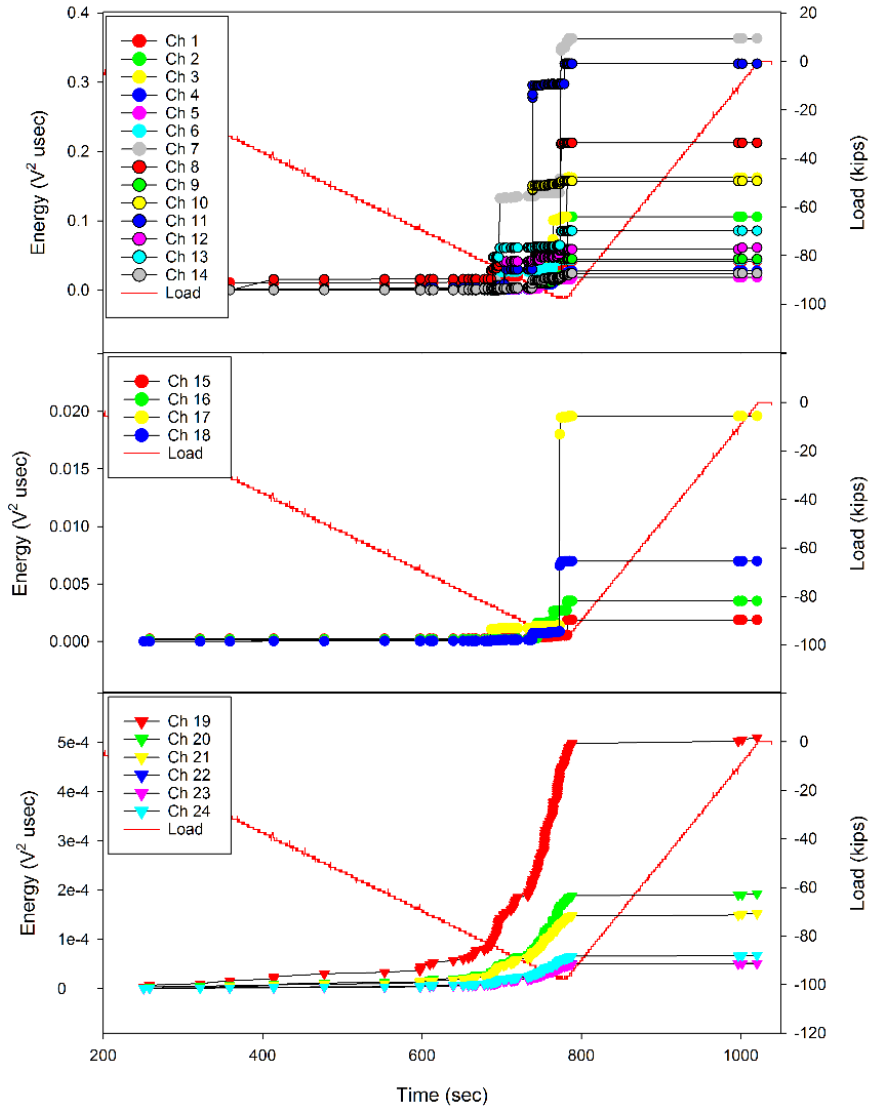


Figure 31. Cumulative Energy: close view. Phase VI: 95.4 kips down-bend. Plot from top: Crown, Bulkheads, and Keel.

4.6.2 Down-bending 95.4 kips and Pressure 13.8 psi (-1.5g + 1.5P) Trial 1, 2, and 3

Loads reached approximately 65 kips and 8.5 psi for the first trial. Lower loads and pressures for the second and third trial generated only 30 events for all three, so no plots are presented.

4.6.3 Down-bending 95.4 kips and Pressure 13.8 psi (-1.5g + 1.5P) Trial 4

Again, as seen in [Figure 32](#), AE starts at moderate loads on loading (approximately 75% of the peak loads) and ends at zero load after unloading. This indicates previous significant damage accumulation.

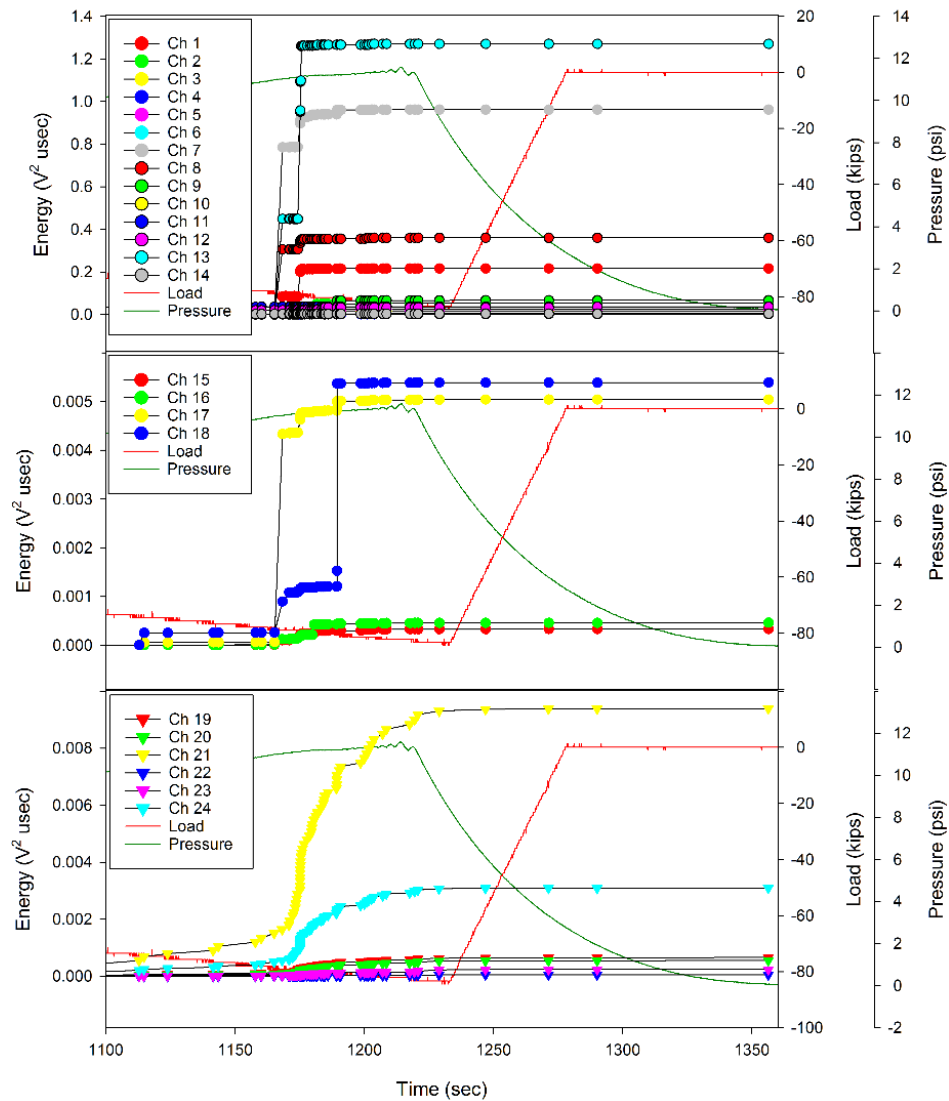


Figure 32. Cumulative Energy: close view. Phase VI: 95.4 kips down-bend + 13.8 psi trial 4. From top: Crown, Bulkheads, and Keel.

4.6.4 Down-bending 95.4 kips and Pressure 13.8 psi (-1.5g + 1.5P) Trial 5

Again, as seen in [Figure 33](#), AE starts at low loads on loading (approximately 30% of peak loads) and ends at zero load on unloading. This indicates previous significant damage accumulation.

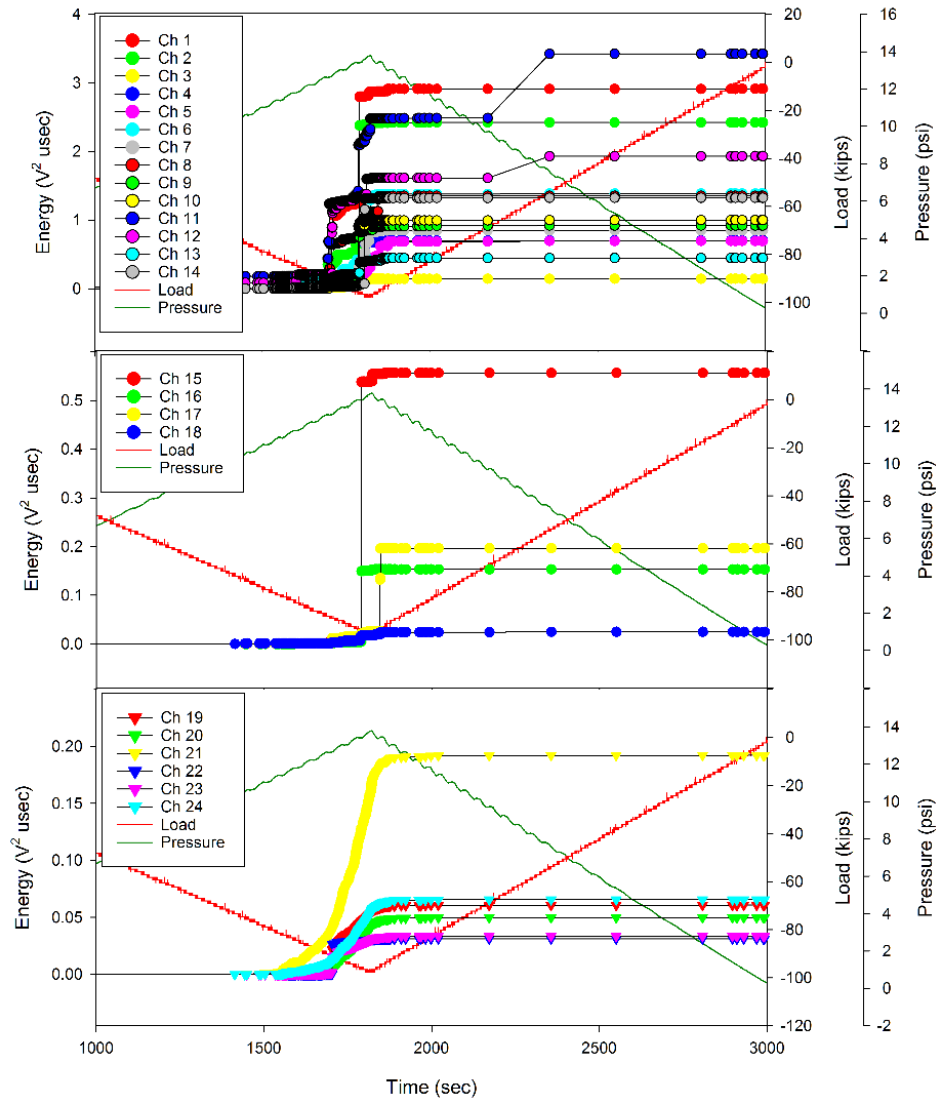


Figure 33. Cumulative Energy: close view. Phase VI: 95.4 kips down-bend + 13.8 psi trial 5. From top: Crown, Bulkheads, and Keel.

4.6.5 Pressure 18.4 psi (2P)

Again, as seen in [Figure 34](#), AE starts at low loads on loading (approximately 25% of peak load) and ends at zero load on unloading. This indicates previous significant damage accumulation.

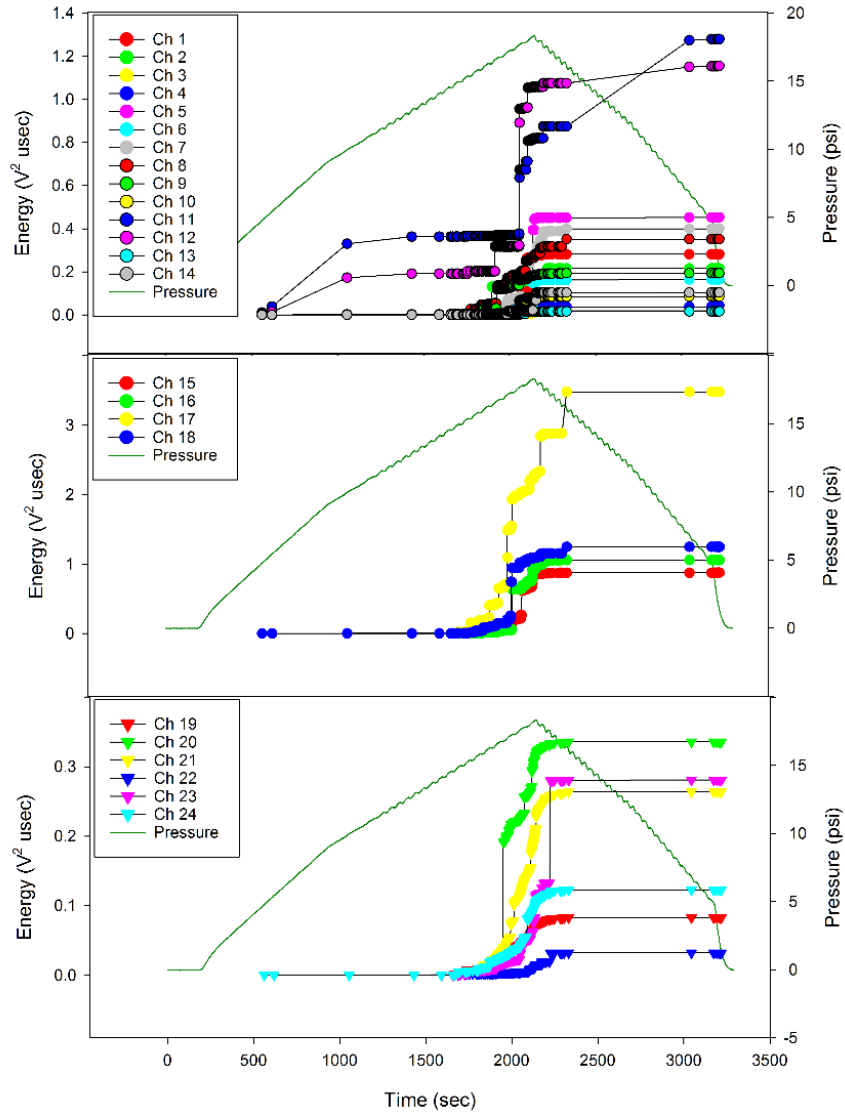


Figure 34. Cumulative Energy: close view. Phase VI: 18.4 psi. Plot from top: Crown, Bulkheads, and Keel.

4.6.6 Up-bending 238.5 kips (3.75g)

As seen in [Figure 35](#), AE starts at near zero load and ends at zero load on unloading. This indicates previous significant damage accumulation. However, distinguishing features are the large energy increases at the crown sensor 6. This evidence combined with the number of previous tests where sensor 6 had significant energy increases, indicates significant structural weakness that existed prior to the weakness introduced by the sawcut.

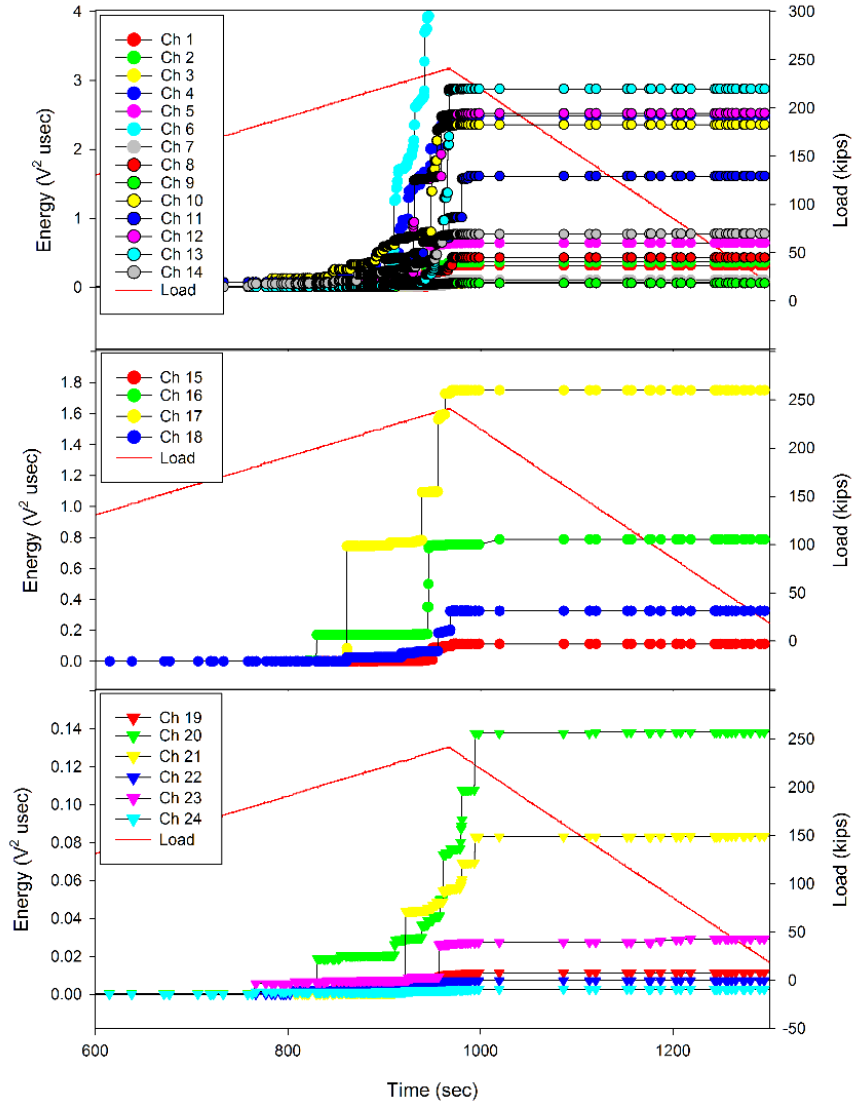


Figure 35. Cumulative Energy: close view. Phase VI: 238.5 kips up-bend. Plot from top: Crown, Bulkheads, and Keel.

4.7 Phase VII Post-Impact Combined Loads Failure Test

This was to be a single test of combined loads where up-bending and pressure were to be varied independently as indicated in [Figures G-1, G-2, and G-3](#) in the appendices.

4.7.1 Trial 1-3

Several restarts occurred with virtually no loading occurring. No AE occurred and no data was saved.

4.7.2 Trial 4

The first portion of the test with an up-bending peak and a pressure hold (nominally 262.4 kips and 13.8 psi) as seen in [Figure 36](#), applies an unprecedented load and a pressure equal to previous unprecedented pressure. At points in the structure where the internal stresses resulting from each of the load and pressure constructively add, the resultant stress can be unprecedented. For the second portion of the test as seen in [Figure 37](#), the load had been previously dropped and held at 238.5 kips and the pressure was removed. The up-bending load was increased back to nominally 262.4 kips before returning to zero.

AE started at very low pressure and up-bending load with significant increases at approximately 200 kips and 11 psi. As seen in [Figure 36](#), activity was most energetic during the pressure hold, which included the peak up-bending load. AE peak cumulative energies are approximately the same order of magnitude for the crown, bulkheads, and keel. The highest are on the crown. The keel is approximately half that of the crown and the bulkheads approximately half of the keel. The AE event rate remained high during the up-bending load hold and while the pressure is returned to zero. However, the events are low energy events after the unloading beginning at approximately 2000 seconds (the peak load 262.4 kips and 13.8 psi). The highest crown sensors in order of decreasing energy are 6, 12 and 5, then 14 and 11. All of these sensors are in or near the buckle failure regions in the upcoming post-sawcut test.

Two periods have rapid increases in cumulative energy. The first, seen in [Figure 36](#), occurs from approximately 1500 to 2000 seconds (210-262.4 kips and 11.5-13.8 psi), during most of the first pressure hold and ramp to the first load peak. The second occurs between approximately 3800 and 3900 seconds (240-262 kips and 0 psi) during the ramp up to the second load peak, as seen in [Figure 37](#). The high AE rates during holds and unloading indicate rapid continuing damage accumulation.

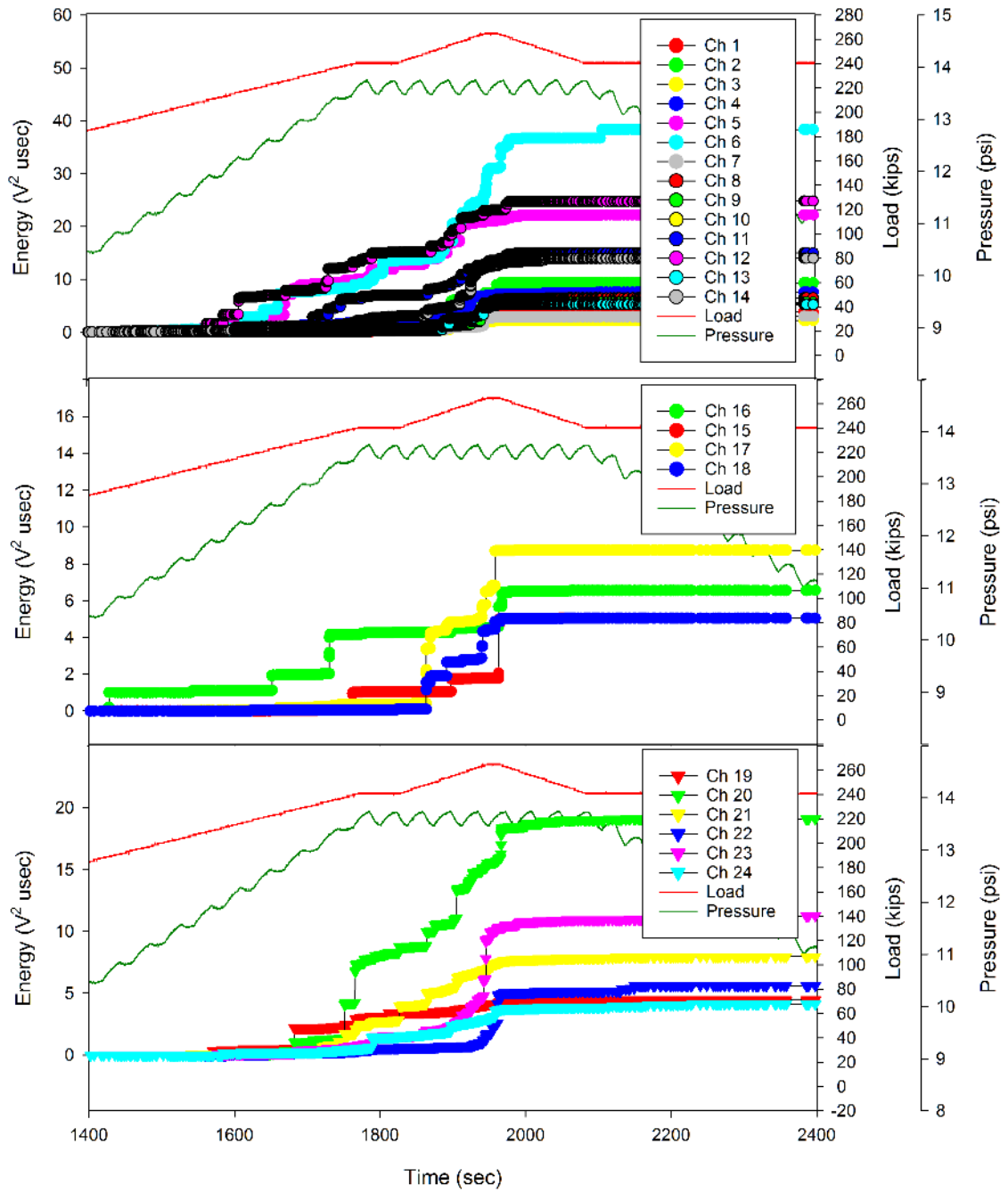


Figure 36. Cumulative Energy: close view. Phase VII: First load and pressure peak. Plot from top: Crown, Bulkheads, and Keel.

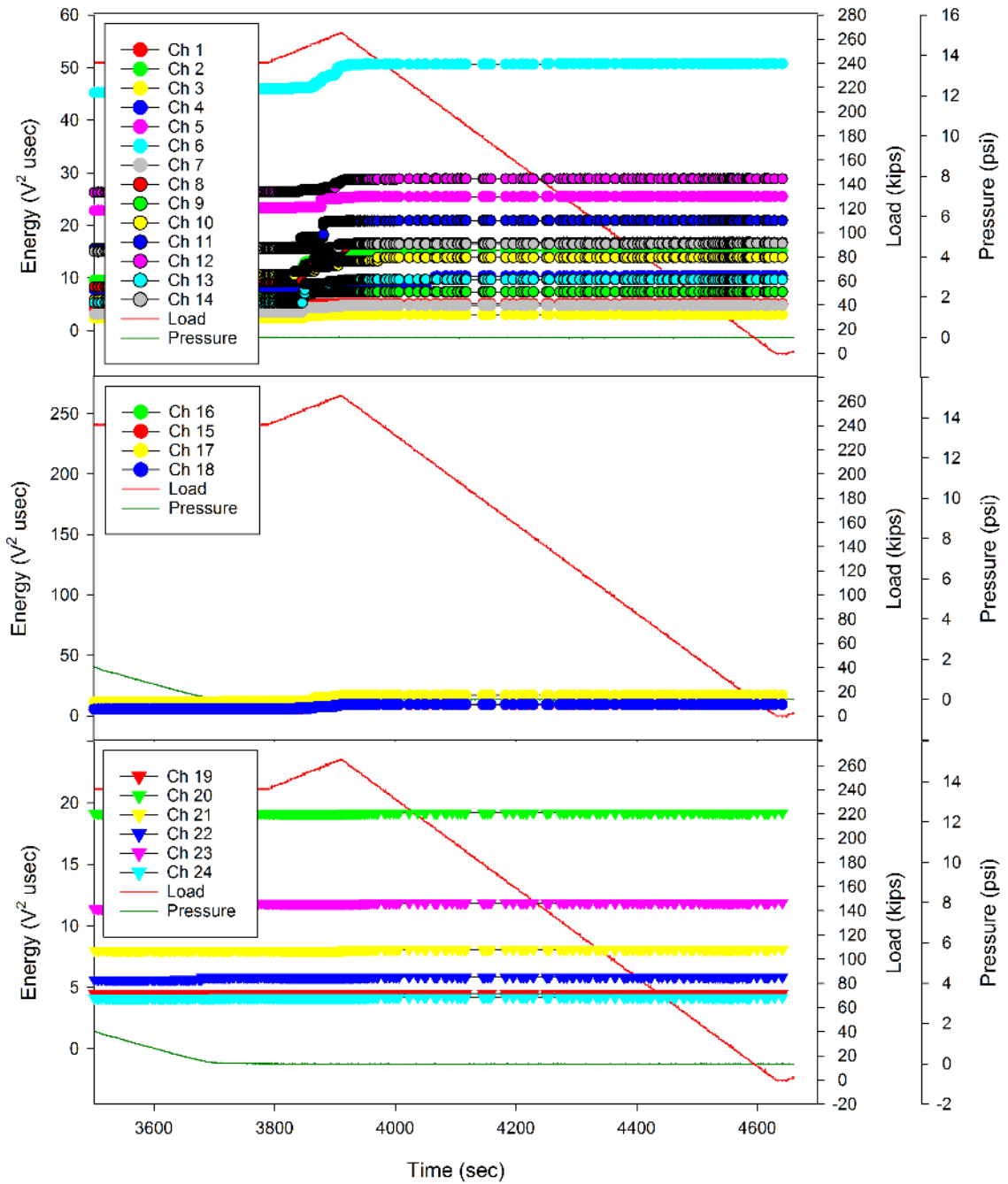


Figure 37. Cumulative Energy: close view. Phase VII: Second load peak, zero pressure. Plot from top: Crown, Bulkheads, and Keel.

4.8 Phase VIII Post-Sawcut Up-bending Failure Test

The frame in the middle of the crown running parallel to the bulkheads was completely severed at the midline prior to this test. This is represented by the black elongated diamond shape between sensors 6 and 12 in [Figure 3](#). During the test an up-bending load was applied until shear buckling failure occurred in the crown and bulkheads.

4.8.1 Trial 1-3

The first three trials were stopped at approximately 33, 31, and 5.5 kips respectively. These peak loads were between 2% and 15% of the previous unprecedented up-bending-only test (Phase VI post impact DUL) and no AE was generated. The previous unprecedented up-bending-only test had AE starting at only a few percent of peak load. The fact that two of these tests went higher than a few percent of previous peak load without generating AE indicates the remaining integrity of the structure. It could be suggested that the sawcut actually redistributed load carrying through less damaged regions than in the previous tests.

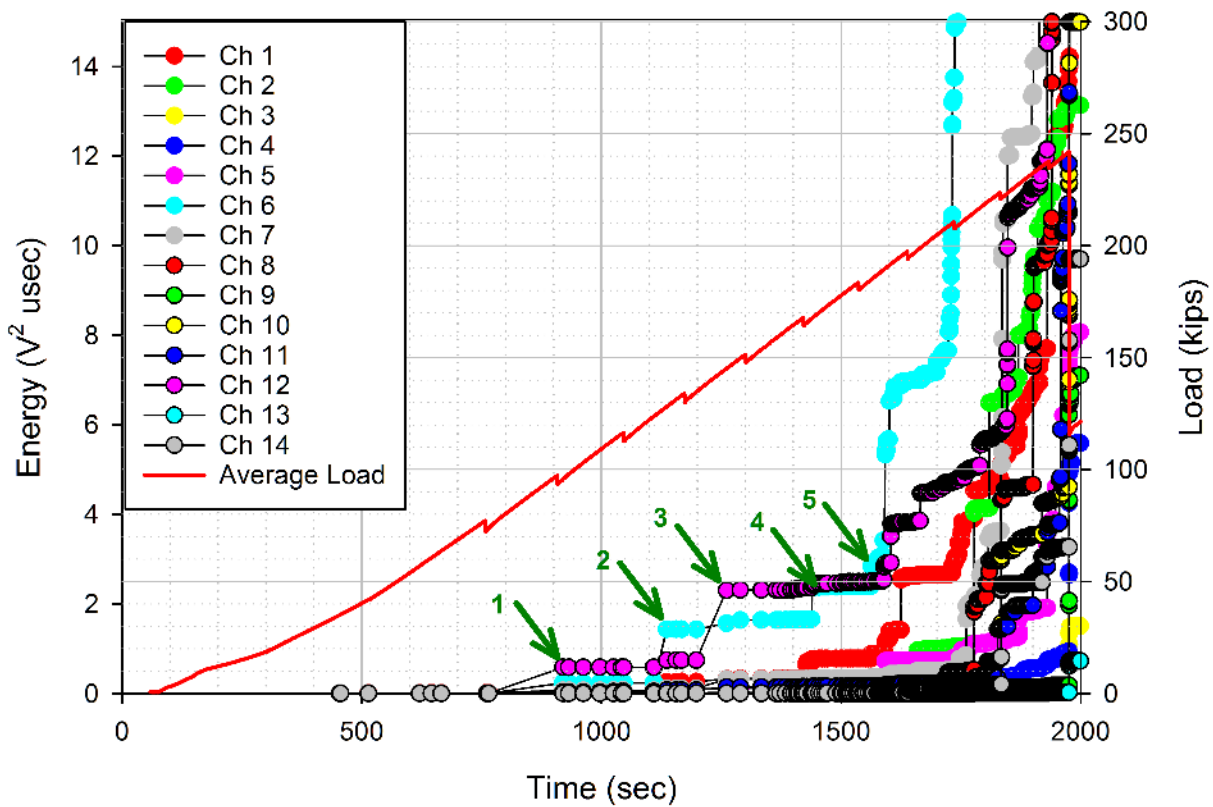


Figure 38. Cumulative Energy: close view. Post-sawcut Up-bend: low energy portion of crown channels before load drop.

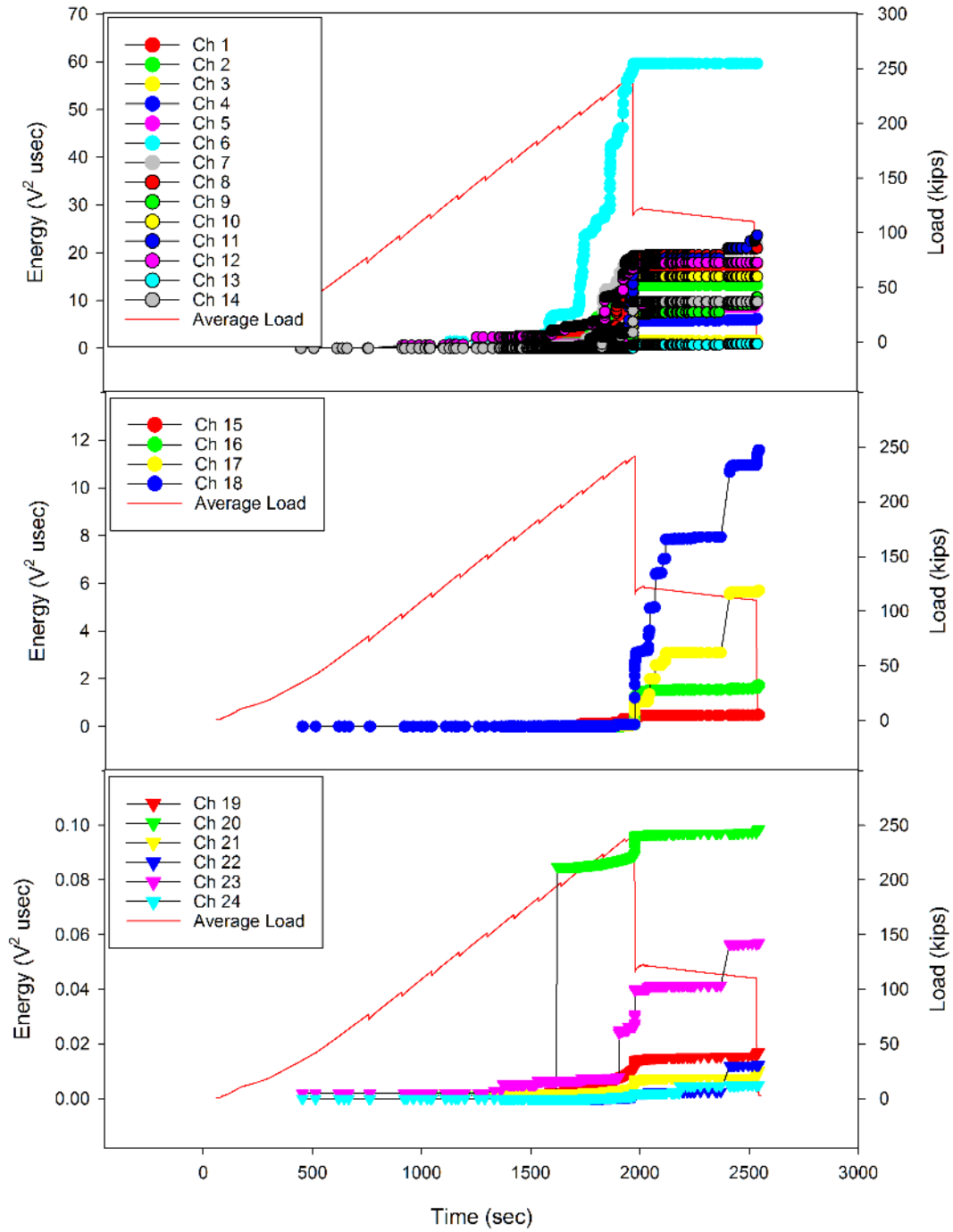


Figure 39. Cumulative Energy: Post-sawcut Up-bend. Plot from top: Crown, Bulkheads, and Keel.

4.8.2 Trial 4 Up-bending to Failure

It should be noted that for this test the cumulative energy is plotted against average load. This is the average of the four load cells at the loading platen. They should have been nominally equal but were not.

Highly localized damage started at tips of the diamond shaped sawcut early in the test at approximately 100 kips and continued during the entire test. As shown in [Figure 38](#), between approximately 100 and 200 kips the damage progression switches back and forth from tip to tip as indicated by the energy jumps at sensors 6 and 12 (located near the sawcut tips) pointed to by the green arrows numbered 1-5. The forward bulkhead tip damage accumulation (sensor 6) begins to dominate from 220 kips on as seen in [Figure 39](#), possibly reducing stresses along the forward bulkhead-crown edge relative to the aft bulkhead-crown edge.

A large load drop indicated in [Figure 38](#) from just below 250 kip to 115 kip, is likely due to the secondary buckle located toward the loading end contiguous to sensors 4, 10, and 14 (one of the blue shaded regions shown in [Figure 3](#)).

5.0 Summary and Conclusions

- AE indications suggest that the prescribed impact damage which created severe fracture, did not affect the failure of the structure, at least in the prescribed locations. The loading conditions created more critical damage than the impacts.
- There are indications that damage accumulation began during the pre-impact limit load tests.
- The locations of the high-energy AE indications from many of these tests is, in general, comparable to the regions of high tensile stress in the structure.
- No AE seemed to indicate any major design flaws with the structure, at least for the prescribed loading conditions.
- The AE indicated that a significant amount of structural integrity remained after completely severing one of the frames.

6.0 References

- [1] Vicroy, D.D. Jegley D.C., Cosentino G. “NASA Blended-Wing-Body Research Overview”. 67th Annual International Conference on Mass Properties Engineering. Seattle, Washington 2008
- [2] Velicki, A. “Damage Arresting Composites for Shaped Vehicles,” NASA CR-2009-215932, Sept. 2009.
- [3] Przekop, A, et al. AIAA SciTech. 55th AIAA/ASME/ASCE/AHS/SC Structures, Structural Dynamics, and Materials Conference. 13-17 January 2014, National Harbor, Maryland.
- [4] Horne, M. R., Madaras, E.I. (2013). “Evaluation of Acoustic Emission SHM of PRSEUS Composite Pressure Cube Tests”. NASA Technical Memo: NASA/TM–2013-217993.
- [5] Nondestructive Testing Handbook Third Edition Vol. 6 Acoustic Emission Testing. American Society of Nondestructive Testing. 2005
- [6] “Standard Practice for Acoustic Emission Examination of Fiberglass Reinforced Plastic Resin (FRP) Tanks/Vessels”. ASTM E1067/ E1067M-11. American Society for Testing and Materials. 2011
- [7] Article RT-6. Section X. Fiber Reinforced Plastic Pressure Vessels. ASME Boiler and Pressure Vessel Code. American Society of Mechanical Engineers. 2015

Appendix A: Pressure Checkout and Phase 1 Checkout Tests

Table of Figures

Figure A-1. Crown AE Cumulative Energy by Channel: Pre-Phase I, Pressure Checkout, 2 psi.....	A3
Figure A-2. Bulkheads AE Cumulative Energy by Channel: Pre-Phase I, Pressure Checkout, 2 psi.....	A4
Figure A-3. Keel AE Cumulative Energy by Channel: Pre-Phase I, Pressure Checkout, 2 psi.....	A5
Figure A-4. Crown AE Cumulative Energy by Channel: Phase I, 31.8 kips down-bending.....	A6
Figure A-5. Bulkheads AE Cumulative Energy by Channel: Phase I, 31.8 kips down-bending.....	A7
Figure A-6. Keel AE Cumulative Energy by Channel: Phase I, 31.8 kips down-bending.....	A8
Figure A-7. Crown AE Cumulative Energy by Channel: Phase I, 79.5 kips up-bending.....	A9
Figure A-8. Bulkheads AE Cumulative Energy by Channel: Phase I, 79.5 kips up-bending.....	A10
Figure A-9. Keel AE Cumulative Energy by Channel: Phase I, 79.5 kips up-bending.....	A11
Figure A-10. Crown AE Cumulative Energy by Channel: Phase I, 31.8 kips down-bending + 4.6 psi.....	A12
Figure A-11. Bulkheads AE Cumulative Energy by Channel: Phase I, 31.8 kips down-bending + 4.6 psi.....	A13
Figure A-12. Keel AE Cumulative Energy by Channel: Phase I, 31.8 kips down-bending + 4.6 psi.....	A14
Figure A-13. Crown AE Cumulative Energy by Channel: Phase I, 79.5 kips up-bending + 4.6 psi.....	A15
Figure A-14. Bulkheads AE Cumulative Energy by Channel: Phase I, 79.5 kips up-bending + 4.6 psi.....	A16
Figure A-15. Keel AE Cumulative Energy by Channel: Phase I, 79.5 kips up-bending + 4.6 psi.....	A17

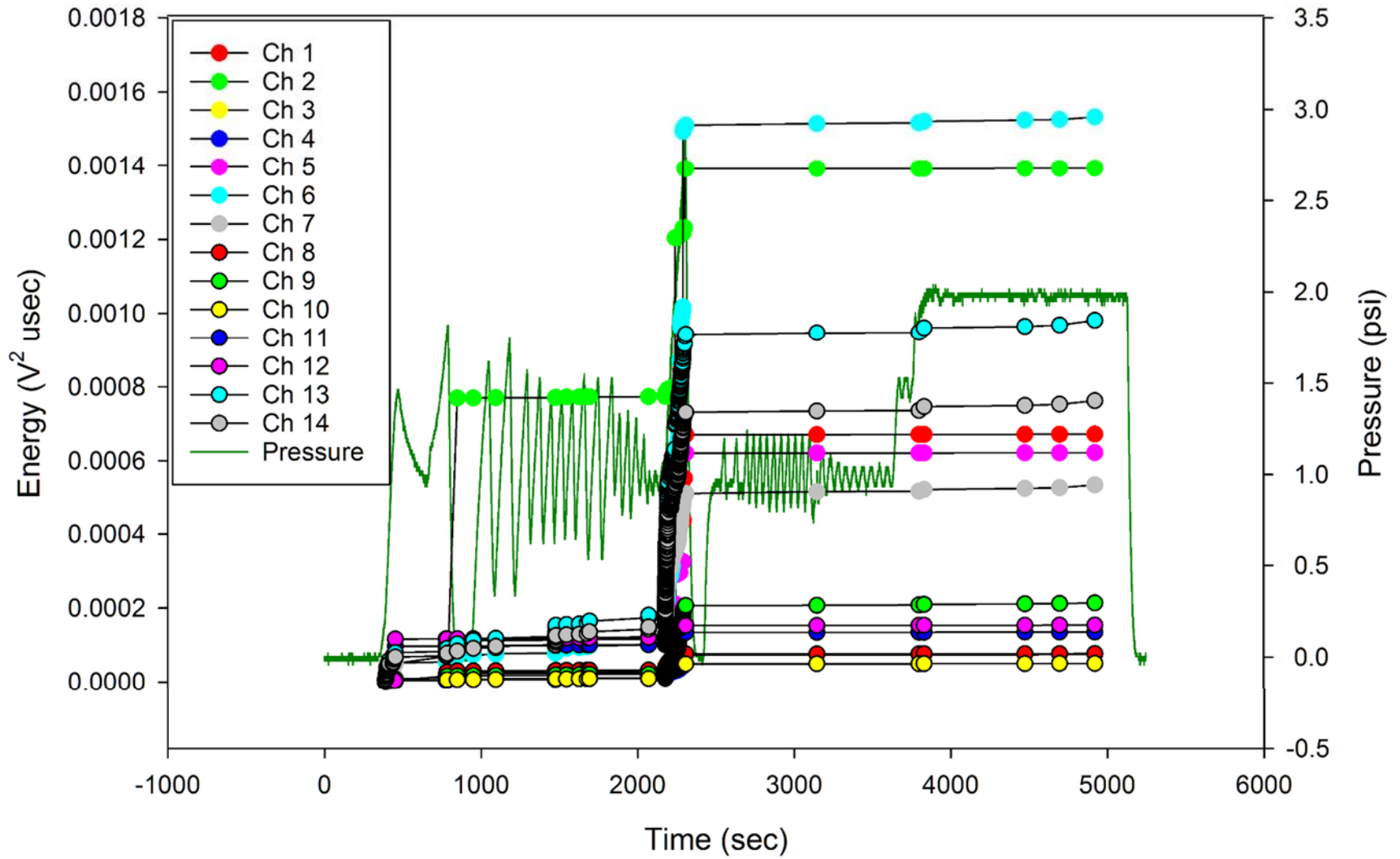


Figure A-1. Crown AE Cumulative Energy by Channel: Pre-Phase I, Pressure Checkout, 2 psi.

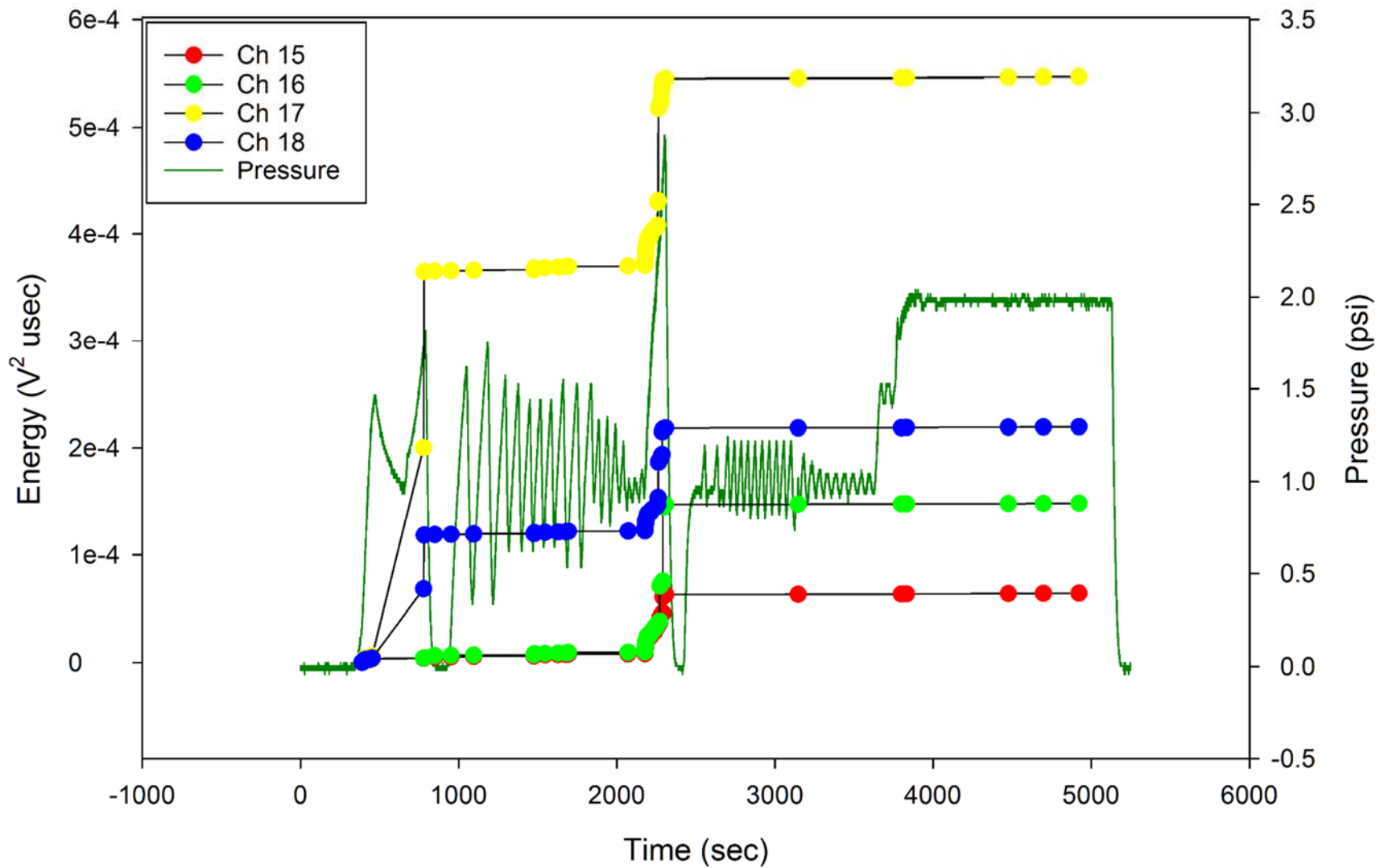


Figure A-2. Bulkheads AE Cumulative Energy by Channel: Pre-Phase I, Pressure Checkout, 2 psi.

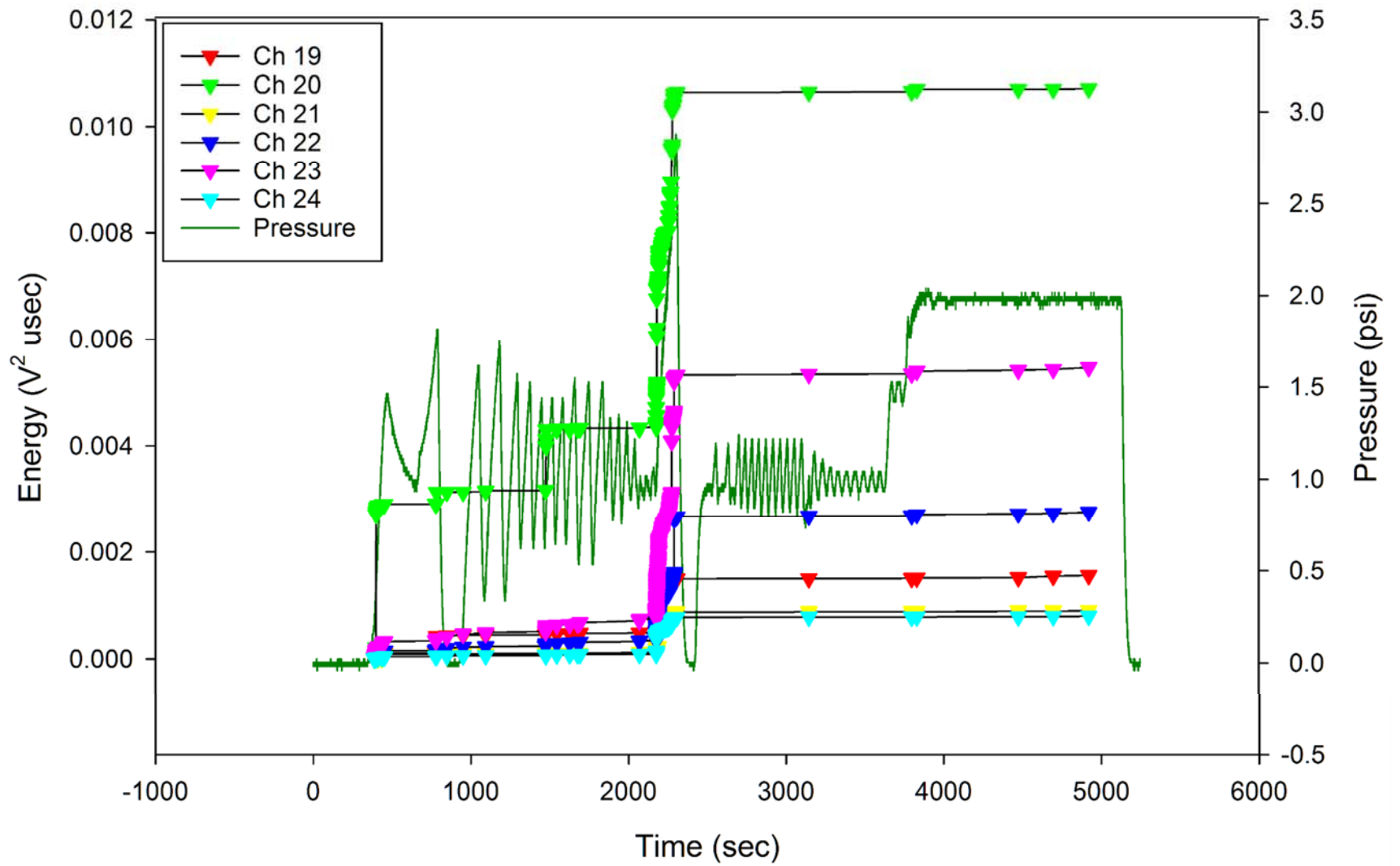


Figure A-3. Keel AE Cumulative Energy by Channel: Pre-Phase I, Pressure Checkout, 2 psi.

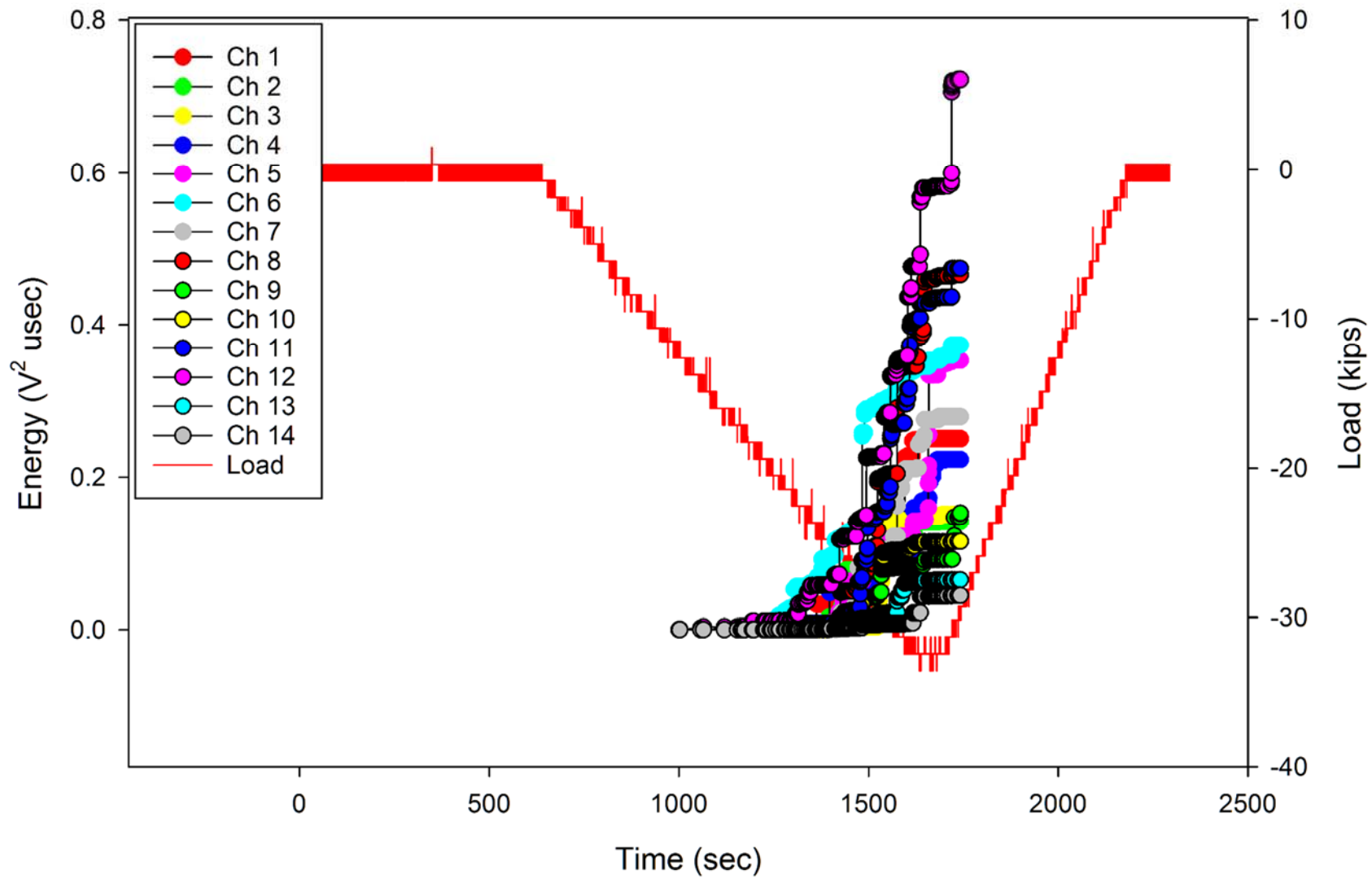


Figure A-4. Crown AE Cumulative Energy by Channel: Phase I, 31.8 kips down-bending.

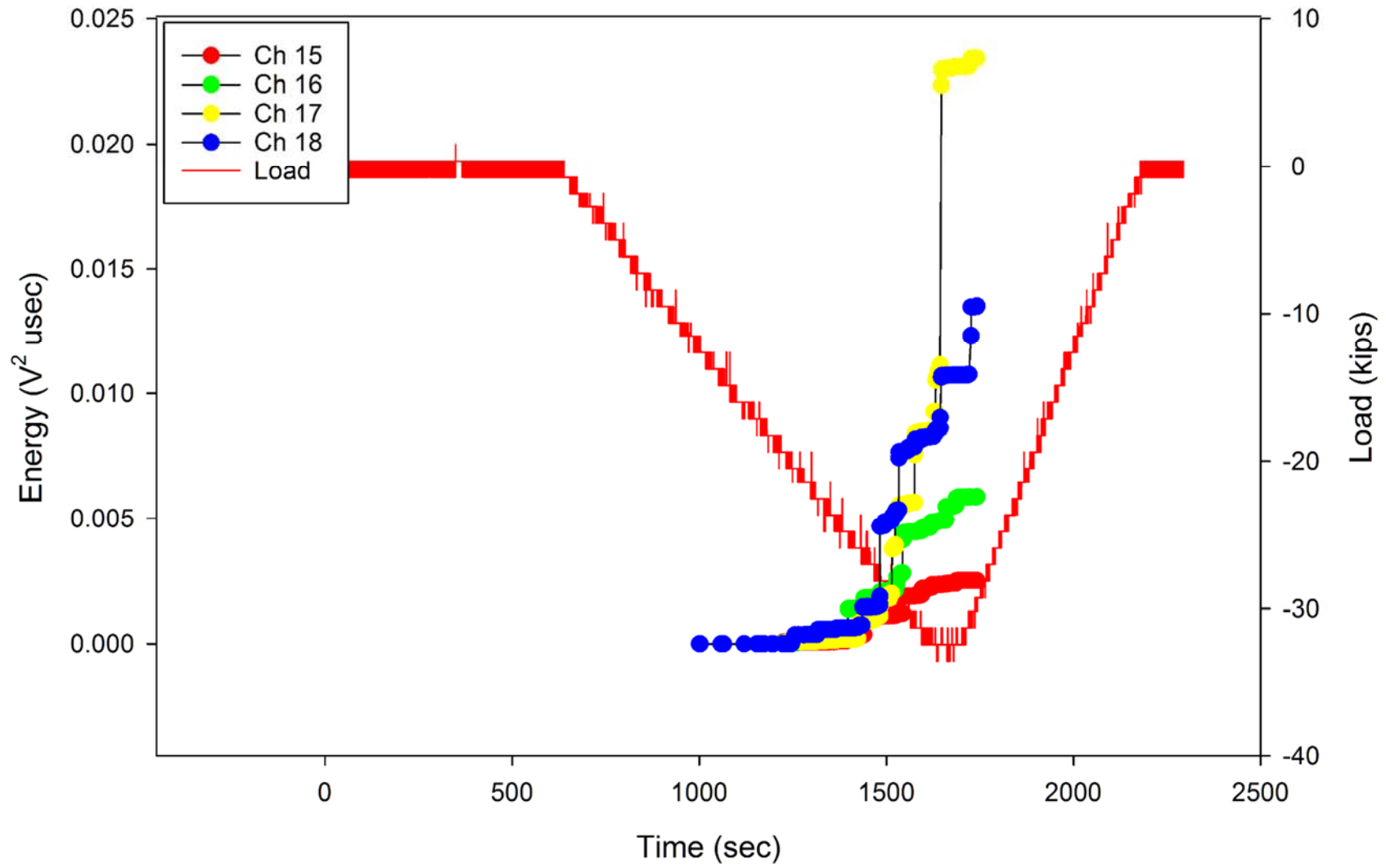


Figure A-5. Bulkheads AE Cumulative Energy by Channel: Phase I, 31.8 kips down-bending.

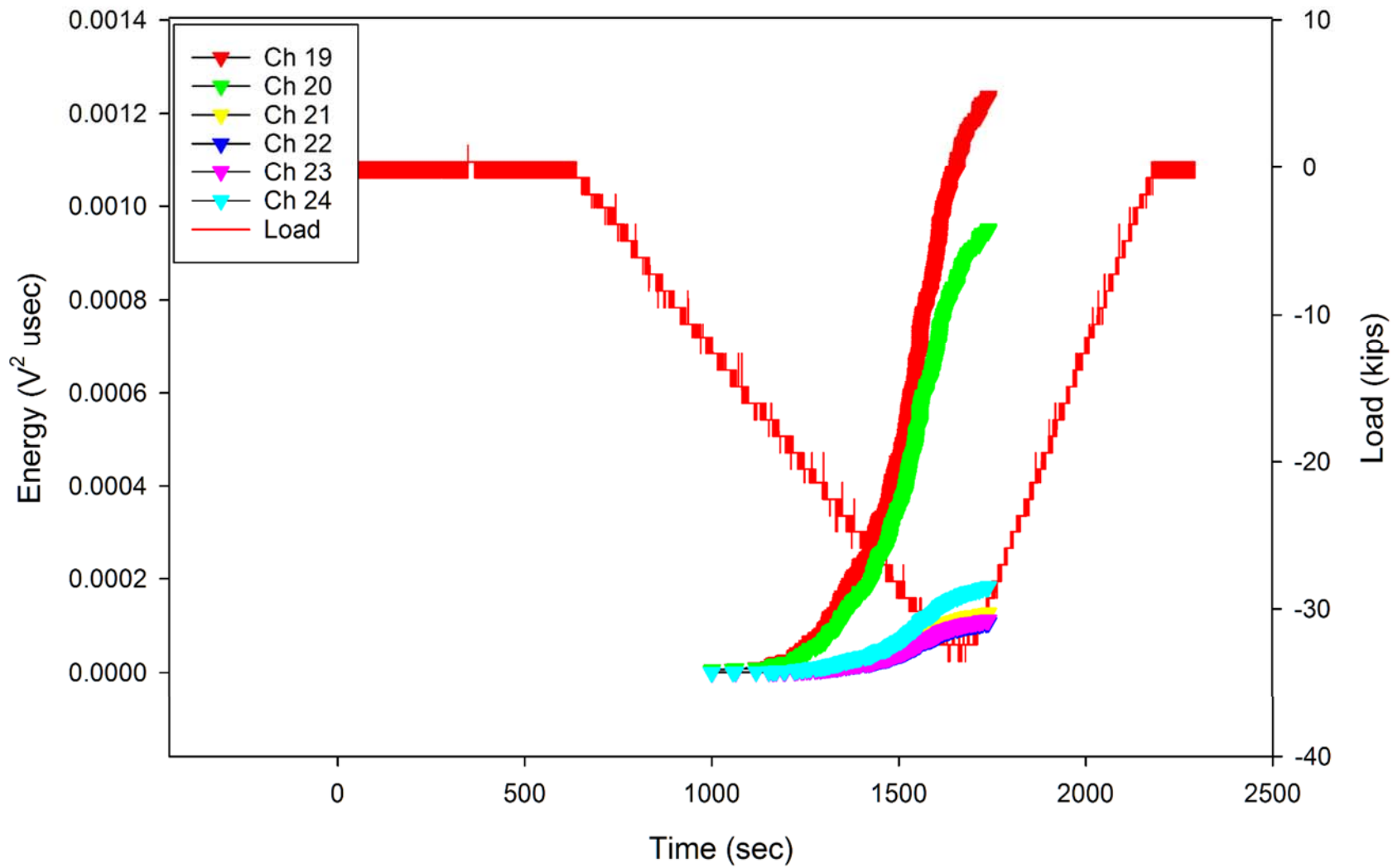


Figure A-6. Keel AE Cumulative Energy by Channel: Phase I, 31.8 kips down-bending.

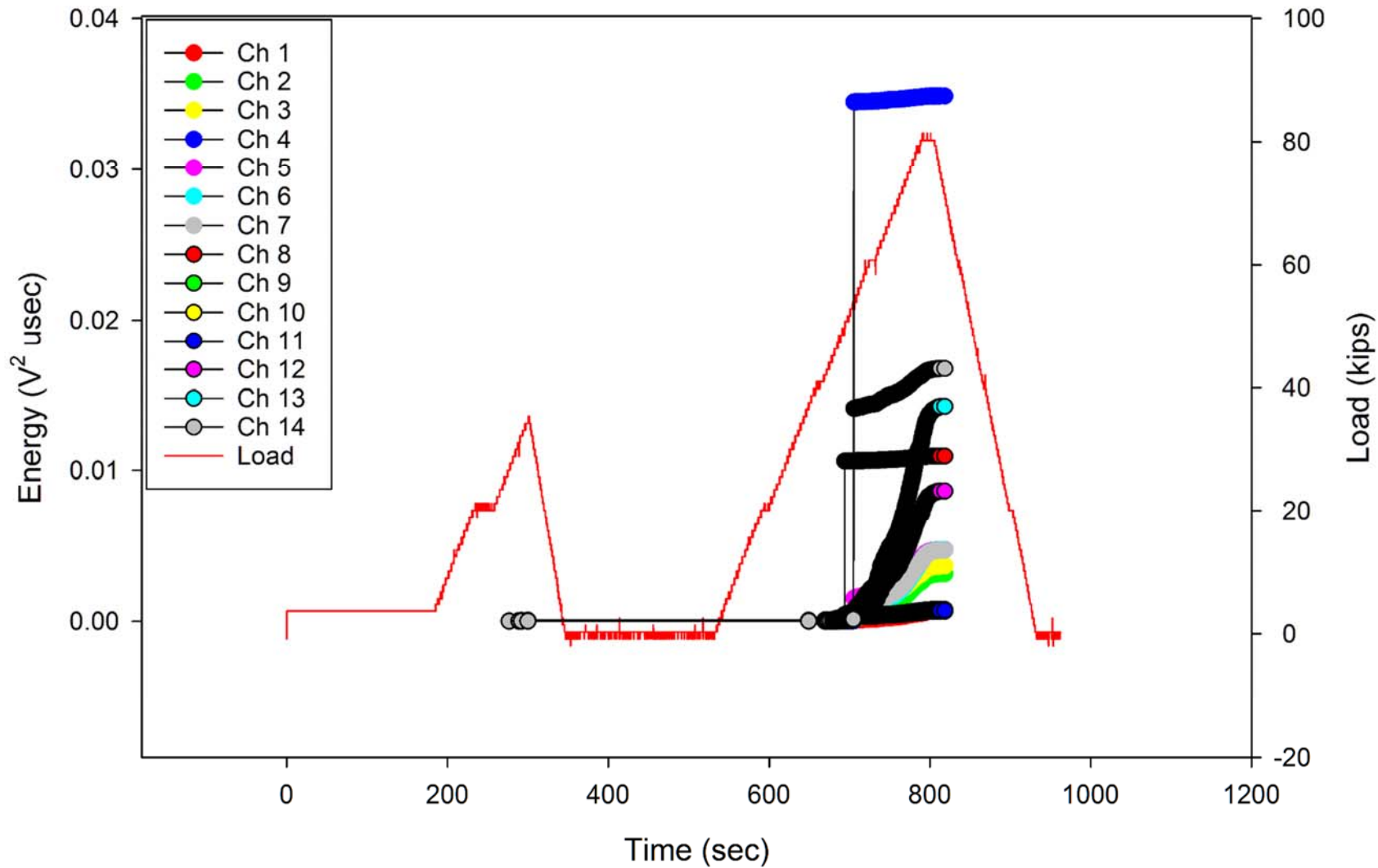


Figure A-7. Crown AE Cumulative Energy by Channel: Phase I, 79.5 kips up-bending.

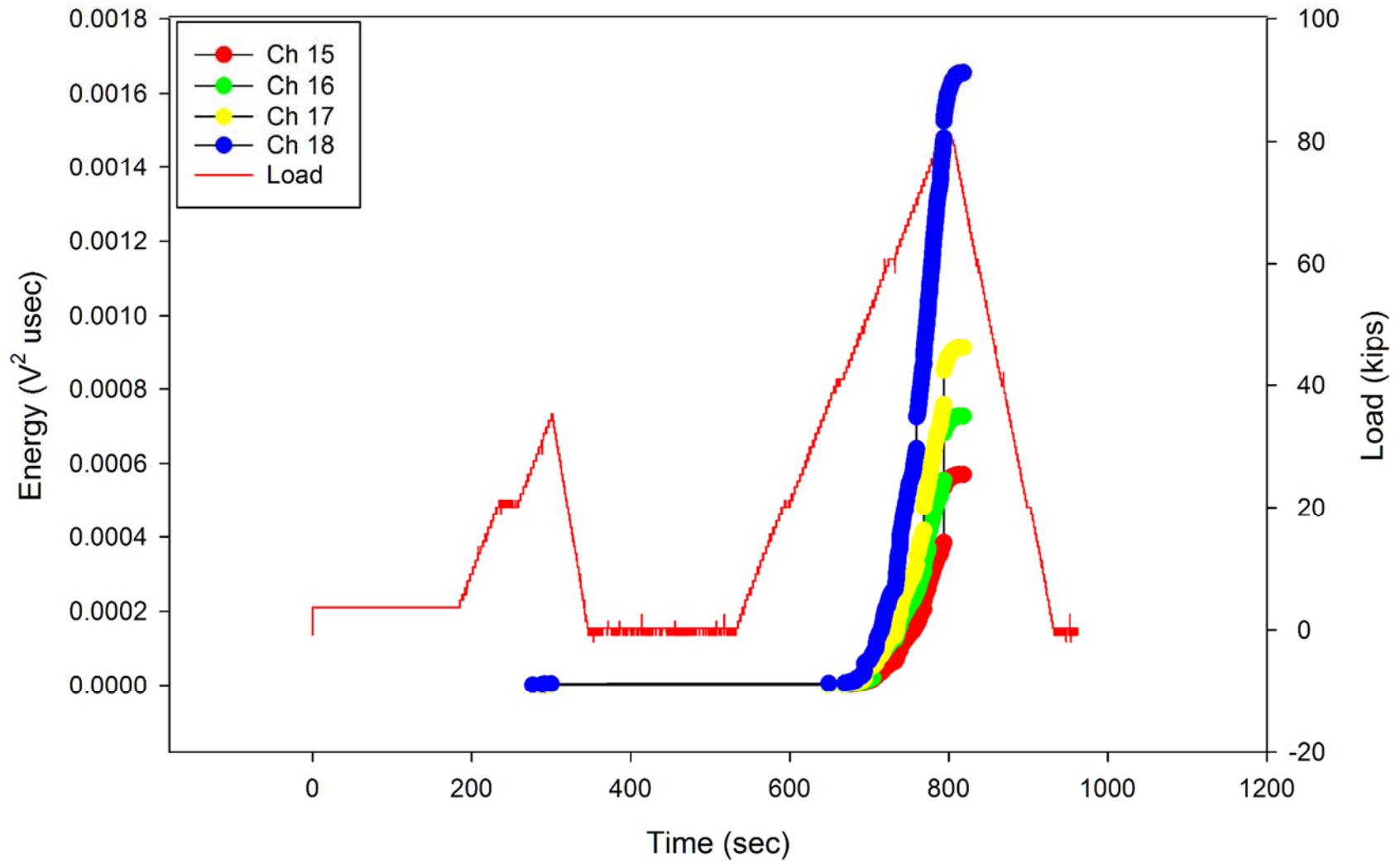


Figure A-8. Bulkheads AE Cumulative Energy by Channel: Phase I, 79.5 kips up-bending.

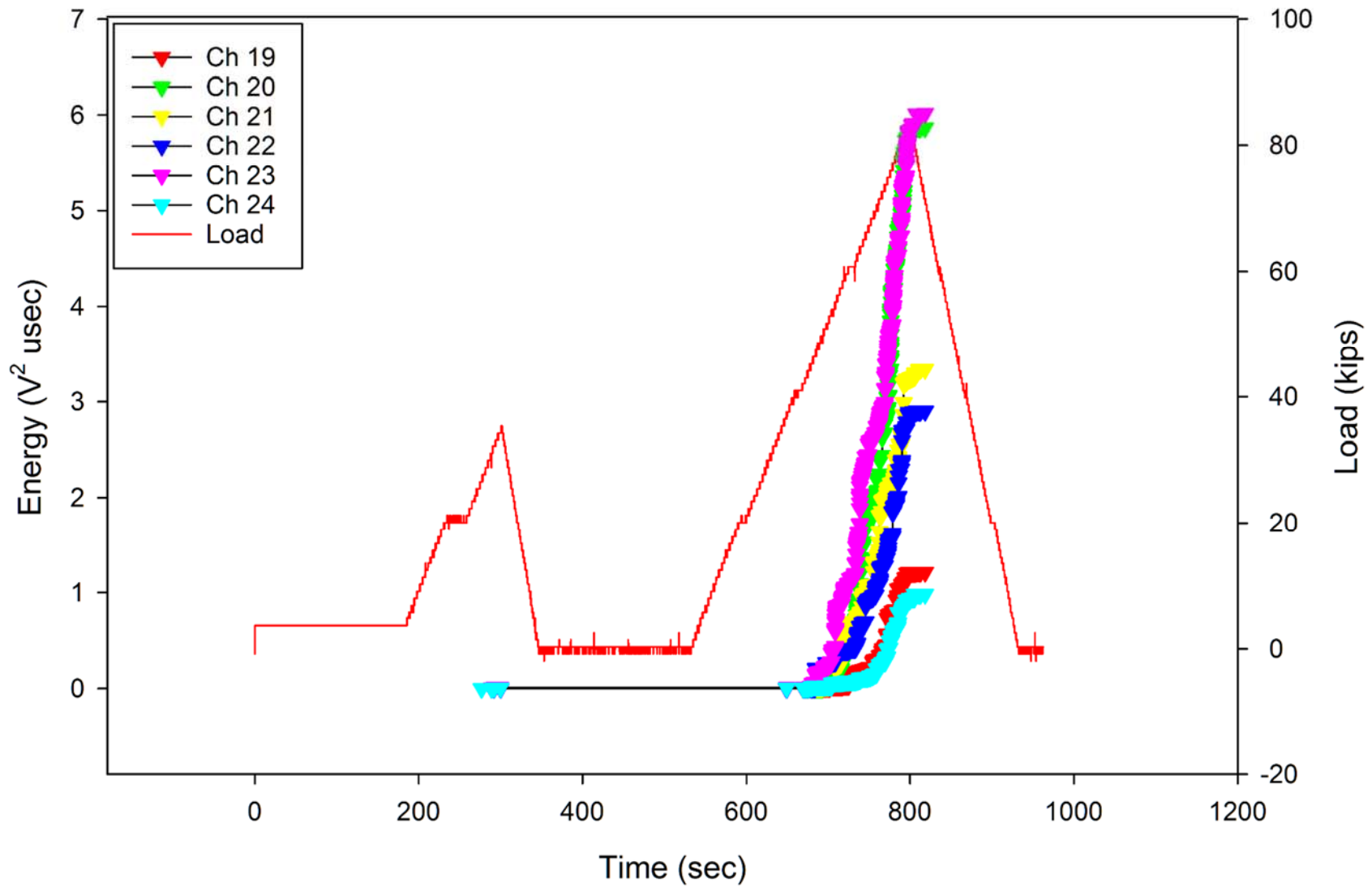


Figure A-9. Keel AE Cumulative Energy by Channel: Phase I, 79.5 kips up-bending.

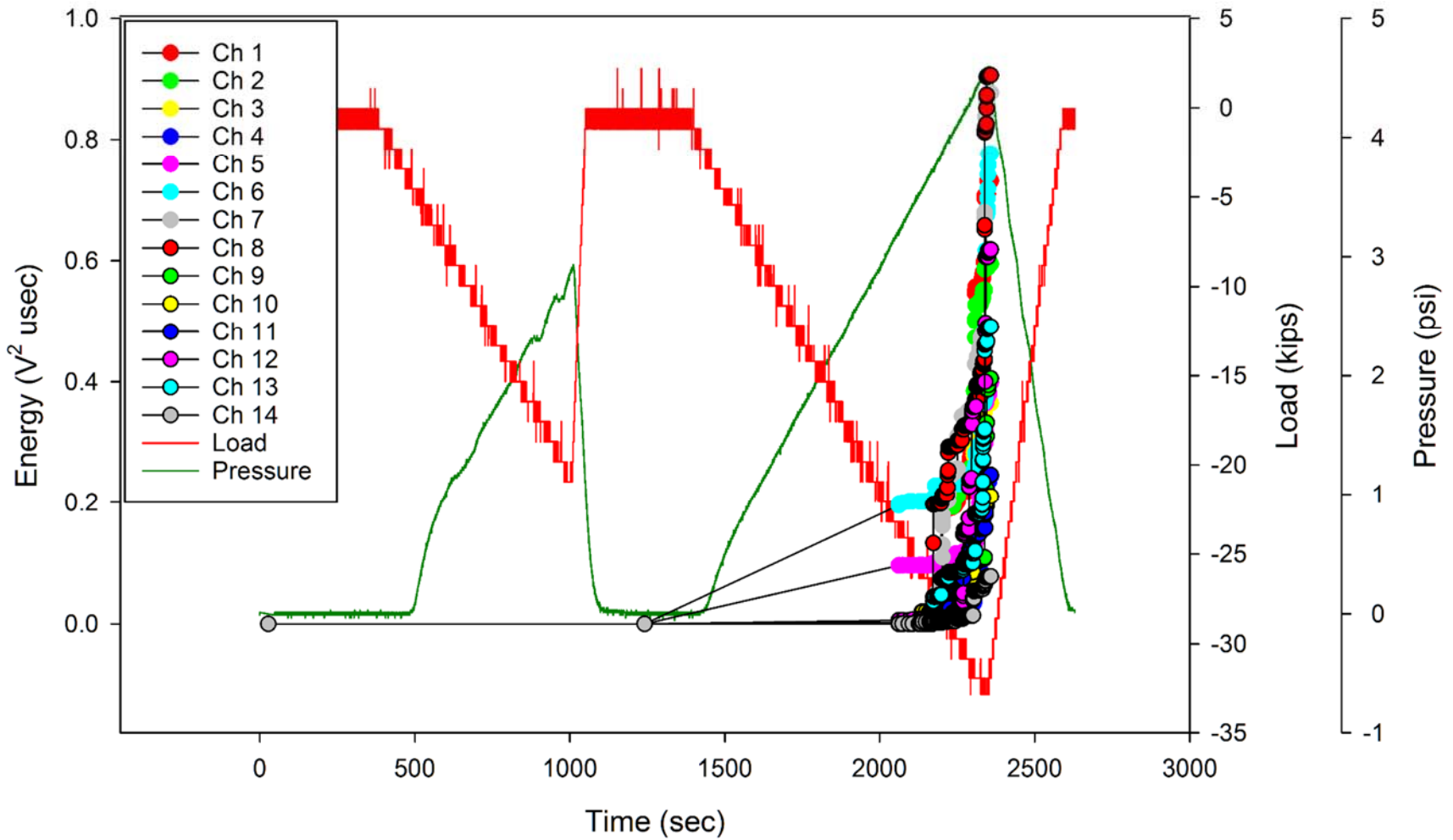


Figure A-10. Crown AE Cumulative Energy by Channel: Phase I, 31.8 kips down-bending + 4.6 psi.

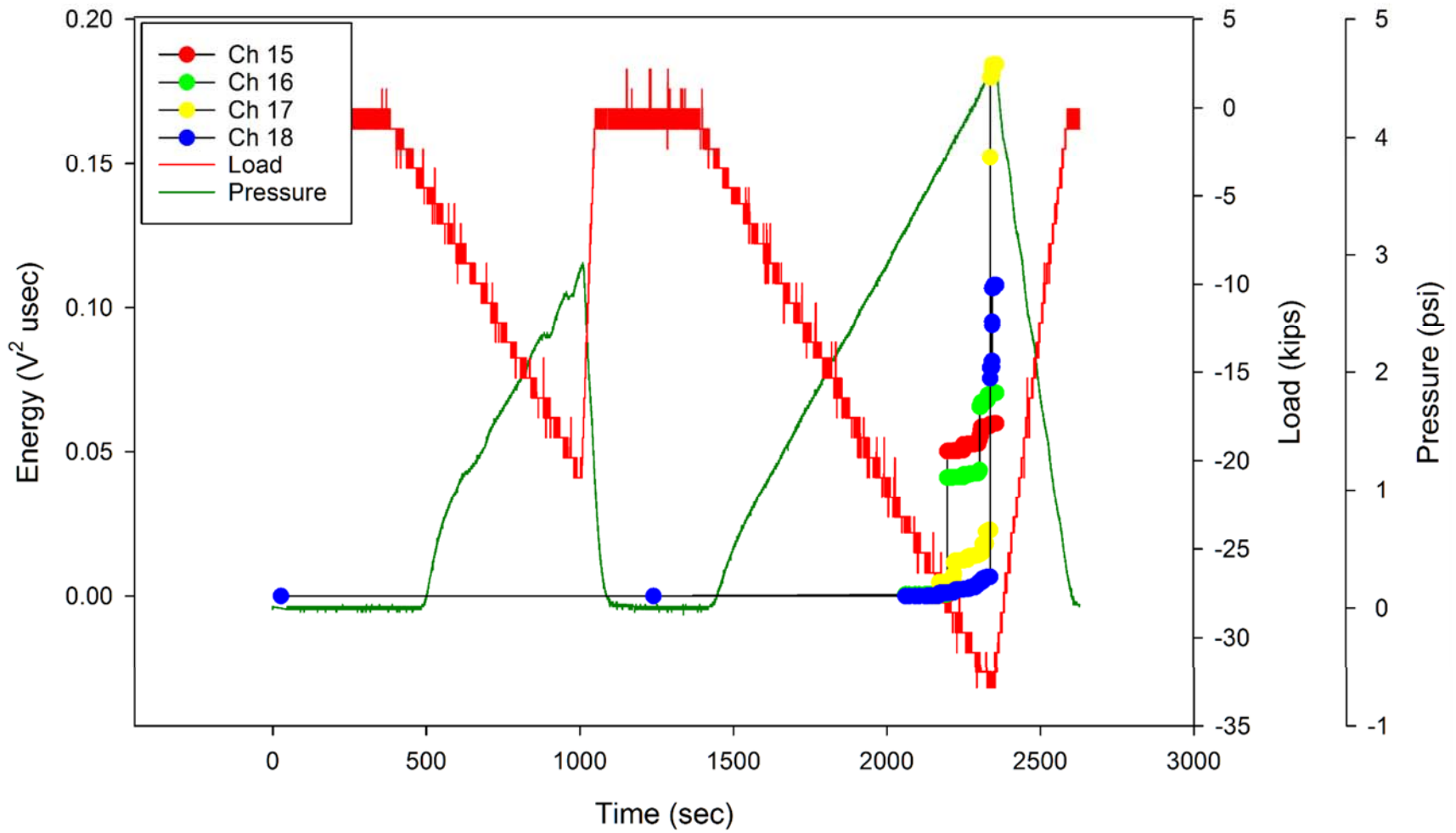


Figure A-11. Bulkheads AE Cumulative Energy by Channel: Phase I, 31.8 kips down-bending + 4.6 psi.

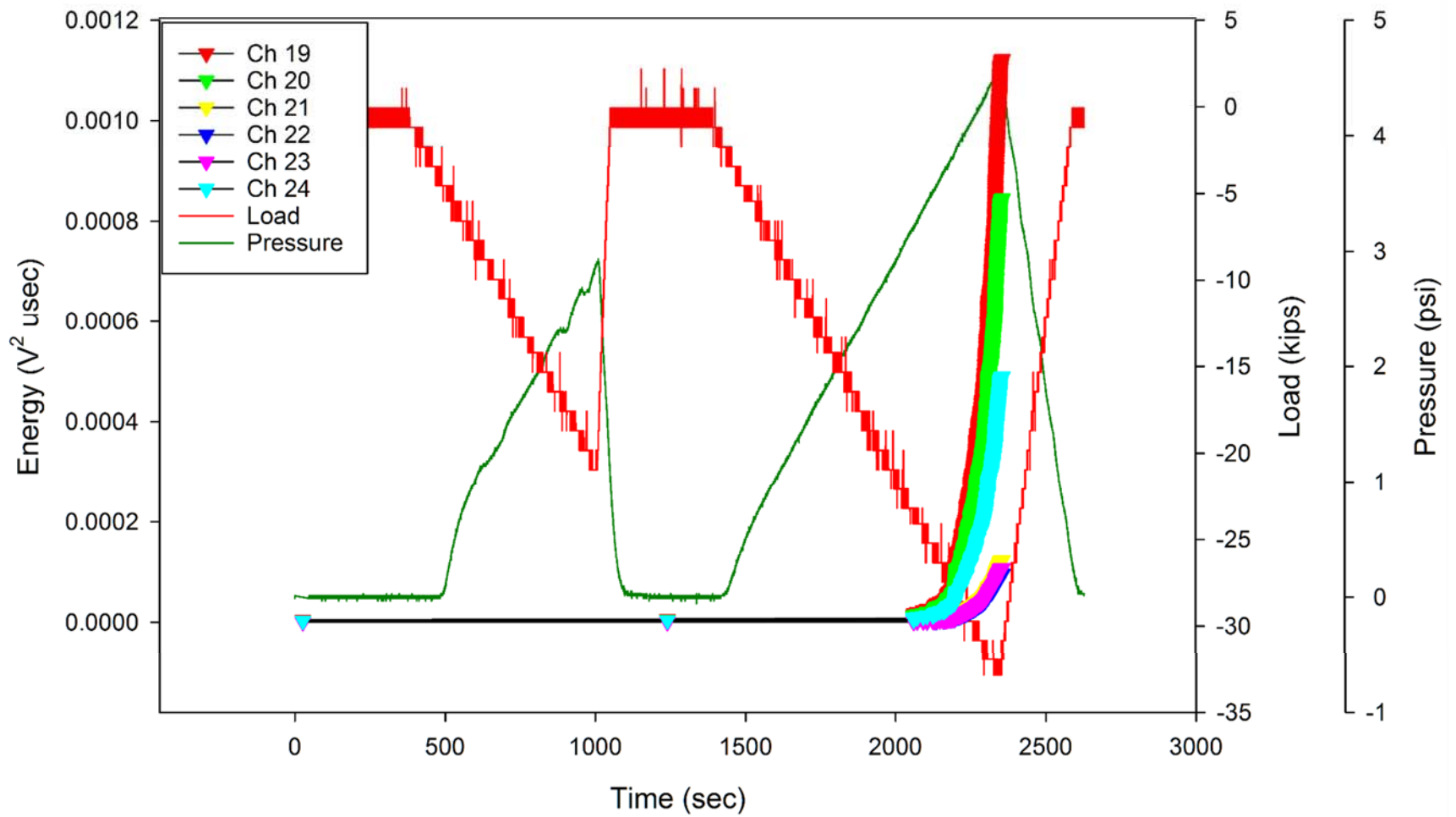


Figure A-12. Keel AE Cumulative Energy by Channel: Phase I, 31.8 kips down-bending + 4.6 psi.

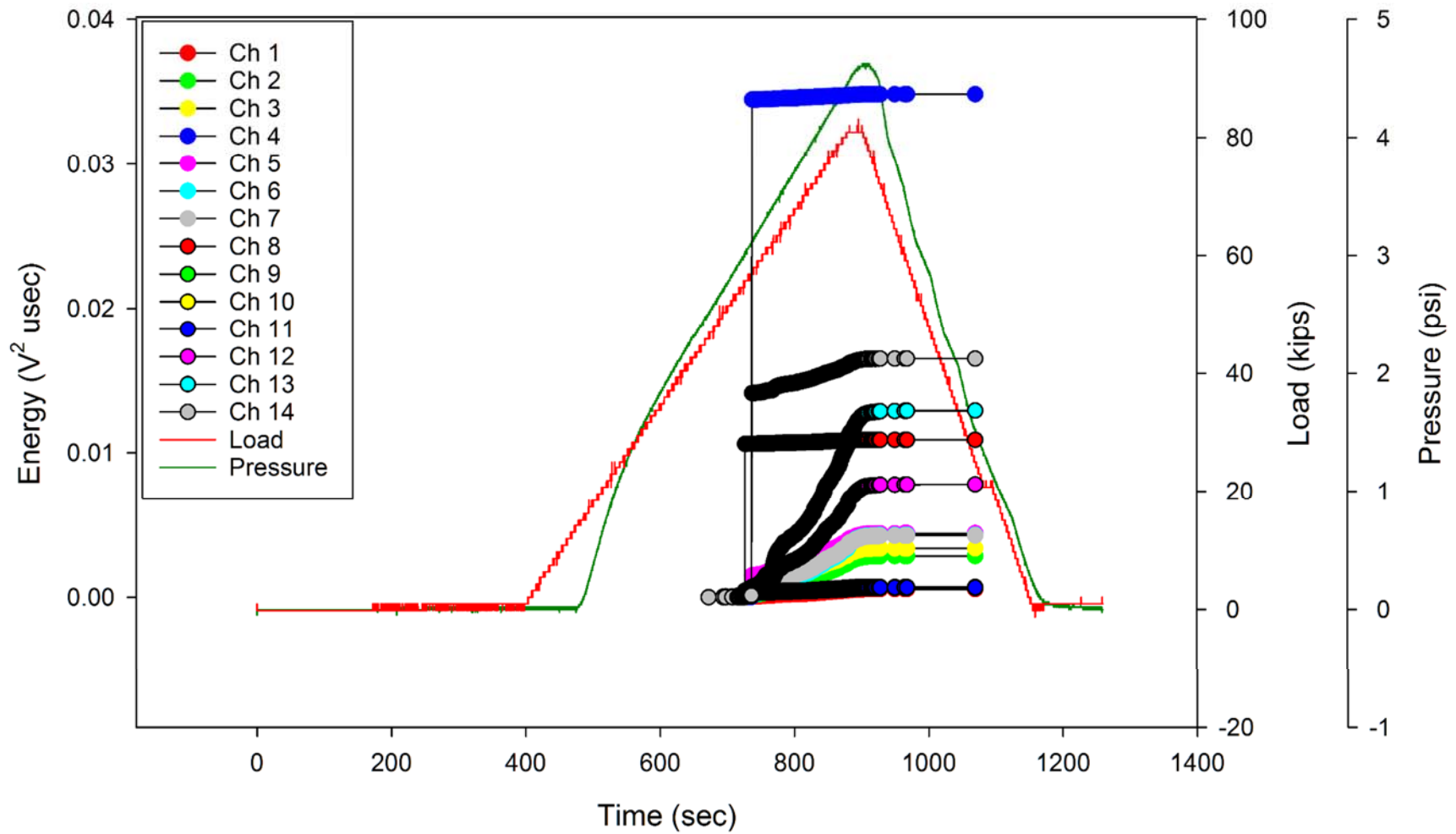


Figure A-13. Crown AE Cumulative Energy by Channel: Phase I, 79.5 kips up-bending + 4.6 psi.

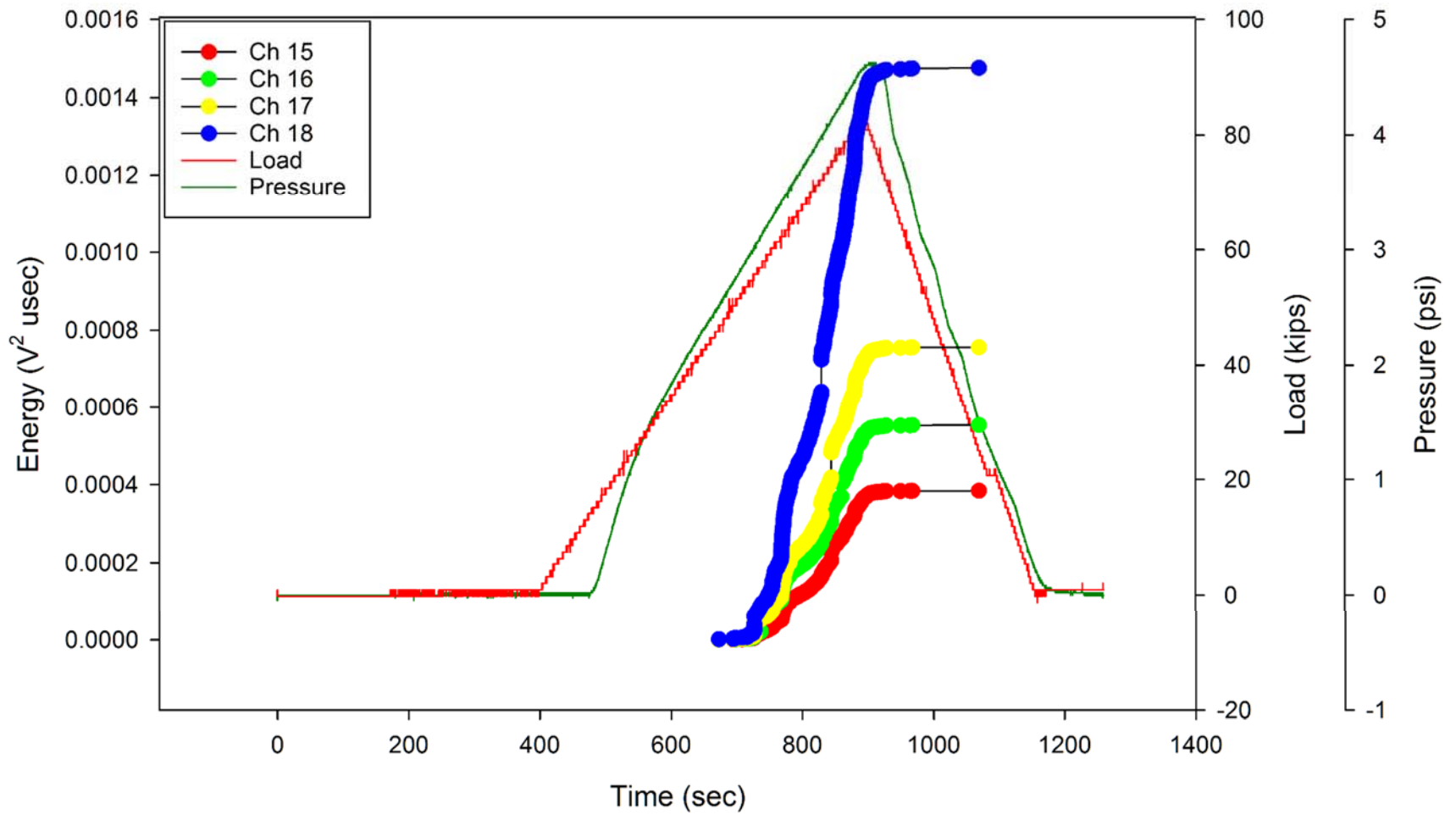


Figure A-14. Bulkheads AE Cumulative Energy by Channel: Phase I, 79.5 kips up-bending + 4.6 psi.

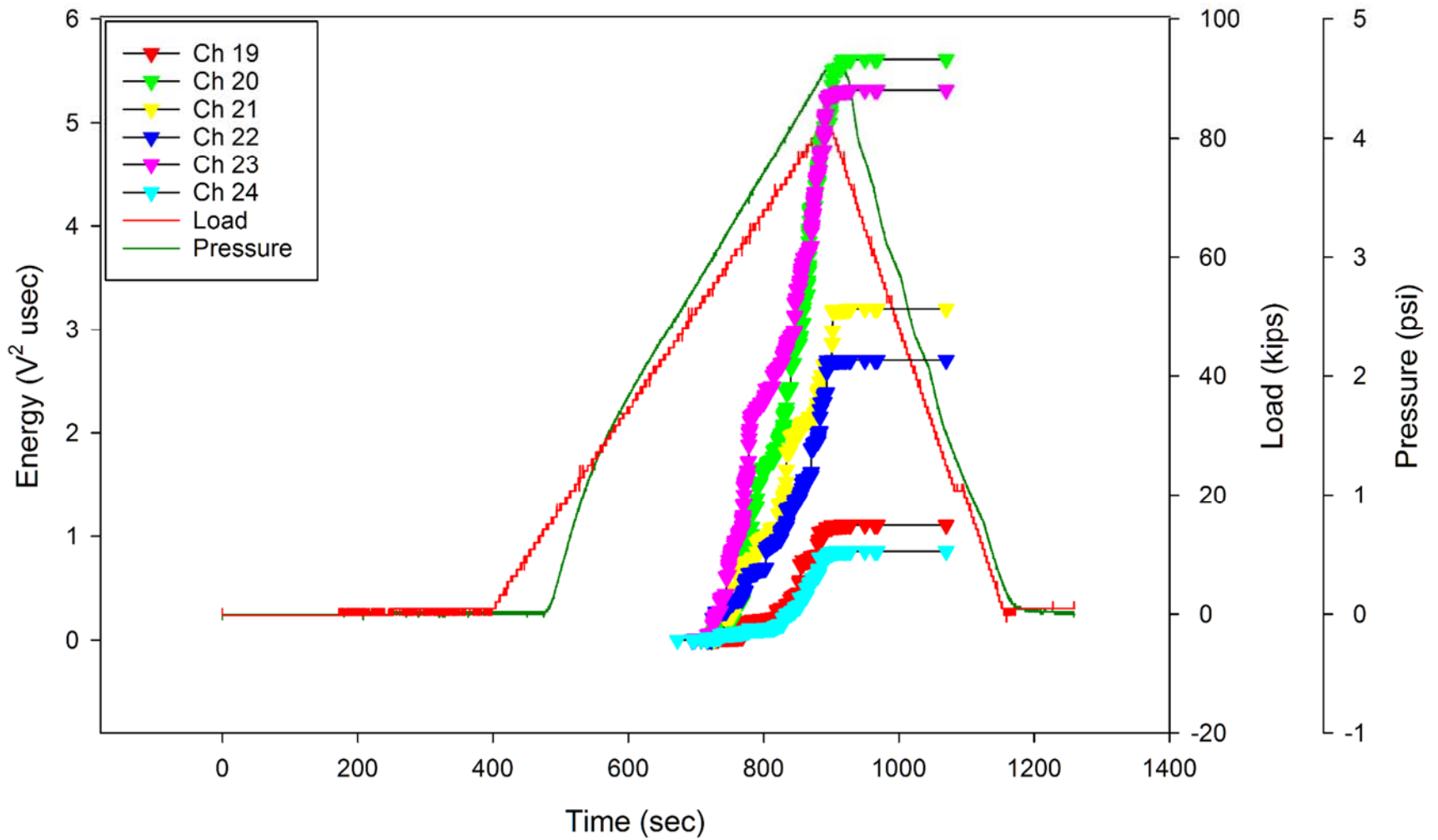


Figure A-15. Keel AE Cumulative Energy by Channel: Phase I, 79.5 kips up-bending + 4.6 psi.

Appendix B: Phase II Design Limit Load (DLL) Tests

Table of Figures

Figure B-1. Crown AE Cumulative Energy by Channel: Phase II, DLL, 12.2 psi.	B3
Figure B-2. Bulkheads AE Cumulative Energy by Channel: Phase II, DLL, 12.2 psi.	B4
Figure B-3. Keel AE Cumulative Energy by Channel: Phase II, DLL, 12.2 psi.	B5
Figure B-4. Crown AE Cumulative Energy by Channel: Phase II, DLL, 63.6 kips down-bending.	B6
Figure B-5. Bulkheads AE Cumulative Energy by Channel: Phase II, DLL, 63.6 kips down-bending.	B7
Figure B-6. Keel AE Cumulative Energy by Channel: Phase II, DLL, 63.6 kips down-bending.	B8
Figure B-7. Crown AE Cumulative Energy by Channel: Phase II, DLL, 63.6 kips down-bending + 9.2 psi.	B9
Figure B-8. Bulkheads AE Cumulative Energy by Channel: Phase II, DLL, 63.6 kips down-bending + 9.2 psi.	B10
Figure B-9. Keel AE Cumulative Energy by Channel: Phase II, DLL, 63.6 kips down-bending + 9.2 psi.	B11
Figure B-10. Crown AE Cumulative Energy by Channel: Phase II, DLL, 159 kips up-bending.	B12
Figure B-11. Bulkheads AE Cumulative Energy by Channel: Phase II, DLL, 159 kips up-bending.	B13
Figure B-12. Keel AE Cumulative Energy by Channel: Phase II, DLL, 159 kips up-bending.	B14
Figure B-13. Crown AE Cumulative Energy by Channel: Phase II, DLL, 159 kips up-bending + 9.2 psi.	B15
Figure B-14. Bulkheads AE Cumulative Energy by Channel: Phase II, DLL, 159 kips up-bending + 9.2 psi.	B16
Figure B-15. Keel AE Cumulative Energy by Channel: Phase II, DLL, 159 kips up-bending + 9.2 psi.	B17

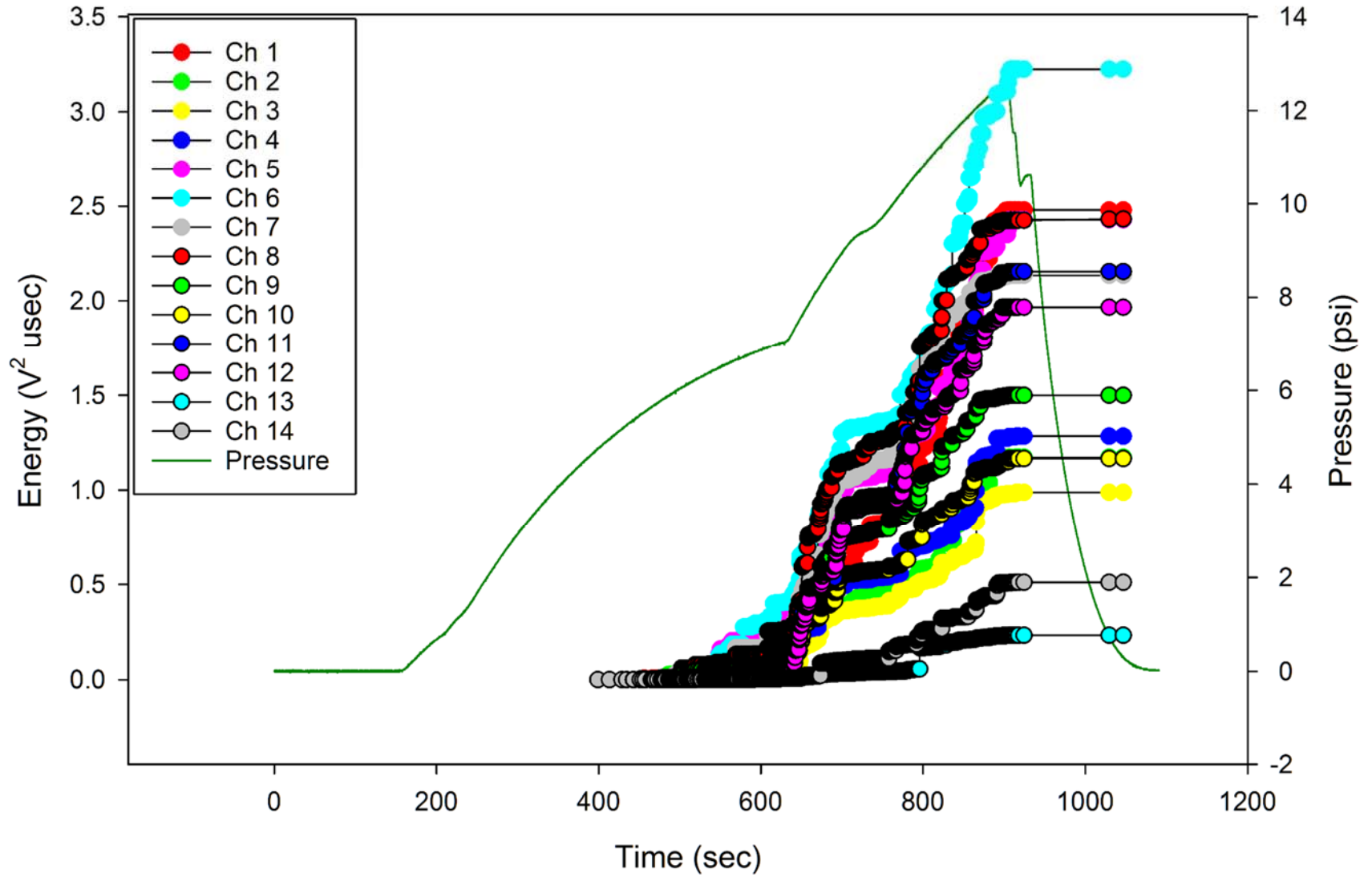


Figure B-1. Crown AE Cumulative Energy by Channel: Phase II, DLL, 12.2 psi.

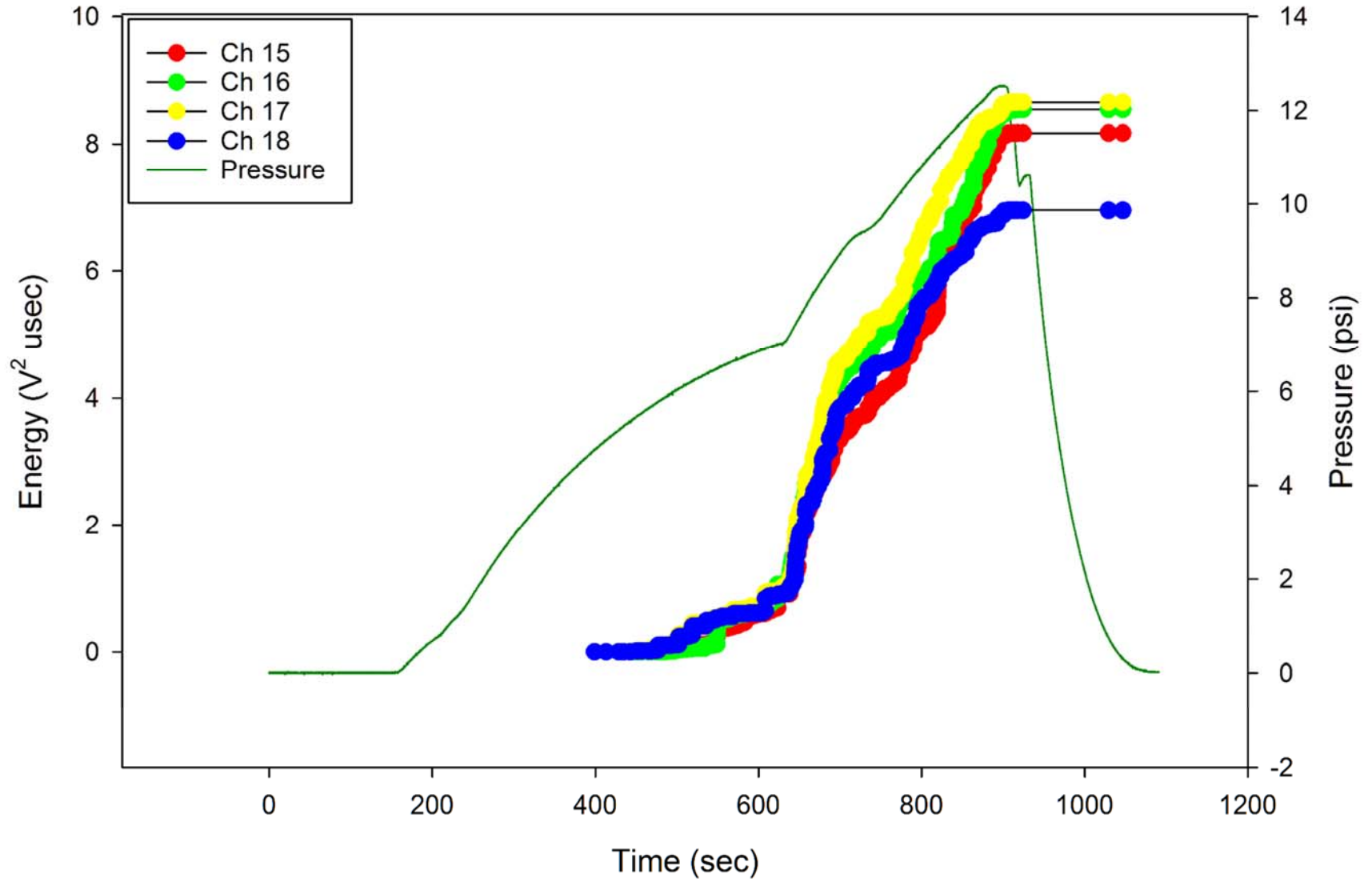


Figure B-2. Bulkheads AE Cumulative Energy by Channel: Phase II, DLL, 12.2 psi.

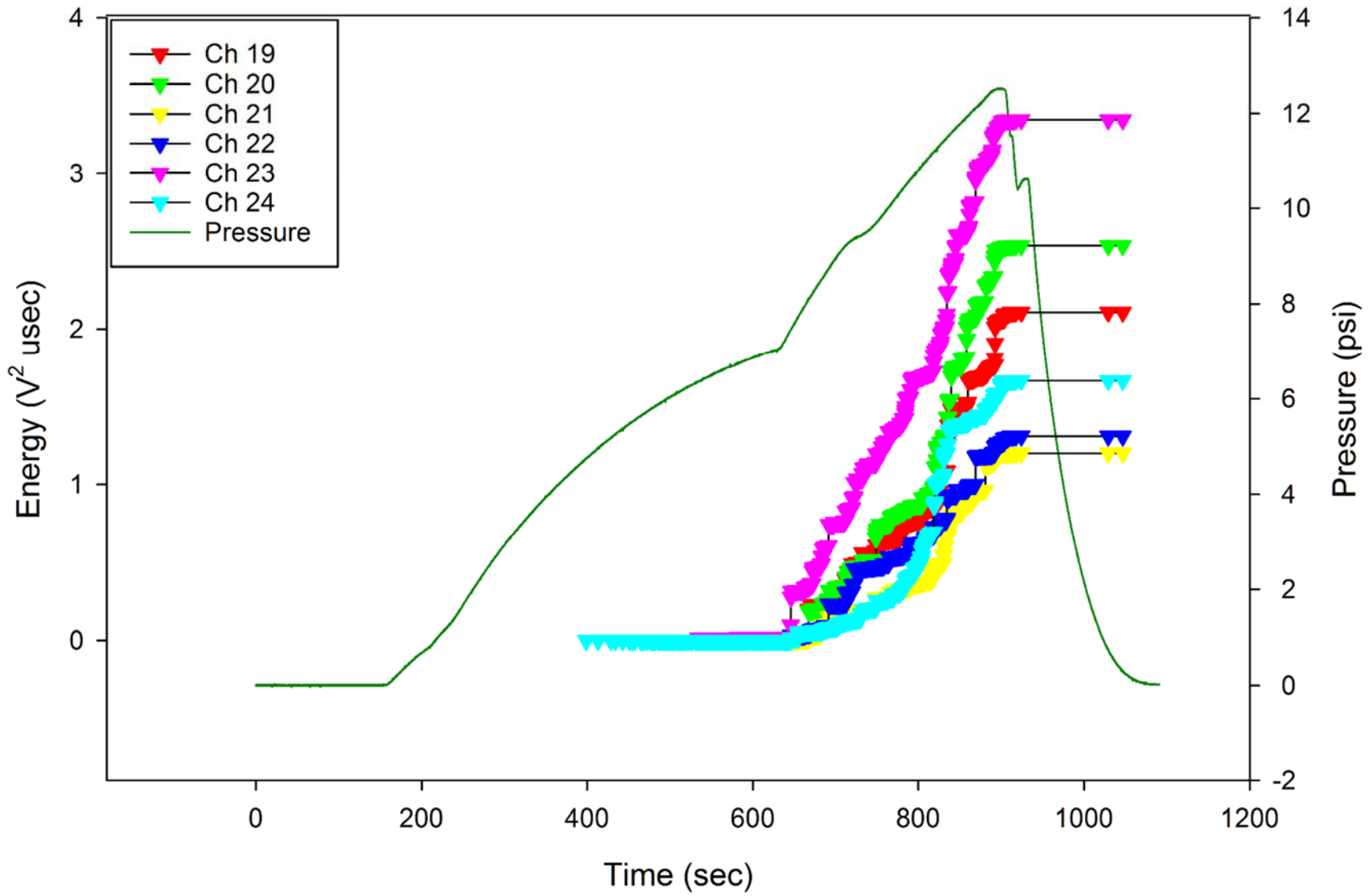


Figure B-3. Keel AE Cumulative Energy by Channel: Phase II, DLL, 12.2 psi.

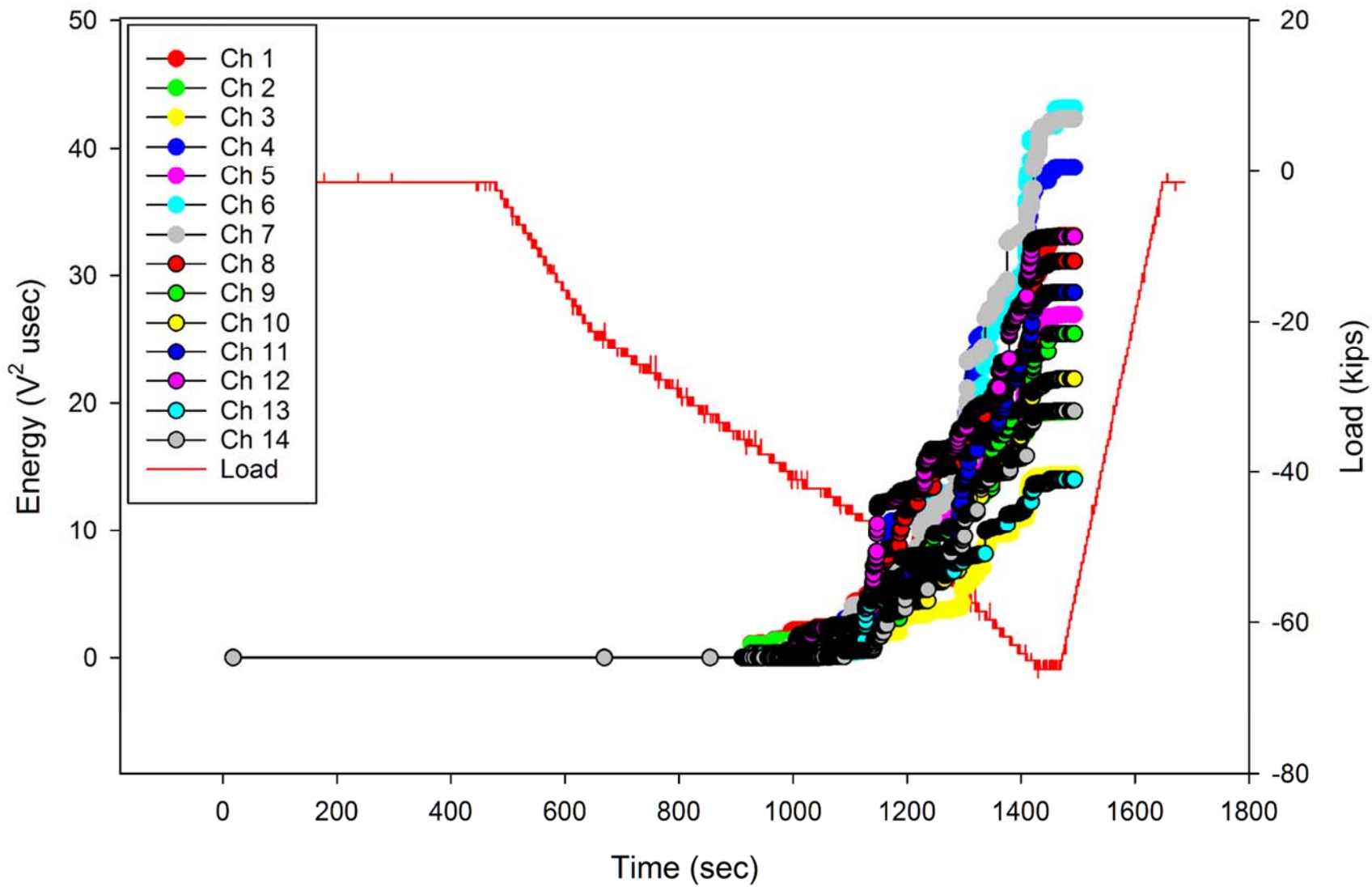


Figure B-4. Crown AE Cumulative Energy by Channel: Phase II, DLL, 63.6 kips down-bending.

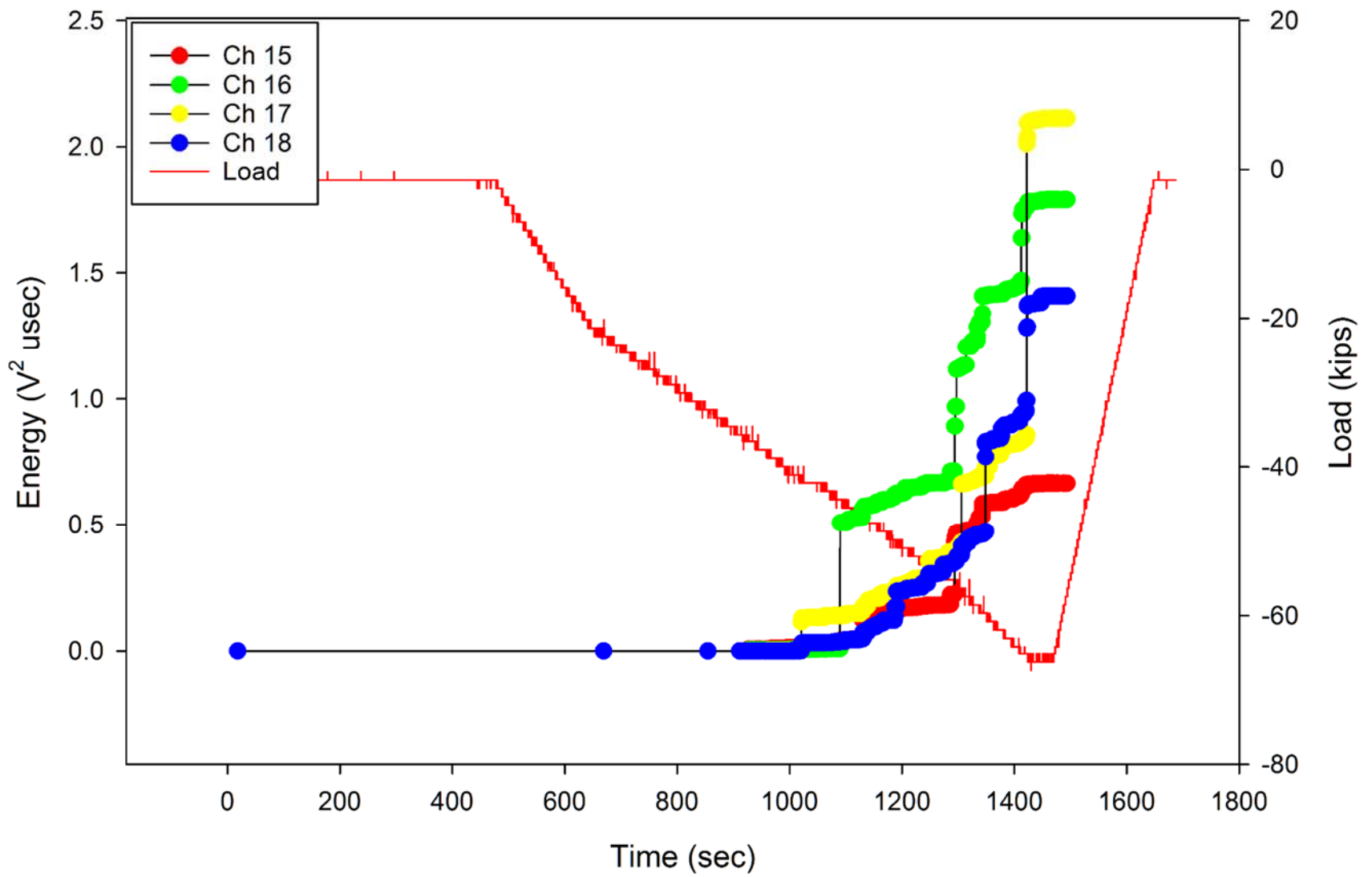


Figure B-5. Bulkheads AE Cumulative Energy by Channel: Phase II, DLL, 63.6 kips down-bending.

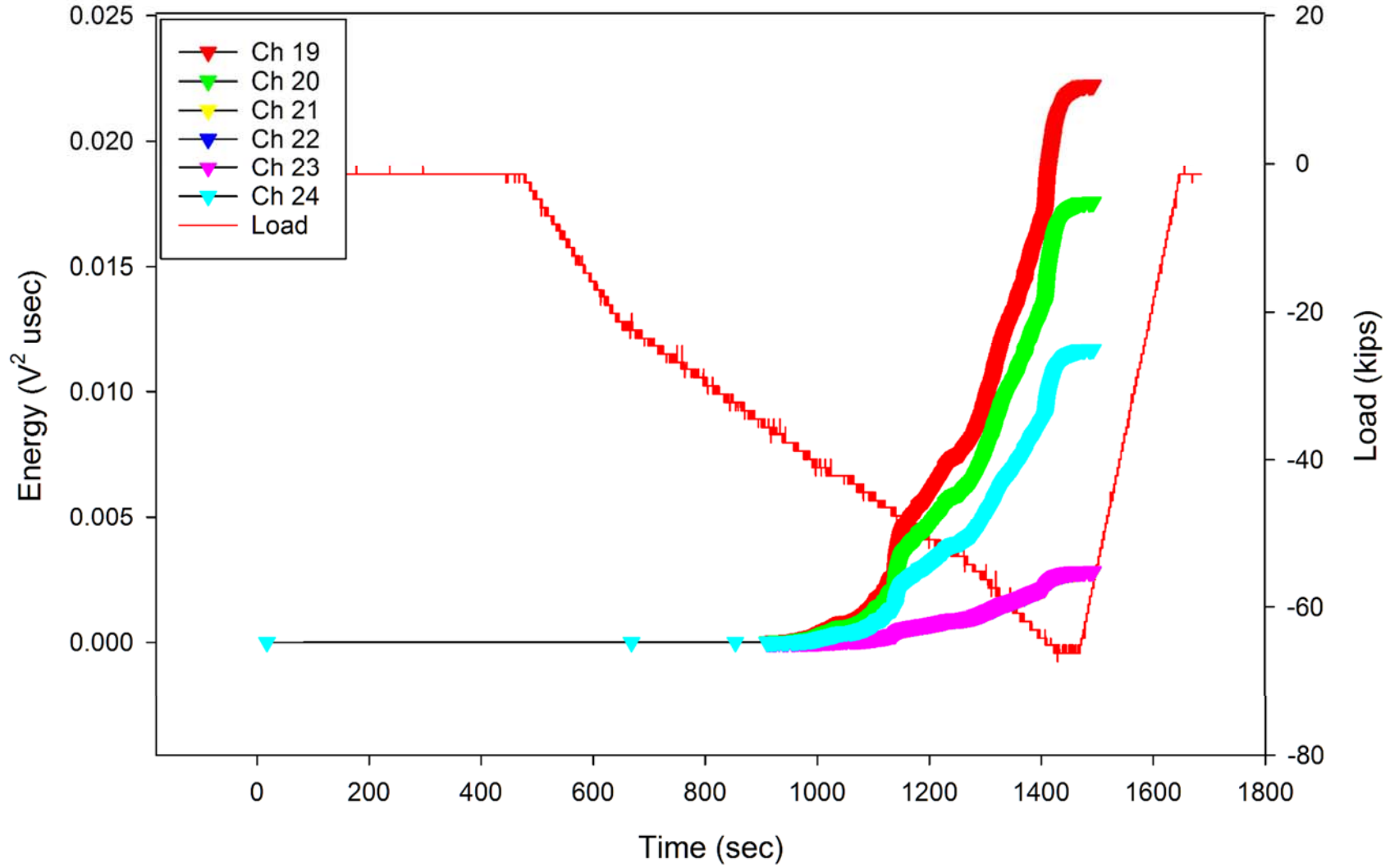


Figure B-6. Keel AE Cumulative Energy by Channel: Phase II, DLL, 63.6 kips down-bending.

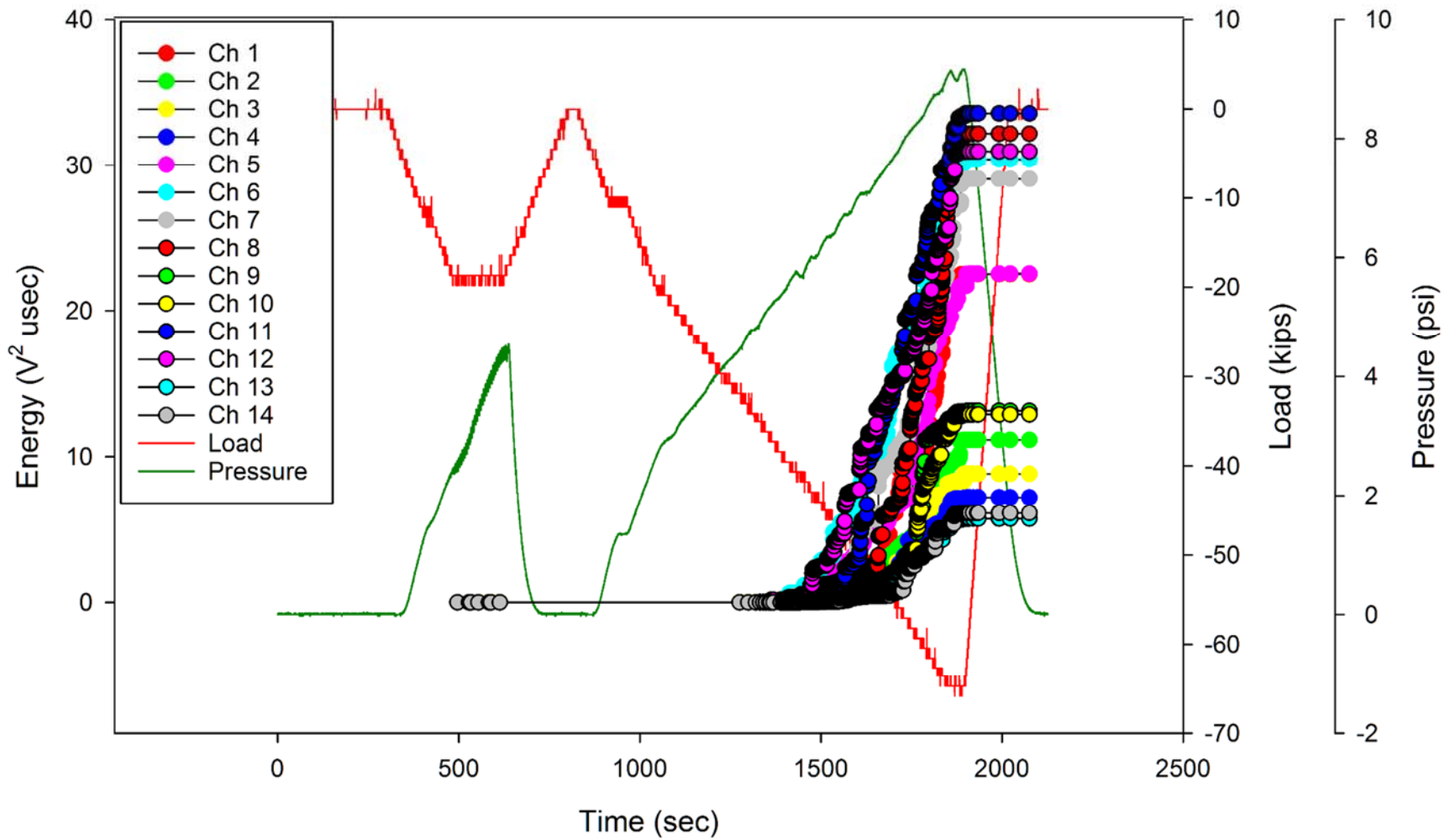


Figure B-7. Crown AE Cumulative Energy by Channel: Phase II, DLL, 63.6 kips down-bending + 9.2 psi.

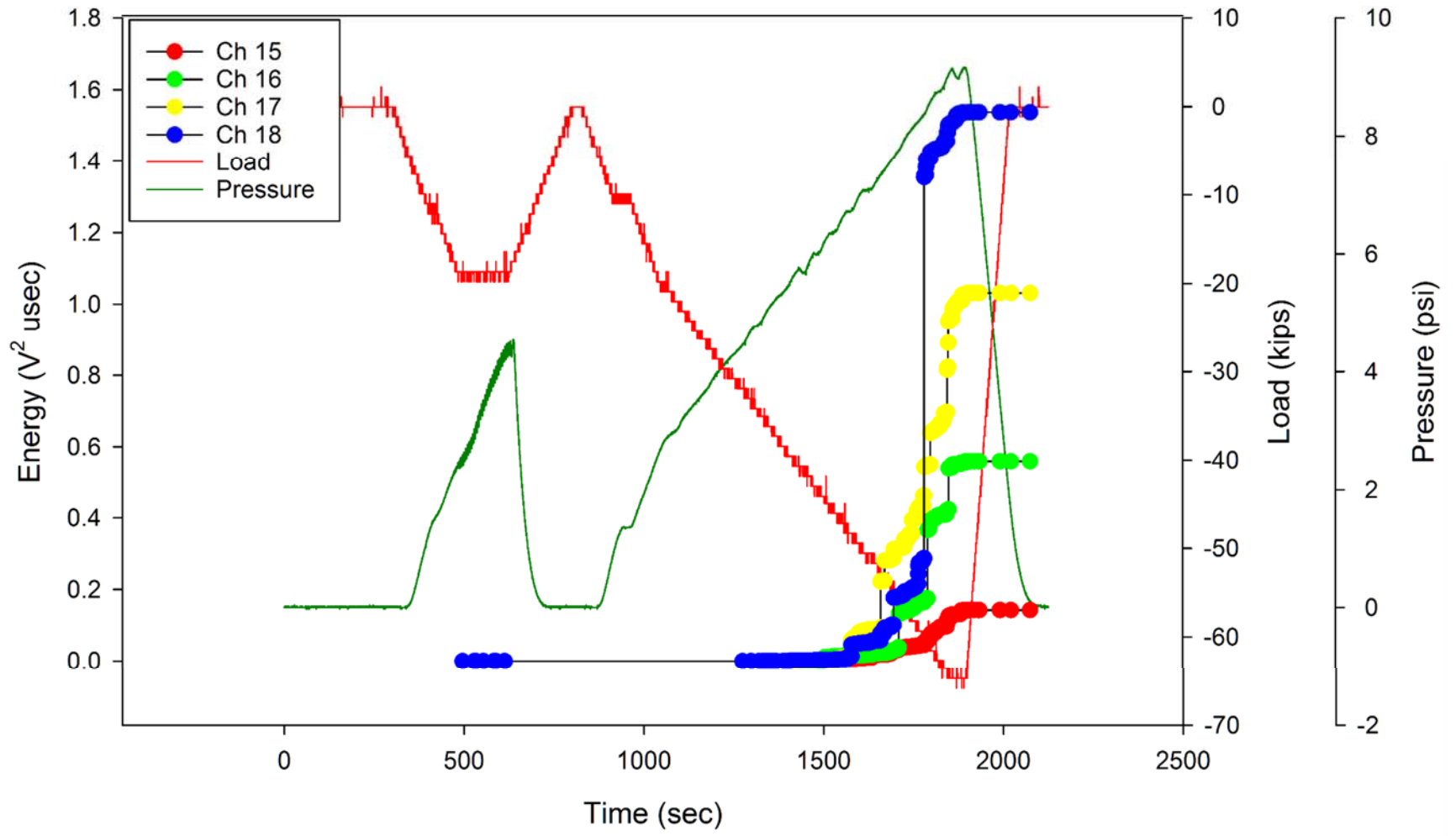


Figure B-8. Bulkheads AE Cumulative Energy by Channel: Phase II, DLL, 63.6 kips down-bending + 9.2 psi.

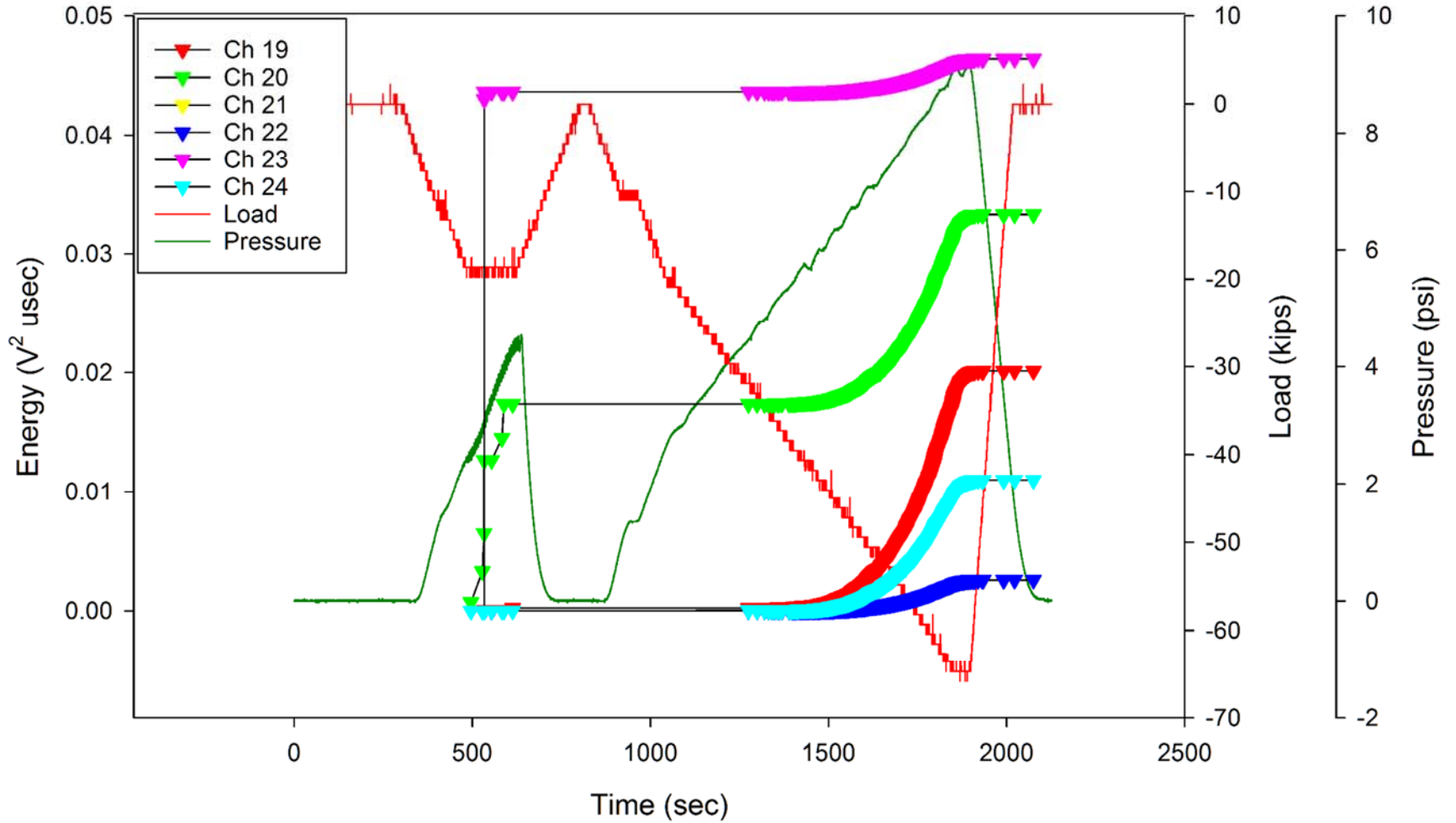


Figure B-9. Keel AE Cumulative Energy by Channel: Phase II, DLL, 63.6 kips down-bending + 9.2 psi.

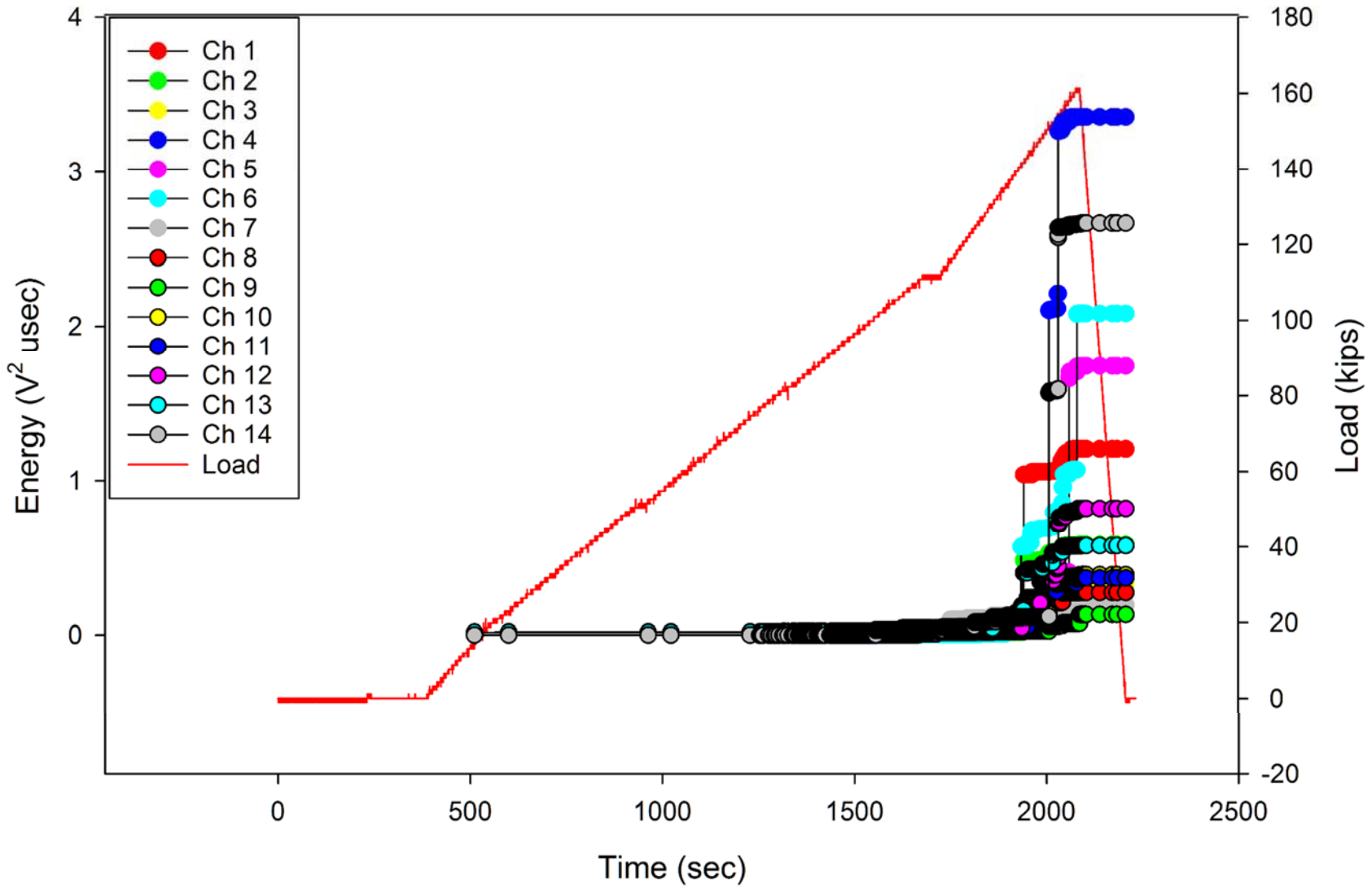


Figure B-10. Crown AE Cumulative Energy by Channel: Phase II, DLL, 159 kips up-bending.

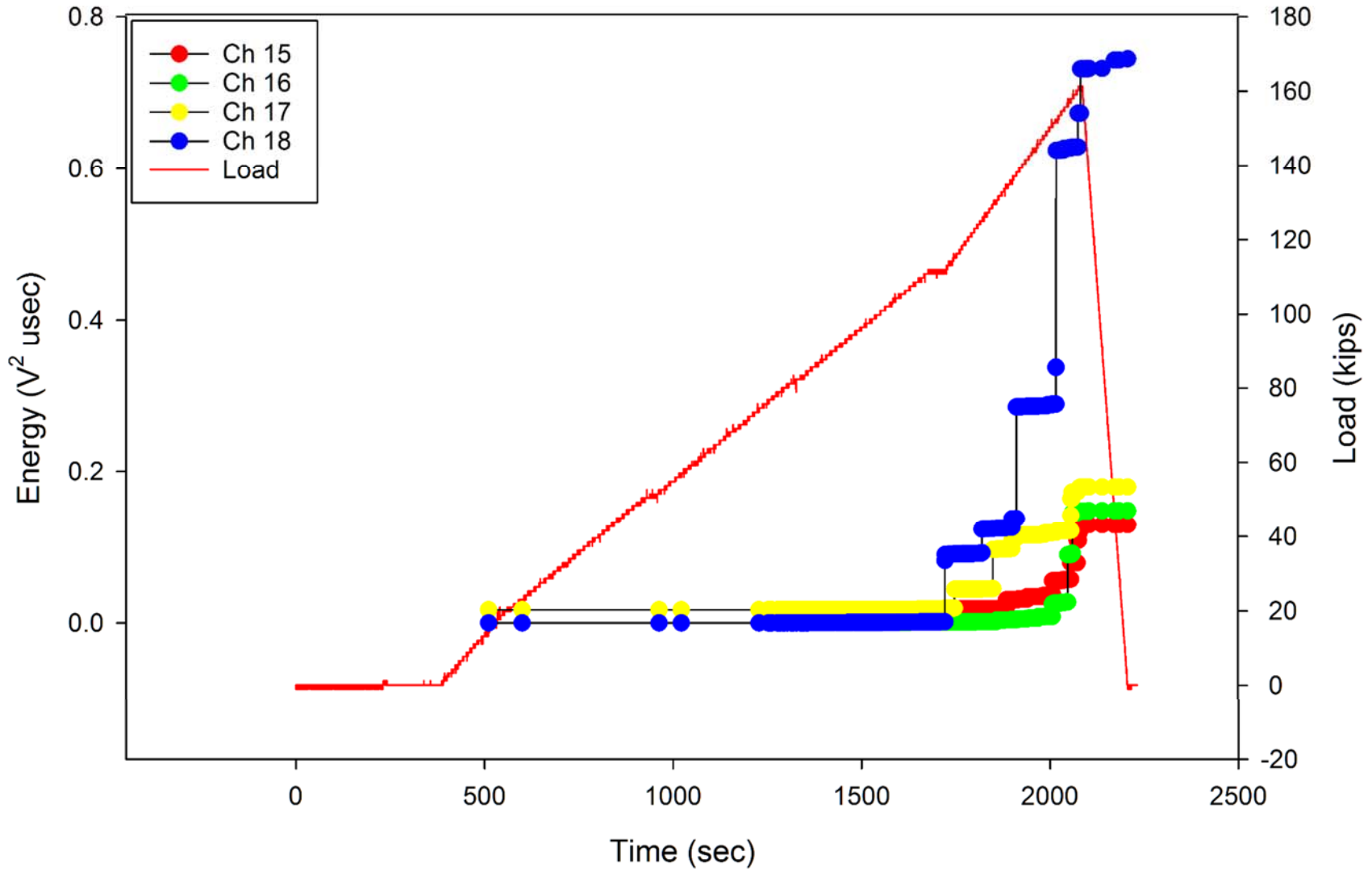


Figure B-11. Bulkheads AE Cumulative Energy by Channel: Phase II, DLL, 159 kips up-bending.

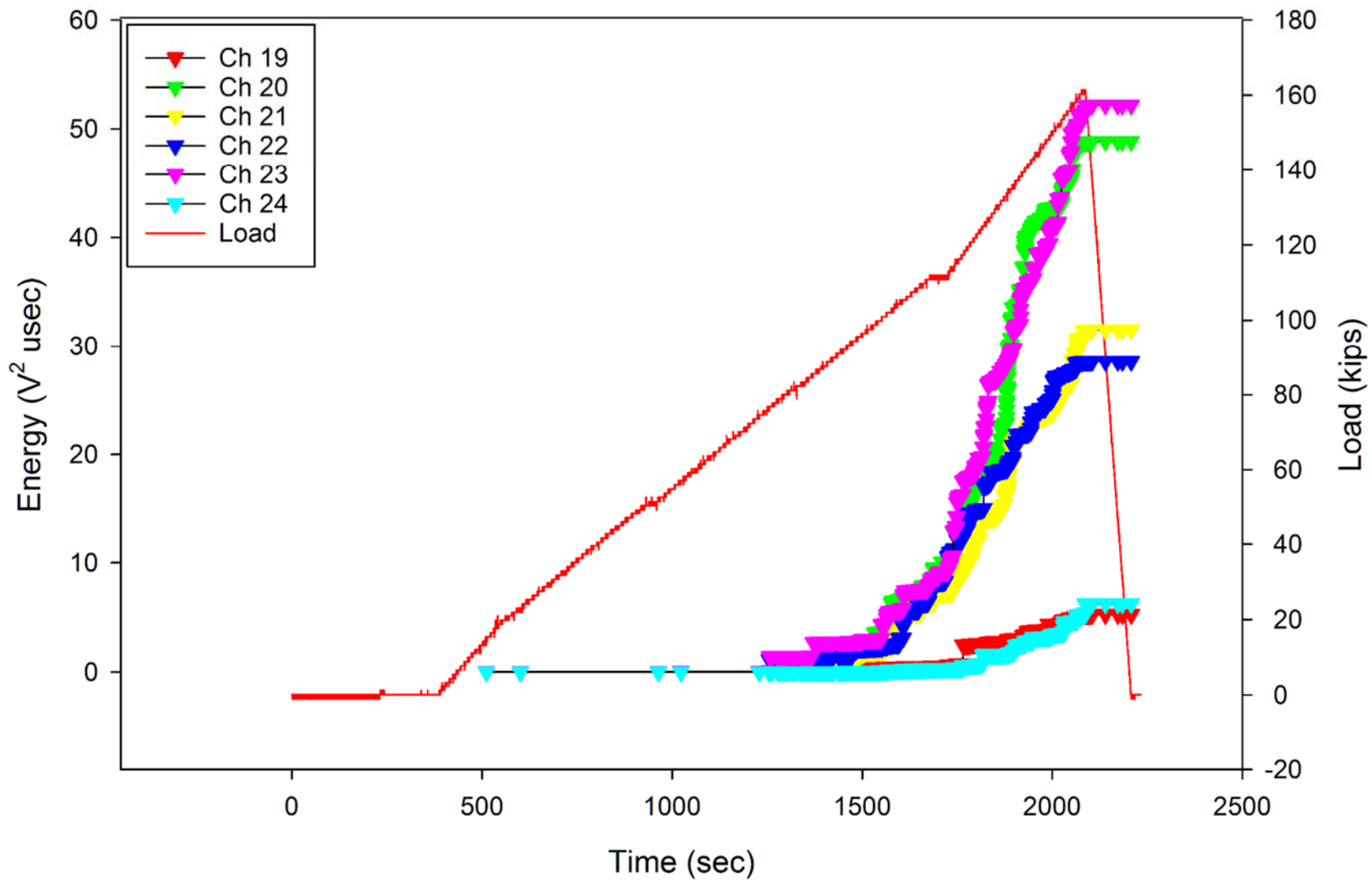


Figure B-12. Keel AE Cumulative Energy by Channel: Phase II, DLL, 159 kips up-bending.

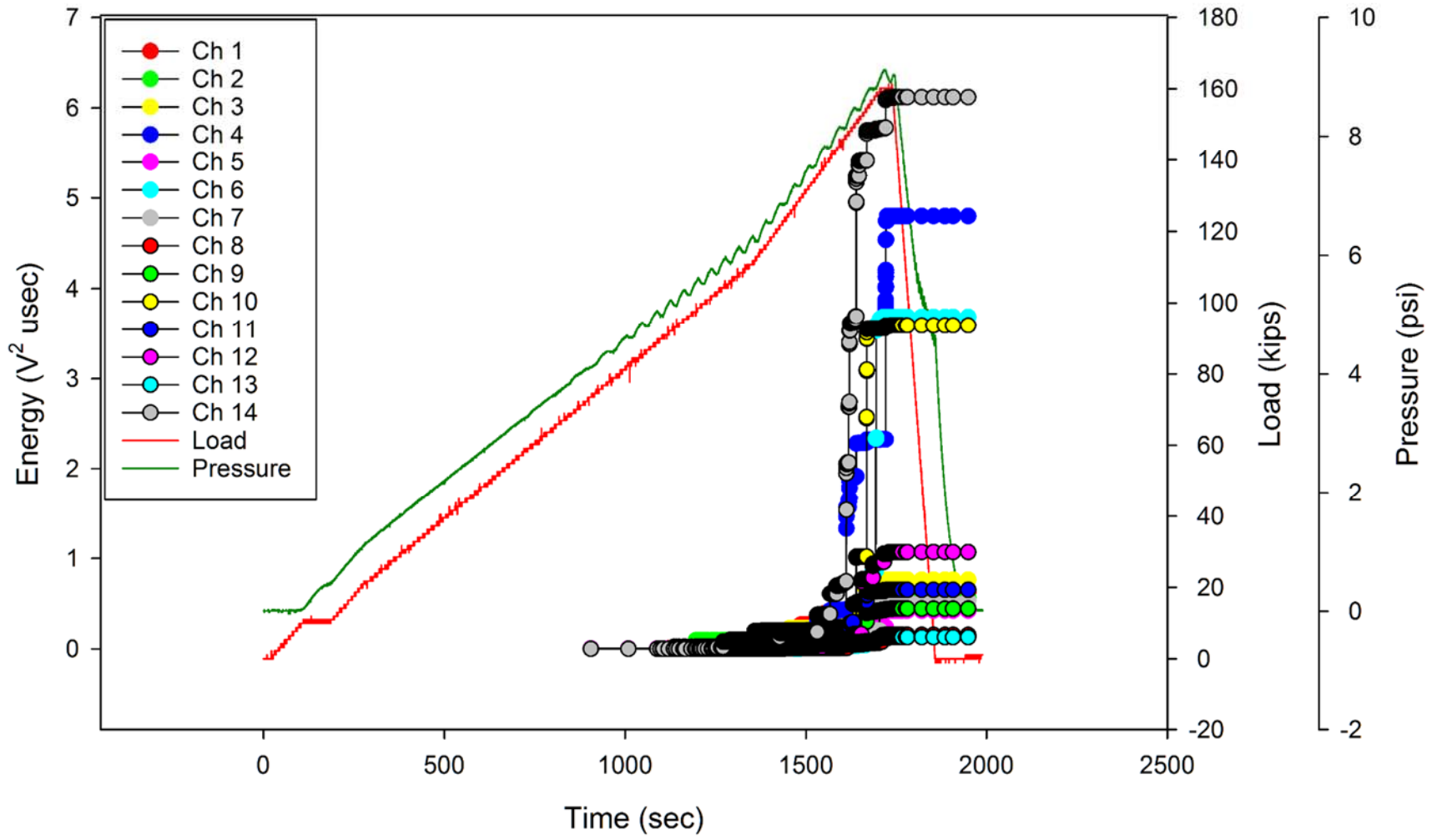


Figure B-13. Crown AE Cumulative Energy by Channel: Phase II, DLL, 159 kips up-bending + 9.2 psi.

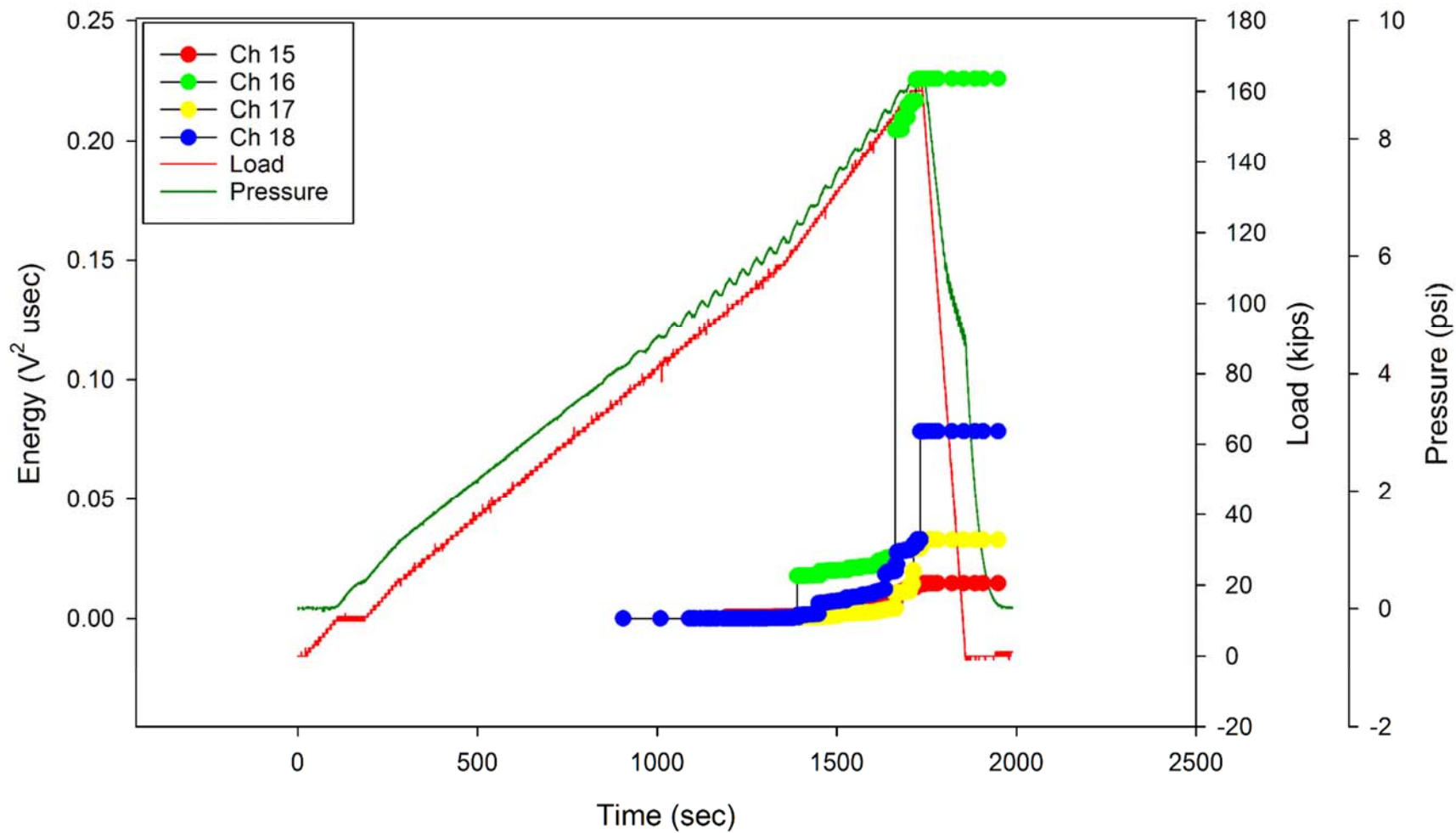


Figure B-14. Bulkheads AE Cumulative Energy by Channel: Phase II, DLL, 159 kips up-bending + 9.2 psi.

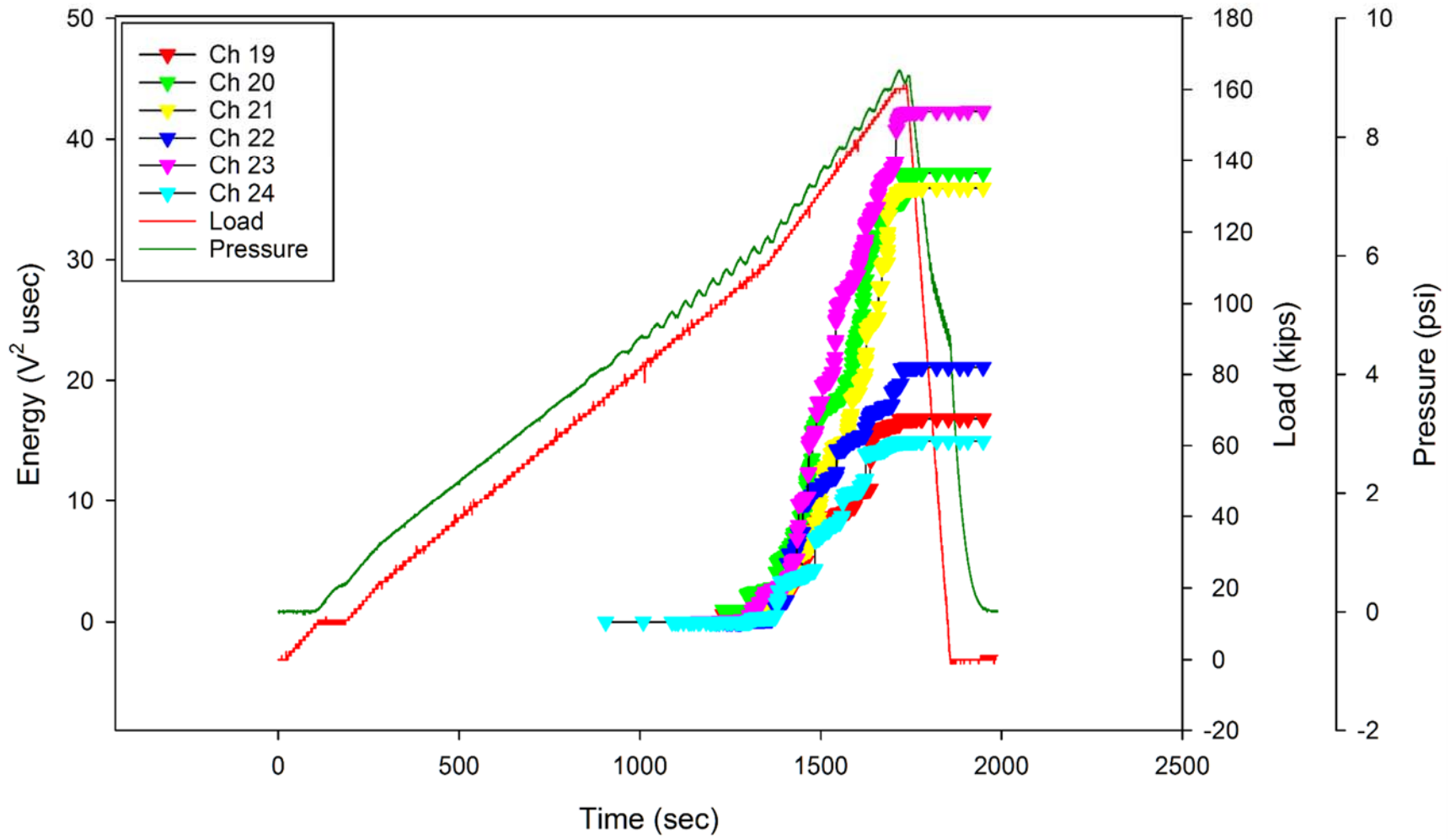


Figure B-15. Keel AE Cumulative Energy by Channel: Phase II, DLL, 159 kips up-bending + 9.2 psi.

Appendix C: Phase III Design Ultimate Load (DUL) Tests

Table of Figures

Figure C-1. Crown AE Cumulative Energy by Channel: Phase III, DUL, 95.4 kips down-bending.	C3
Figure C-2. Bulkheads AE Cumulative Energy by Channel: Phase III, DUL, 95.4 kips down-bending.	C4
Figure C-3. Keel AE Cumulative Energy by Channel: Phase III, DUL, 95.4 kips down-bending.	C5
Figure C-4. Crown AE Cumulative Energy by Channel: Phase III, DUL, 95.4 kips down-bending +13.8 psi.	C6
Figure C-5. Bulkheads AE Cumulative Energy by Channel: Phase III, DUL, 95.4 kips down-bending +13.8 psi.	C7
Figure C-6. Keel AE Cumulative Energy by Channel: Phase III, DUL, 95.4 kips down-bending +13.8 psi.	C8
Figure C-7. Crown AE Cumulative Energy by Channel: Phase III, DUL, 238.5 kips up-bending, Trial 1.	C9
Figure C-8. Bulkheads AE Cumulative Energy by Channel: Phase III, DUL, 238.5 kips up-bending, Trial 1.	C10
Figure C-9. Keel AE Cumulative Energy by Channel Ph III DUL, 238.5 kips up-bending, Trial 1.	C11
Figure C-10. Crown AE Cumulative Energy by Channel: Phase III, DUL, 238.5 kips up-bending, Trial 2.	C12
Figure C-11. Bulkheads AE Cumulative Energy by Channel Ph III DUL, 238.5 kips up-bending, Trial 2.	C13
Figure C-12. Keel AE Cumulative Energy by Channel: Phase III, DUL, 238.5 kips up-bending, Trial 2.	C14
Figure C-13. Crown AE Cumulative Energy by Channel: Phase III, DUL, 238.5 kips up-bending + 13.8 psi.	C15
Figure C-14. Bulkheads AE Cumulative Energy by Channel: Phase III, DUL, 238.5 kips up-bending + 13.8 psi.	C16
Figure C-15. Keel AE Cumulative Energy by Channel: Phase III, DUL, 238.5 kips up-bending + 13.8 psi.	C17
Figure C-16. Crown AE Cumulative Energy by Channel: Phase III, DUL, 18.4 psi, Trial 1.	C18
Figure C-17. Bulkheads AE Cumulative Energy by Channel: Phase III, DUL, 18.4 psi, Trial 1.	C19
Figure C-18. Keel AE Cumulative Energy by Channel: Phase III, DUL, 18.4 psi, Trial 1.	C20
Figure C-19. Crown AE Cumulative Energy by Channel: Phase III, DUL, 18.4 psi, Trial 2.	C21
Figure C-20. Bulkheads AE Cumulative Energy by Channel: Phase III, DUL, 18.4 psi, Trial 2.	C22
Figure C-21. Keel AE Cumulative Energy by Channel: Phase III, DUL, 18.4 psi, Trial 2.	C23

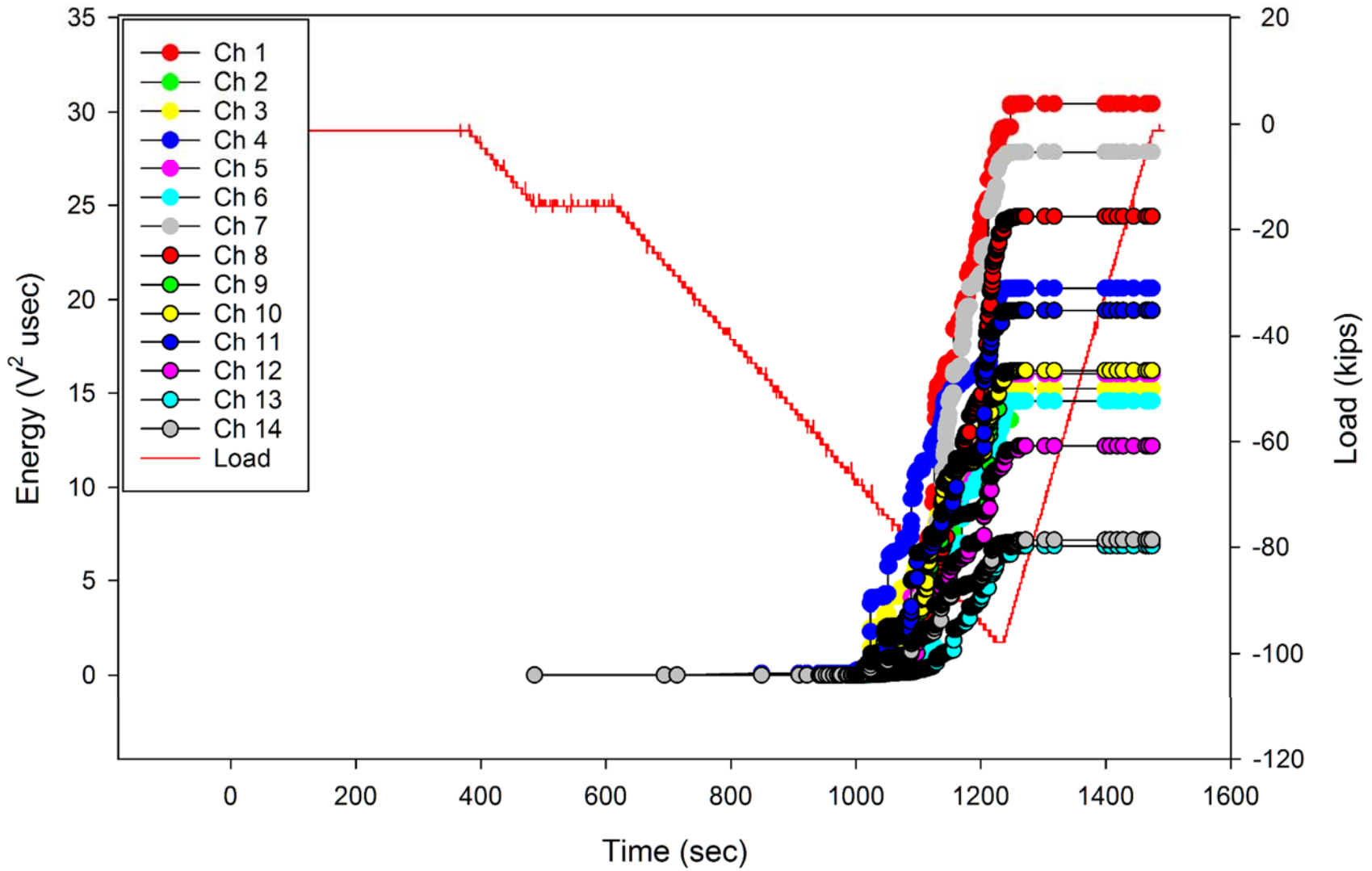


Figure C-1. Crown AE Cumulative Energy by Channel: Phase III, DUL, 95.4 kips down-bending.

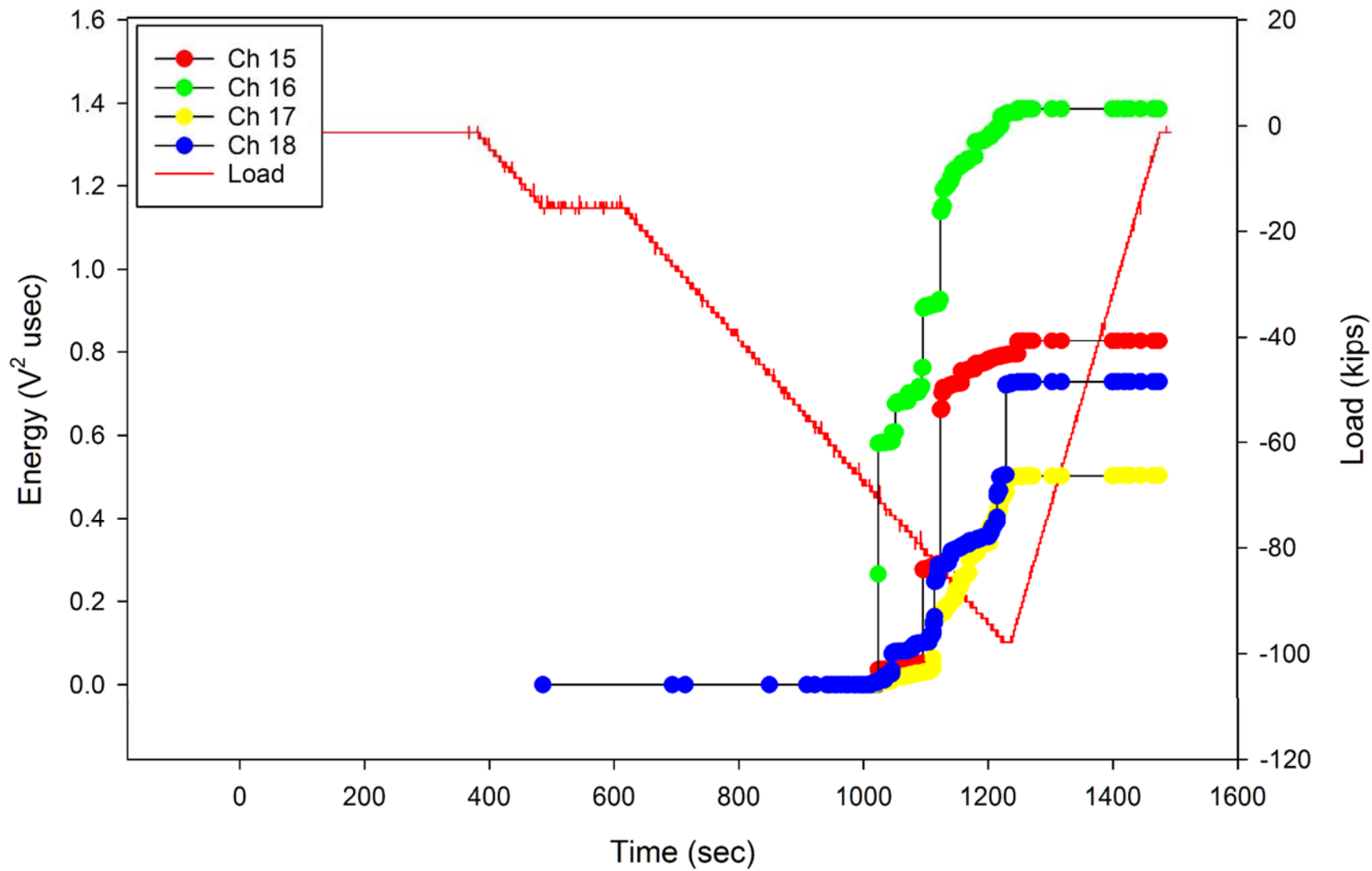


Figure C-2. Bulkheads AE Cumulative Energy by Channel: Phase III, DUL, 95.4 kips down-bending.

C4

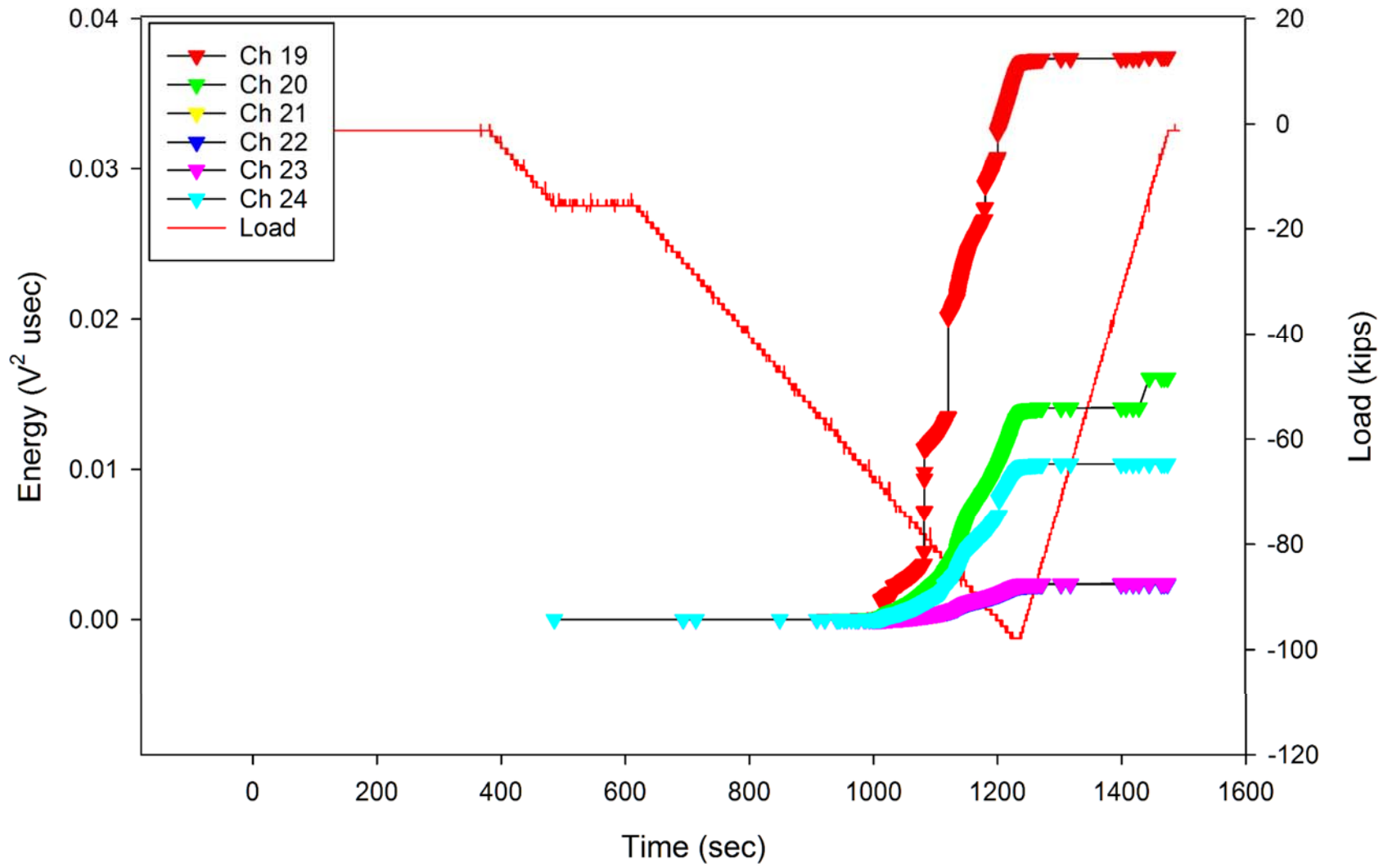


Figure C-3. Keel AE Cumulative Energy by Channel: Phase III, DUL, 95.4 kips down-bending.

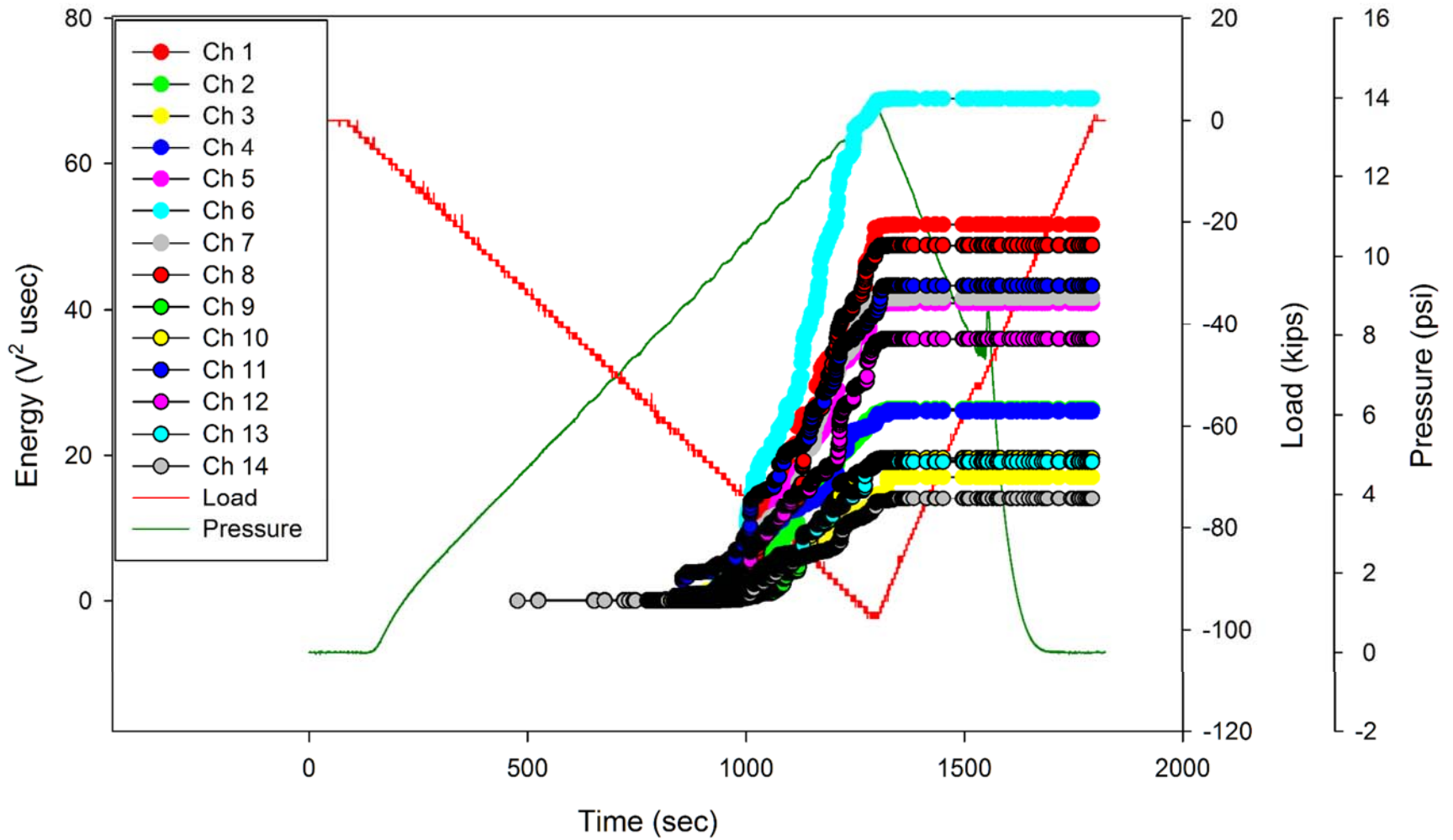


Figure C-4. Crown AE Cumulative Energy by Channel: Phase III, DUL, 95.4 kips down-bending +13.8 psi.

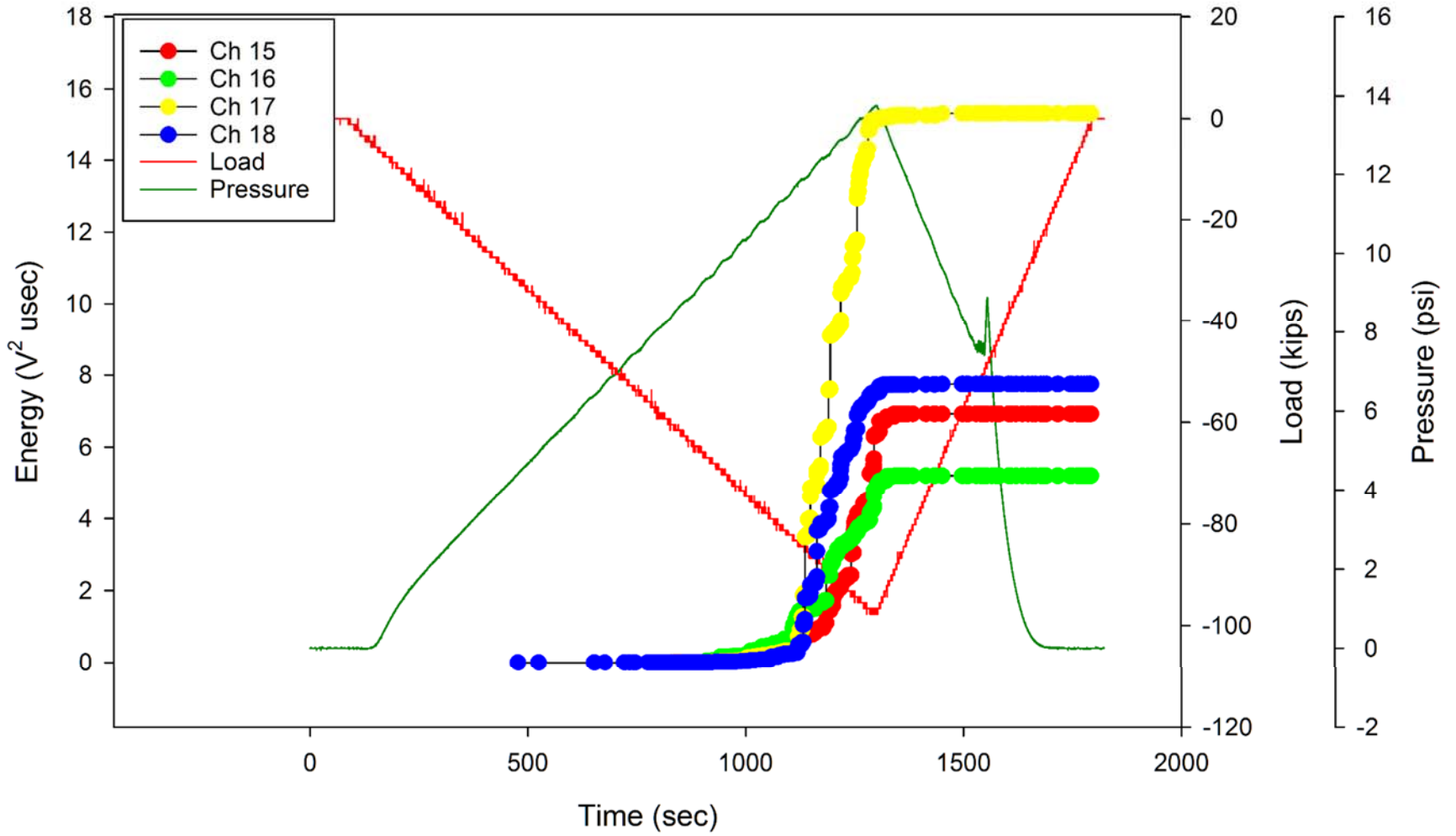


Figure C-5. Bulkheads AE Cumulative Energy by Channel: Phase III, DUL, 95.4 kips down-bending +13.8 psi.

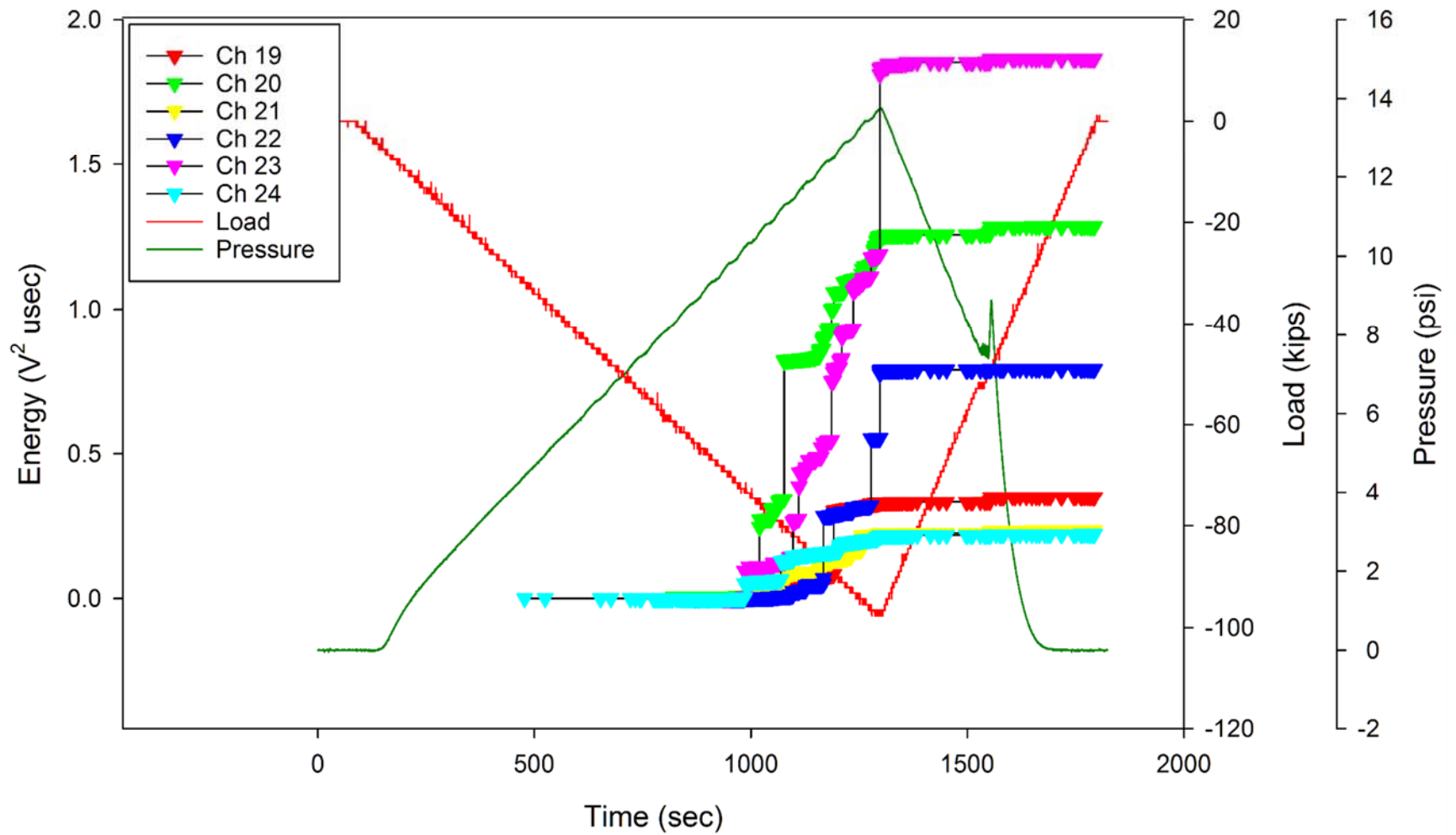


Figure C-6. Keel AE Cumulative Energy by Channel: Phase III, DUL, 95.4 kips down-bending +13.8 psi.

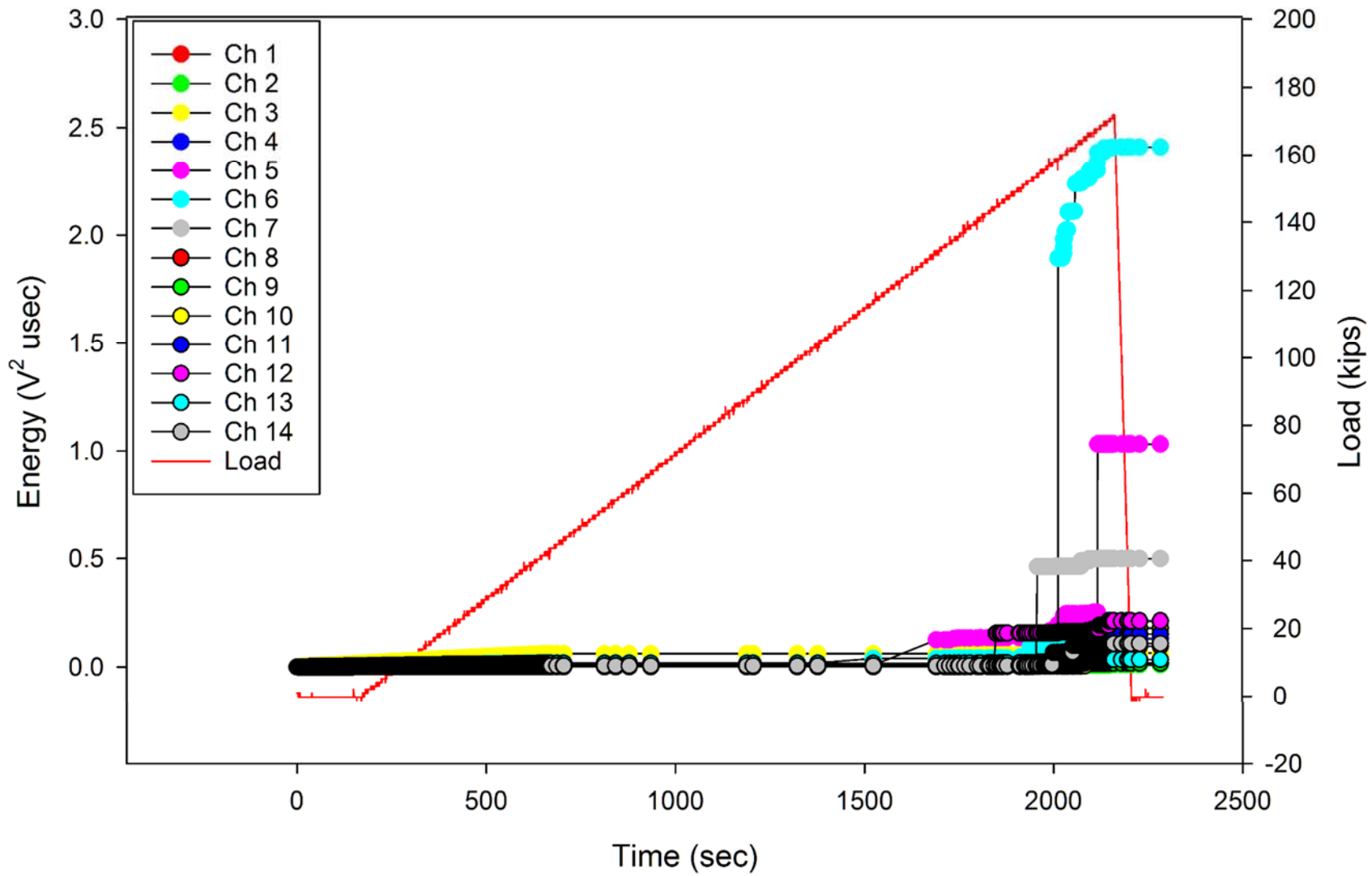


Figure C-7. Crown AE Cumulative Energy by Channel: Phase III, DUL, 238.5 kips up-bending, Trial 1.

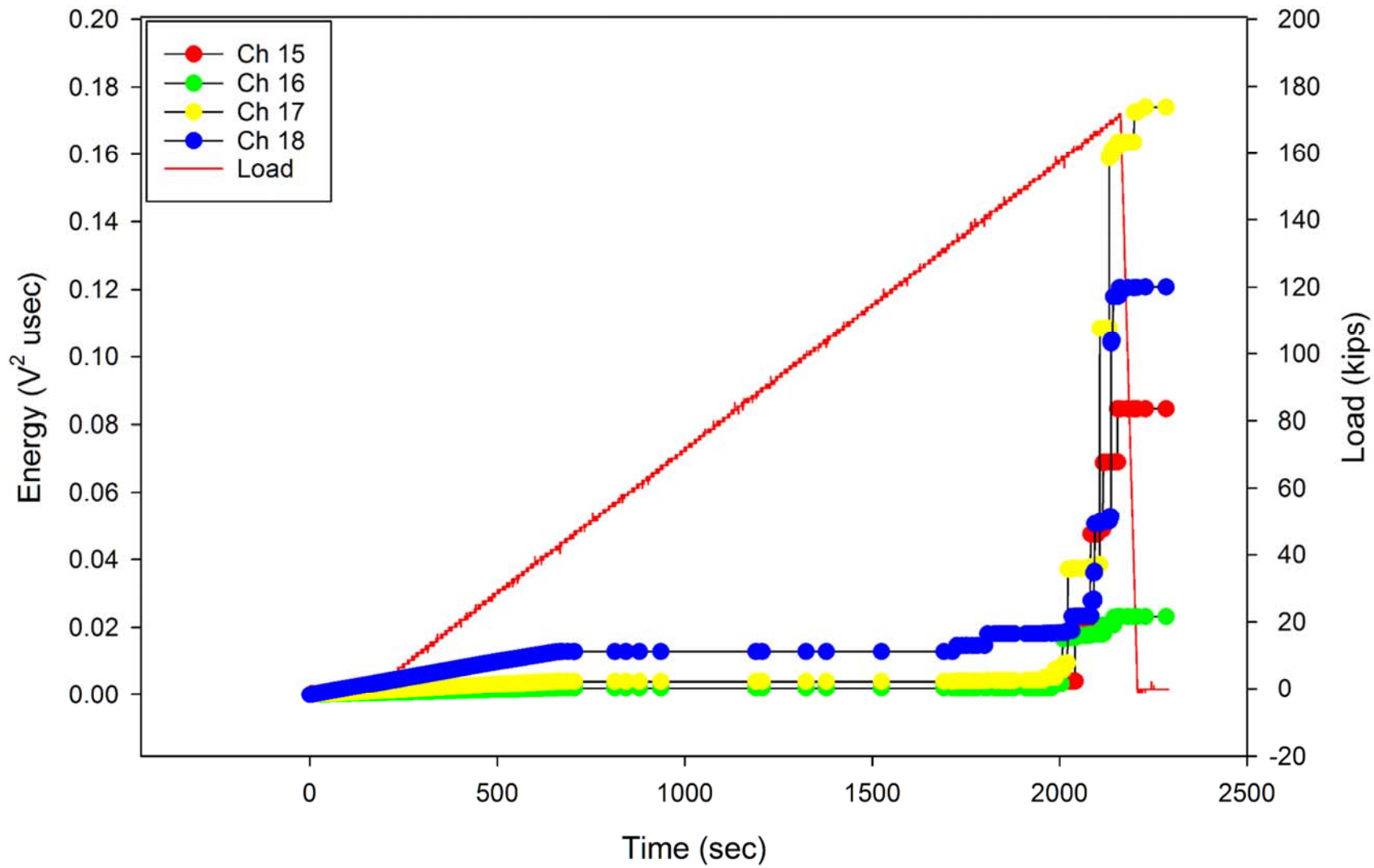


Figure C-8. Bulkheads AE Cumulative Energy by Channel: Phase III, DUL, 238.5 kips up-bending, Trial 1.
C10

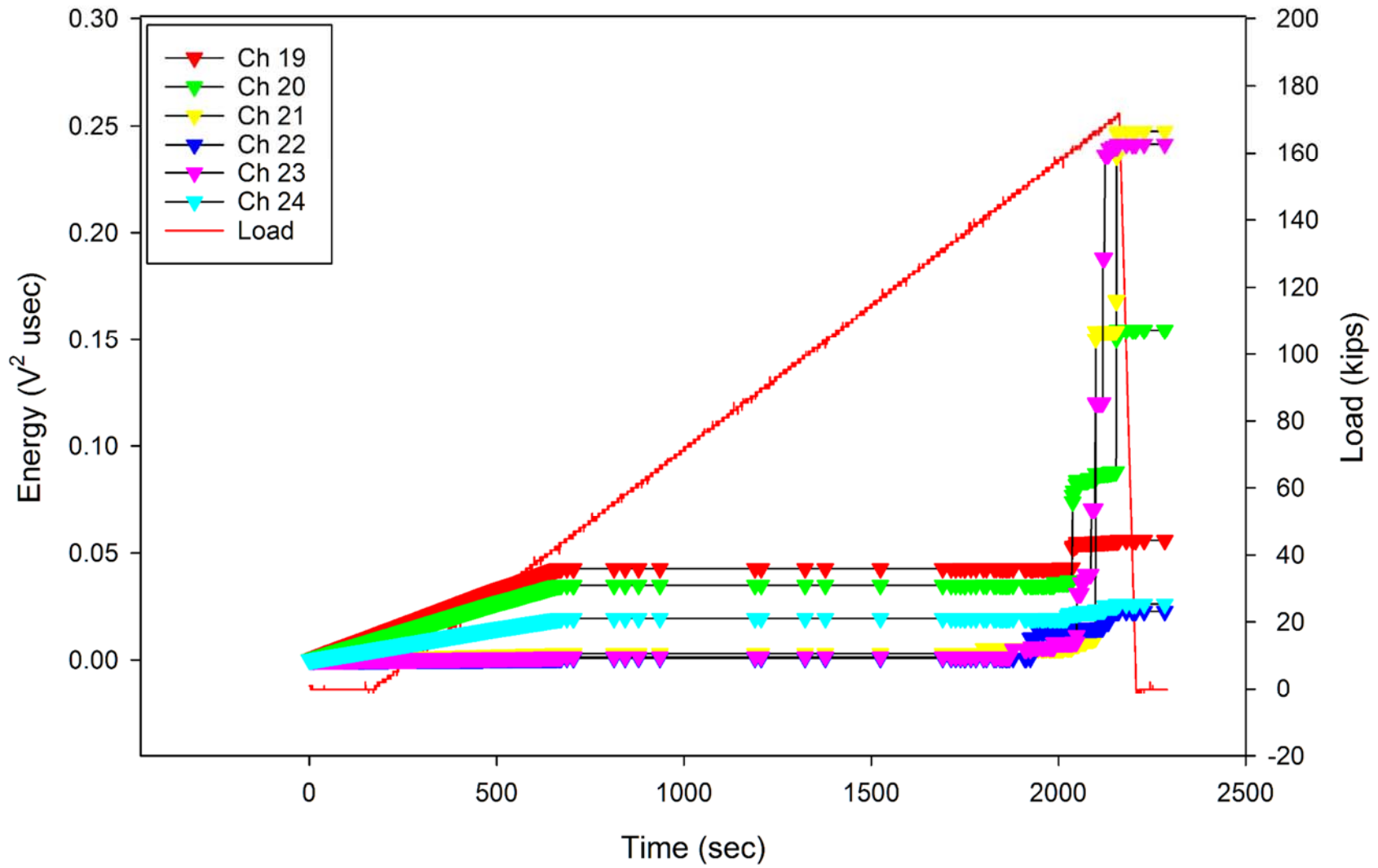


Figure C-9. Keel AE Cumulative Energy by Channel Ph III DUL, 238.5 kips up-bending, Trial 1.

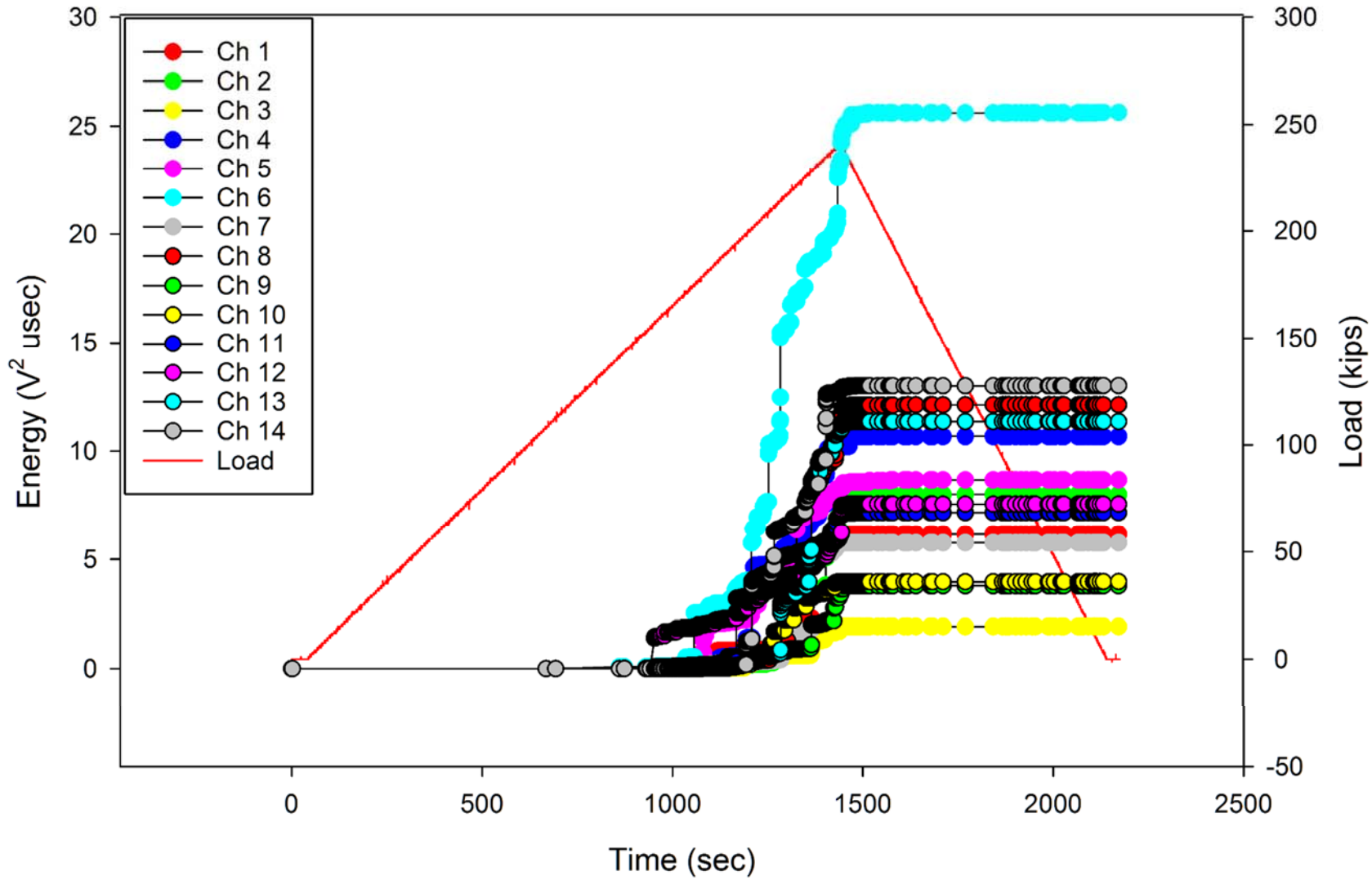


Figure C-10. Crown AE Cumulative Energy by Channel: Phase III, DUL, 238.5 kips up-bending, Trial 2.

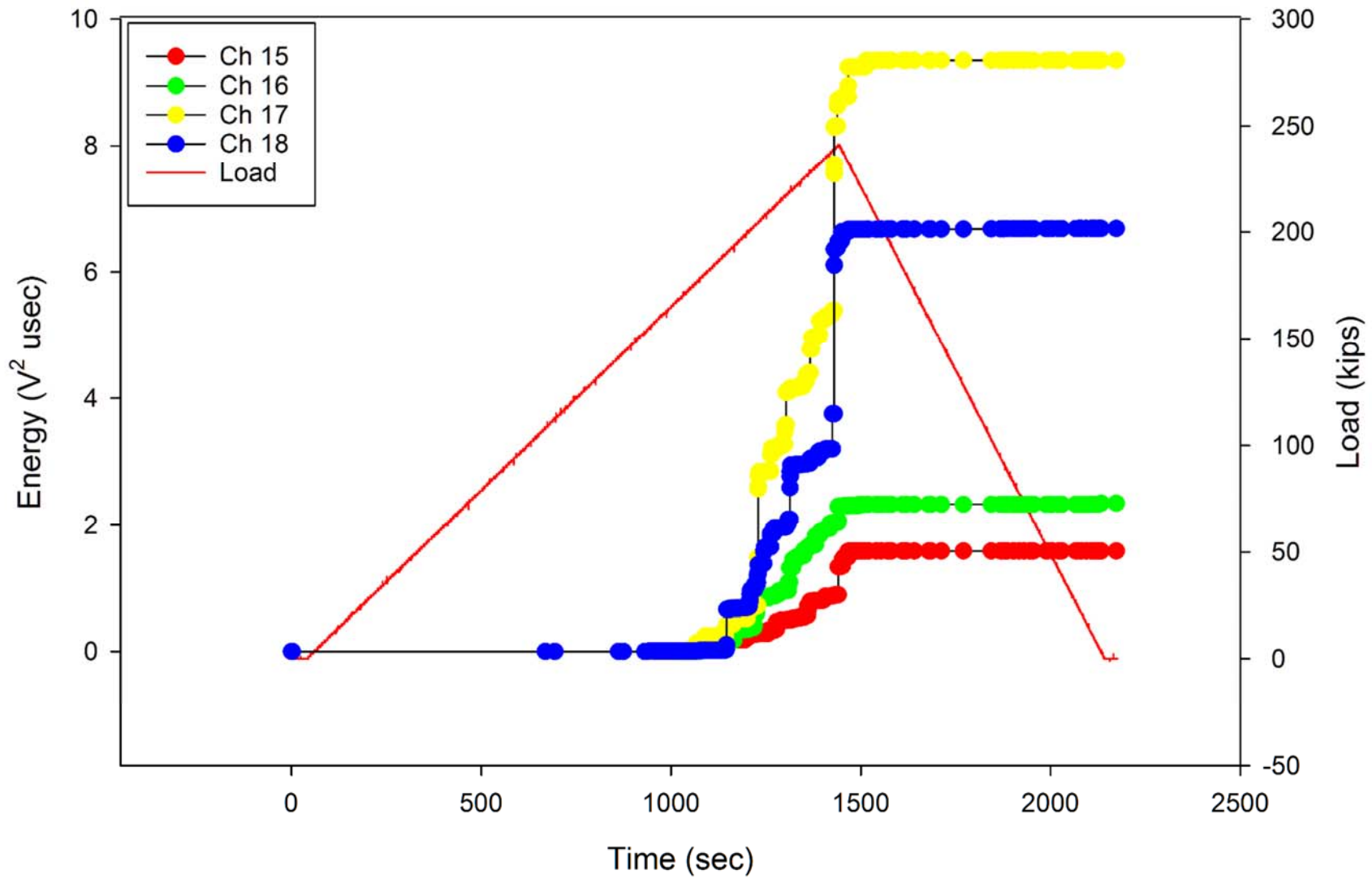


Figure C-11. Bulkheads AE Cumulative Energy by Channel Ph III DUL, 238.5 kips up-bending, Trial 2.
C13

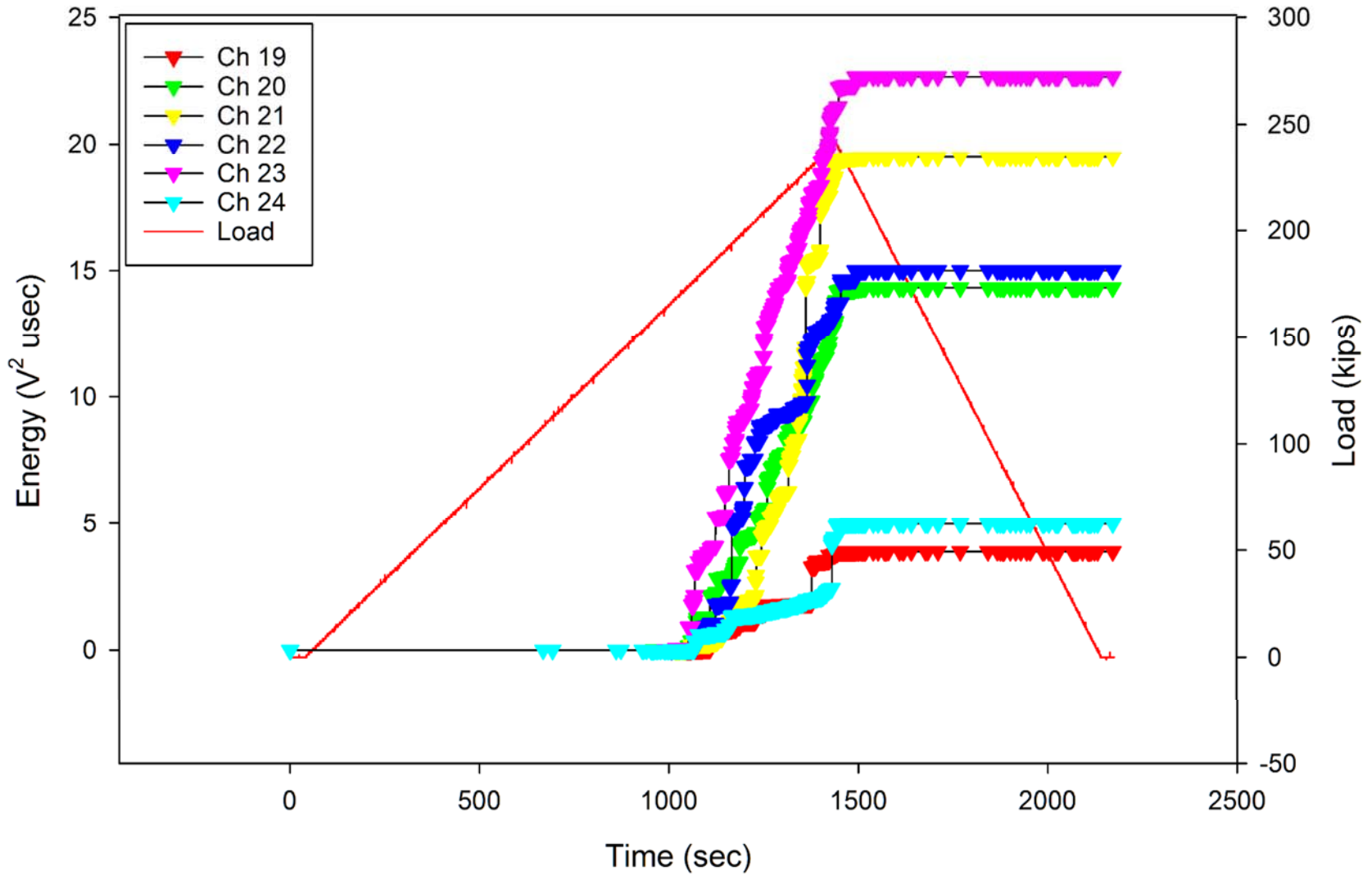


Figure C-12. Keel AE Cumulative Energy by Channel: Phase III, DUL, 238.5 kips up-bending, Trial 2.

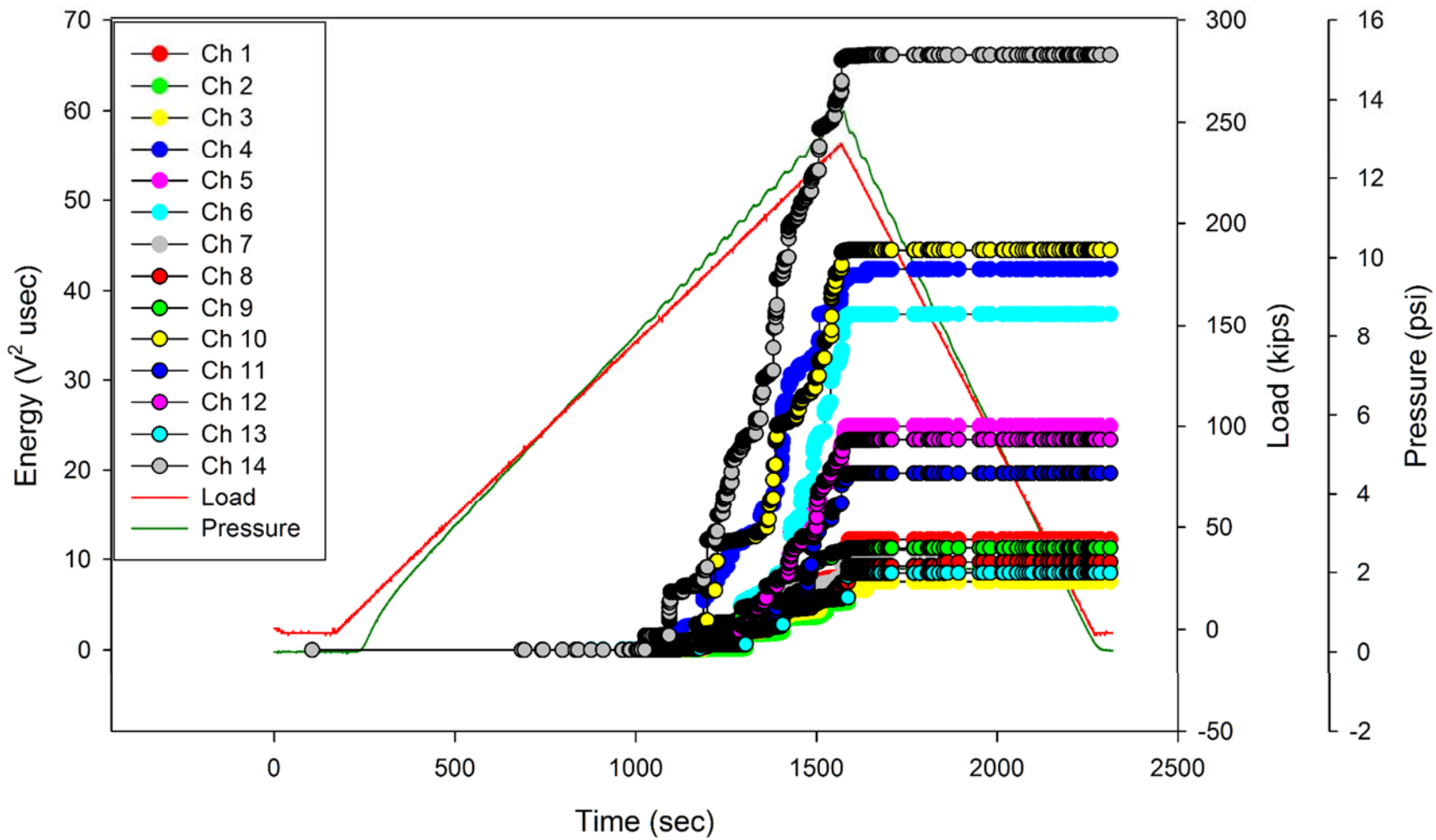


Figure C-13. Crown AE Cumulative Energy by Channel: Phase III, DUL, 238.5 kips up-bending + 13.8 psi.

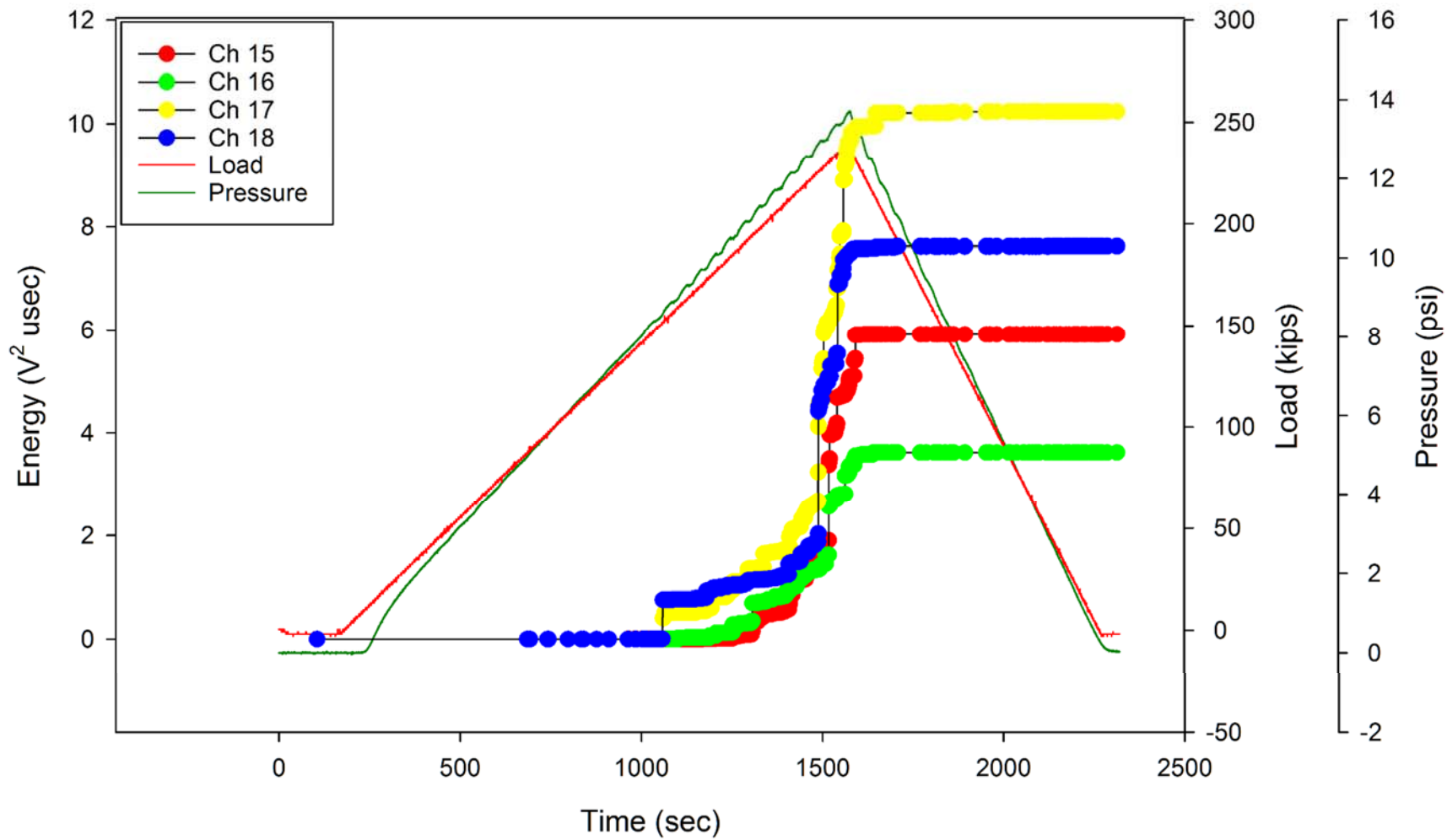


Figure C-14. Bulkheads AE Cumulative Energy by Channel: Phase III, DUL, 238.5 kips up-bending + 13.8 psi.

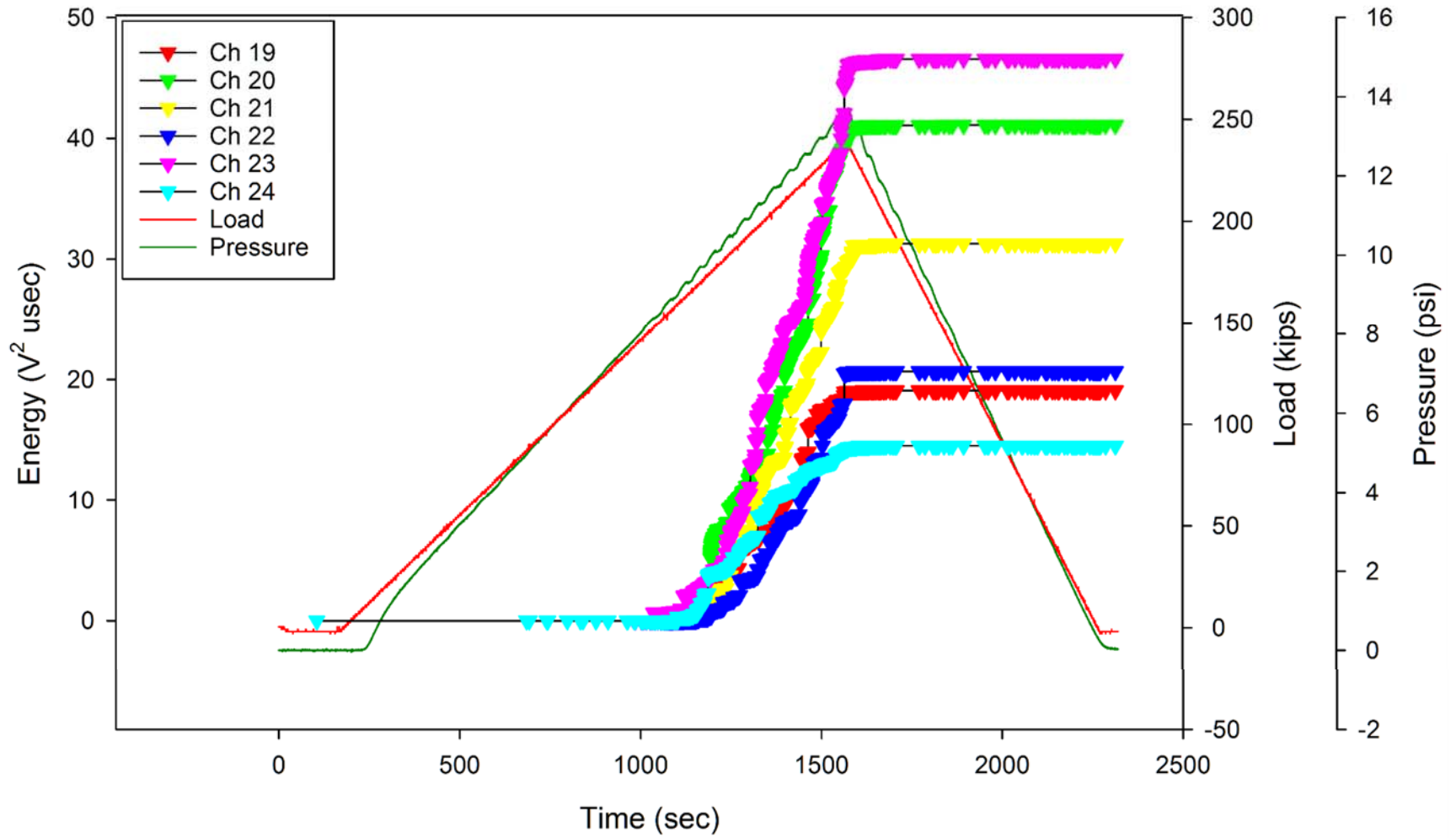


Figure C-15. Keel AE Cumulative Energy by Channel: Phase III, DUL, 238.5 kips up-bending + 13.8 psi.

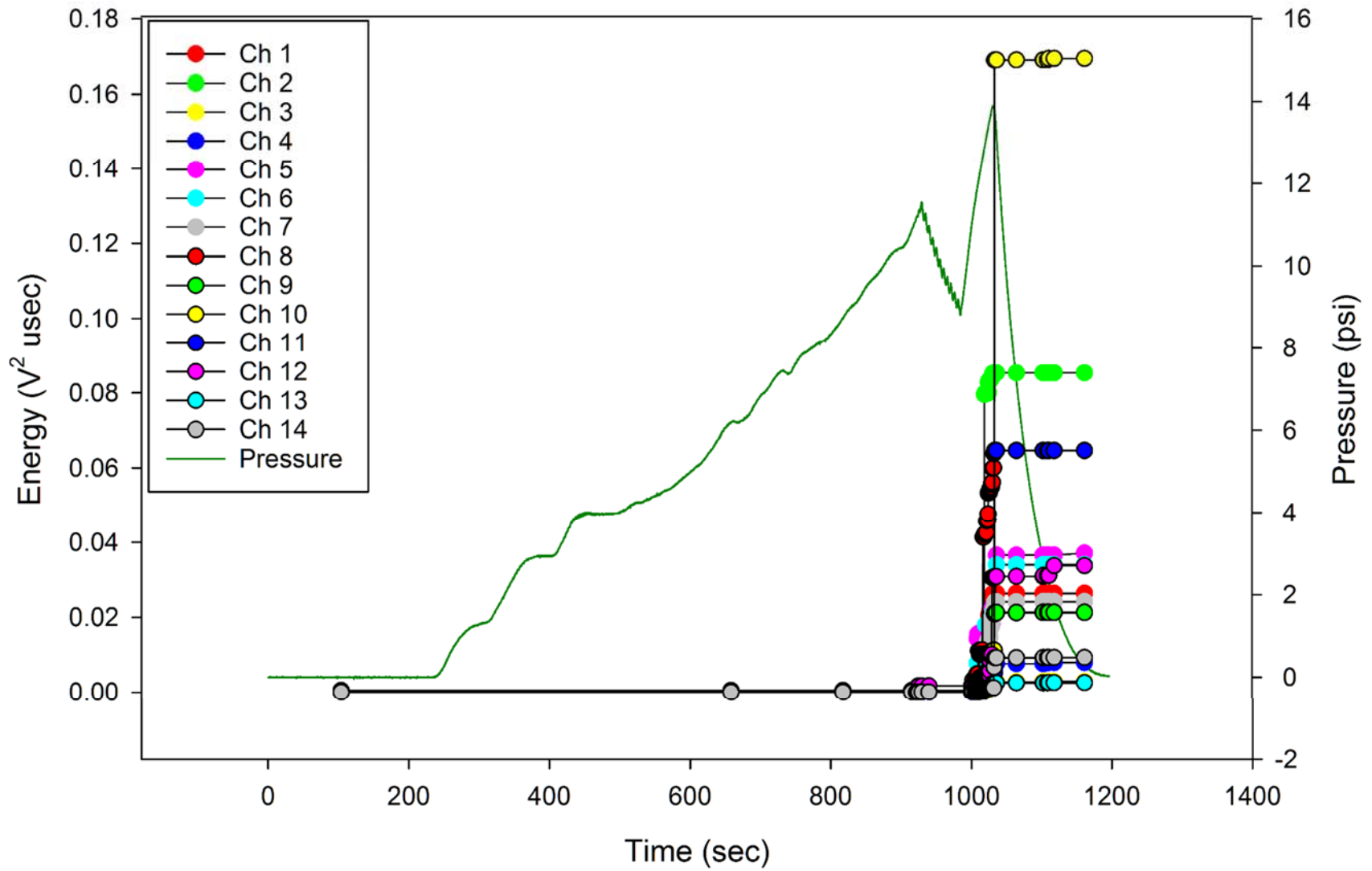


Figure C-16. Crown AE Cumulative Energy by Channel: Phase III, DUL, 18.4 psi, Trial 1.

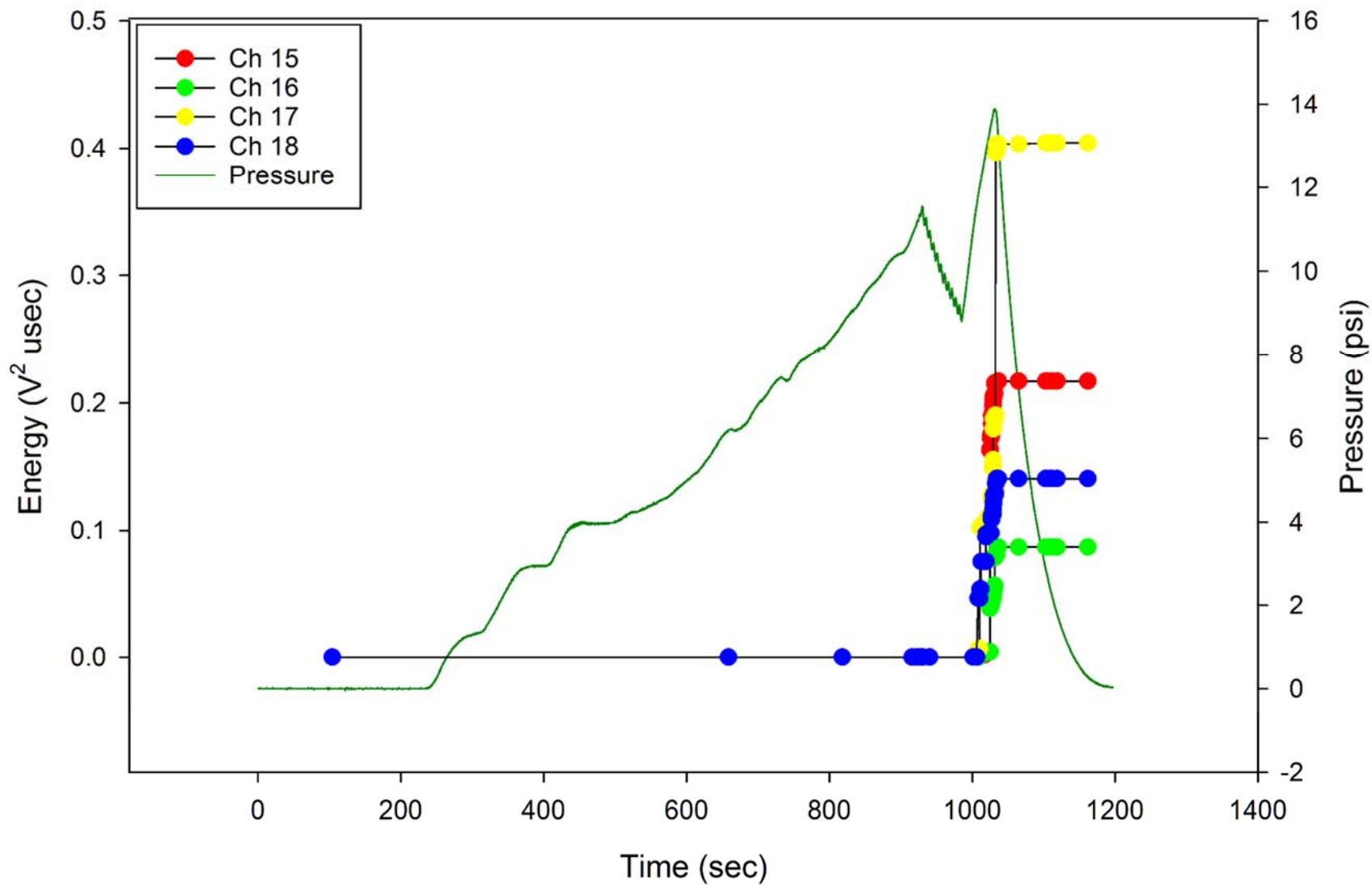


Figure C-17. Bulkheads AE Cumulative Energy by Channel: Phase III, DUL, 18.4 psi, Trial 1.

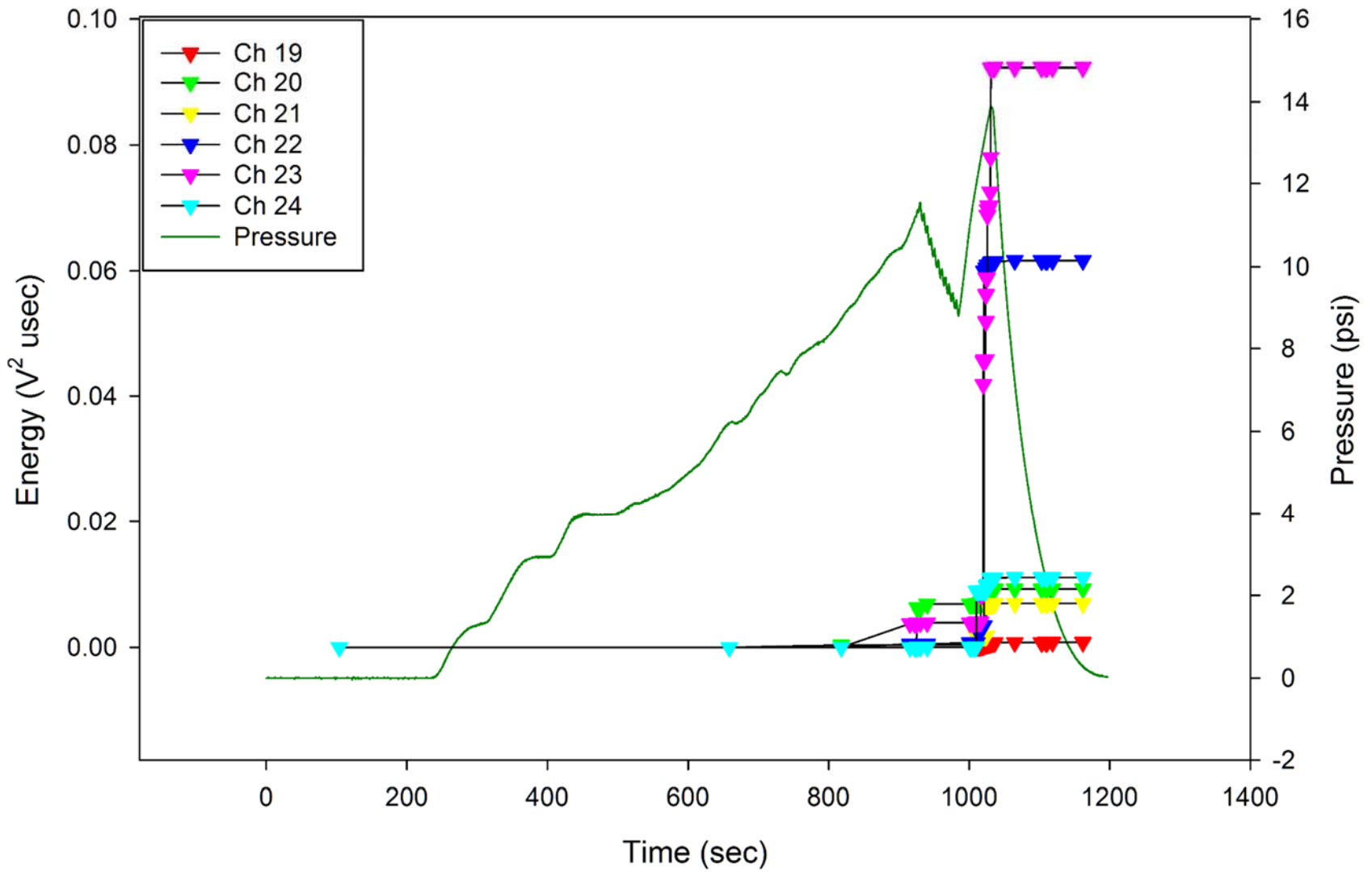


Figure C-18. Keel AE Cumulative Energy by Channel: Phase III, DUL, 18.4 psi, Trial 1.

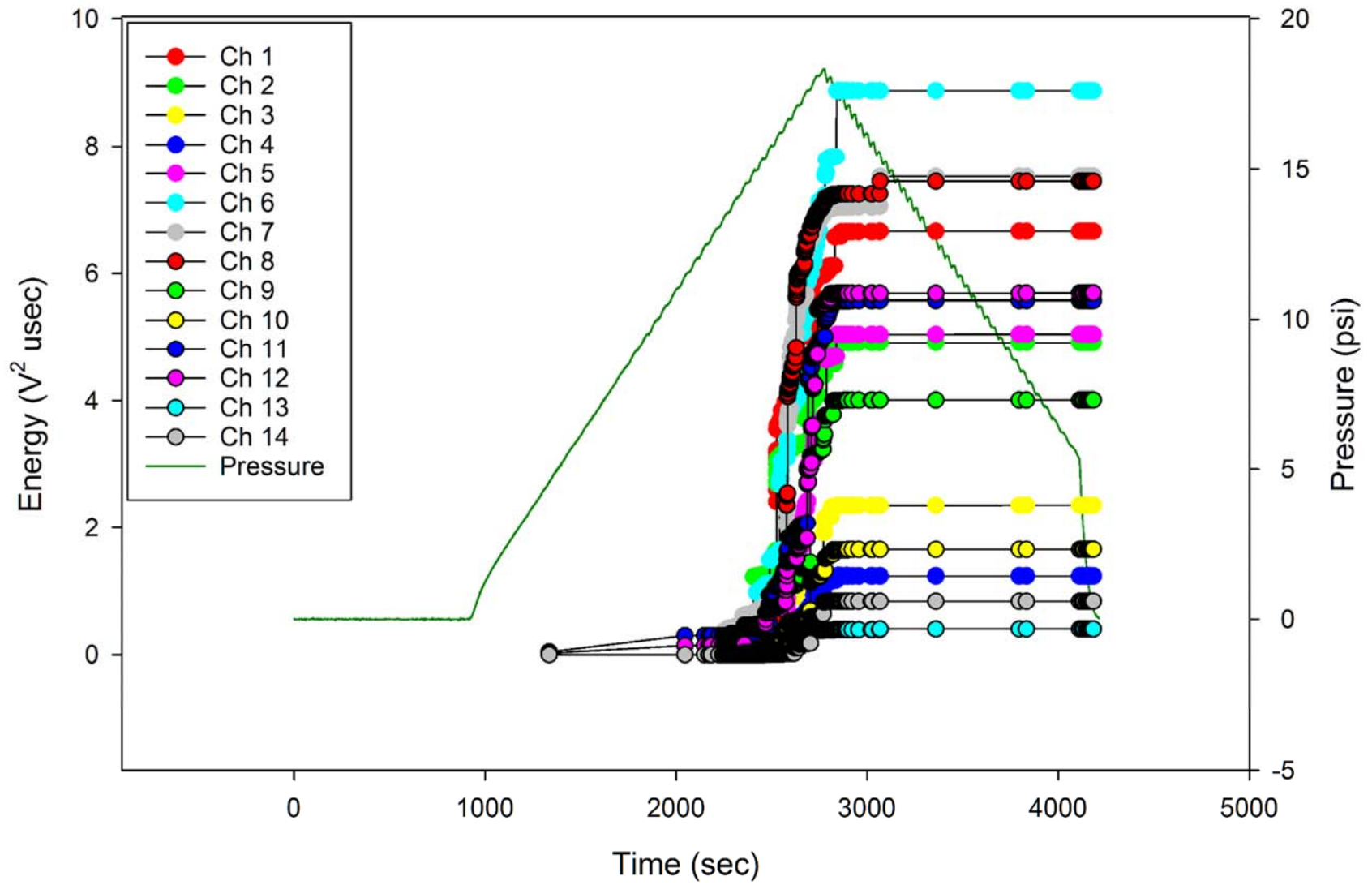


Figure C-19. Crown AE Cumulative Energy by Channel: Phase III, DUL, 18.4 psi, Trial 2.

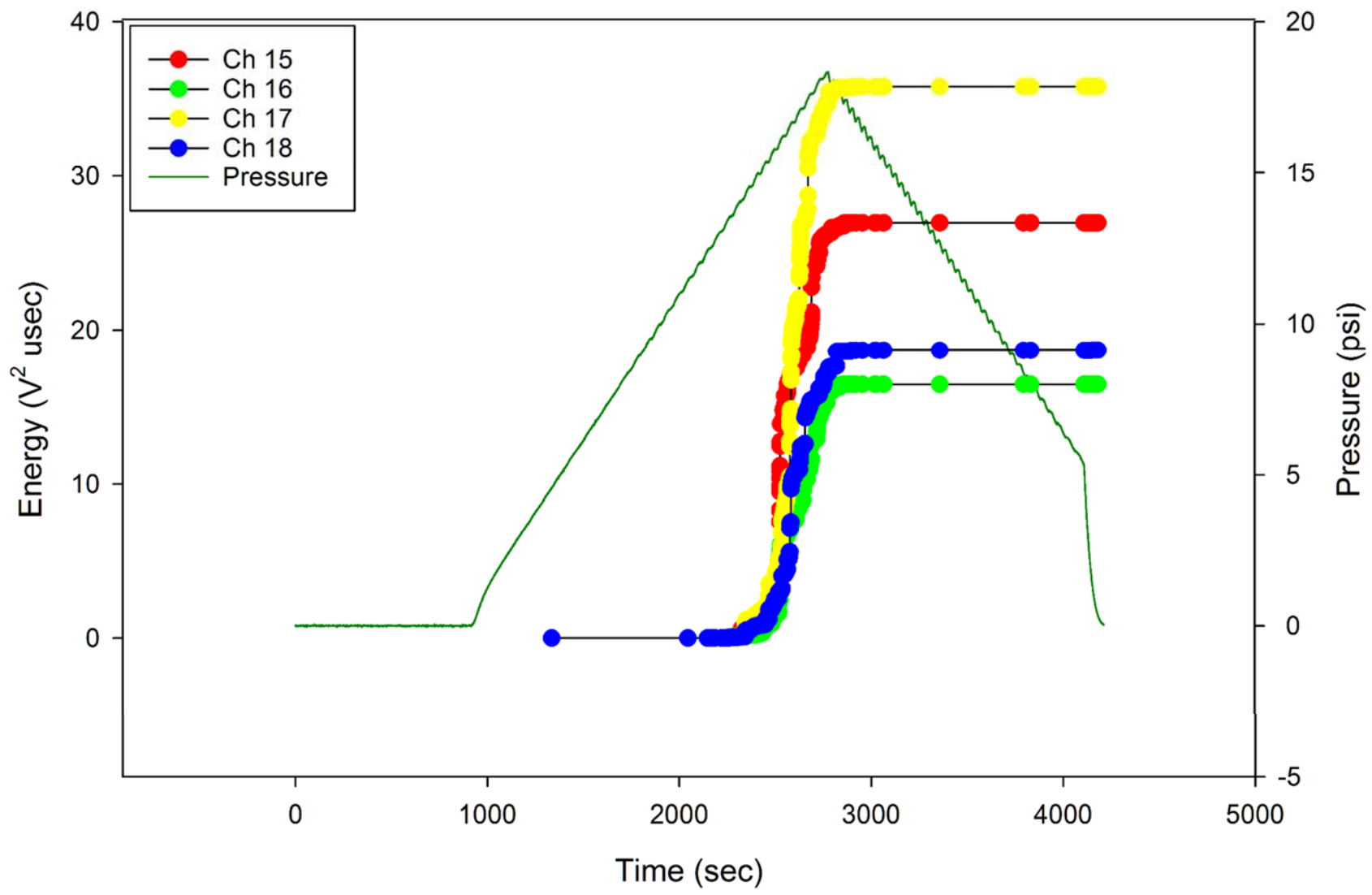


Figure C-20. Bulkheads AE Cumulative Energy by Channel: Phase III, DUL, 18.4 psi, Trial 2.

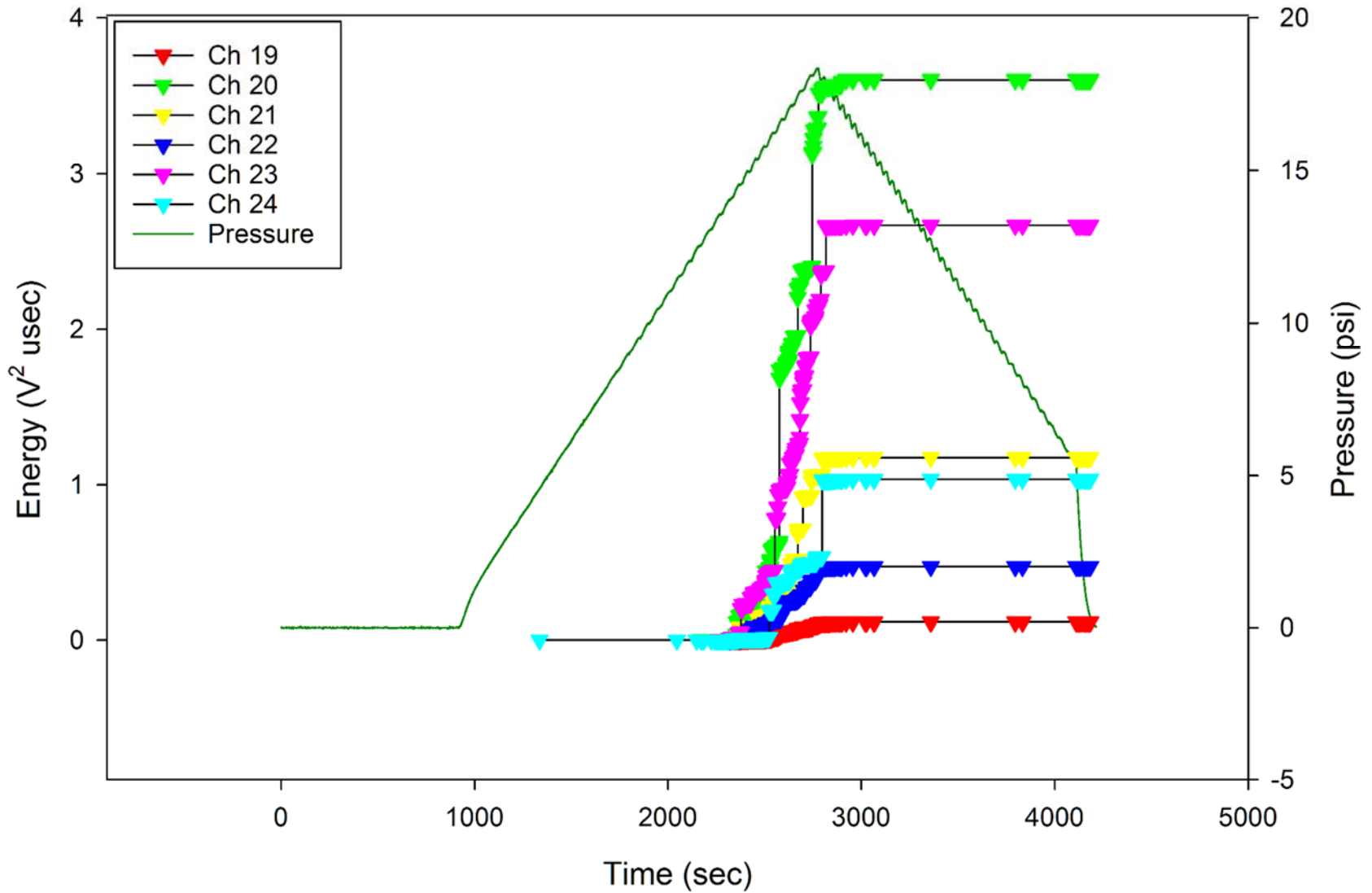


Figure C-21. Keel AE Cumulative Energy by Channel: Phase III, DUL, 18.4 psi, Trial 2.

Appendix D: Phase IV Post-Impact Checkout (PIC) Tests

Table of Figures

Figure D-1. Crown AE Cumulative Energy by Channel: Phase IV, PIC, 4.6 psi.	D3
Figure D-2. Bulkheads AE Cumulative Energy by Channel: Phase IV, PIC, 4.6 psi.	D4
Figure D-3. Keel AE Cumulative Energy by Channel: Phase IV, PIC, 4.6 psi.	D5
Figure D-4. Crown AE Cumulative Energy by Channel: Phase IV, PIC, 31.8 kips down-bending.	D6
Figure D-5. Bulkheads AE Cumulative Energy by Channel: Phase IV, PIC, 31.8 kips down-bending.	D7
Figure D-6. Keel AE Cumulative Energy by Channel: Phase IV, PIC, 31.8 kips down-bending.	D8
Figure D-7. Crown AE Cumulative Energy by Channel: Phase IV, PIC, 79.5 kips up-bending.	D9
Figure D-8. Bulkheads AE Cumulative Energy by Channel: Phase IV, PIC, 79.5 kips up-bending.	D10
Figure D-9. Keel AE Cumulative Energy by Channel: Phase IV, PIC, 79.5 kips up-bending.	D11
Figure D-10. Crown AE Cumulative Energy by Channel: Phase IV, PIC, 31.8 kips down-bending + 4.6 psi.	D12
Figure D-11. Bulkheads AE Cumulative Energy by Channel: Phase IV, PIC, 31.8 kips down-bending + 4.6 psi.	D13
Figure D-12. Keel AE Cumulative Energy by Channel: Phase IV, PIC, 31.8 kips down-bending + 4.6 psi.	D14
Figure D-13. Crown AE Cumulative Energy by Channel: Phase IV, PIC, 79.5 kips up-bending + 4.6 psi.	D15
Figure D-14. Bulkheads AE Cumulative Energy by Channel: Phase IV, PIC, 79.5 kips up-bending + 4.6 psi.	D16
Figure D-15. Keel AE Cumulative Energy by Channel: Phase IV, PIC, 79.5 kips up-bending + 4.6 psi.	D17

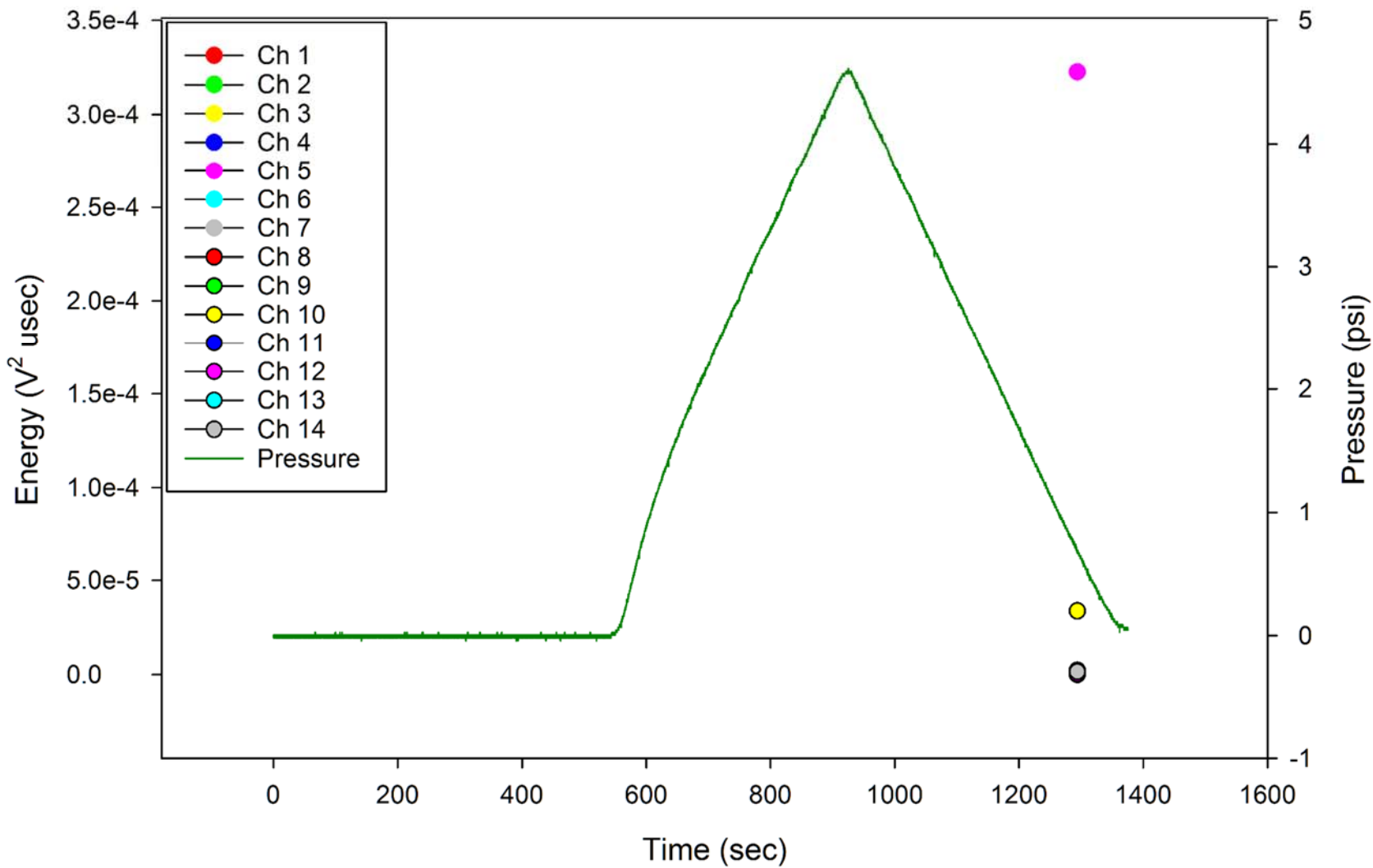


Figure D-1. Crown AE Cumulative Energy by Channel: Phase IV, PIC, 4.6 psi.

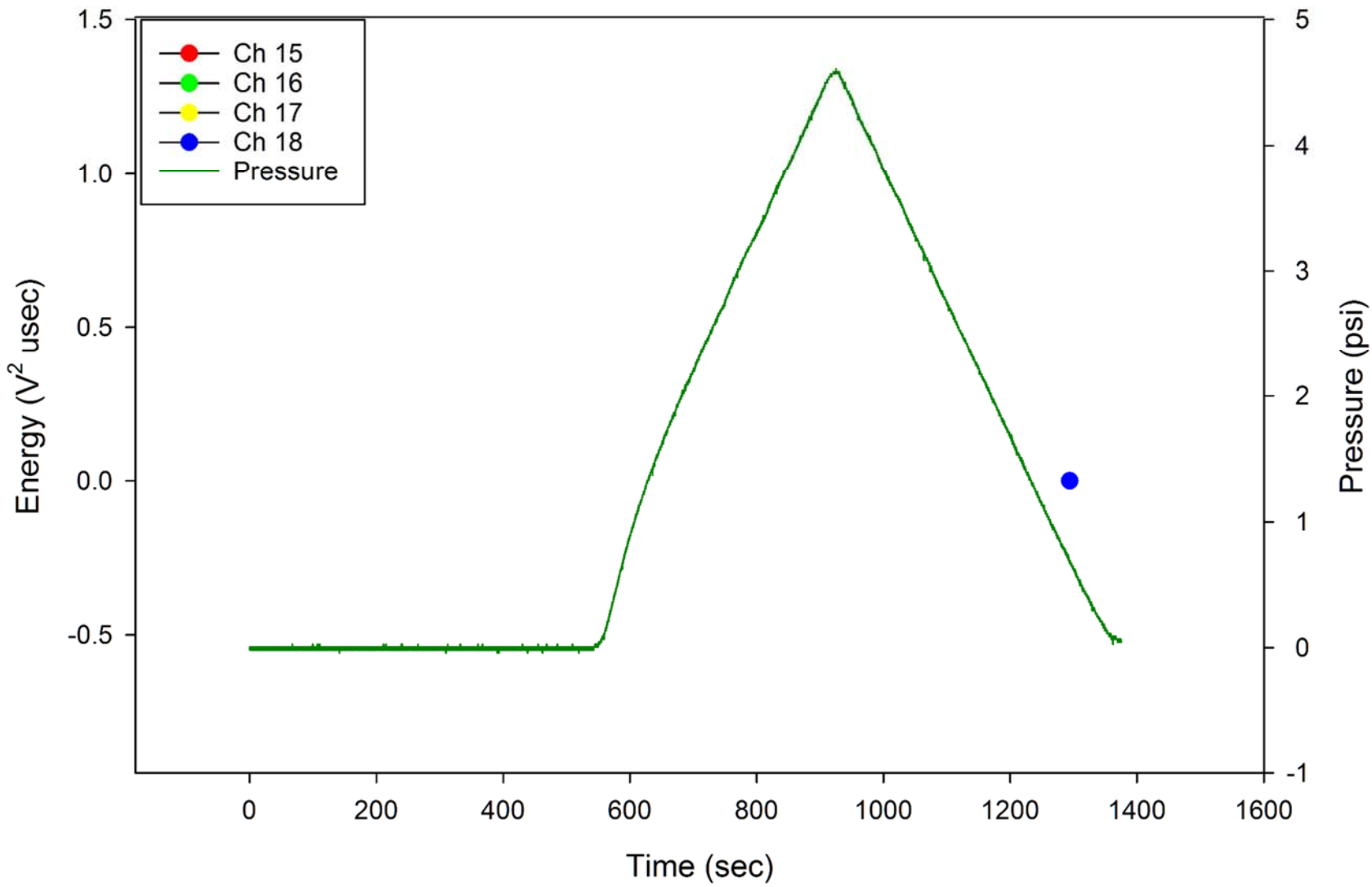


Figure D-2. Bulkheads AE Cumulative Energy by Channel: Phase IV, PIC, 4.6 psi.

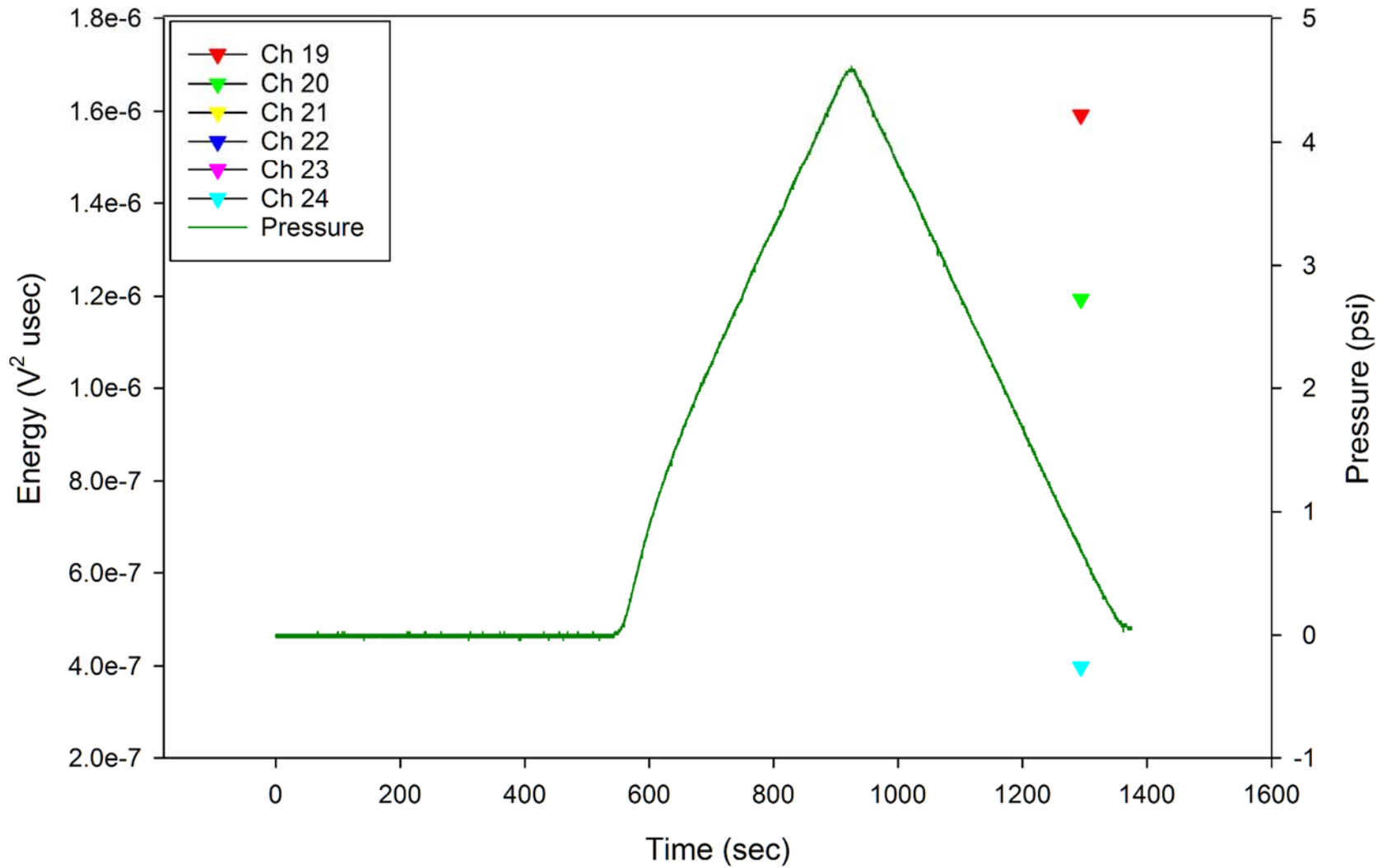


Figure D-3. Keel AE Cumulative Energy by Channel: Phase IV, PIC, 4.6 psi.

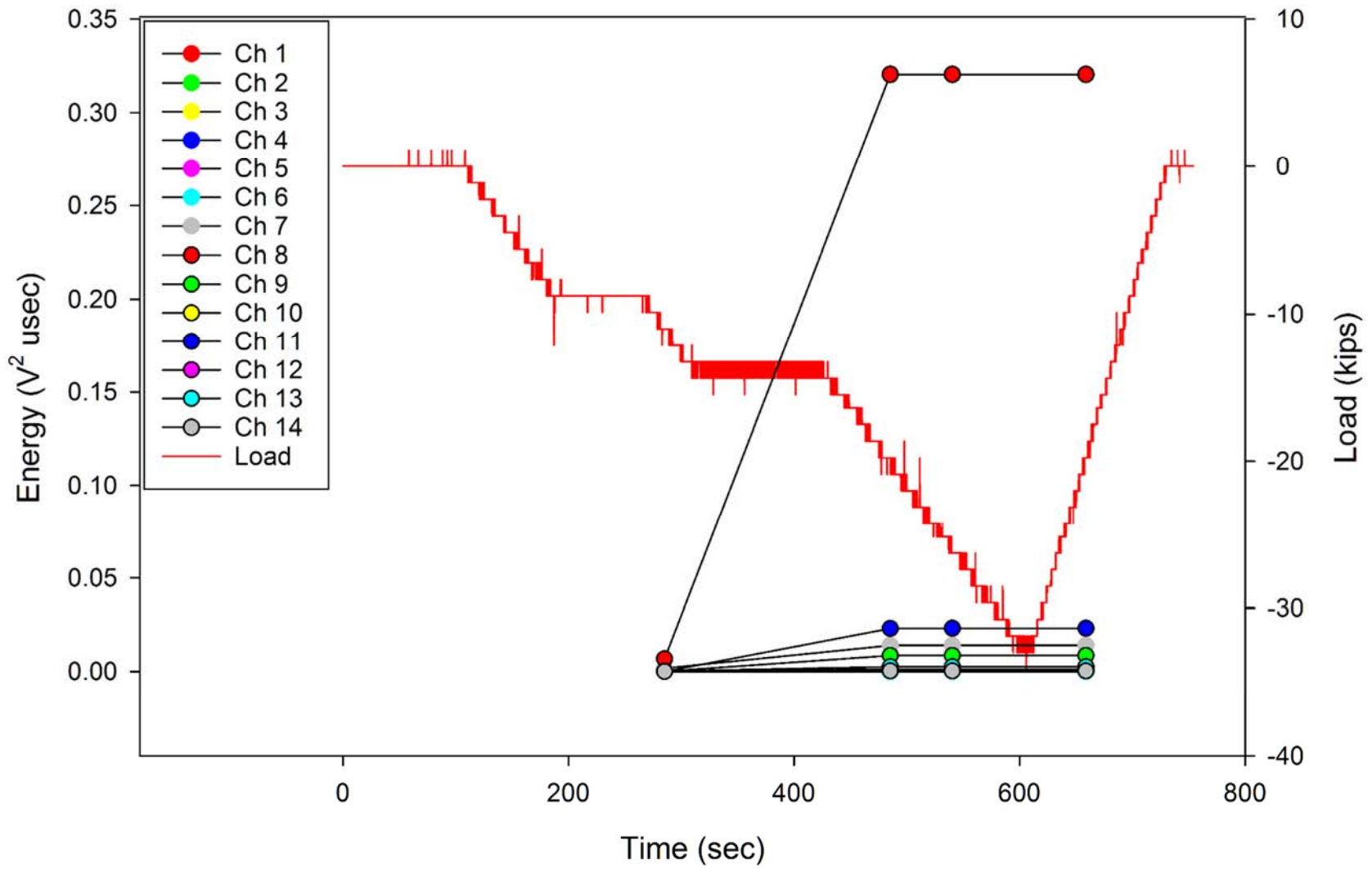


Figure D-4. Crown AE Cumulative Energy by Channel: Phase IV, PIC, 31.8 kips down-bending.

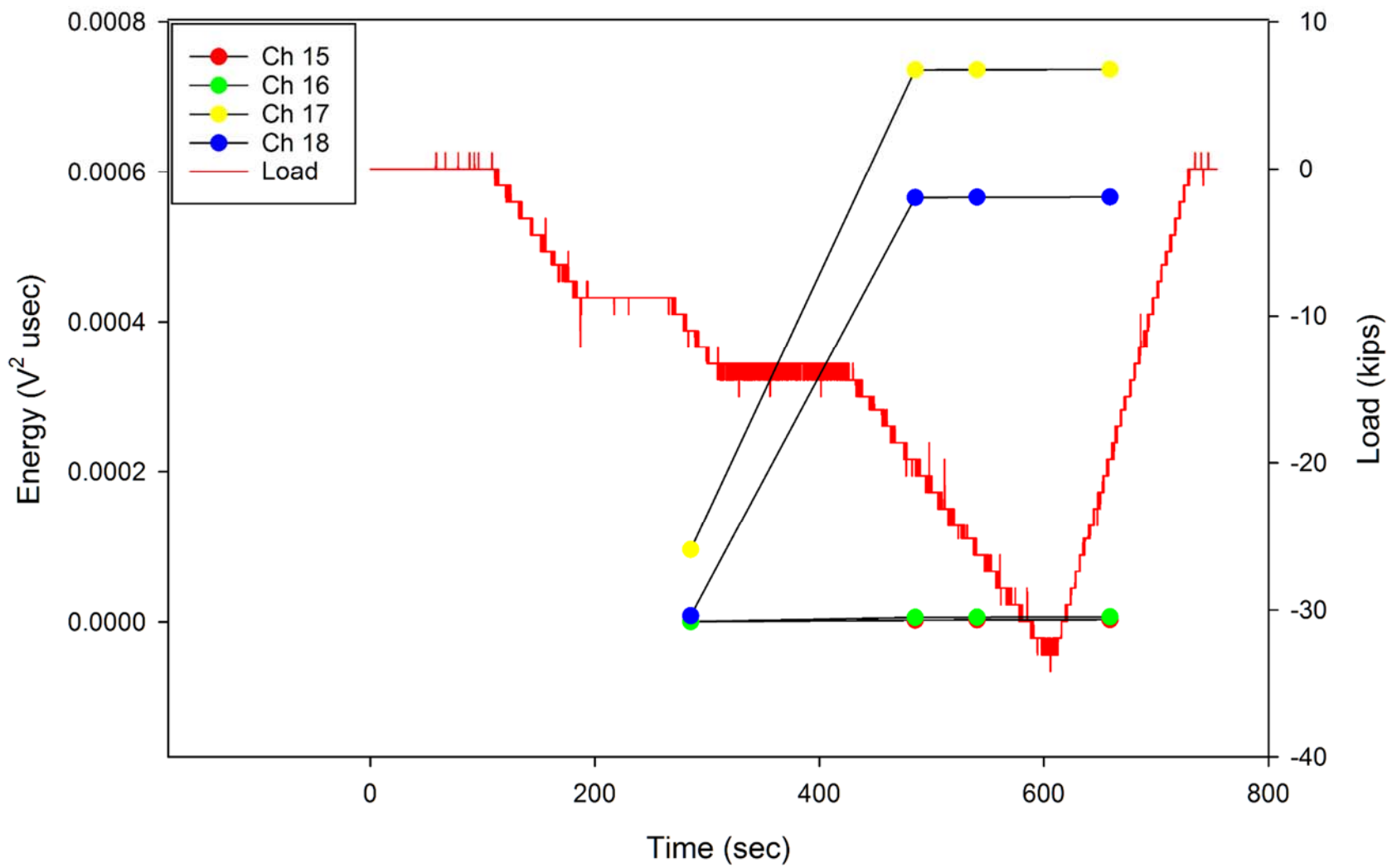


Figure D-5. Bulkheads AE Cumulative Energy by Channel: Phase IV, PIC, 31.8 kips down-bending.

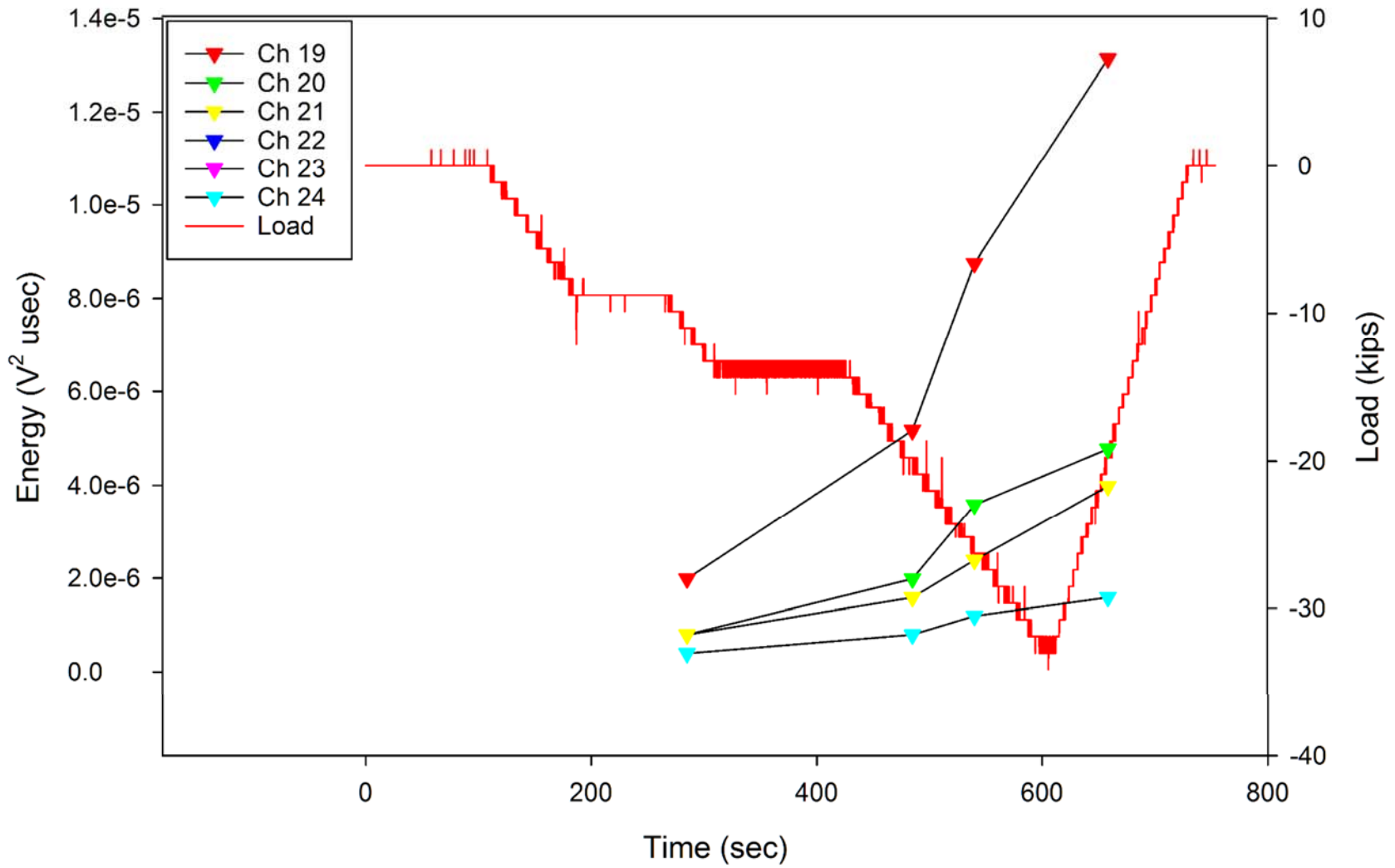


Figure D-6. Keel AE Cumulative Energy by Channel: Phase IV, PIC, 31.8 kips down-bending.

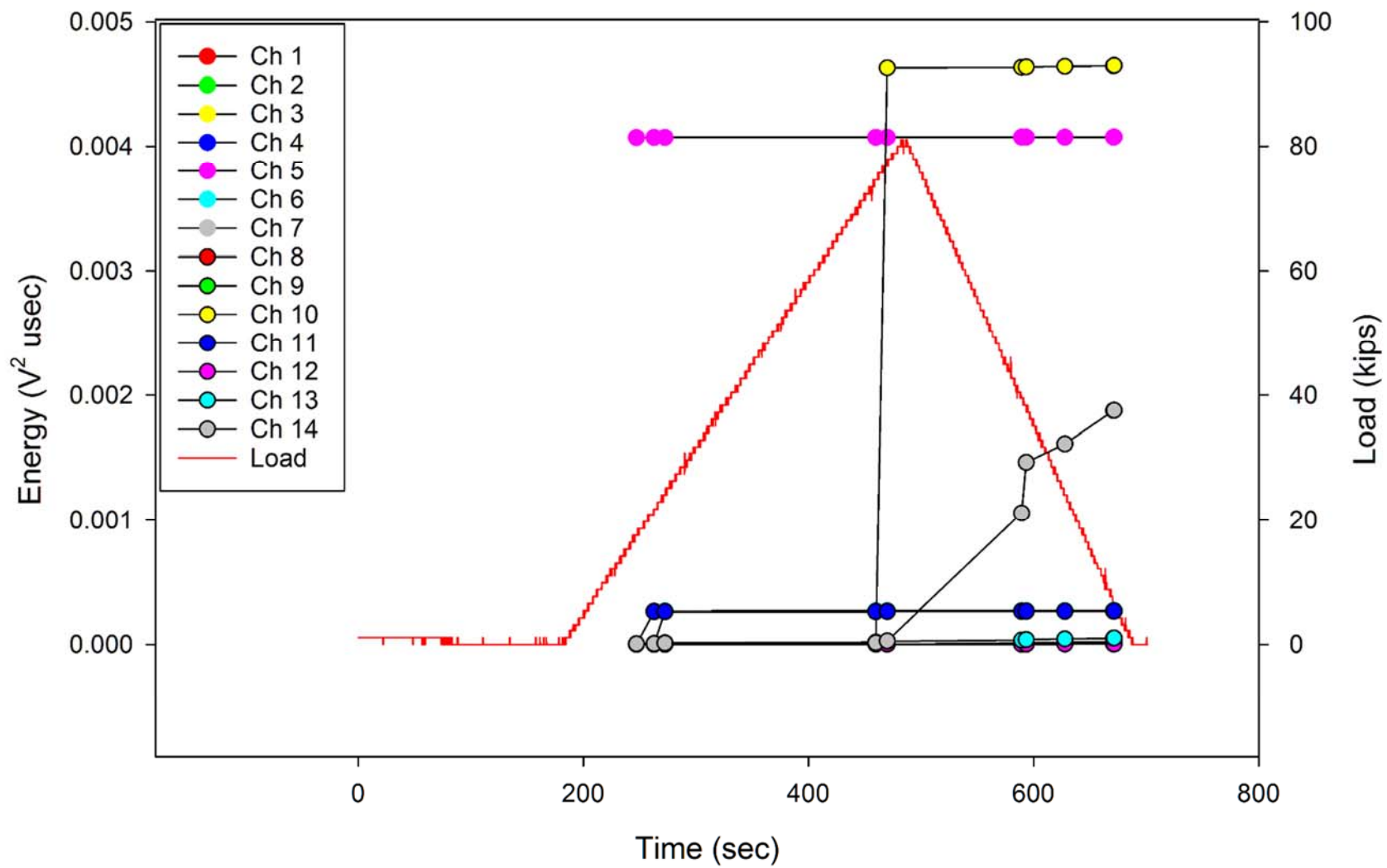


Figure D-7. Crown AE Cumulative Energy by Channel: Phase IV, PIC, 79.5 kips up-bending.

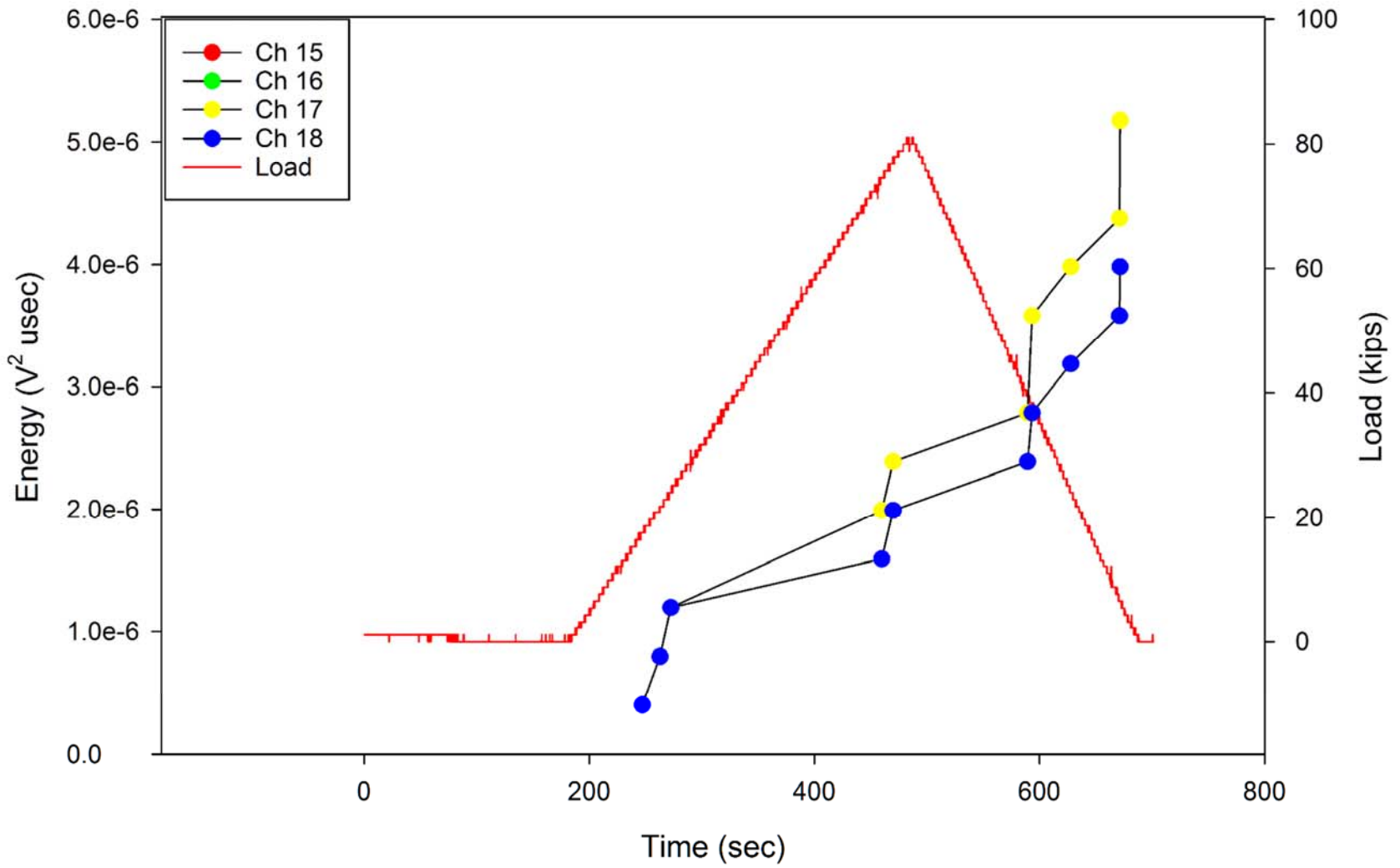


Figure D-8. Bulkheads AE Cumulative Energy by Channel: Phase IV, PIC, 79.5 kips up-bending.

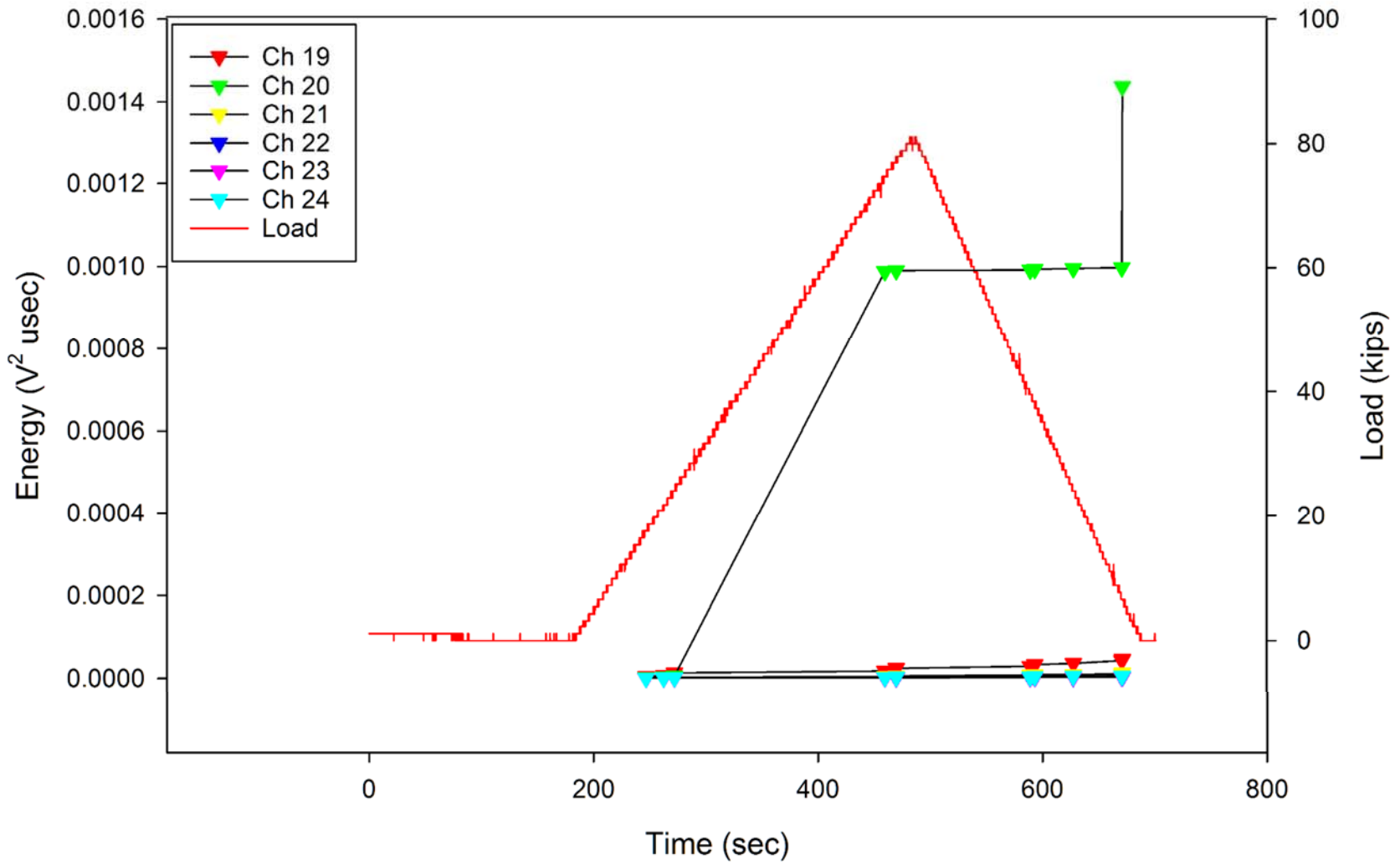


Figure D-9. Keel AE Cumulative Energy by Channel: Phase IV, PIC, 79.5 kips up-bending.

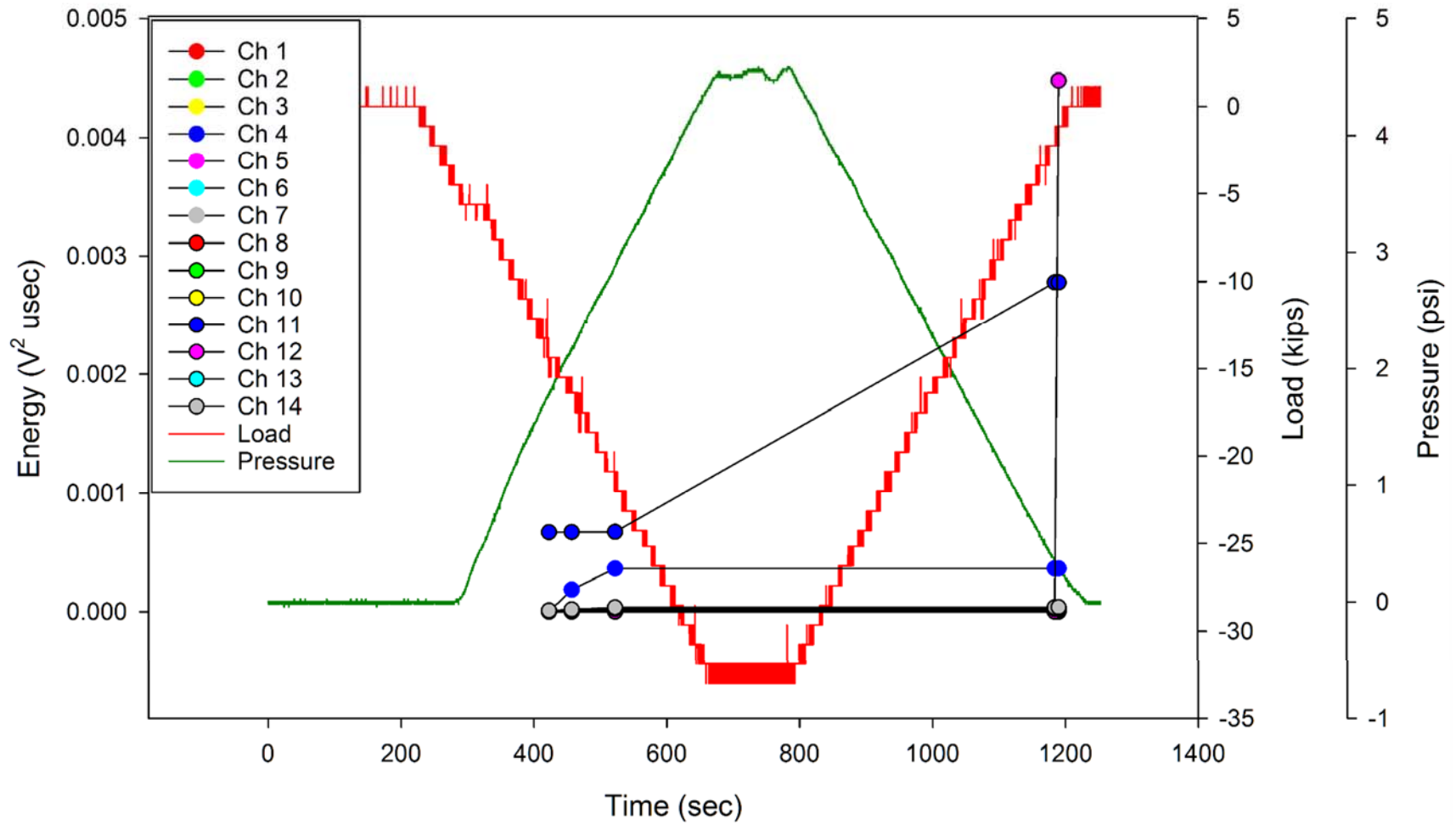


Figure D-10. Crown AE Cumulative Energy by Channel: Phase IV, PIC, 31.8 kips down-bending + 4.6 psi.

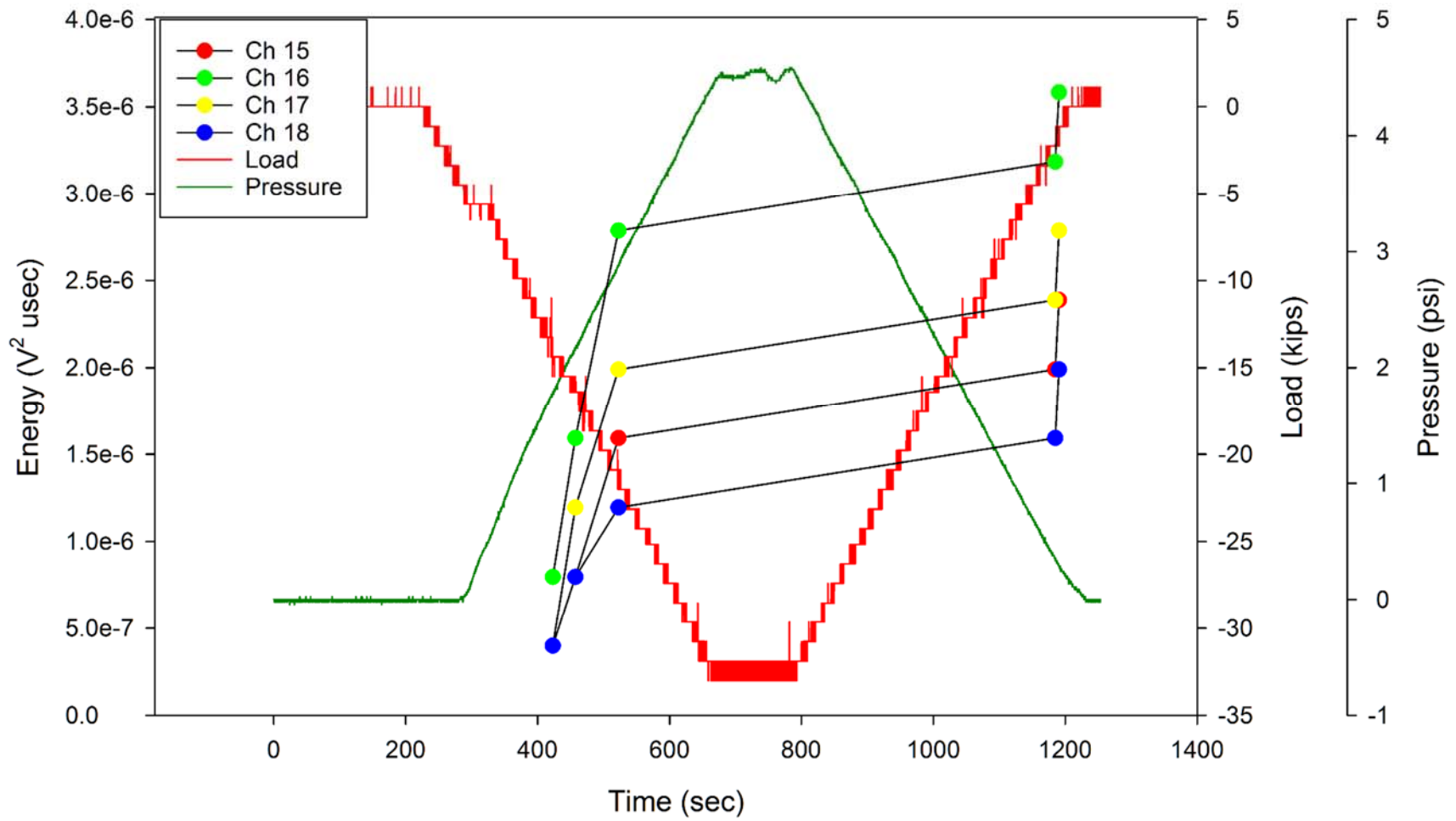


Figure D-11. Bulkheads AE Cumulative Energy by Channel: Phase IV, PIC, 31.8 kips down-bending + 4.6 psi.

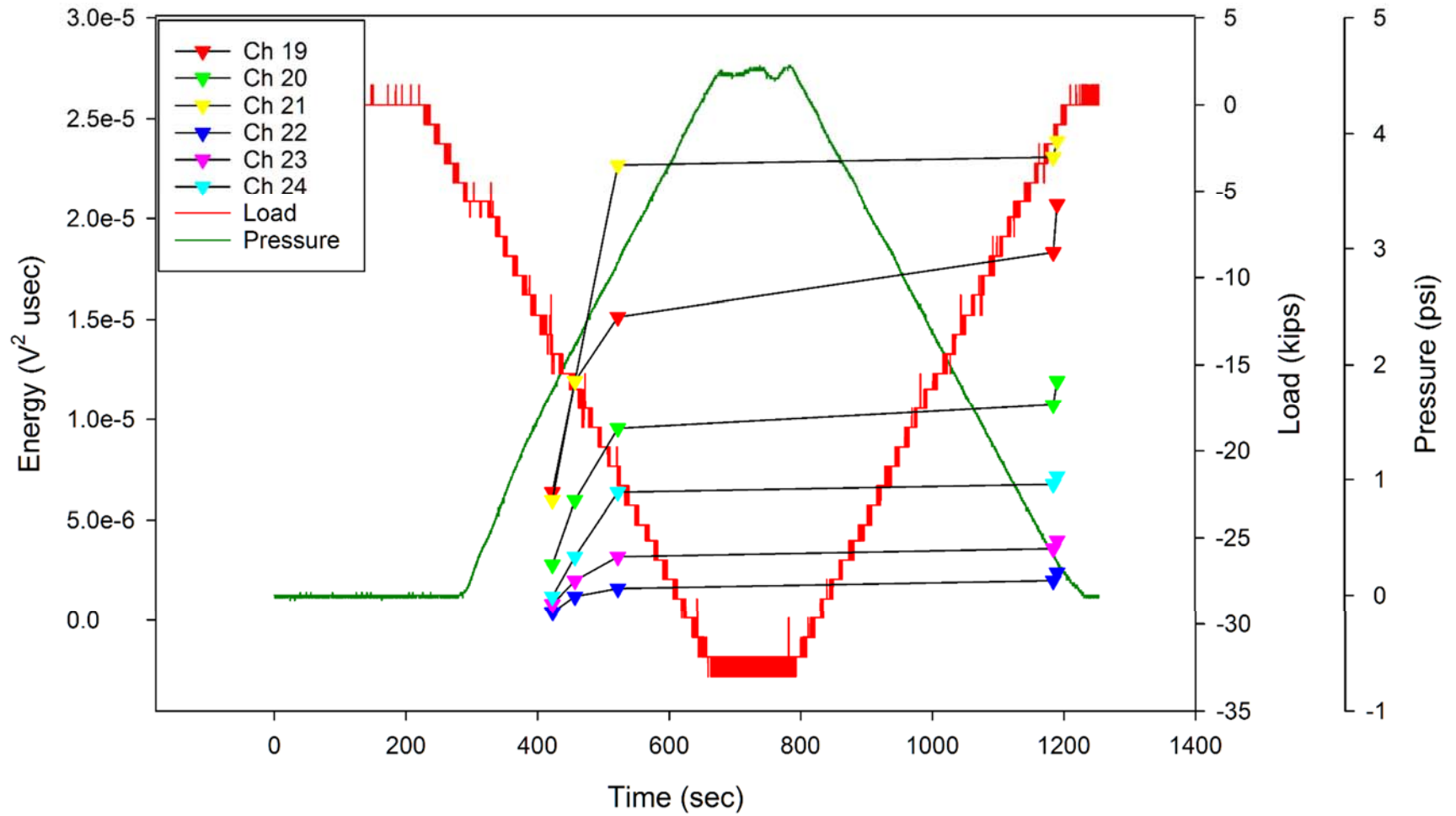


Figure D-12. Keel AE Cumulative Energy by Channel: Phase IV, PIC, 31.8 kips down-bending + 4.6 psi.

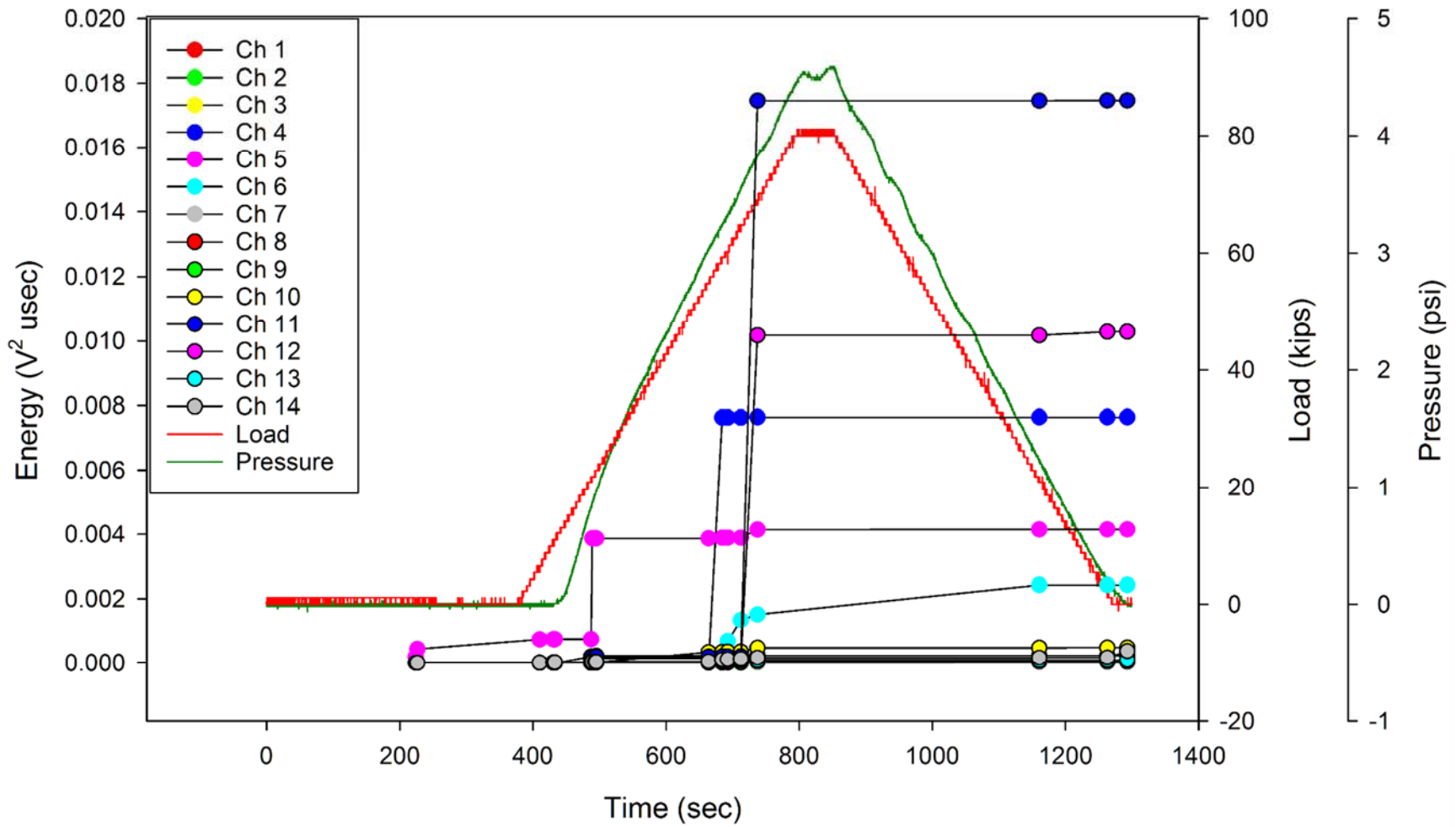


Figure D-13. Crown AE Cumulative Energy by Channel: Phase IV, PIC, 79.5 kips up-bending + 4.6 psi.

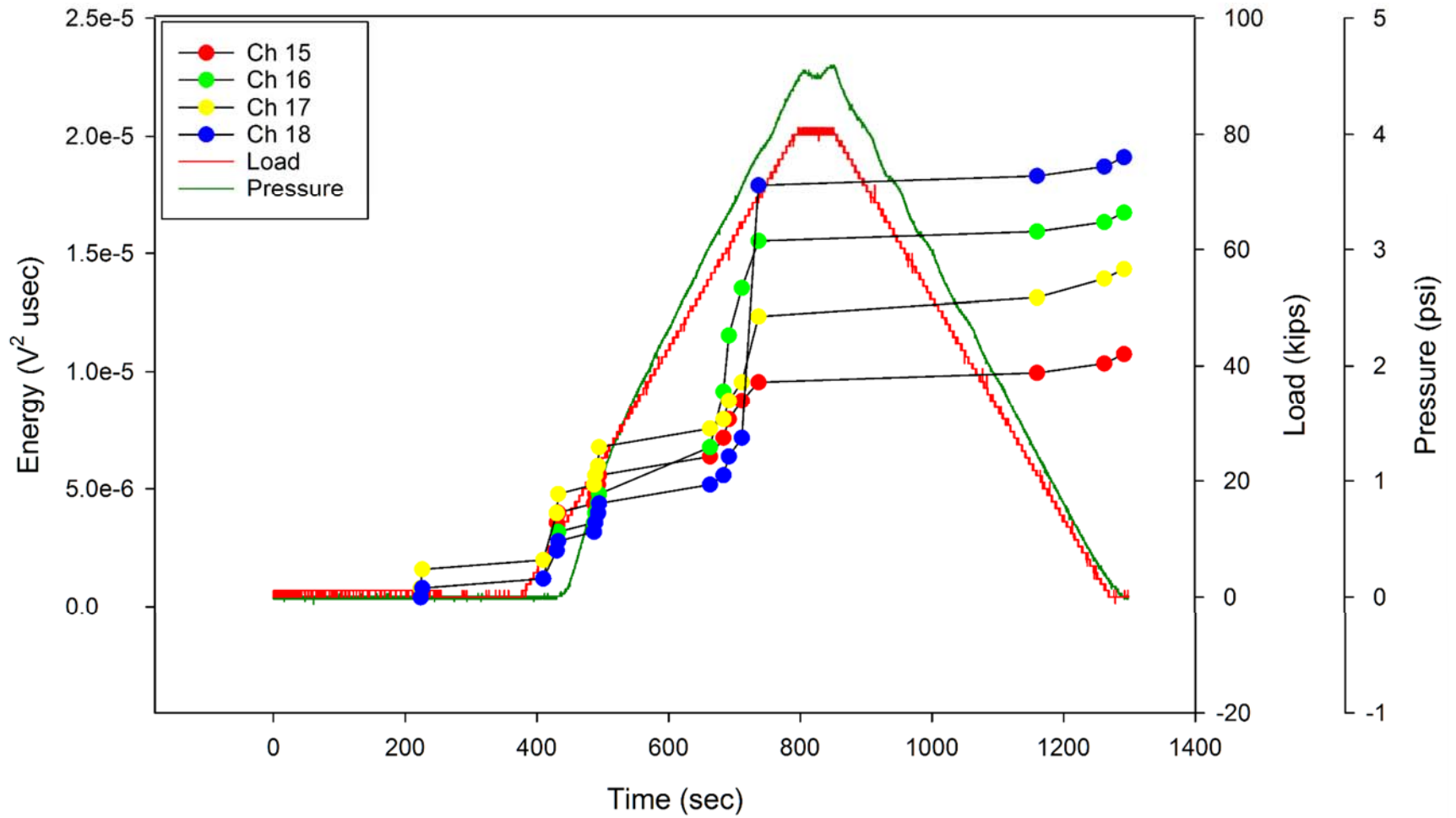


Figure D-14. Bulkheads AE Cumulative Energy by Channel: Phase IV, PIC, 79.5 kips up-bending + 4.6 psi.

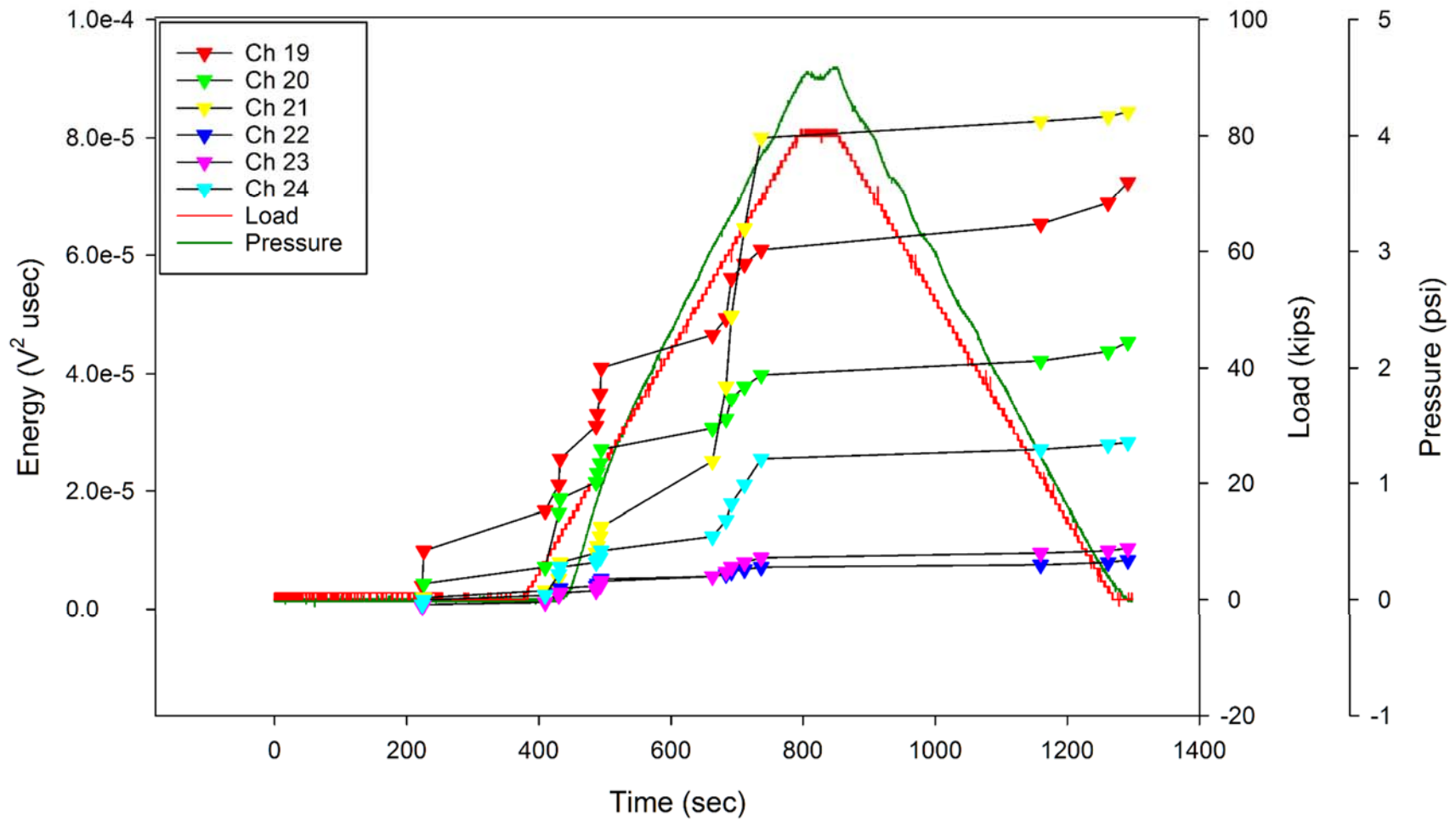


Figure D-15. Keel AE Cumulative Energy by Channel: Phase IV, PIC, 79.5 kips up-bending + 4.6 psi.

Appendix E: Phase V Post-impact DLL (PI DLL) Tests

Table of Figures

Figure E-1. Crown AE Cumulative Energy by Channel: Phase V, PI DLL, 63.6 kips down-bending.....	E3
Figure E-2. Bulkheads AE Cumulative Energy by Channel: Phase V, PI DLL, 63.6 kips down-bending.....	E4
Figure E-3. Keel AE Cumulative Energy by Channel: Phase V, PI DLL, 63.6 kips down-bending.....	E5
Figure E-4. Crown AE Cumulative Energy by Channel: Phase V, PI DLL, 63.6 kips down-bending + 9.2 psi.....	E6
Figure E-5. Bulkheads AE Cumulative Energy by Channel: Phase V, PI DLL, 63.6 kips down-bending + 9.2 psi.....	E7
Figure E-6. Keel AE Cumulative Energy by Channel: Phase V, PI DLL, 63.6 kips down-bending + 9.2 psi.....	E8
Figure E-7. Crown AE Cumulative Energy by Channel: Phase V, PI DLL, 12.2 psi.....	E9
Figure E-8. Bulkheads AE Cumulative Energy by Channel: Phase V, PI DLL, 12.2 psi.....	E10
Figure E-9. Keel AE Cumulative Energy by Channel: Phase V, PI DLL, 12.2 psi.....	E11
Figure E-10. Crown AE Cumulative Energy by Channel: Phase V, PI DLL, 159 kips up-bending.....	E12
Figure E-11. Bulkheads AE Cumulative Energy by Channel: Phase V, PI DLL, 159 kips up-bending.....	E13
Figure E-12. Keel AE Cumulative Energy by Channel: Phase V, PI DLL, 159 kips up-bending.....	E14
Figure E-13. Crown AE Cumulative Energy by Channel: Phase V, PI DLL, 159 kips up-bending + 9.2 psi.....	E15
Figure E-14. Bulkheads AE Cumulative Energy by Channel: Phase V, PI DLL, 159 kips up-bending + 9.2 psi.....	E16
Figure E-15. Keel AE Cumulative Energy by Channel: Phase V, PI DLL, 159 kips up-bending + 9.2 psi.....	E17

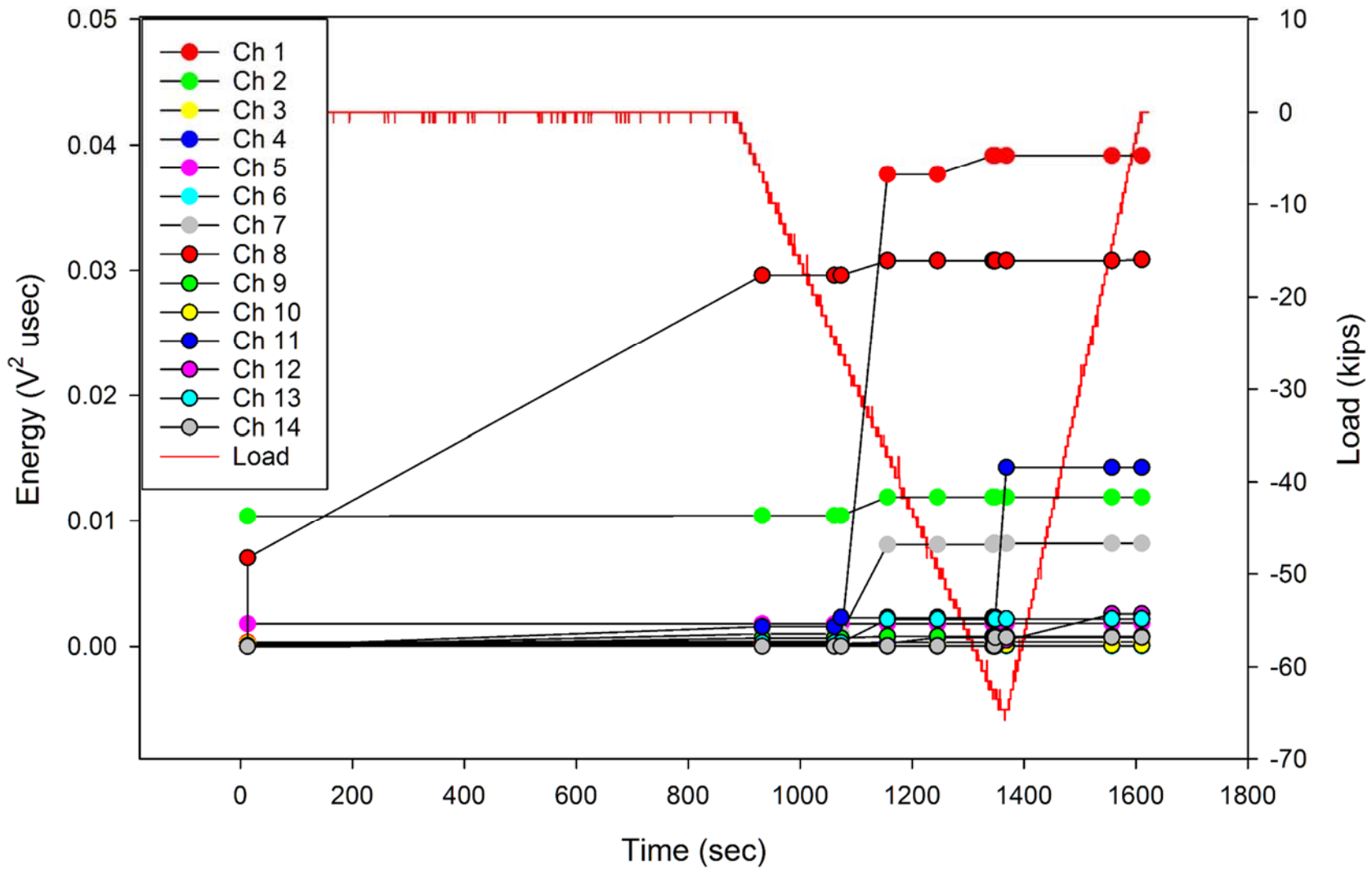


Figure E-1. Crown AE Cumulative Energy by Channel: Phase V, PI DLL, 63.6 kips down-bending.

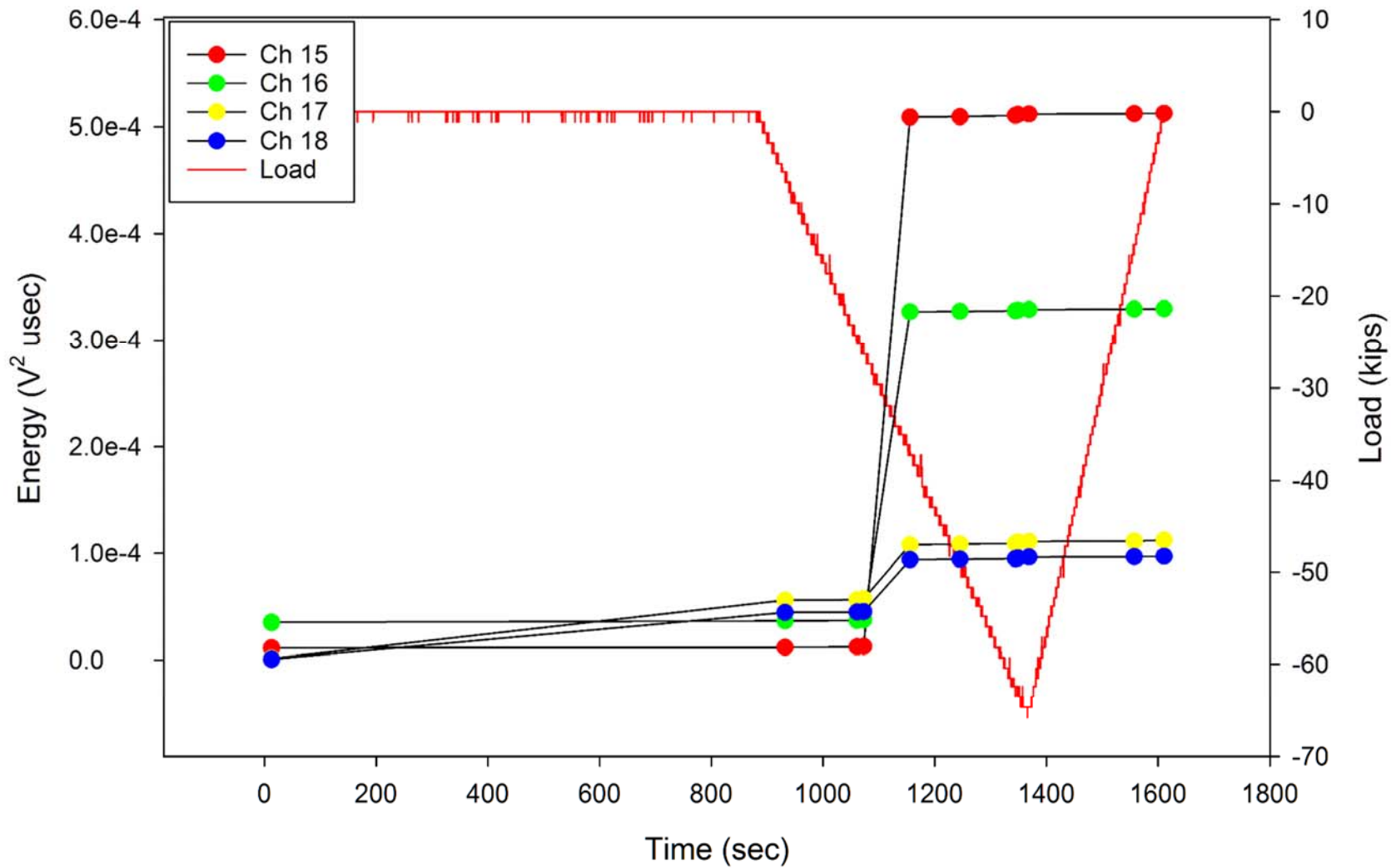


Figure E-2. Bulkheads AE Cumulative Energy by Channel: Phase V, PI DLL, 63.6 kips down-bending.

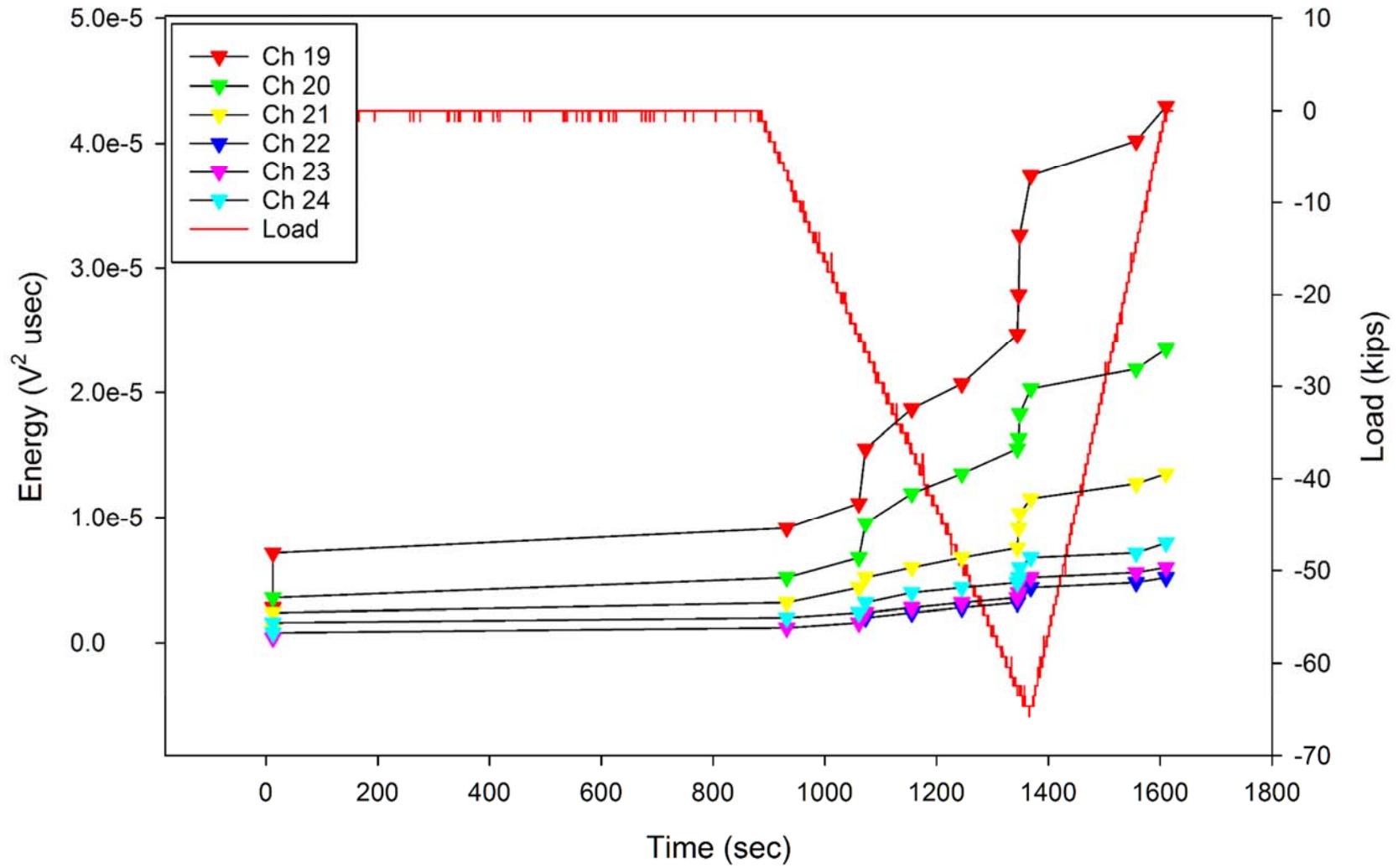


Figure E-3. Keel AE Cumulative Energy by Channel: Phase V, PI DLL, 63.6 kips down-bending.

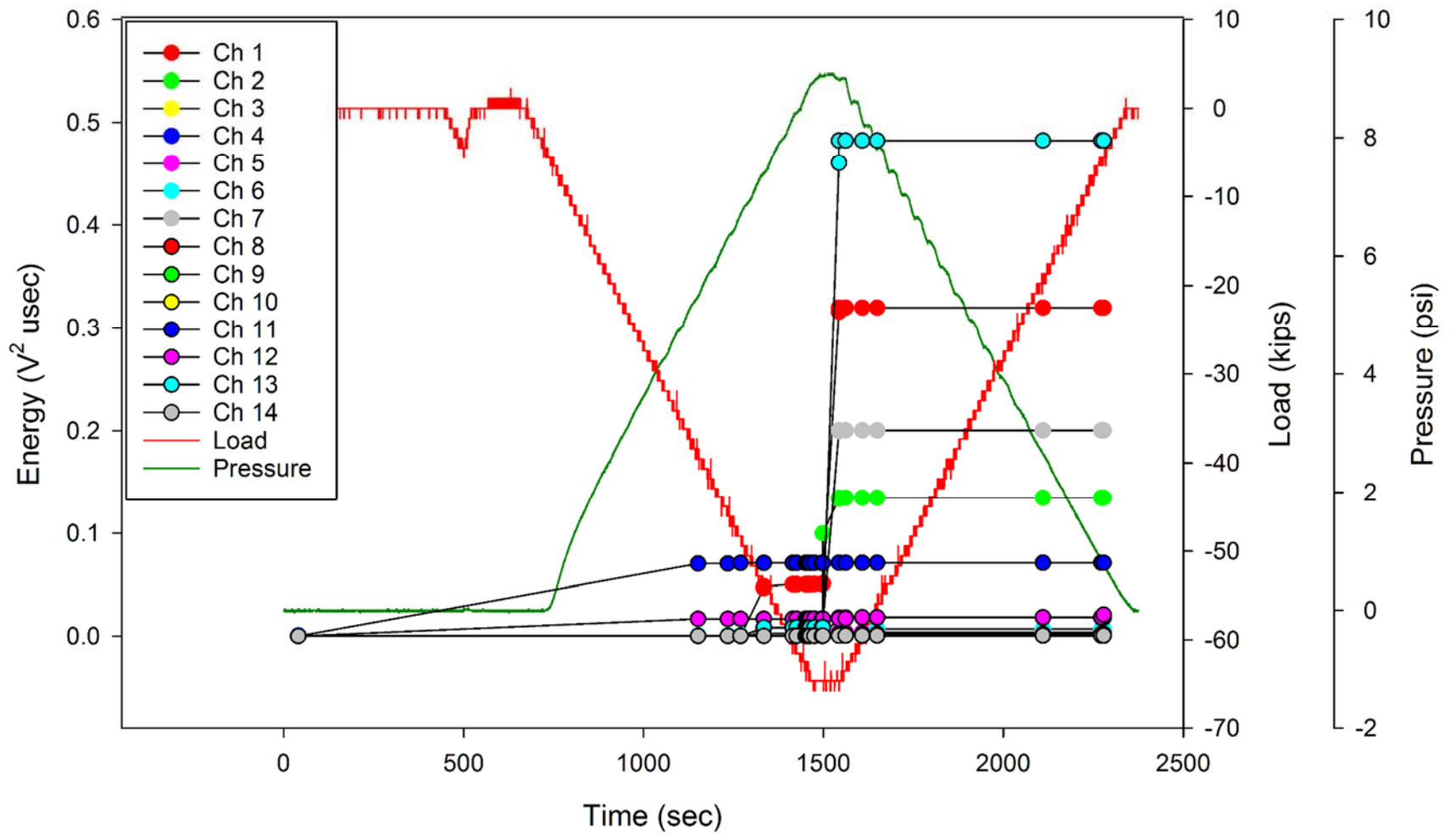


Figure E-4. Crown AE Cumulative Energy by Channel: Phase V, PI DLL, 63.6 kips down-bending + 9.2 psi.

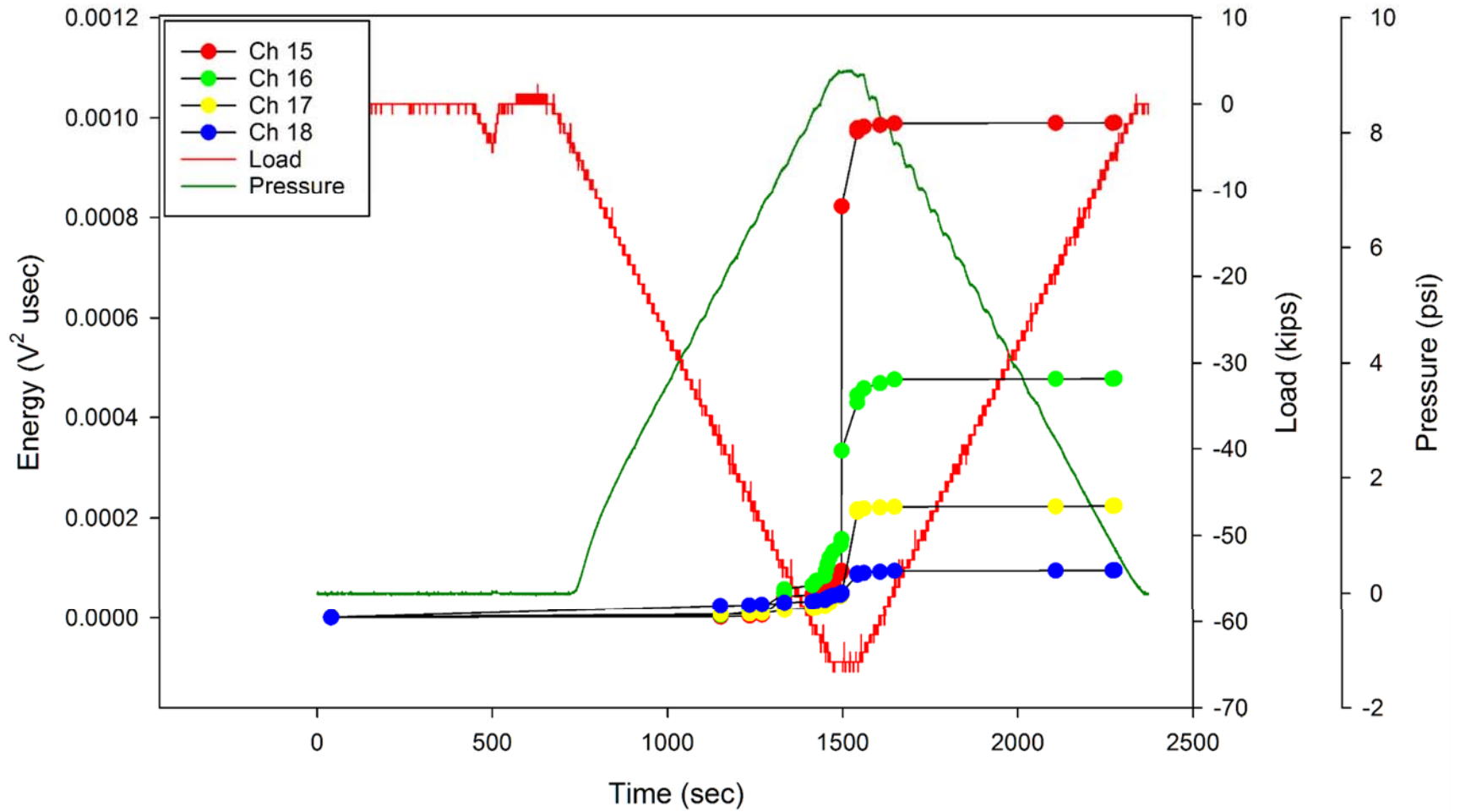


Figure E-5. Bulkheads AE Cumulative Energy by Channel: Phase V, PI DLL, 63.6 kips down-bending + 9.2 psi.

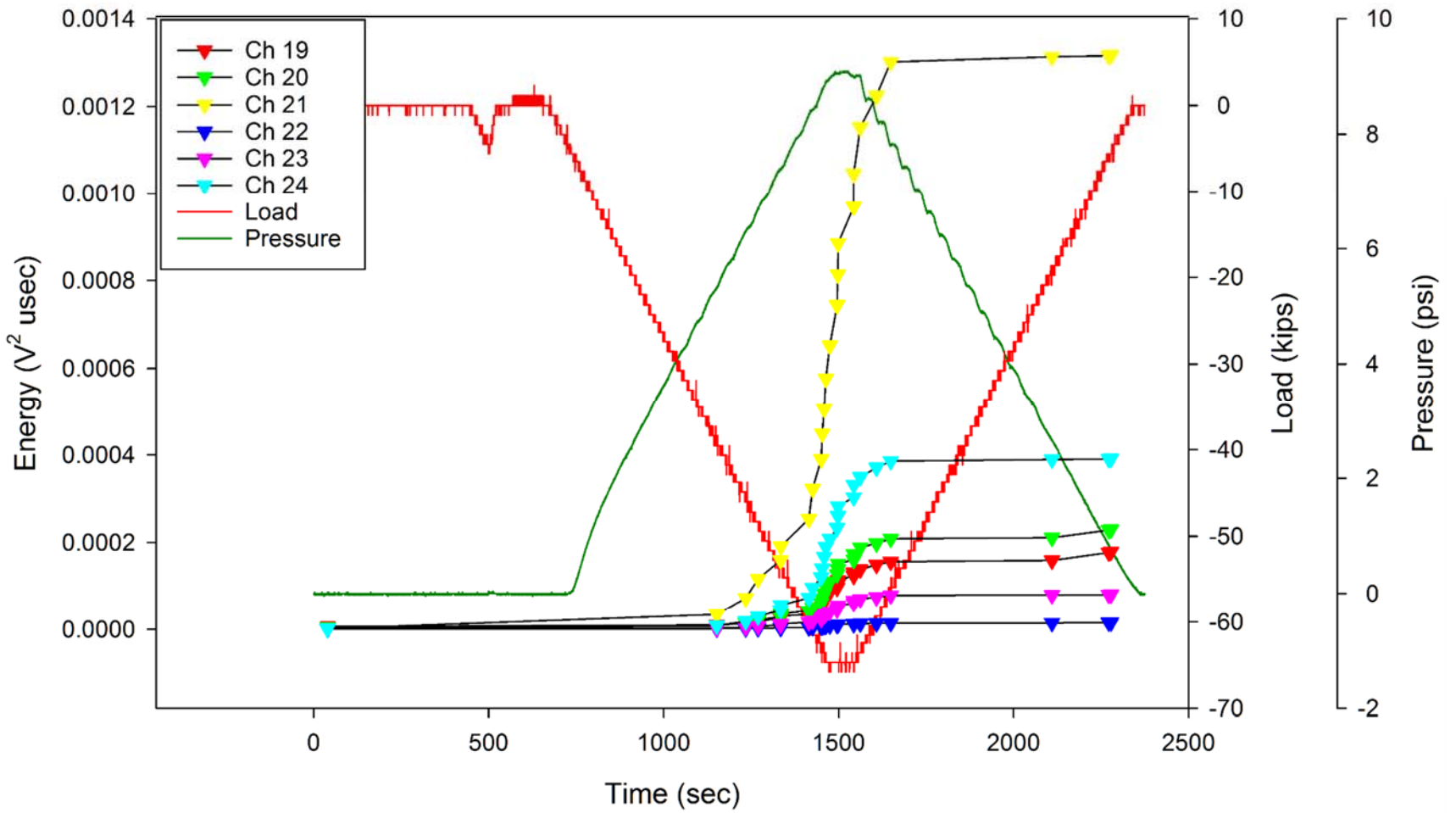


Figure E-6. Keel AE Cumulative Energy by Channel: Phase V, PI DLL, 63.6 kips down-bending + 9.2 psi.

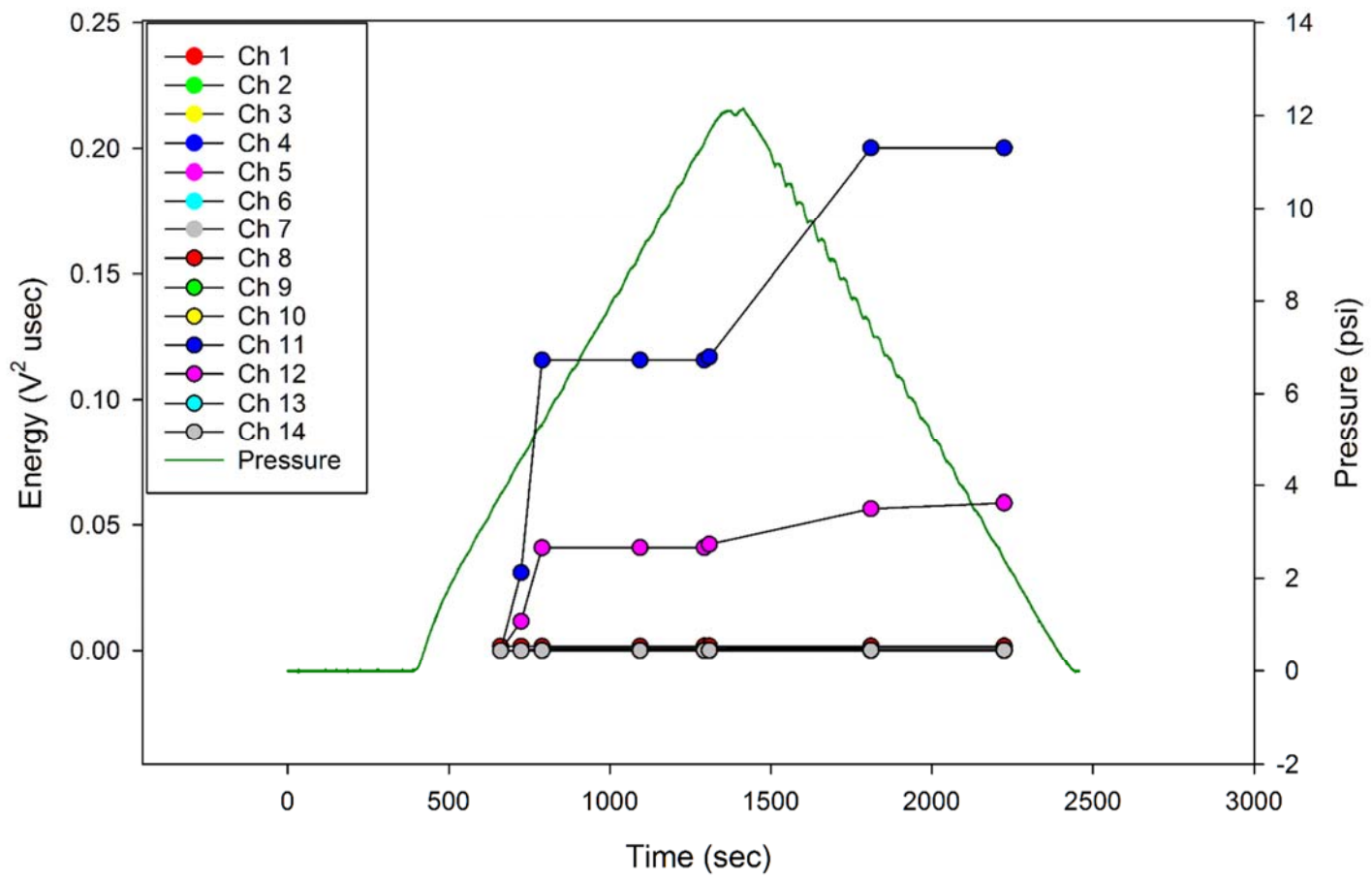


Figure E-7. Crown AE Cumulative Energy by Channel: Phase V, PI DLL, 12.2 psi.

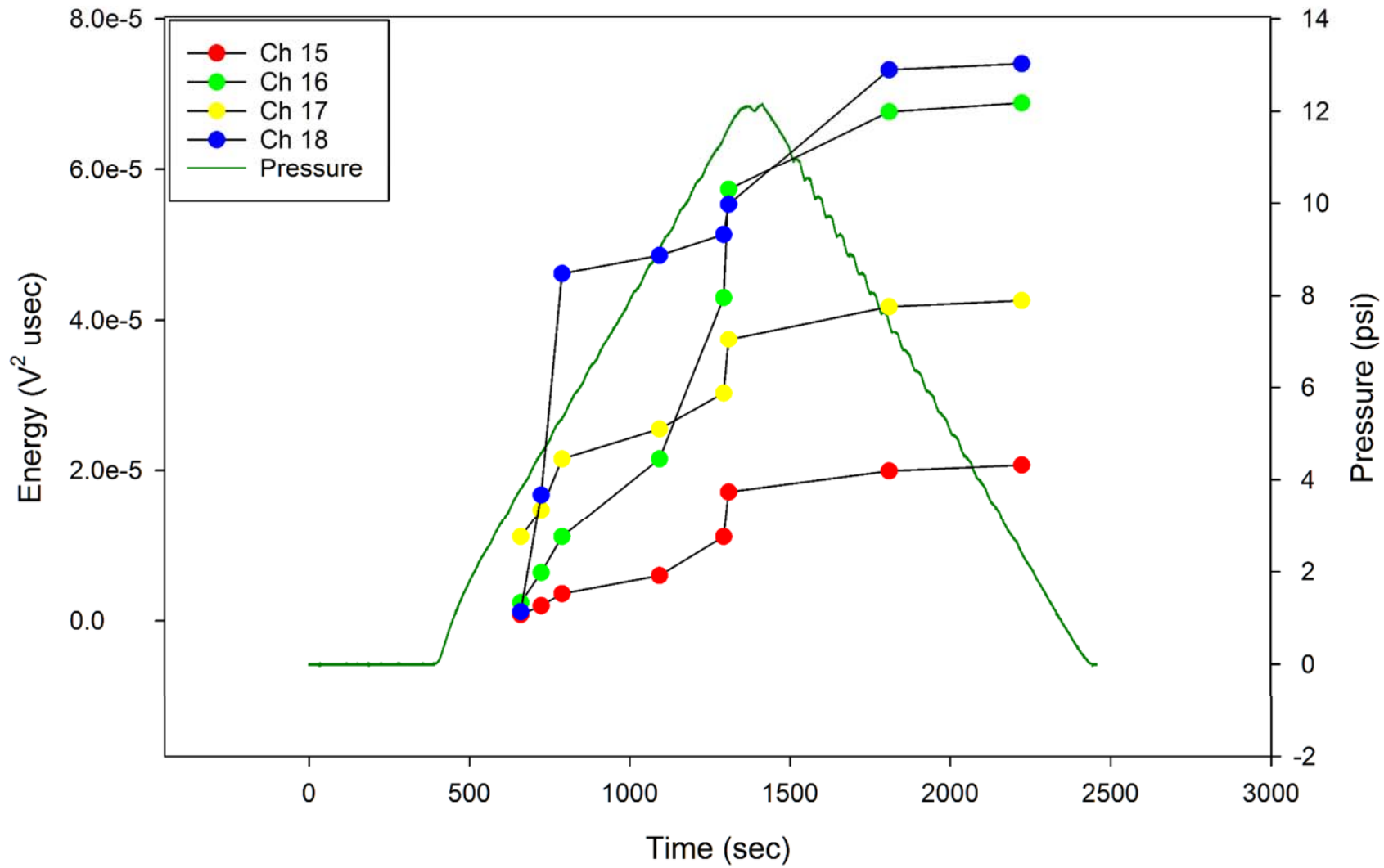


Figure E-8. Bulkheads AE Cumulative Energy by Channel: Phase V, PI DLL, 12.2 psi.

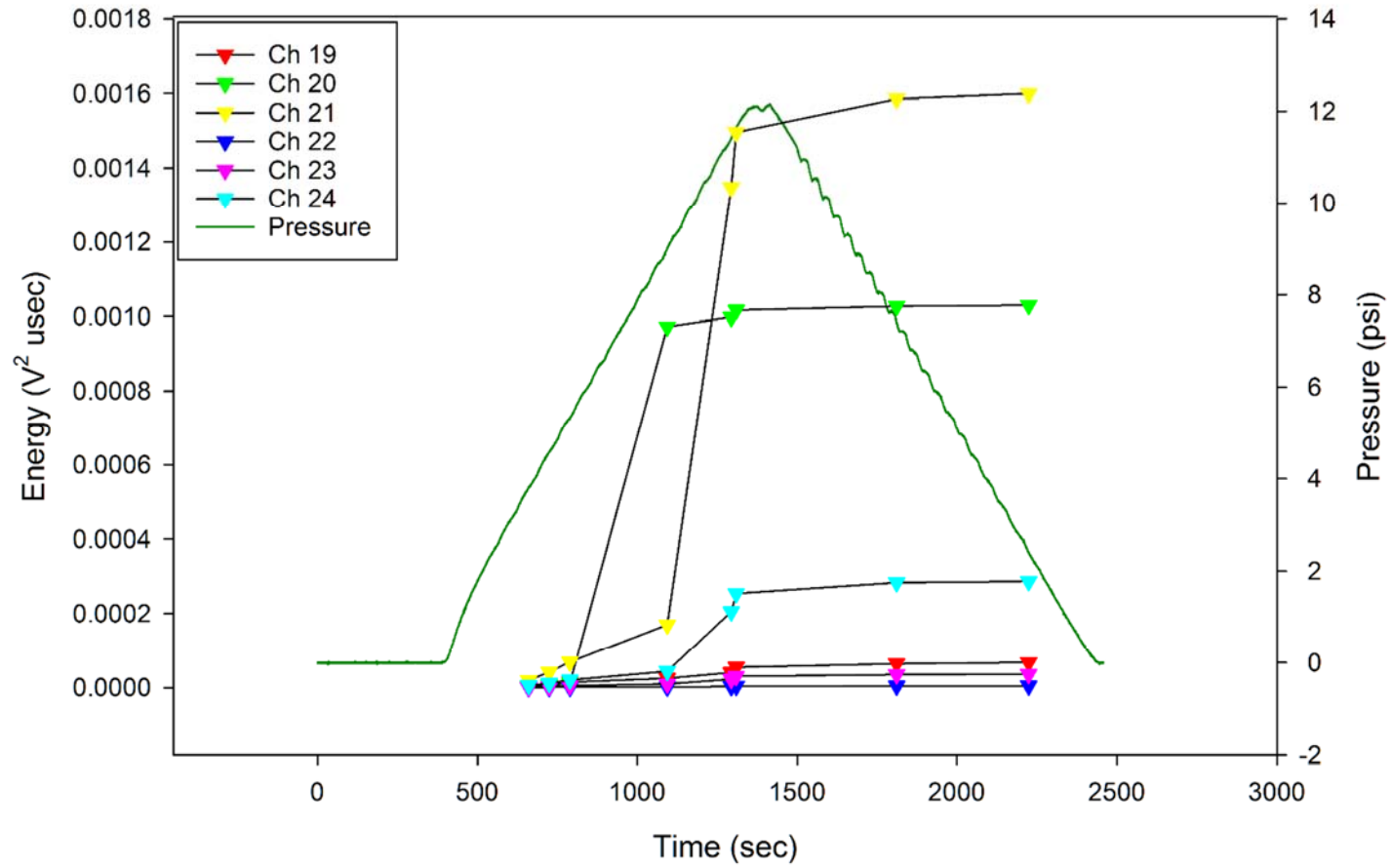


Figure E-9. Keel AE Cumulative Energy by Channel: Phase V, PI DLL, 12.2 psi.

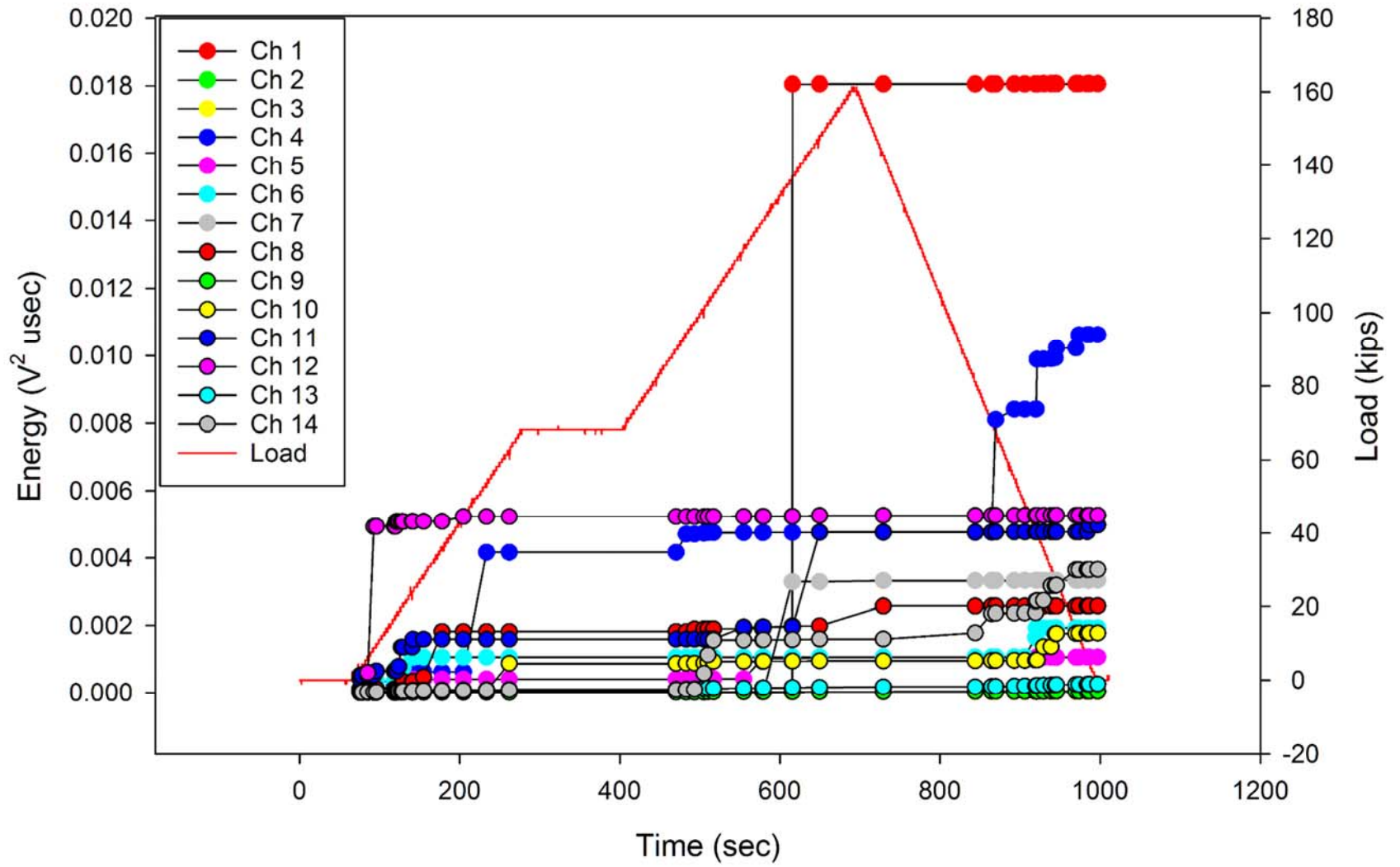


Figure E-10. Crown AE Cumulative Energy by Channel: Phase V, PI DLL, 159 kips up-bending.

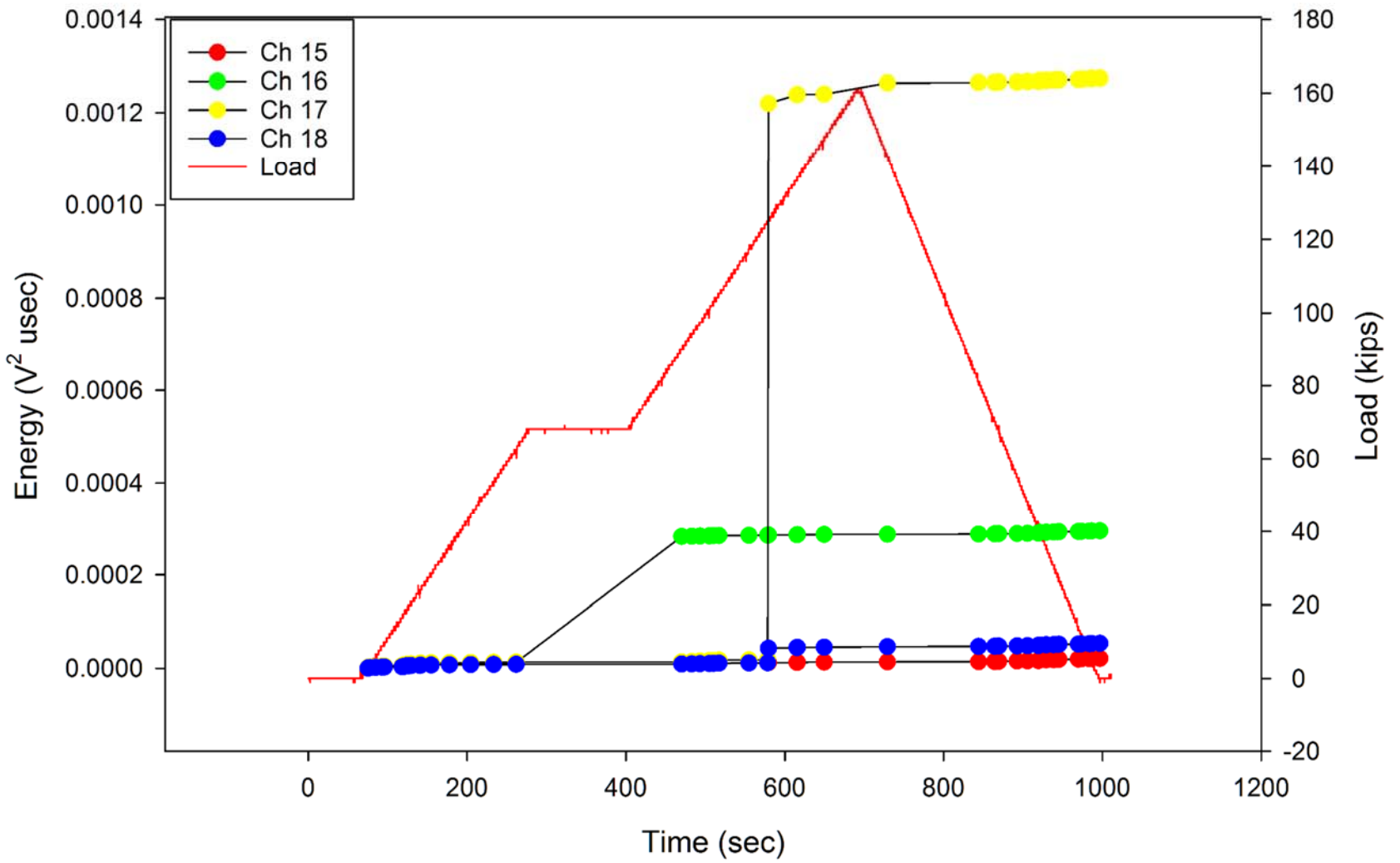


Figure E-11. Bulkheads AE Cumulative Energy by Channel: Phase V, PI DLL, 159 kips up-bending.

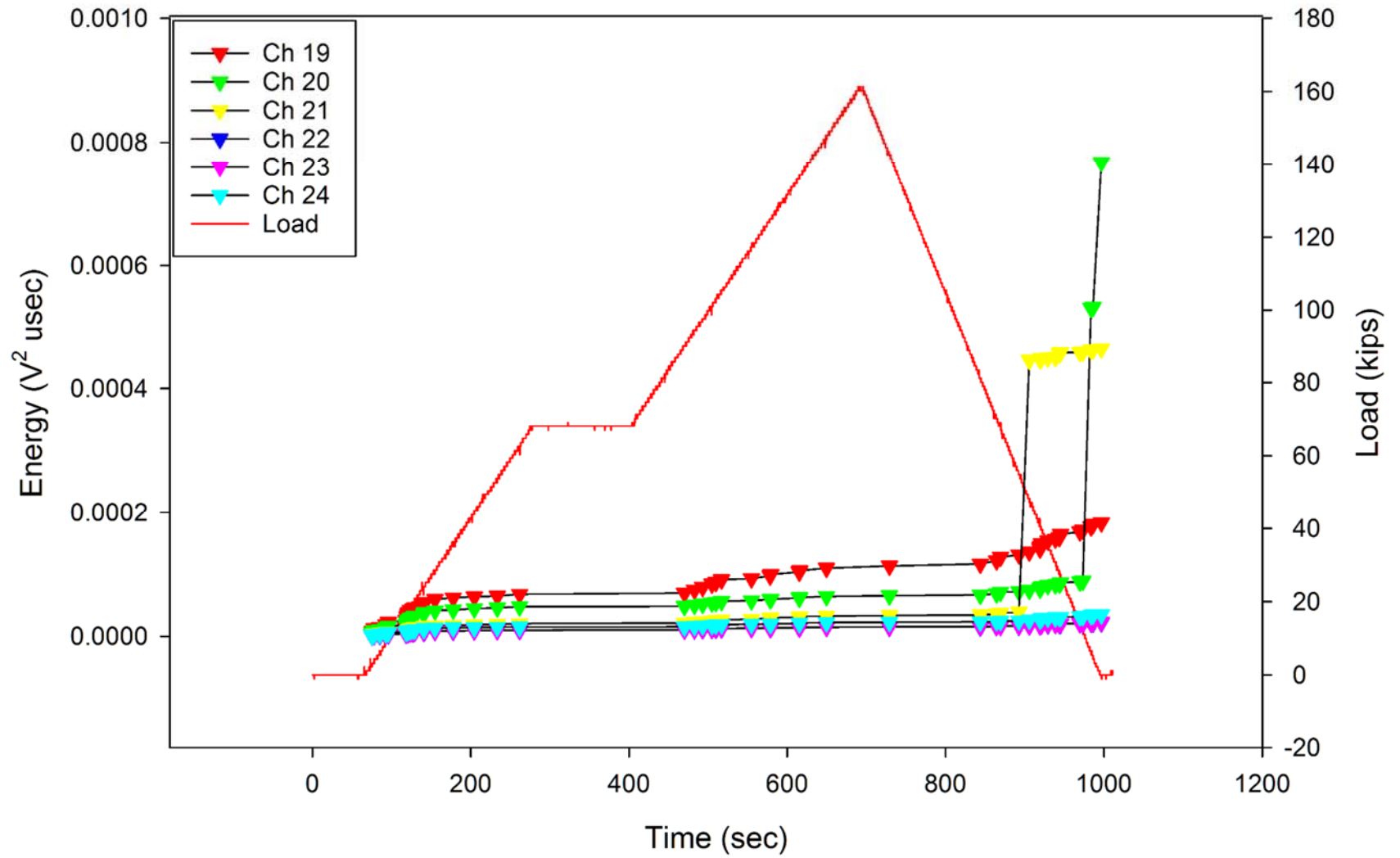


Figure E-12. Keel AE Cumulative Energy by Channel: Phase V, PI DLL, 159 kips up-bending.

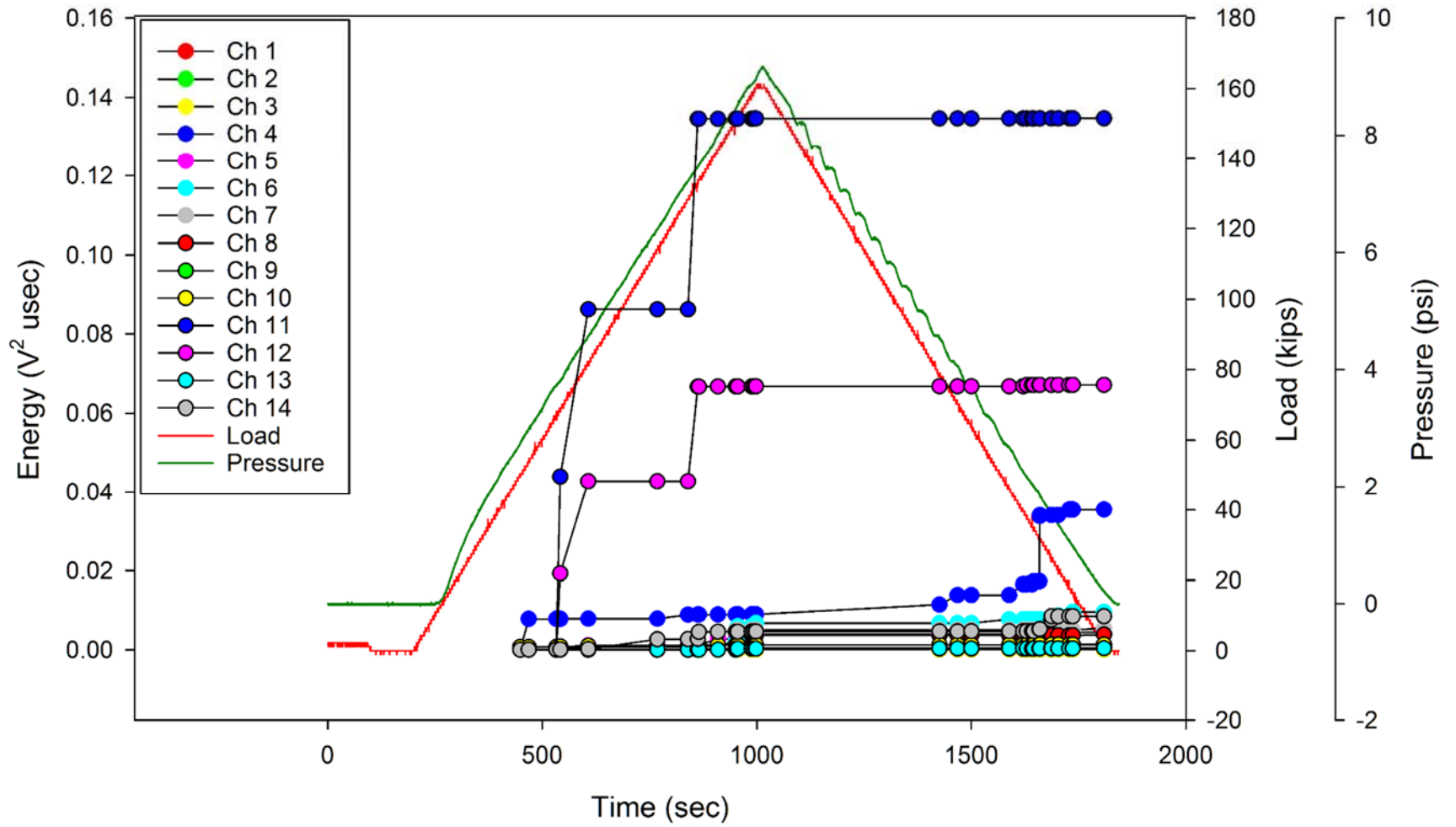


Figure E-13. Crown AE Cumulative Energy by Channel: Phase V, PI DLL, 159 kips up-bending + 9.2 psi.

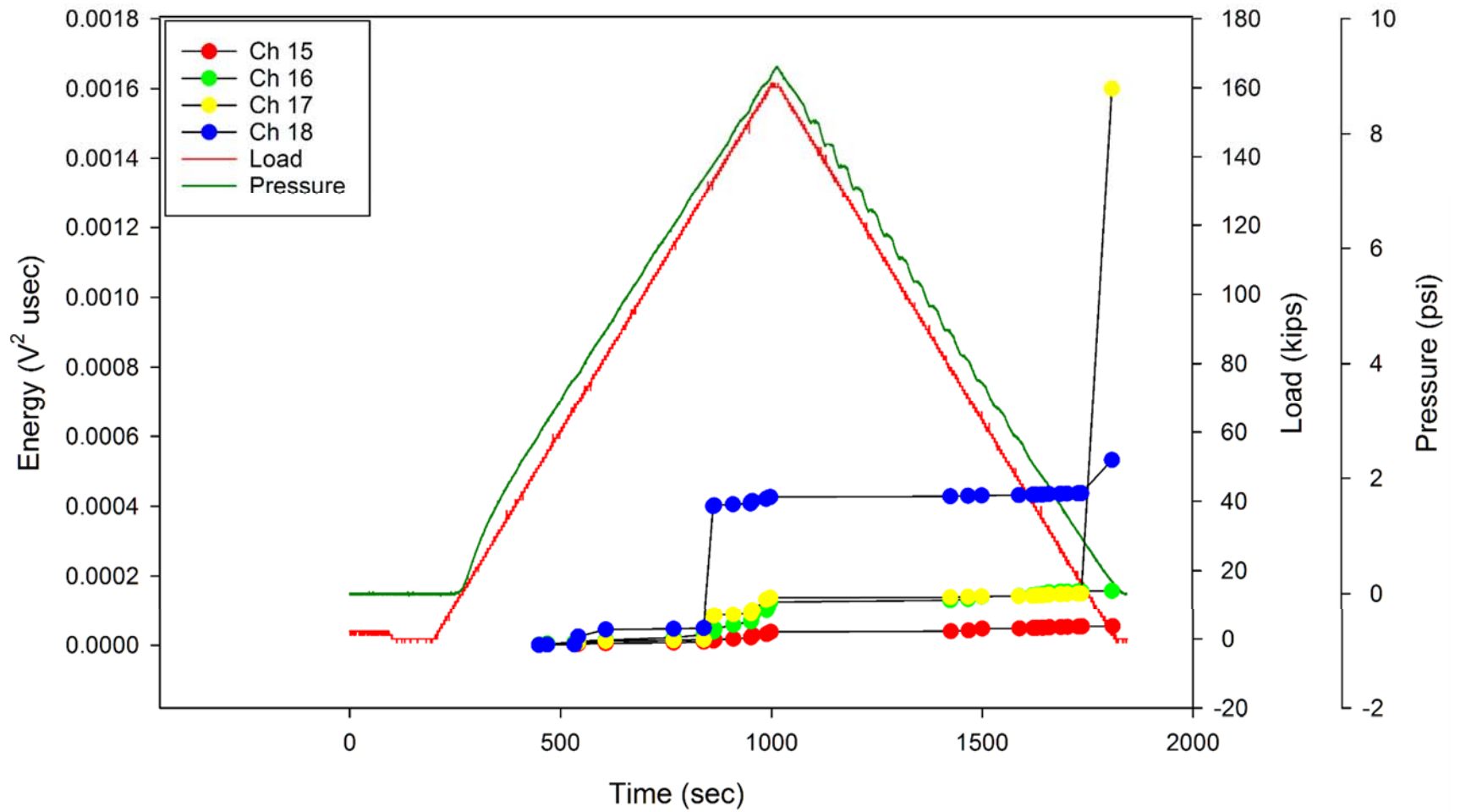


Figure E-14. Bulkheads AE Cumulative Energy by Channel: Phase V, PI DLL, 159 kips up-bending + 9.2 psi.

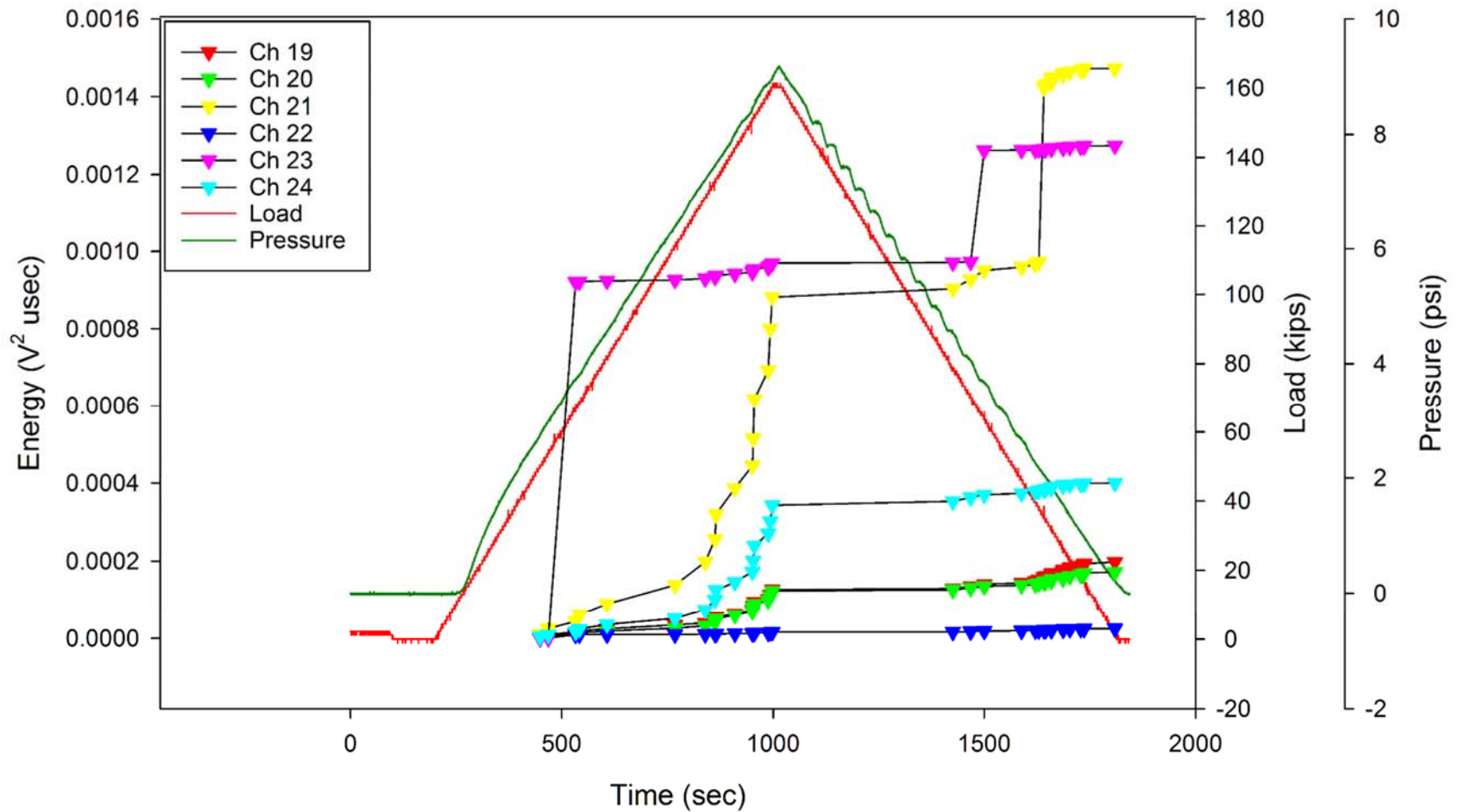


Figure E-15. Keel AE Cumulative Energy by Channel: Phase V, PI DLL, 159 kips up-bending + 9.2 psi.

Appendix F: Phase VI Post-impact DUL (PI DUL) Tests

Table of Figures

Figure F-1. Crown AE Cumulative Energy by Channel: Phase VI, PI DUL, 95.4 kips down-bending.	F3
Figure F-2. Bulkheads AE Cumulative Energy by Channel: Phase VI, PI DUL, 95.4 kips down-bending.	F4
Figure F-3. Keel AE Cumulative Energy by Channel: Phase VI, PI DUL, 95.4 kips down-bending.	F5
Figure F-4. Crown AE Cumulative Energy by Channel: Phase VI, PI DUL, 95.4 kips down-bending + 13.8 psi, Trial 1.	F6
Figure F-5. Bulkheads AE Cumulative Energy by Channel: Phase VI, PI DUL, 95.4 kips down-bending + 13.8 psi, Trial 1.	F7
Figure F-6. Keel AE Cumulative Energy by Channel: Phase VI, PI DUL, 95.4 kips down-bending + 13.8 psi, Trial 1.	F8
Figure F-7. Crown AE Cumulative Energy by Channel: Phase VI, PI DUL, 95.4 kips down-bending + 13.8 psi, Trial 2.	F9
Figure F-8. Bulkheads AE Cumulative Energy by Channel: Phase VI, PI DUL, 95.4 kips down-bending + 13.8 psi, Trial 2.	F10
Figure F-9. Keel AE Cumulative Energy by Channel: Phase VI, PI DUL, 95.4 kips down-bending + 13.8 psi, Trial 2.	F11
Figure F-10. Crown AE Cumulative Energy by Channel: Phase VI, PI DUL, 95.4 kips down-bending + 13.8 psi, Trial 3.	F12
Figure F-11. Bulkheads AE Cumulative Energy by Channel: Phase VI, PI DUL, 95.4 kips down-bending + 13.8 psi, Trial 3.	F13
Figure F-12. Keel AE Cumulative Energy by Channel: Phase VI, PI DUL, 95.4 kips down-bending + 13.8 psi, Trial 3.	F14
Figure F-13. Crown AE Cumulative Energy by Channel: Phase VI, PI DUL, 95.4 kips down-bending + 13.8 psi, Trial 4.	F15
Figure F-14. Bulkheads AE Cumulative Energy by Channel: Phase VI, PI DUL, 95.4 kips down-bending + 13.8 psi, Trial 4.	F16
Figure F-15. Keel AE Cumulative Energy by Channel: Phase VI, PI DUL, 95.4 kips down-bending + 13.8 psi, Trial 4.	F17
Figure F-16. Crown AE Cumulative Energy by Channel: Phase VI, PI DUL, 95.4 kips down-bending + 13.8 psi, Trial 5.	F18
Figure F-17. Bulkheads AE Cumulative Energy by Channel: Phase VI, PI DUL, 95.4 kips down-bending + 13.8 psi, Trial 5.	F19
Figure F-18. Keel AE Cumulative Energy by Channel: Phase VI, PI DUL, 95.4 kips down-bending + 13.8 psi, Trial 5.	F20
Figure F-19. Crown AE Cumulative Energy by Channel: Phase VI, PI DUL, 18.4 psi.	F21
Figure F-20. Bulkheads AE Cumulative Energy by Channel: Phase VI, PI DUL, 18.4 psi.	F22
Figure F-21. Keel AE Cumulative Energy by Channel: Phase VI, PI DUL, 18.4 psi.	F23
Figure F-22. Crown AE Cumulative Energy by Channel: Phase VI, PI DUL, 238.5 kips up-bending.	F24
Figure F-23. Bulkheads AE Cumulative Energy by Channel: Phase VI, PI DUL, 238.5 kips up-bending.	F25
Figure F-24. Keel AE Cumulative Energy by Channel: Phase VI, PI DUL, 238.5 kips up-bending.	F26

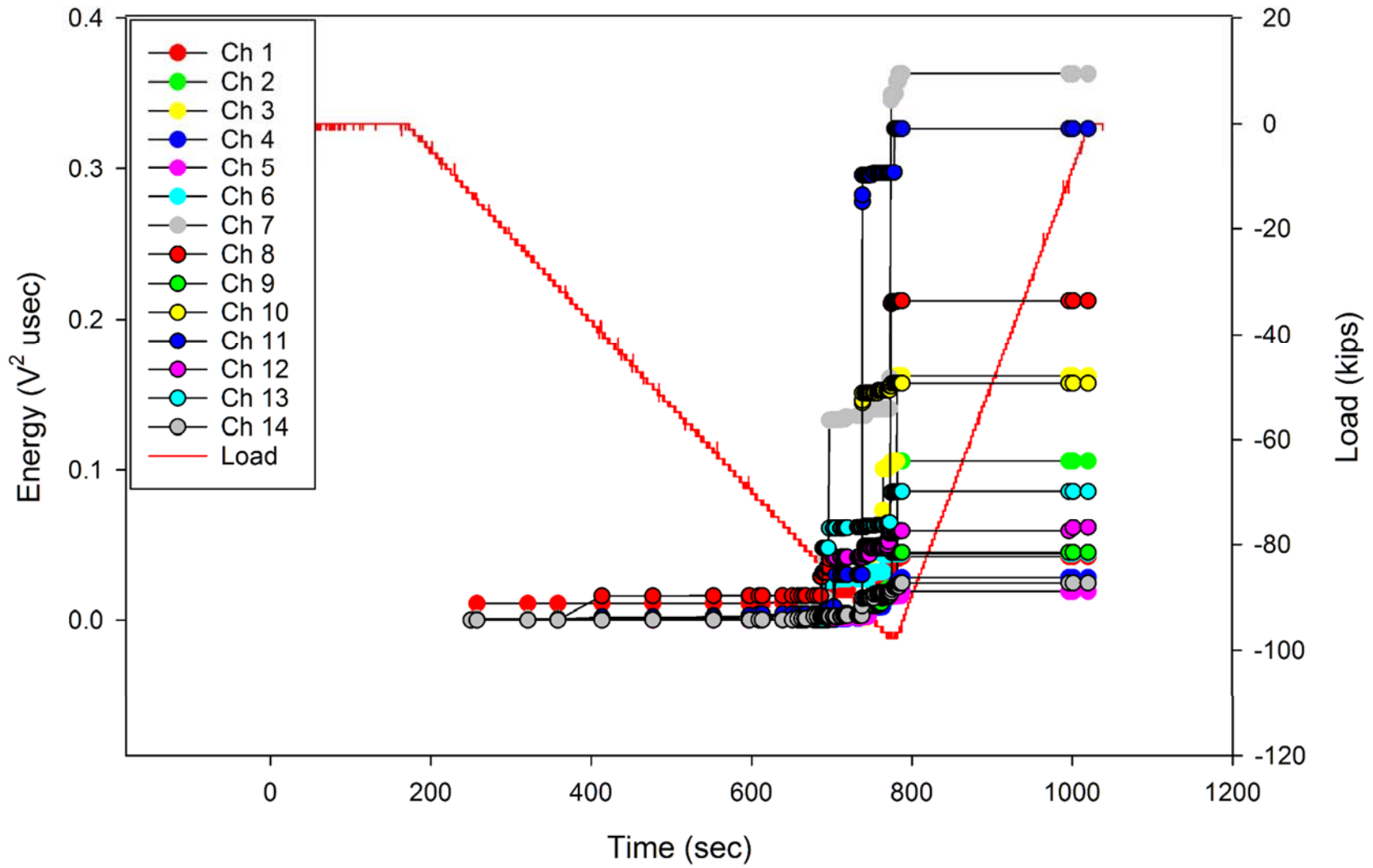


Figure F-1. Crown AE Cumulative Energy by Channel: Phase VI, PI DUL, 95.4 kips down-bending.

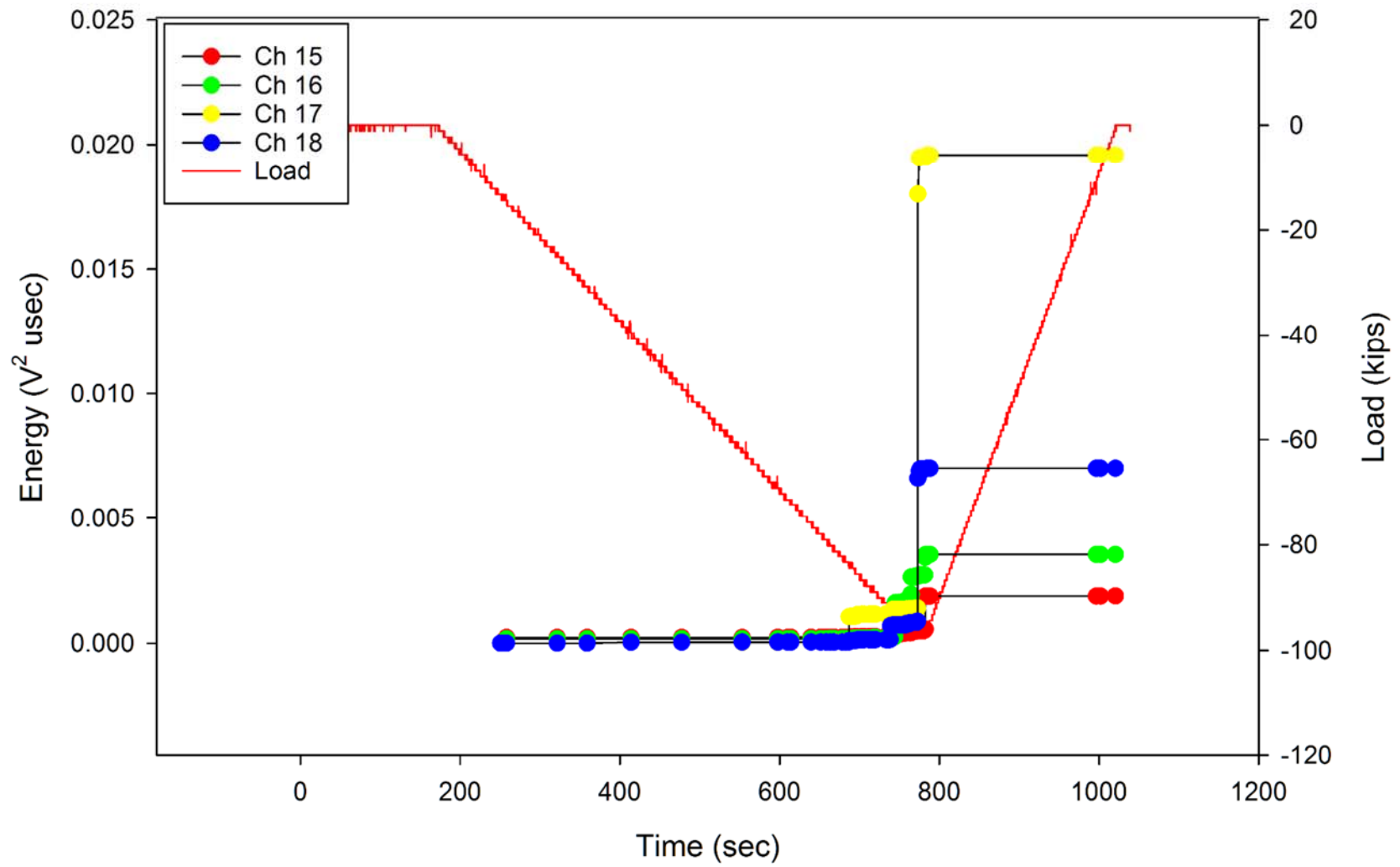


Figure F-2. Bulkheads AE Cumulative Energy by Channel: Phase VI, PI DUL, 95.4 kips down-bending.

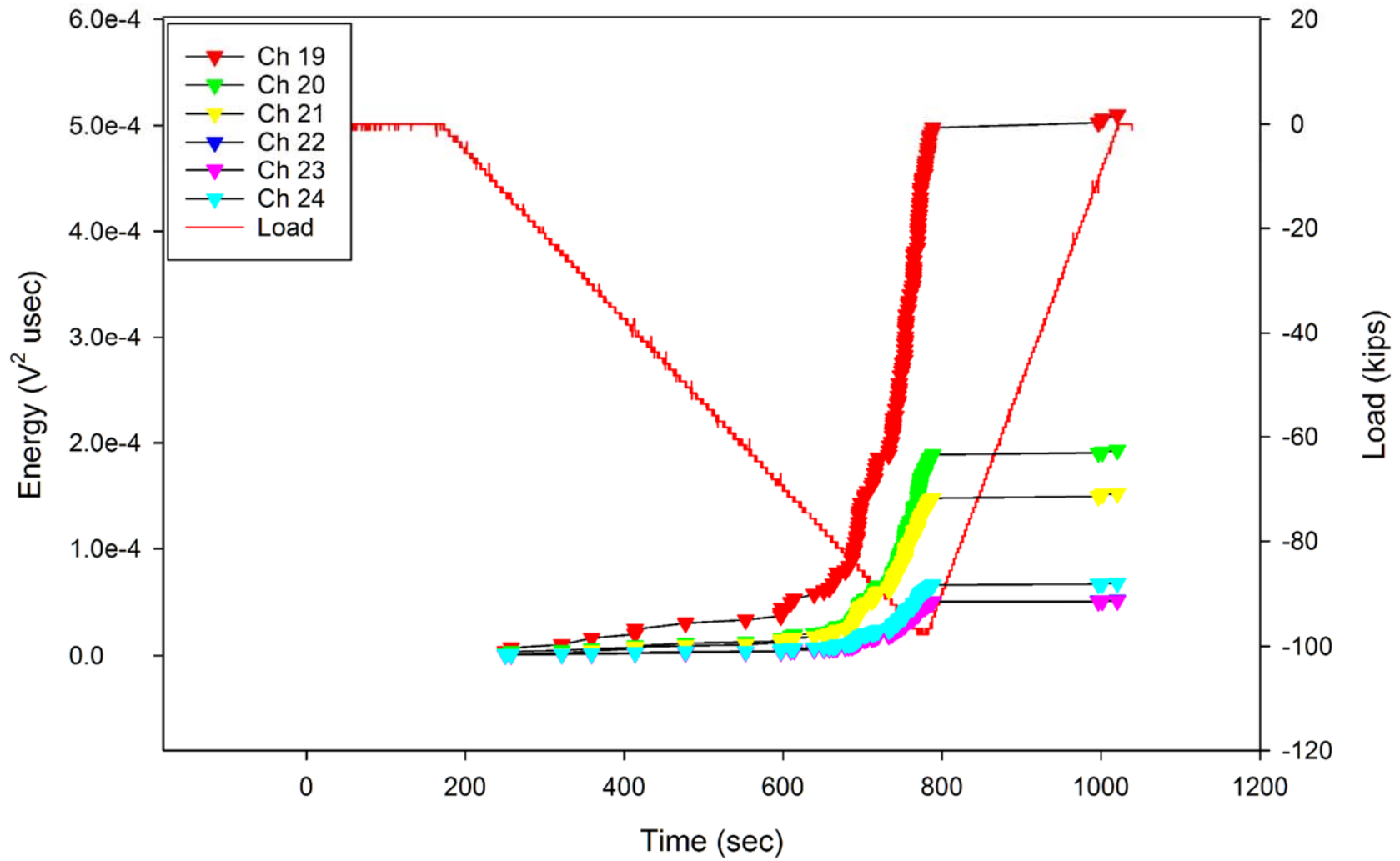


Figure F-3. Keel AE Cumulative Energy by Channel: Phase VI, PI DUL, 95.4 kips down-bending.

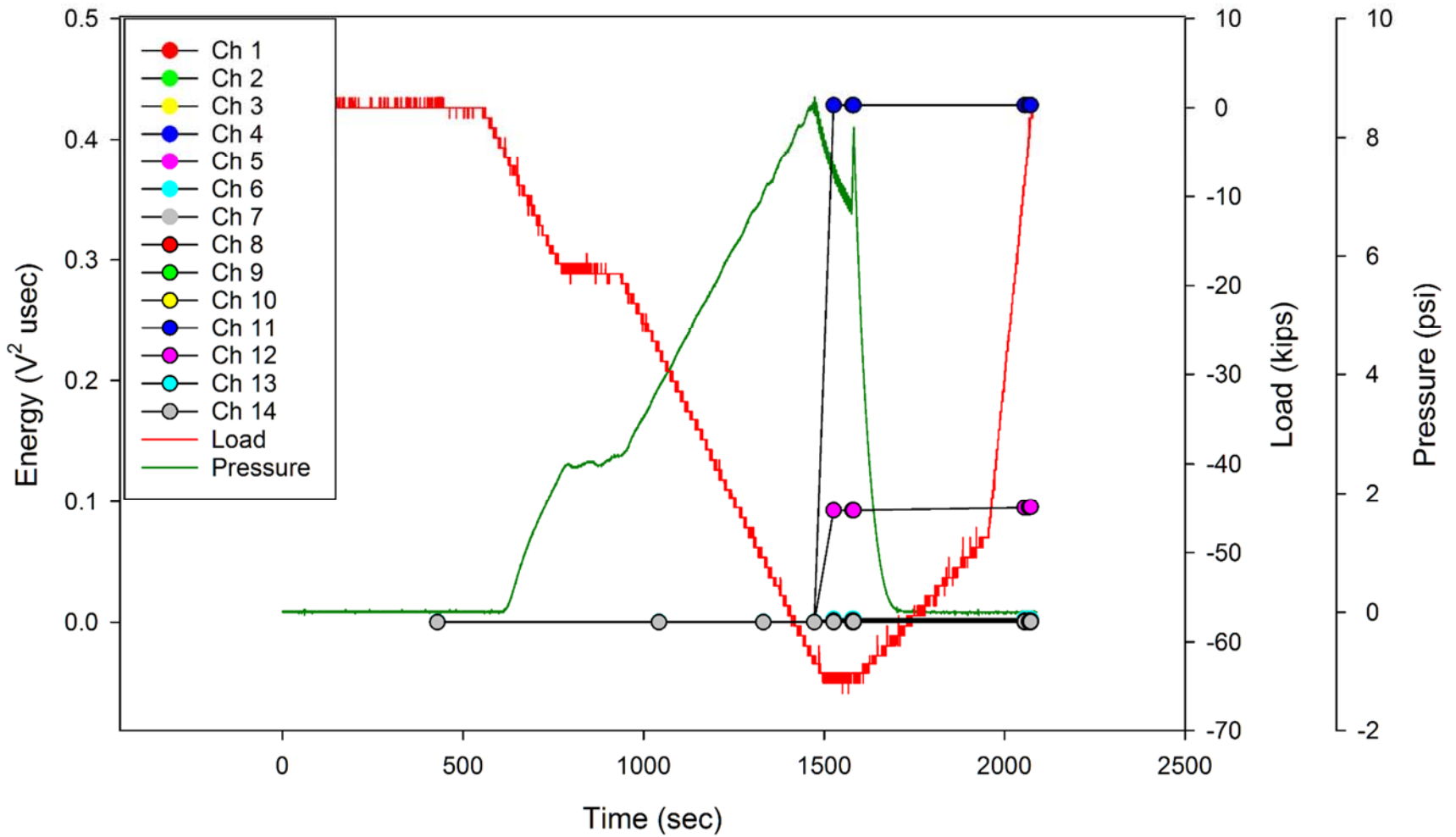


Figure F-4. Crown AE Cumulative Energy by Channel: Phase VI, PI DUL, 95.4 kips down-bending + 13.8 psi, Trial 1.

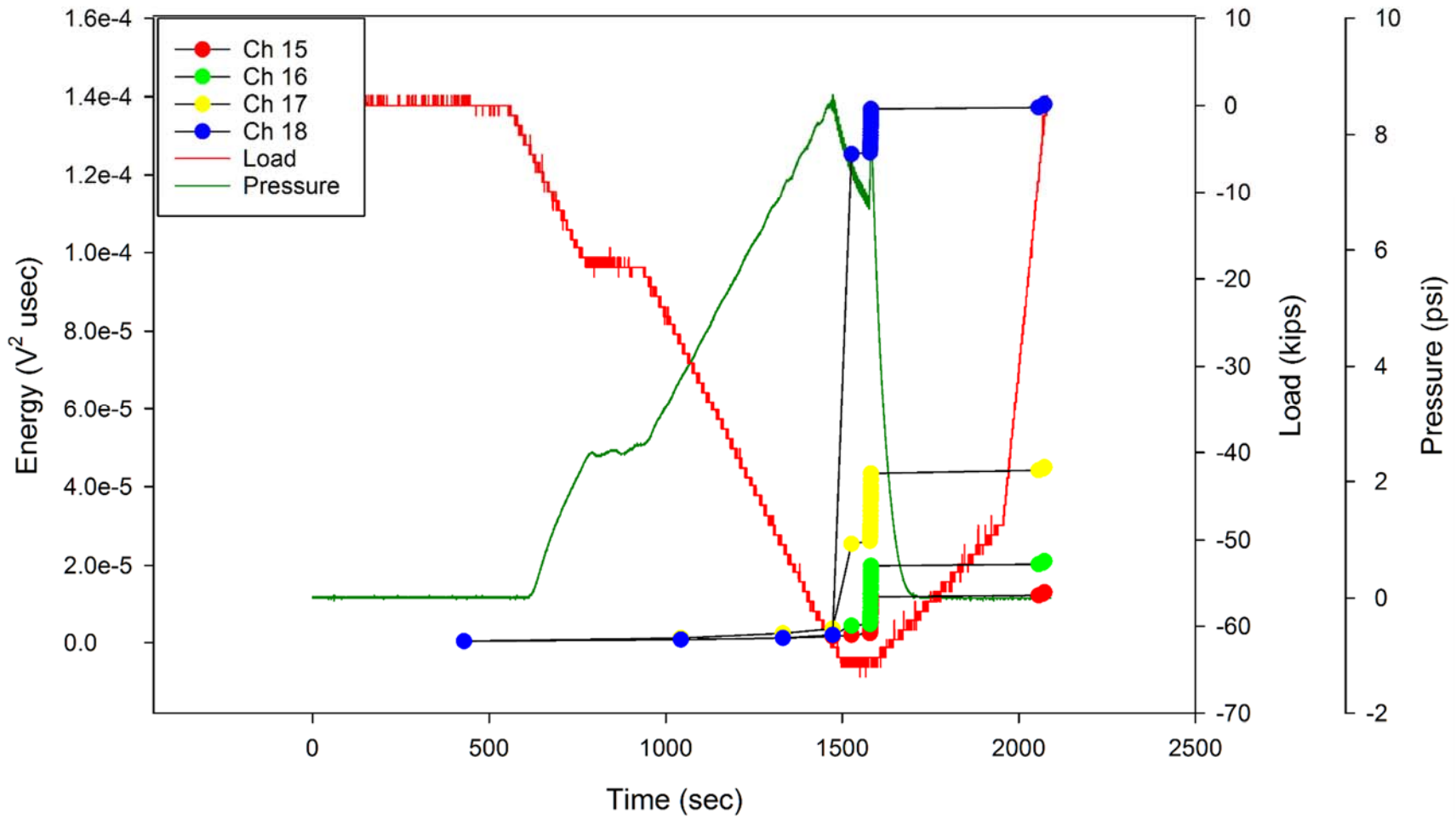


Figure F-5. Bulkheads AE Cumulative Energy by Channel: Phase VI, PI DUL, 95.4 kips down-bending + 13.8 psi, Trial 1.

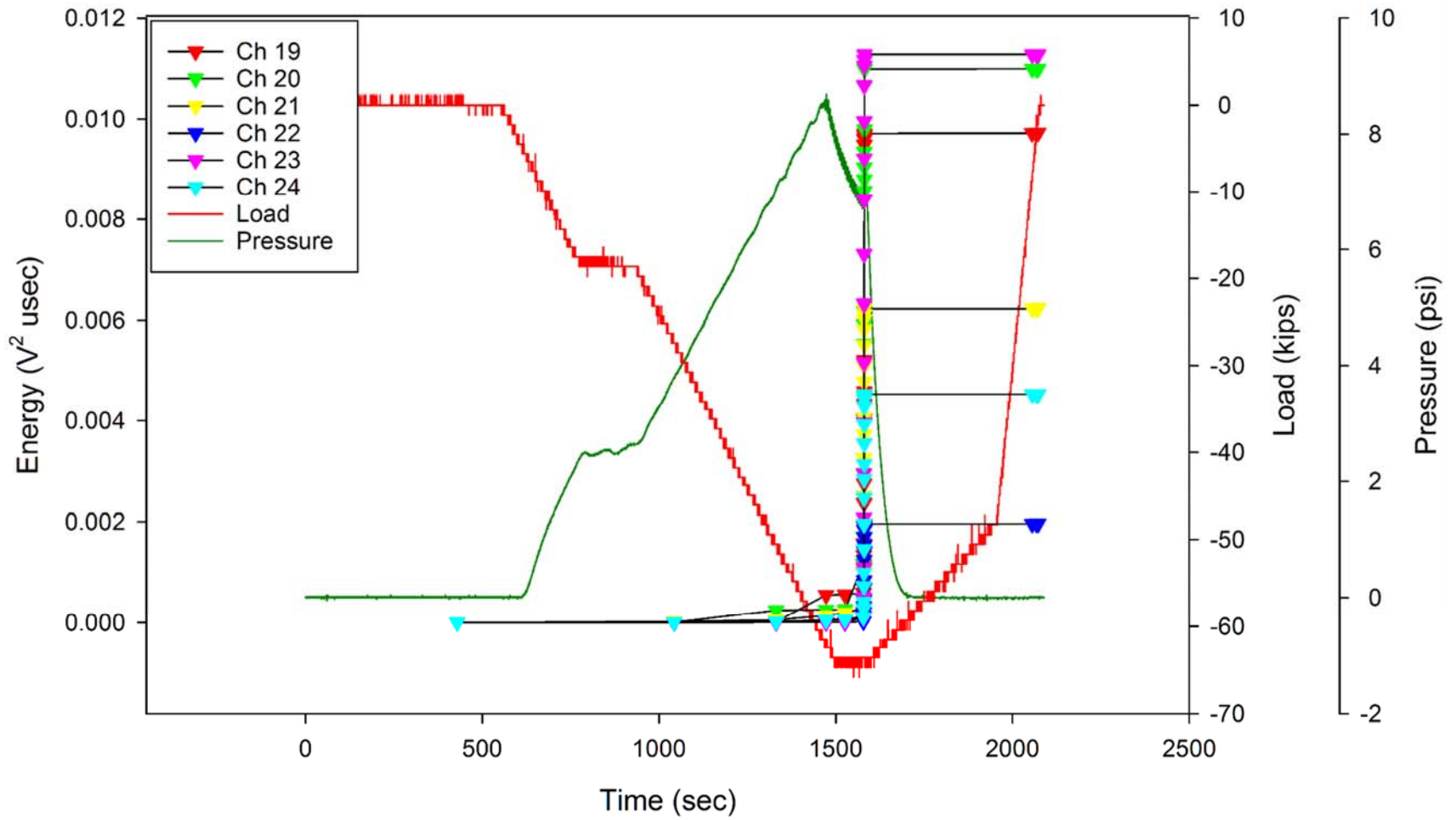


Figure F-6. Keel AE Cumulative Energy by Channel: Phase VI, PI DUL, 95.4 kips down-bending + 13.8 psi, Trial 1.

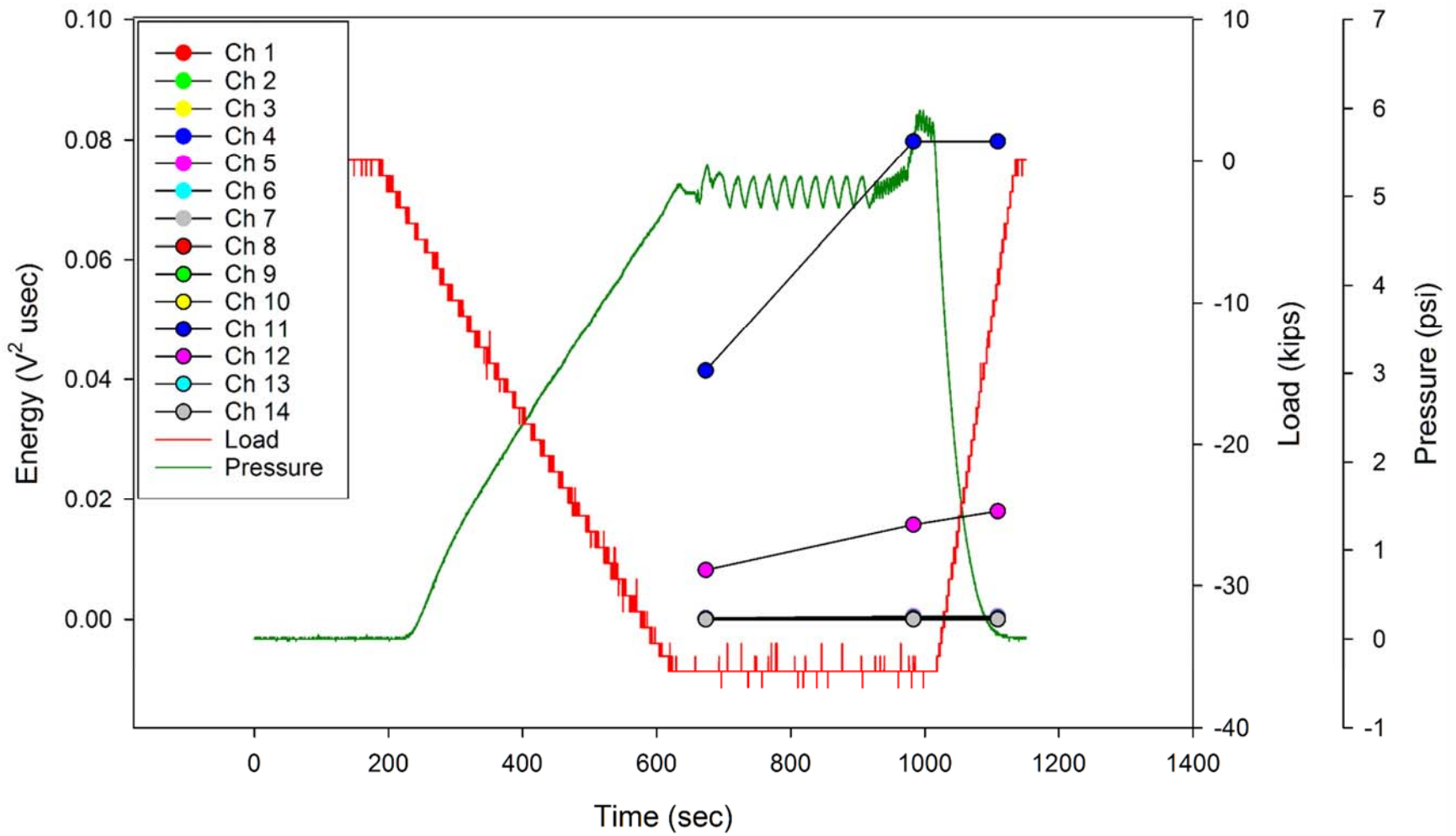


Figure F-7. Crown AE Cumulative Energy by Channel: Phase VI, PI DUL, 95.4 kips down-bending + 13.8 psi, Trial 2.

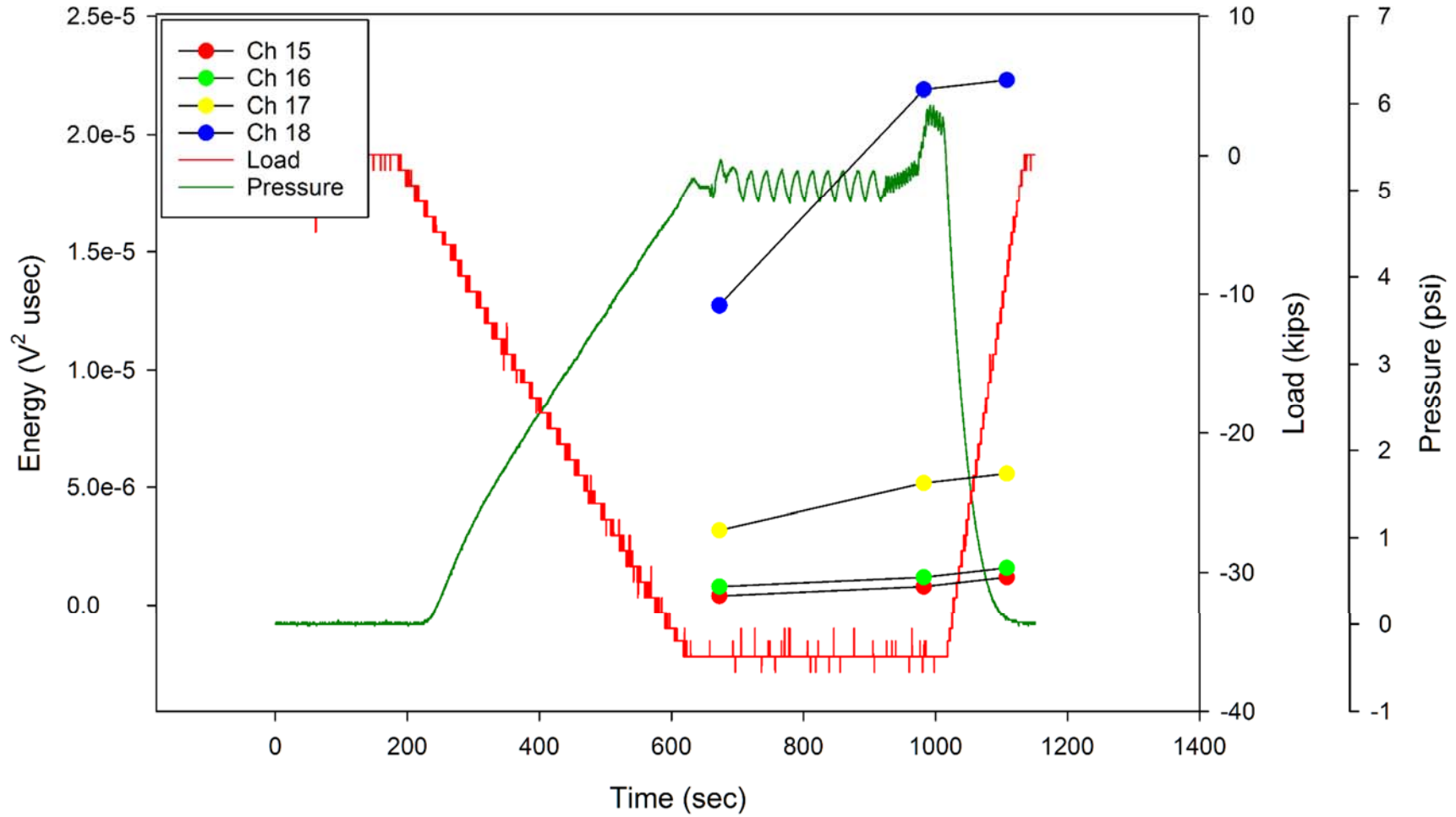


Figure F-8. Bulkheads AE Cumulative Energy by Channel: Phase VI, PI DUL, 95.4 kips down-bending + 13.8 psi, Trial 2.

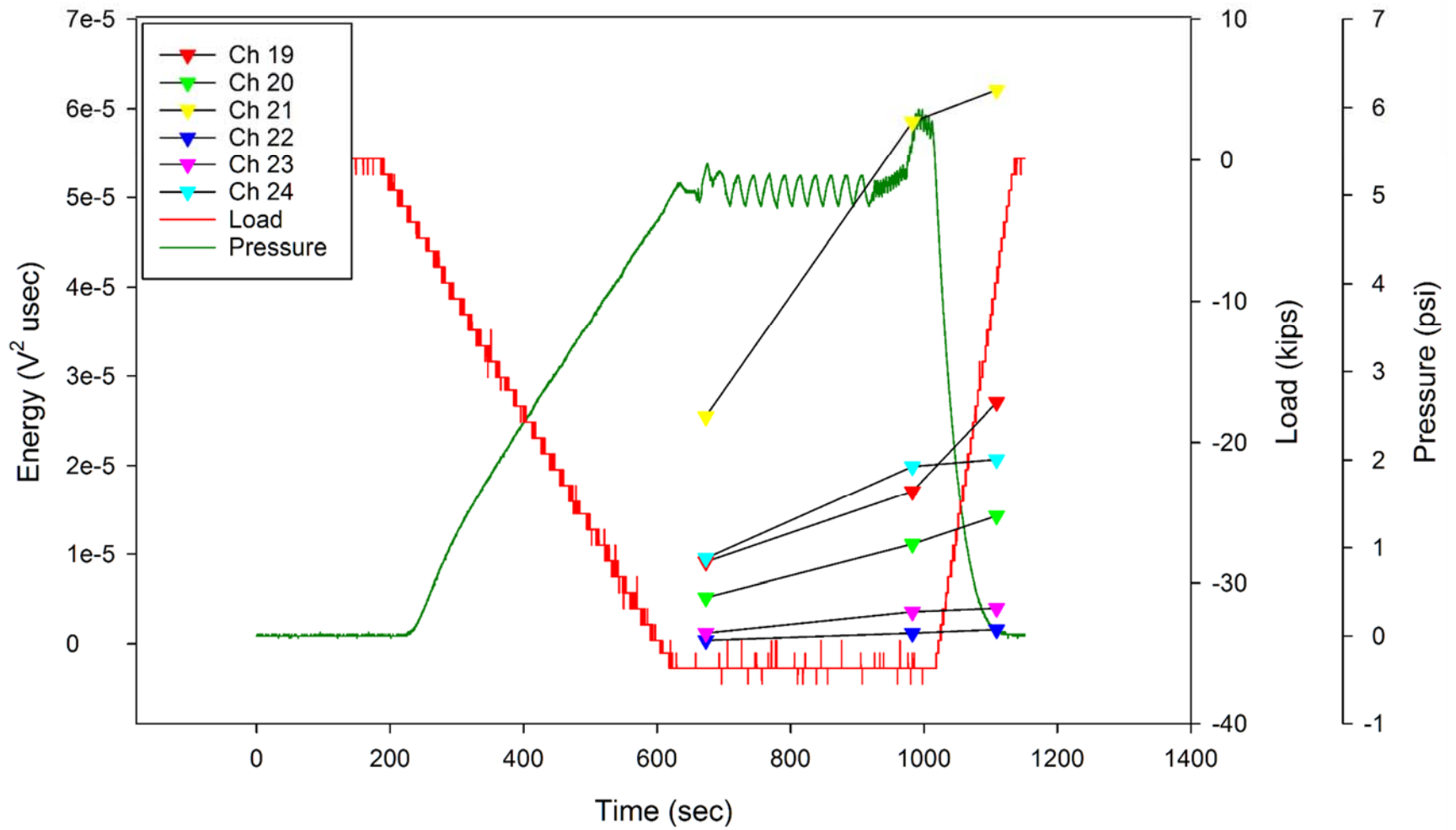


Figure F-9. Keel AE Cumulative Energy by Channel: Phase VI, PI DUL, 95.4 kips down-bending + 13.8 psi, Trial 2.

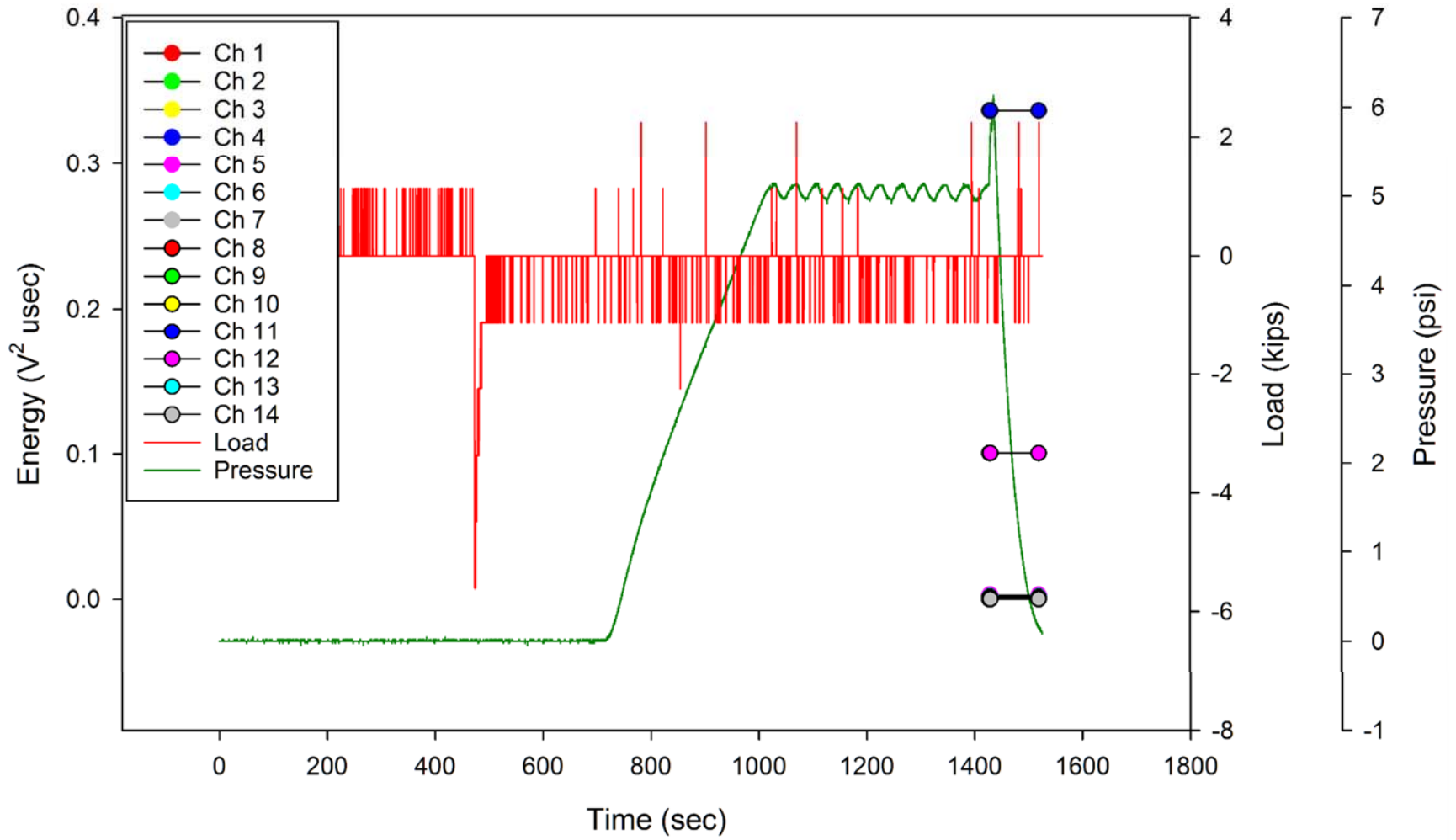


Figure F-10. Crown AE Cumulative Energy by Channel: Phase VI, PI DUL, 95.4 kips down-bending + 13.8 psi, Trial 3.

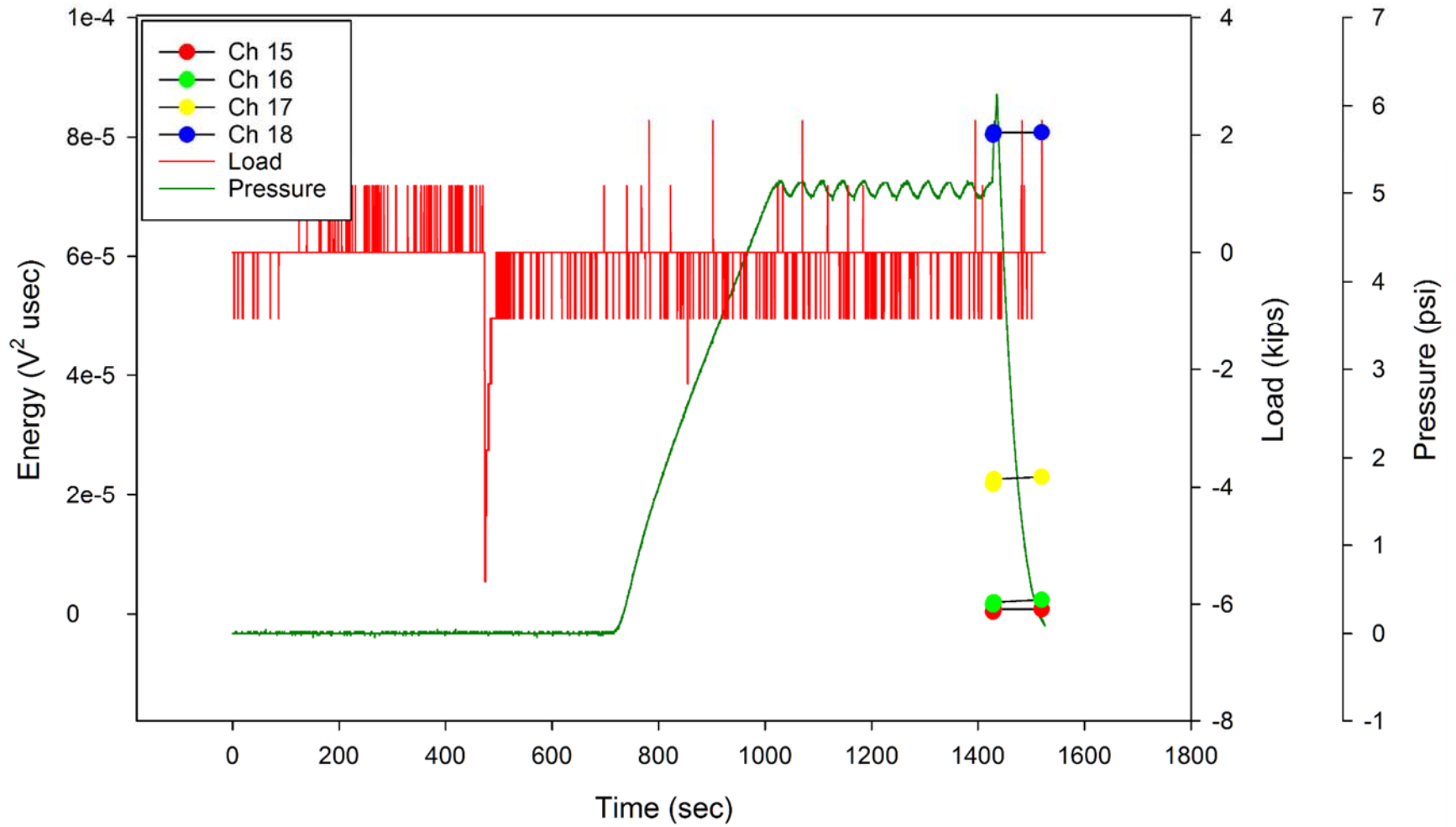


Figure F-11. Bulkheads AE Cumulative Energy by Channel: Phase VI, PI DUL, 95.4 kips down-bending + 13.8 psi, Trial 3.

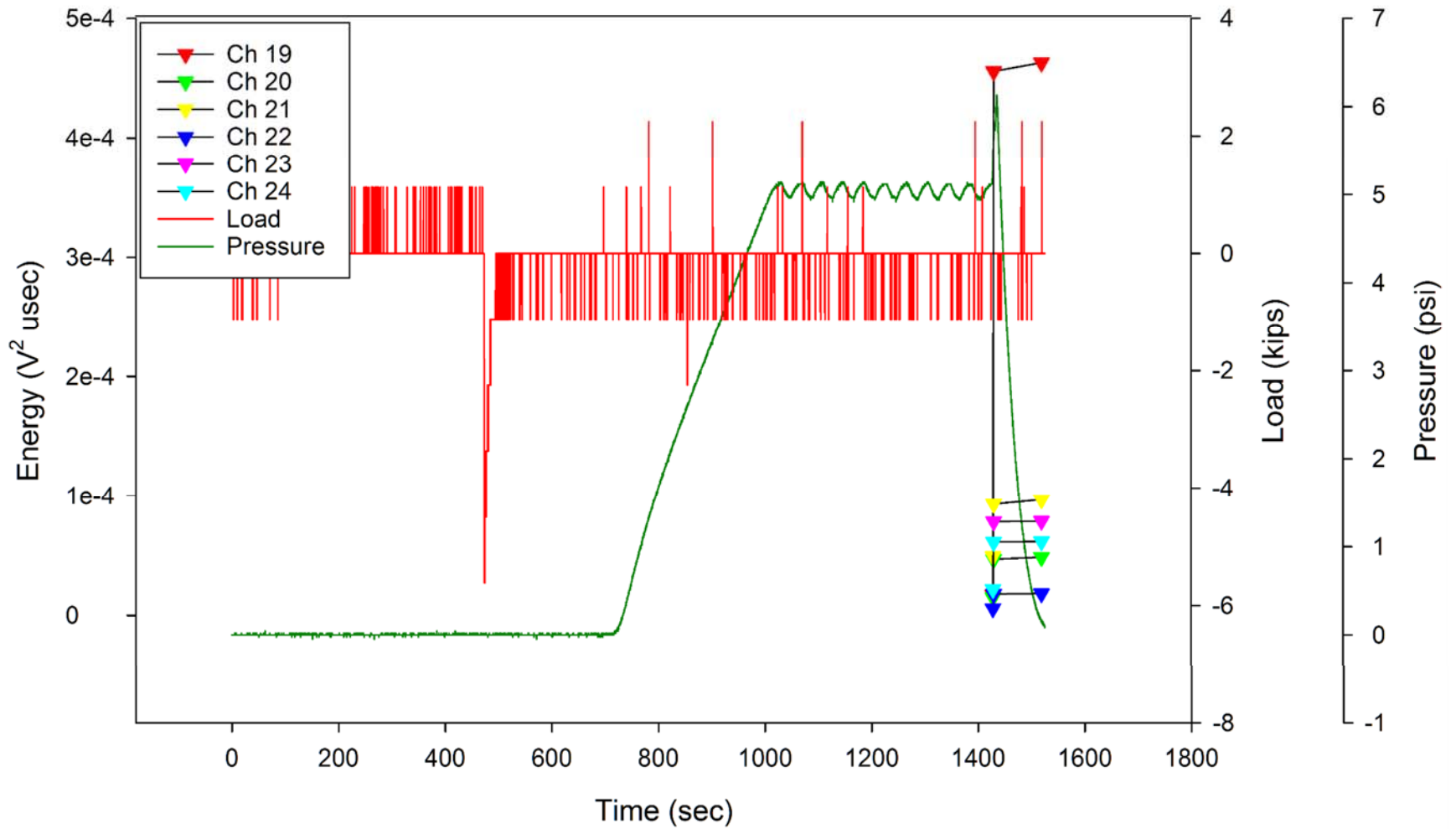


Figure F-12. Keel AE Cumulative Energy by Channel: Phase VI, PI DUL, 95.4 kips down-bending + 13.8 psi, Trial 3.

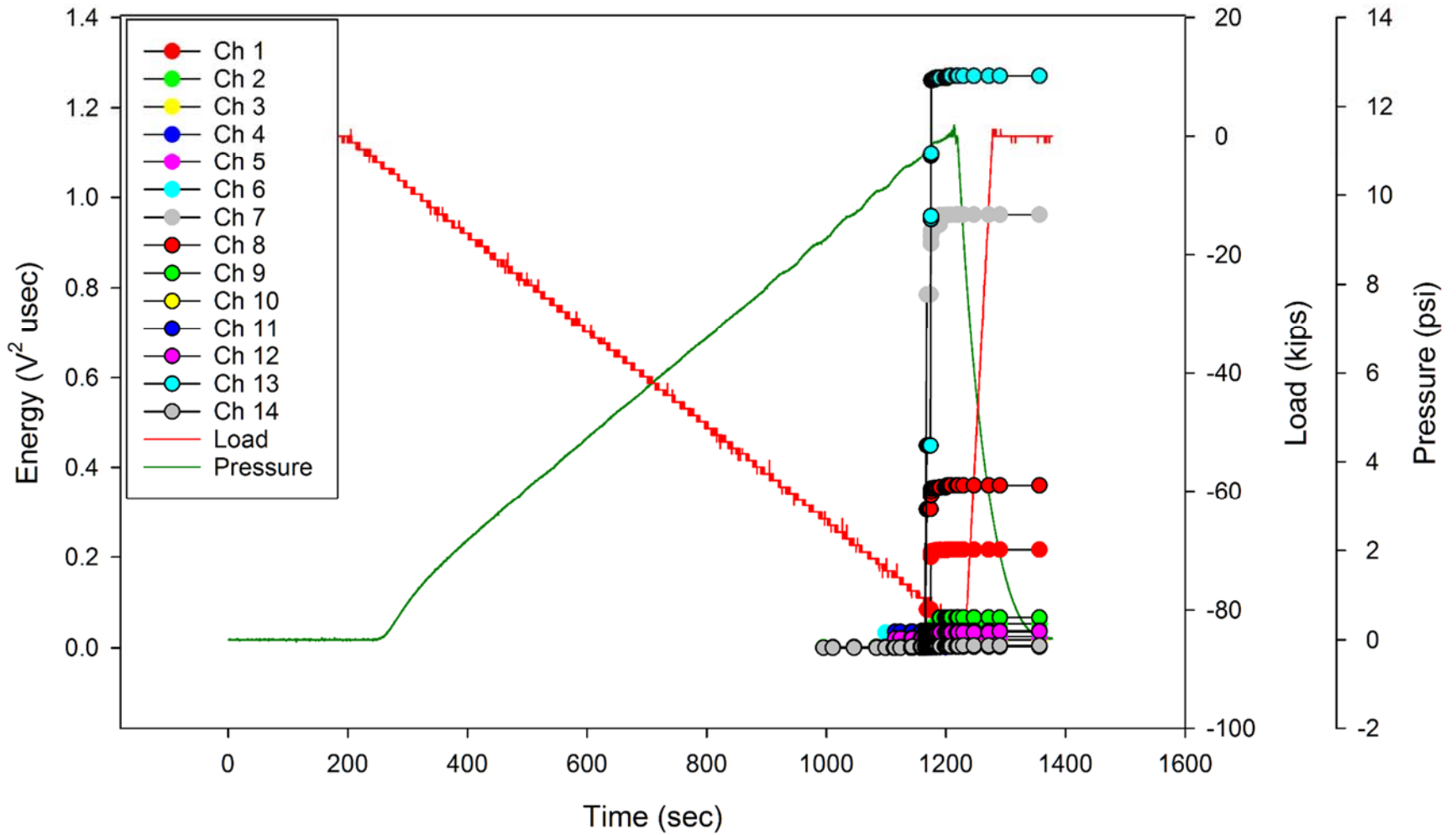


Figure F-13. Crown AE Cumulative Energy by Channel: Phase VI, PI DUL, 95.4 kips down-bending + 13.8 psi, Trial 4.

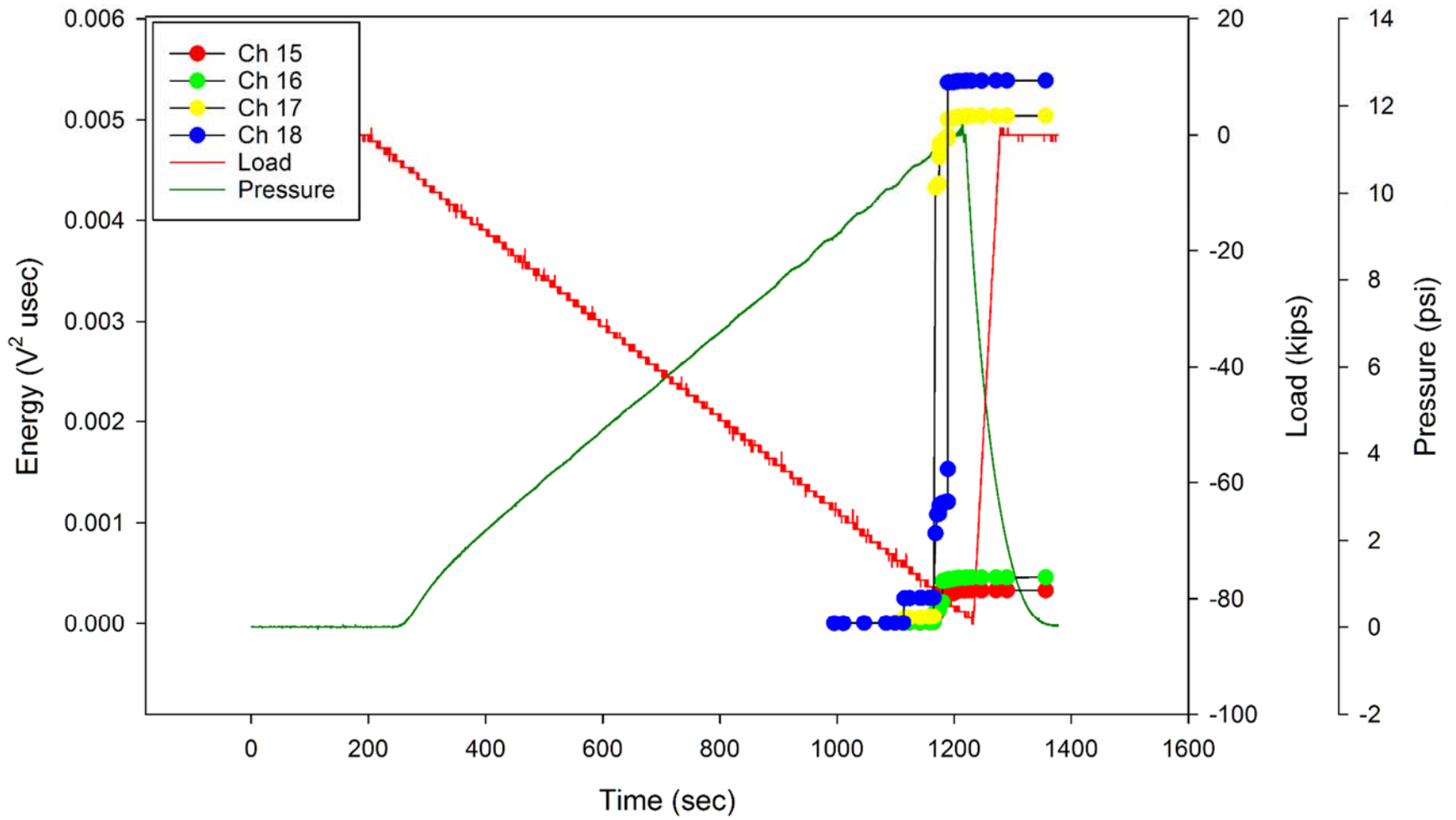


Figure F-14. Bulkheads AE Cumulative Energy by Channel: Phase VI, PI DUL, 95.4 kips down-bending + 13.8 psi, Trial 4.

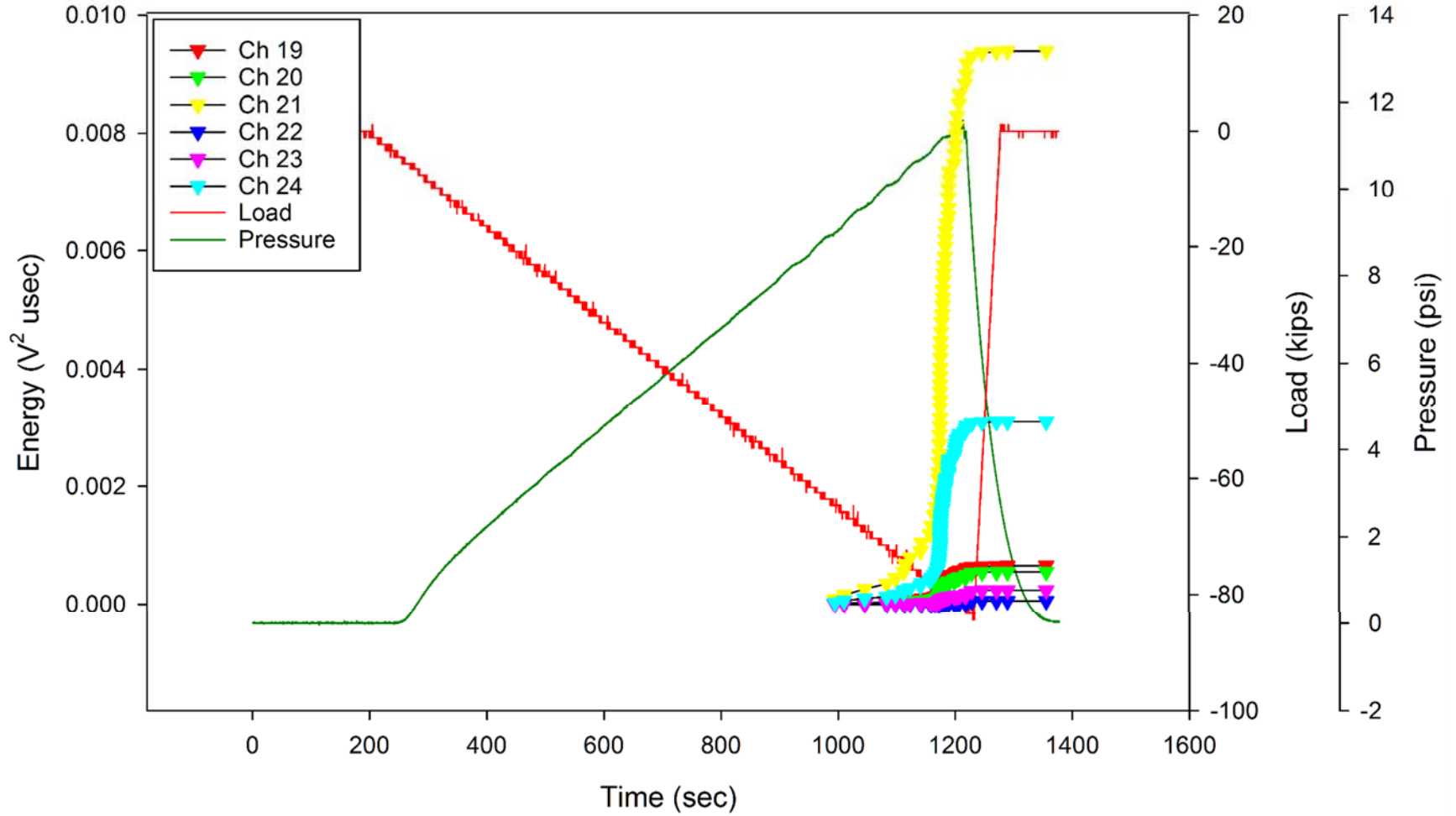


Figure F-15. Keel AE Cumulative Energy by Channel: Phase VI, PI DUL, 95.4 kips down-bending + 13.8 psi, Trial 4.

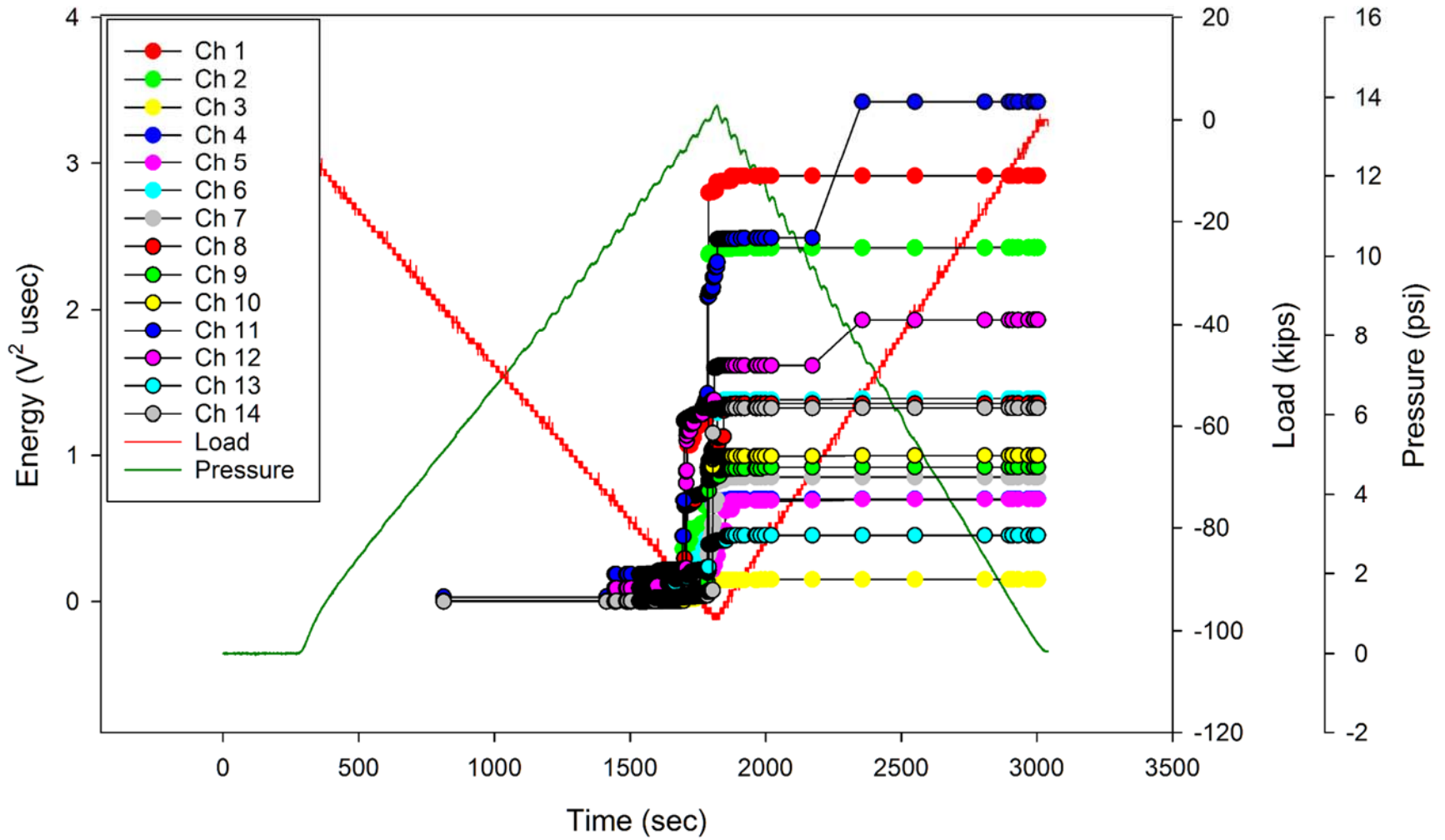


Figure F-16. Crown AE Cumulative Energy by Channel: Phase VI, PI DUL, 95.4 kips down-bending + 13.8 psi, Trial 5.

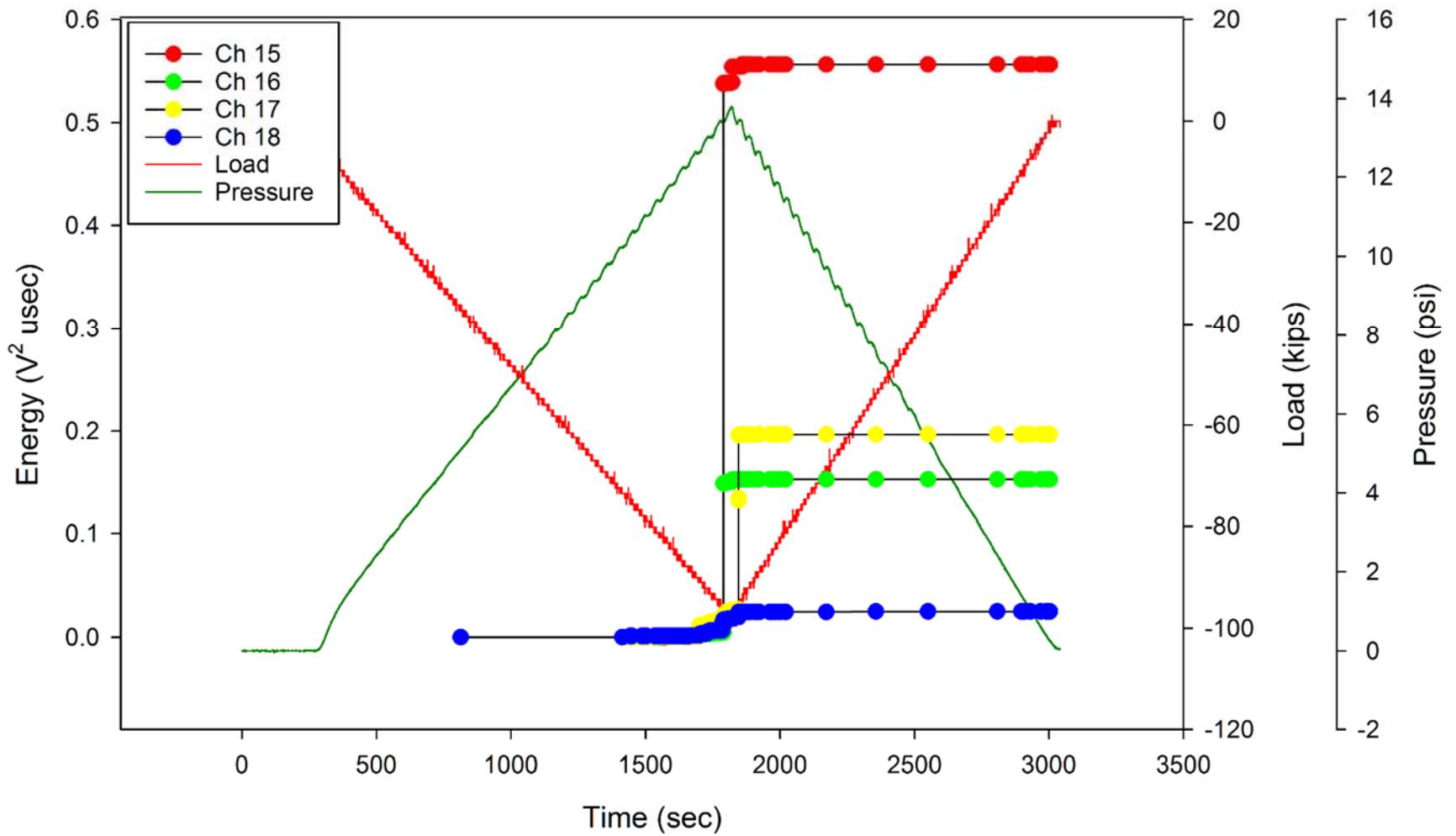


Figure F-17. Bulkheads AE Cumulative Energy by Channel: Phase VI, PI DUL, 95.4 kips down-bending + 13.8 psi, Trial 5.

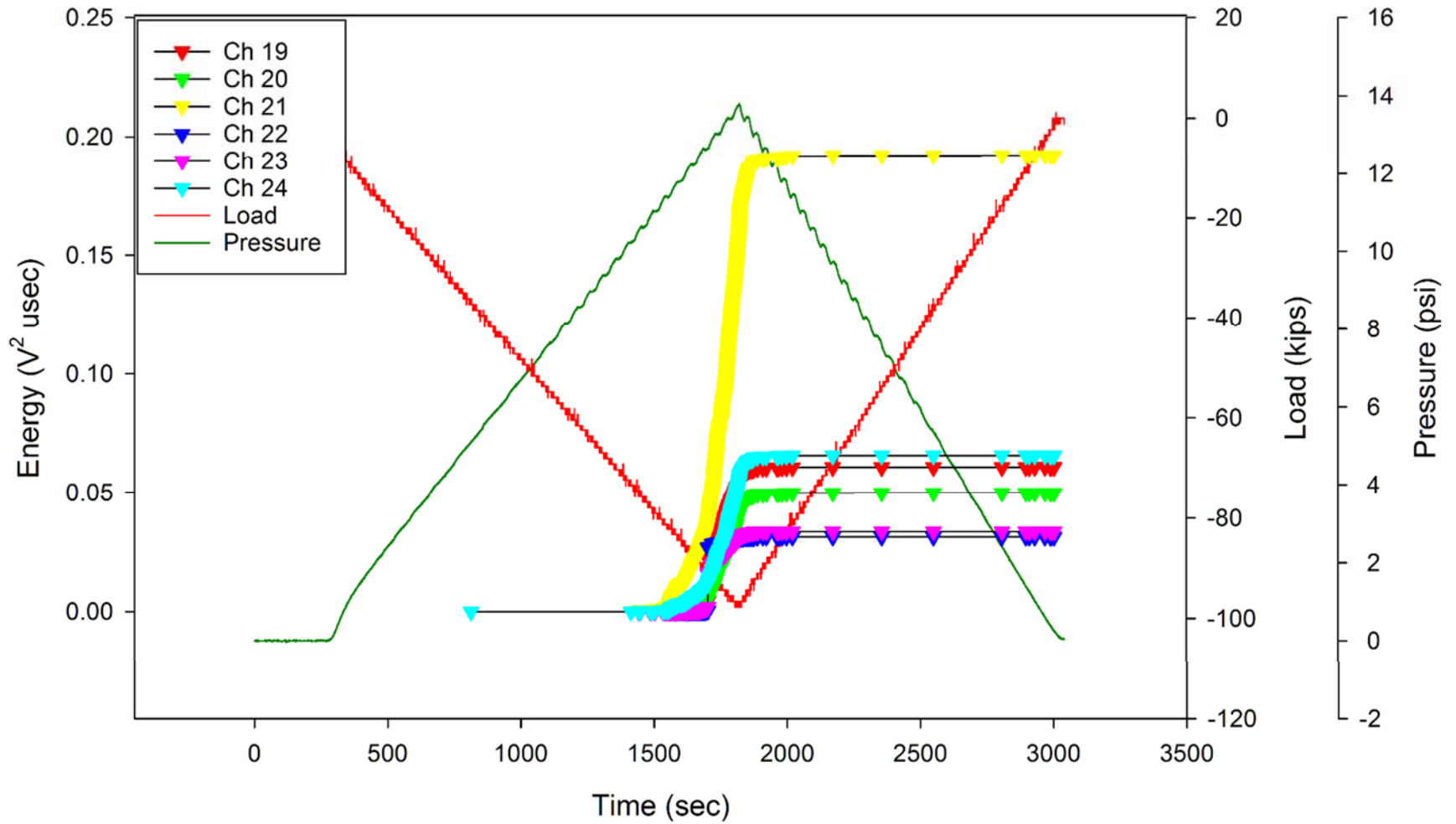


Figure F-18. Keel AE Cumulative Energy by Channel: Phase VI, PI DUL, 95.4 kips down-bending + 13.8 psi, Trial 5.

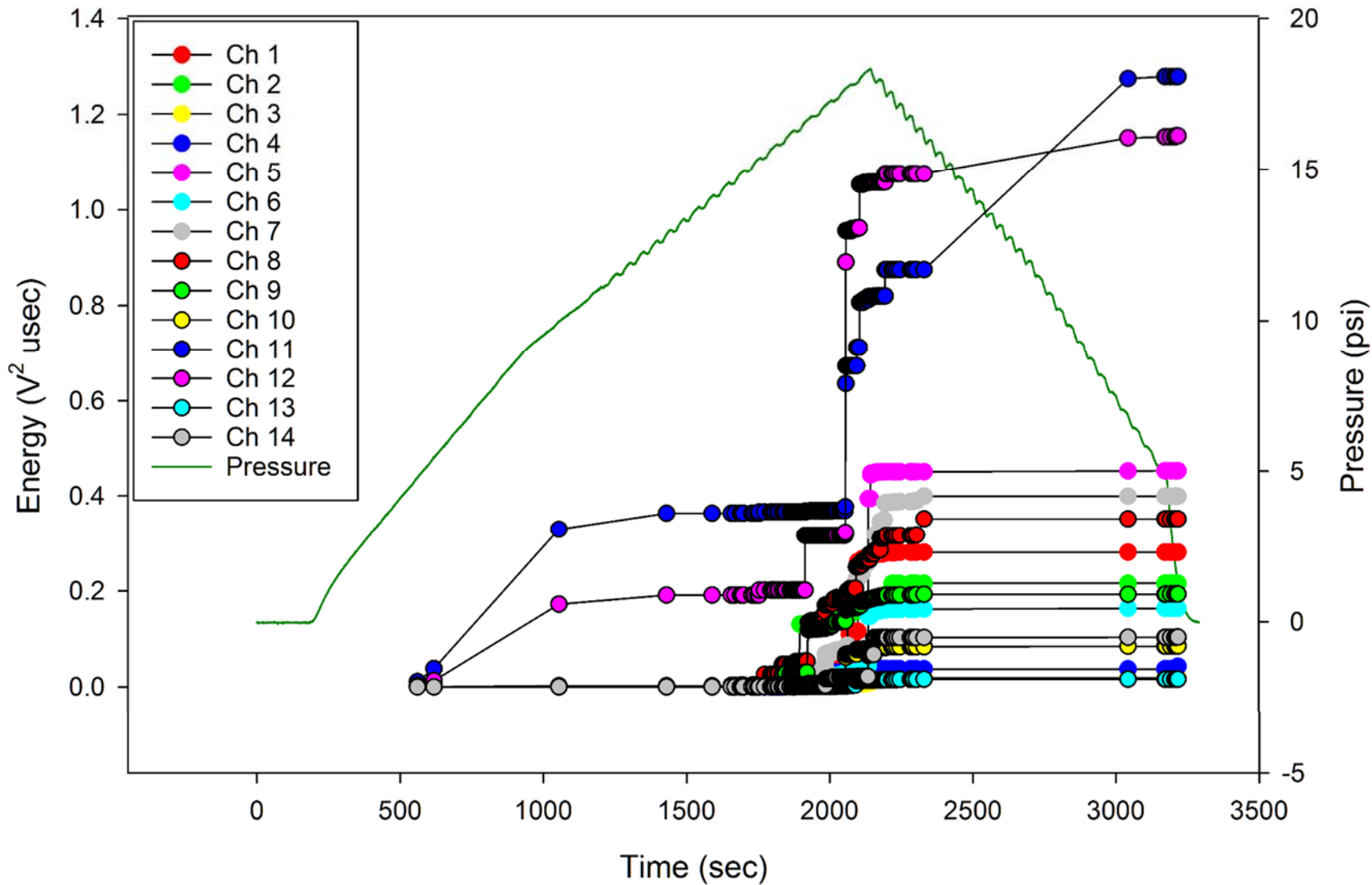


Figure F-19. Crown AE Cumulative Energy by Channel: Phase VI, PI DUL, 18.4 psi.

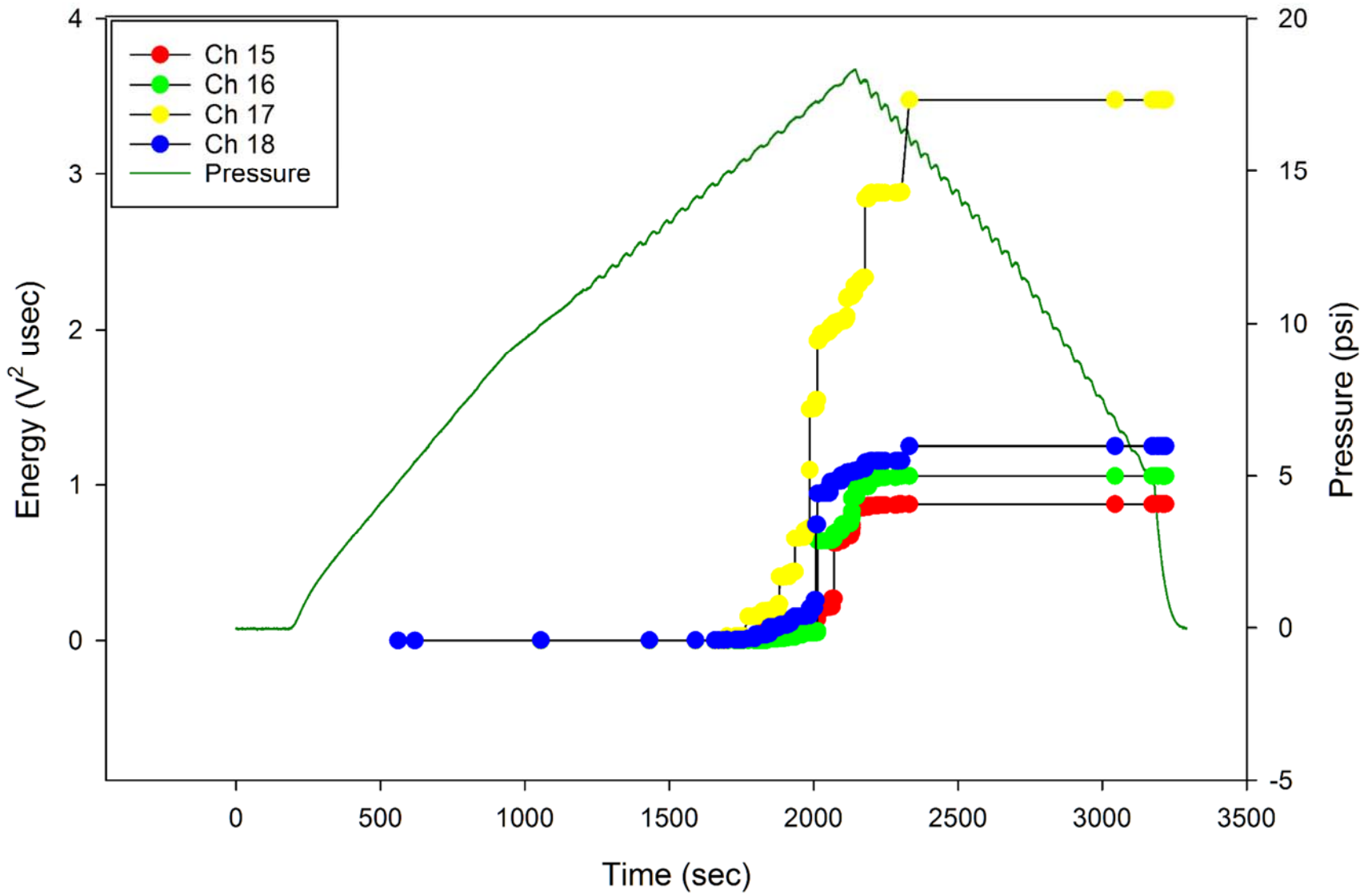


Figure F-20. Bulkheads AE Cumulative Energy by Channel: Phase VI, PI DUL, 18.4 psi.

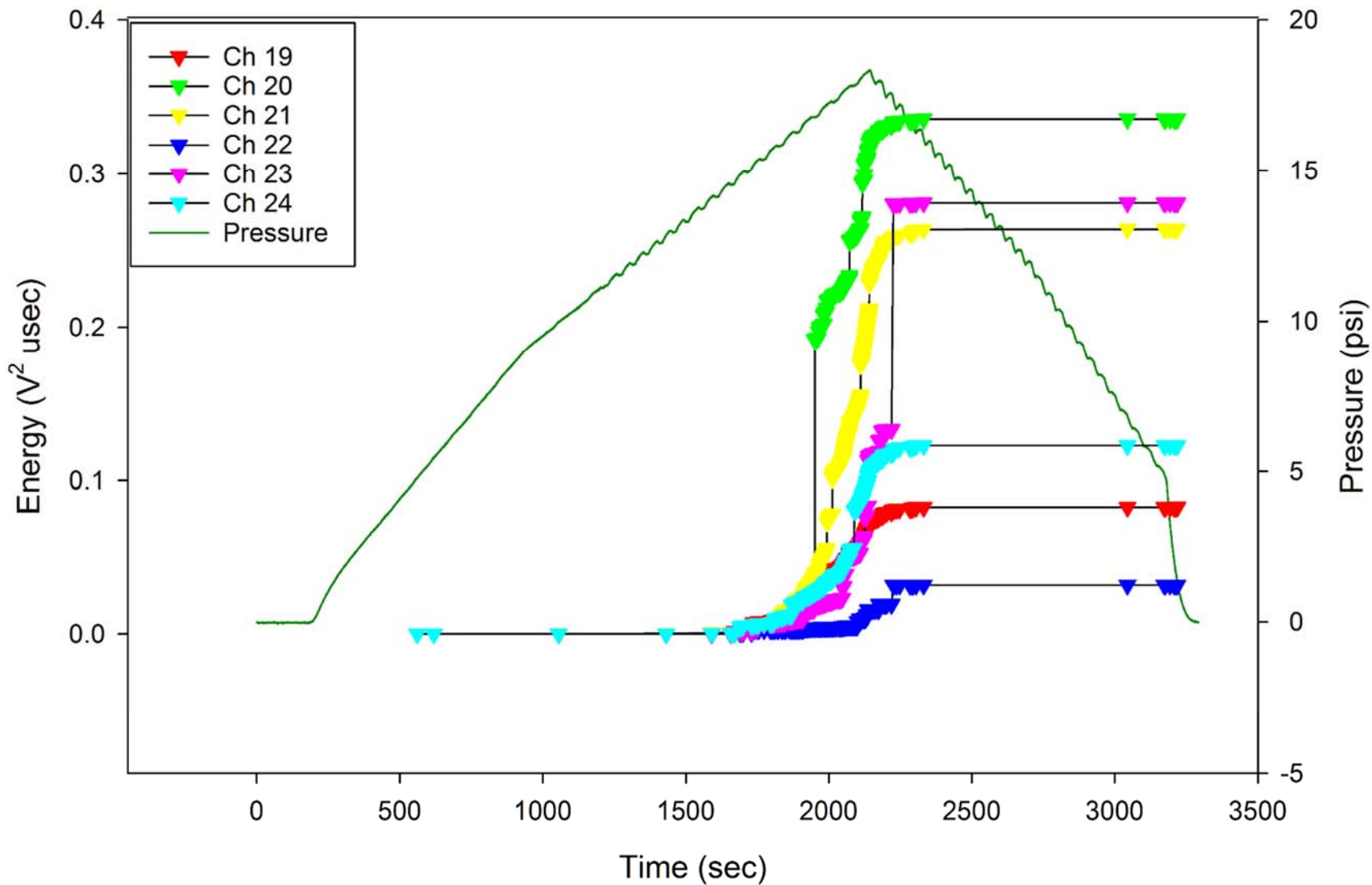


Figure F-21. Keel AE Cumulative Energy by Channel: Phase VI, PI DUL, 18.4 psi.

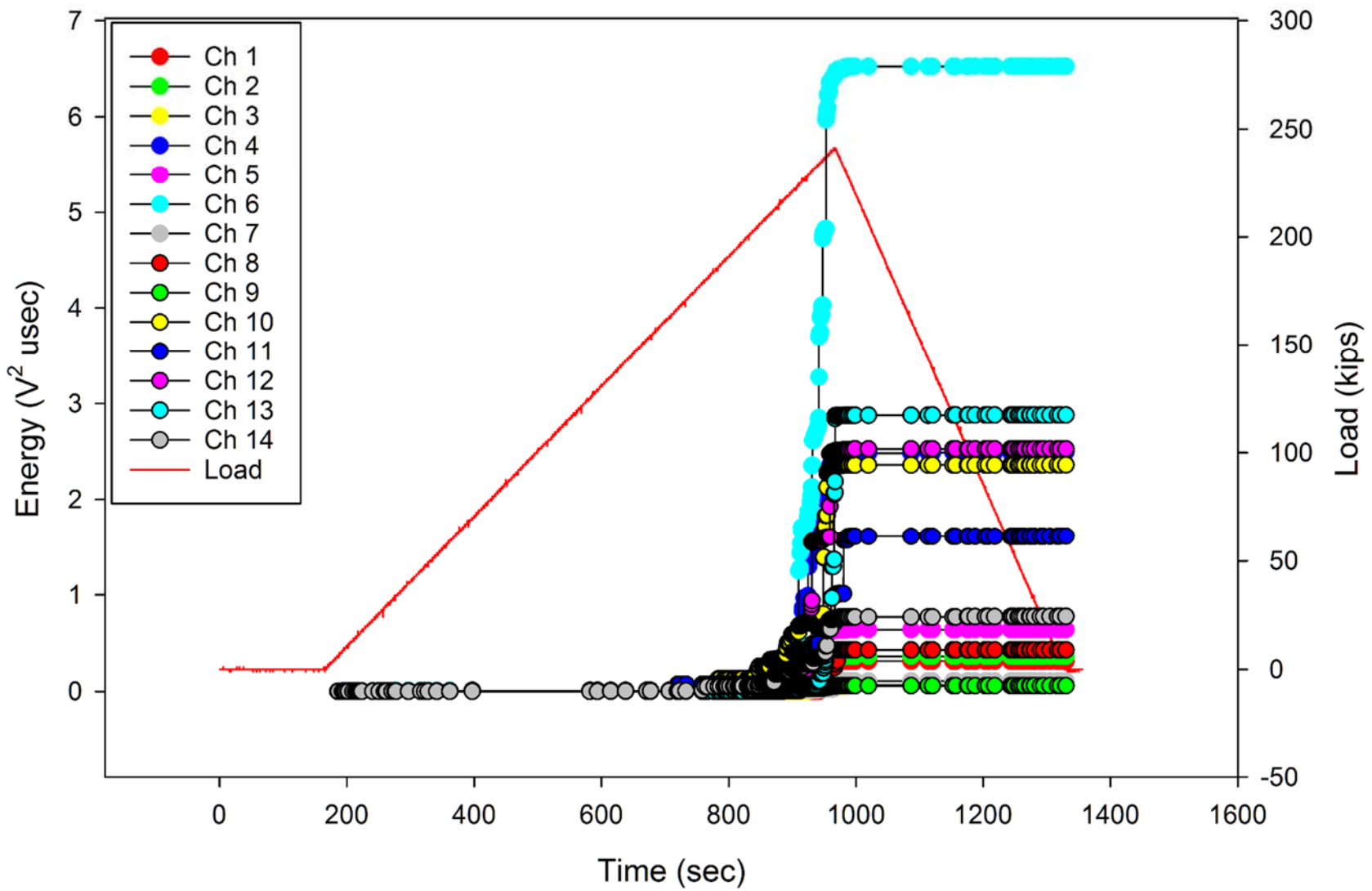


Figure F-22. Crown AE Cumulative Energy by Channel: Phase VI, PI DUL, 238.5 kips up-bending.

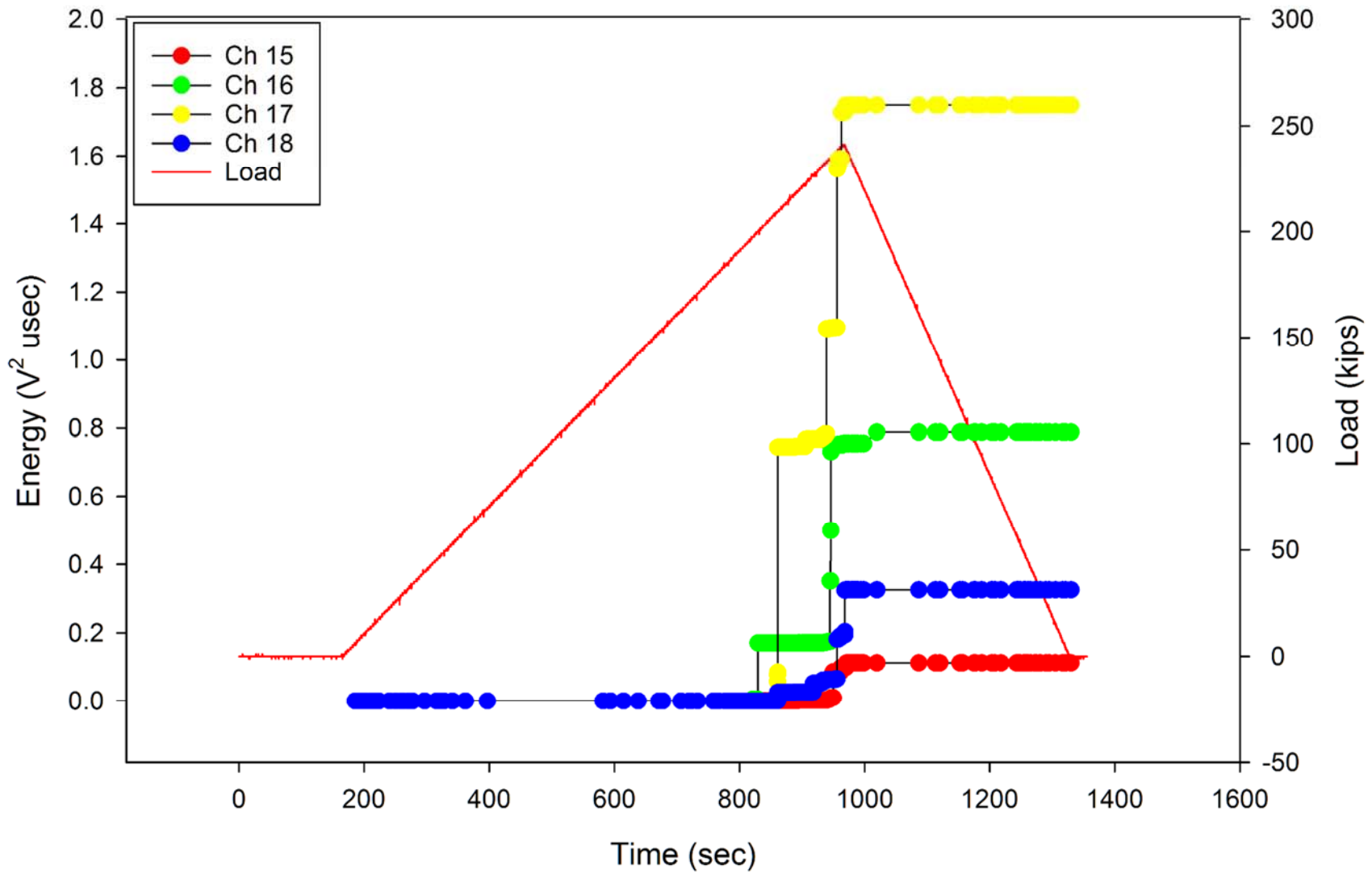


Figure F-23. Bulkheads AE Cumulative Energy by Channel: Phase VI, PI DUL, 238.5 kips up-bending.

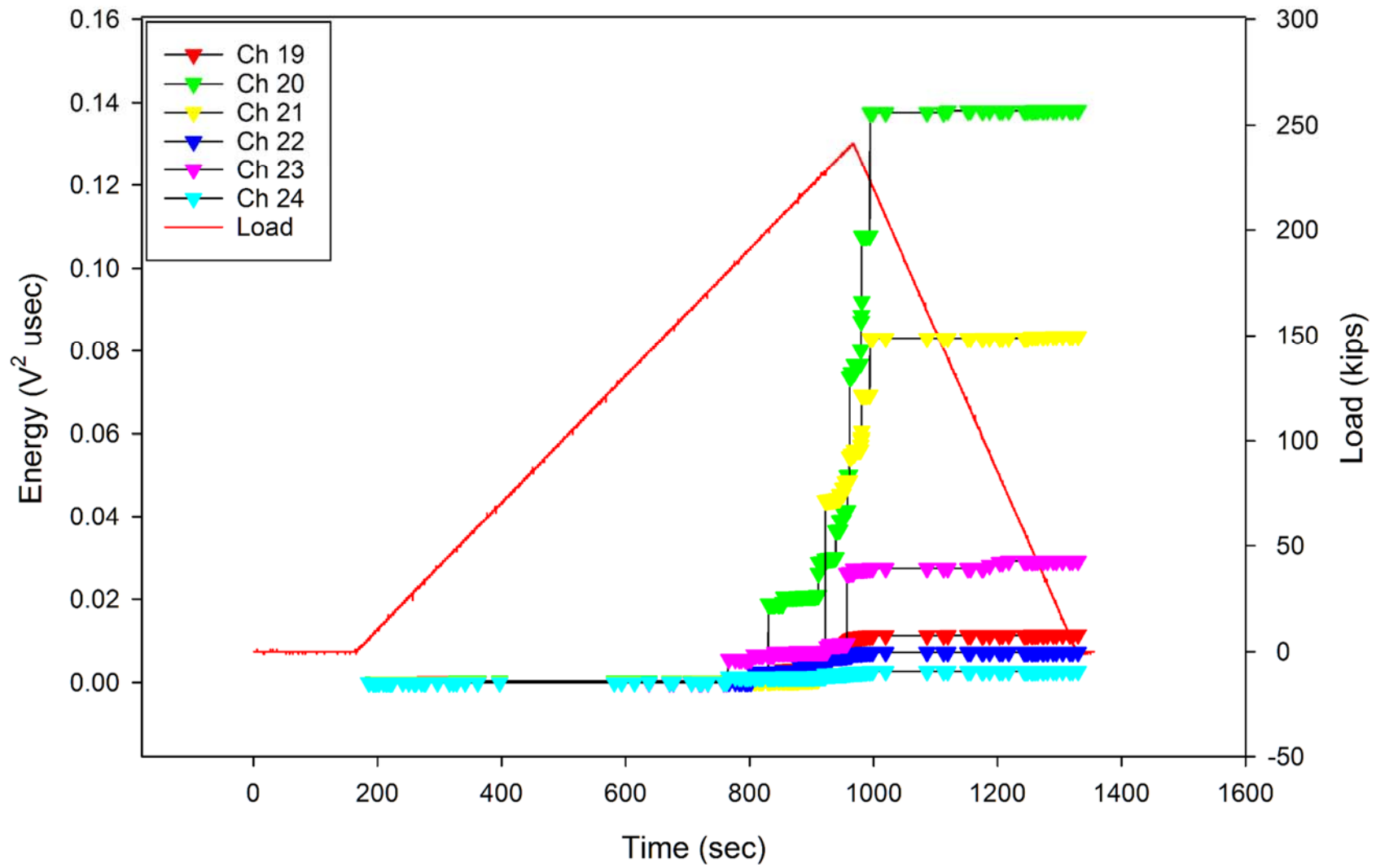


Figure F-24. Keel AE Cumulative Energy by Channel: Phase VI, PI DUL, 238.5 kips up-bending.

Appendix G: Phase VII Post-impact Combined Loads (PICL) Failure Test

Table of Figures

Figure G-1. Crown AE Cumulative Energy by Channel: Phase VII, PICL Failure.	G3
Figure G-2. Bulkheads AE Cumulative Energy by Channel: Phase VII, PICL Failure.....	G4
Figure G-3. Keel AE Cumulative Energy by Channel: Phase VII, PICL Failure.....	G5

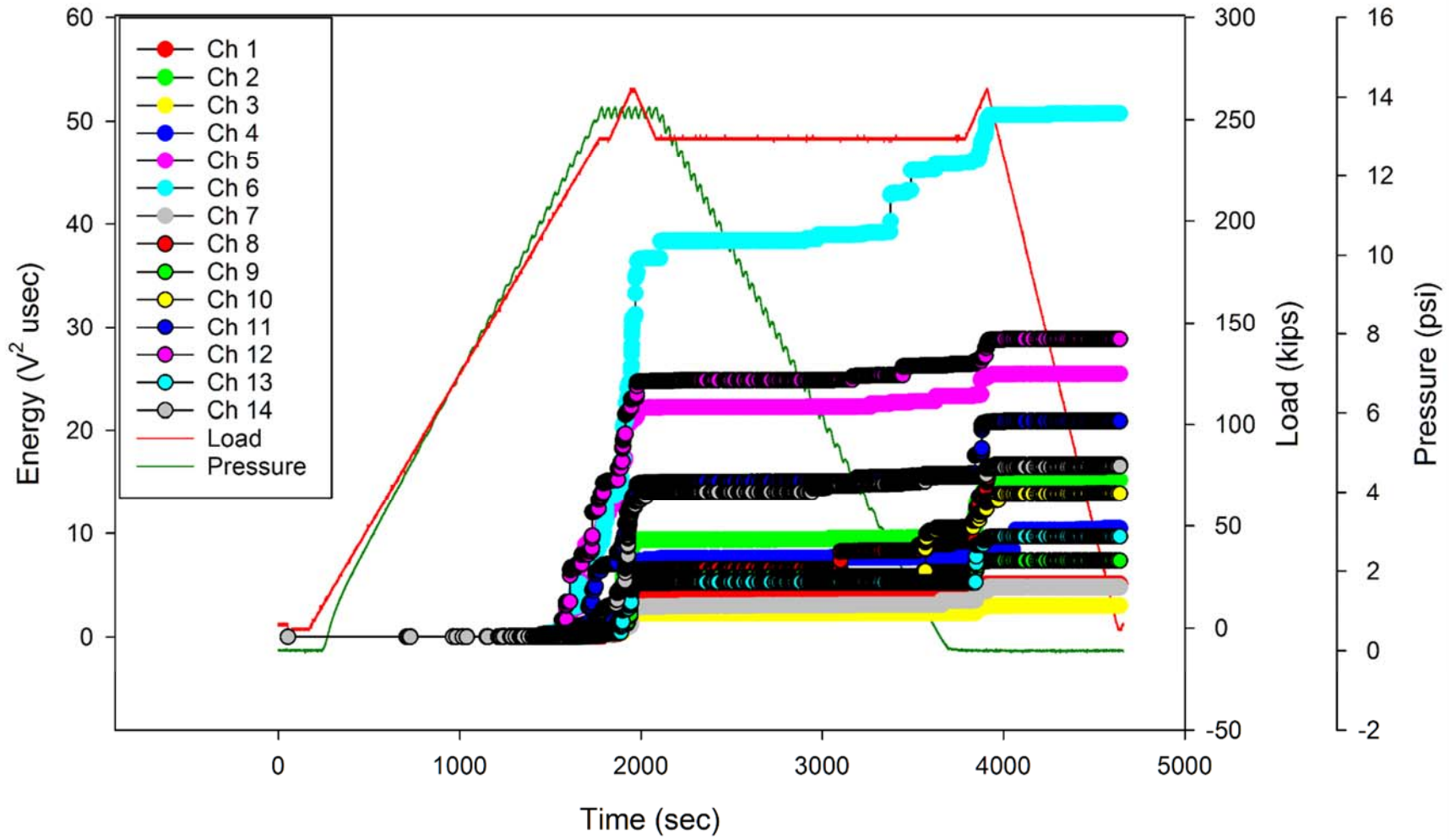


Figure G-1. Crown AE Cumulative Energy by Channel: Phase VII, PICL Failure.

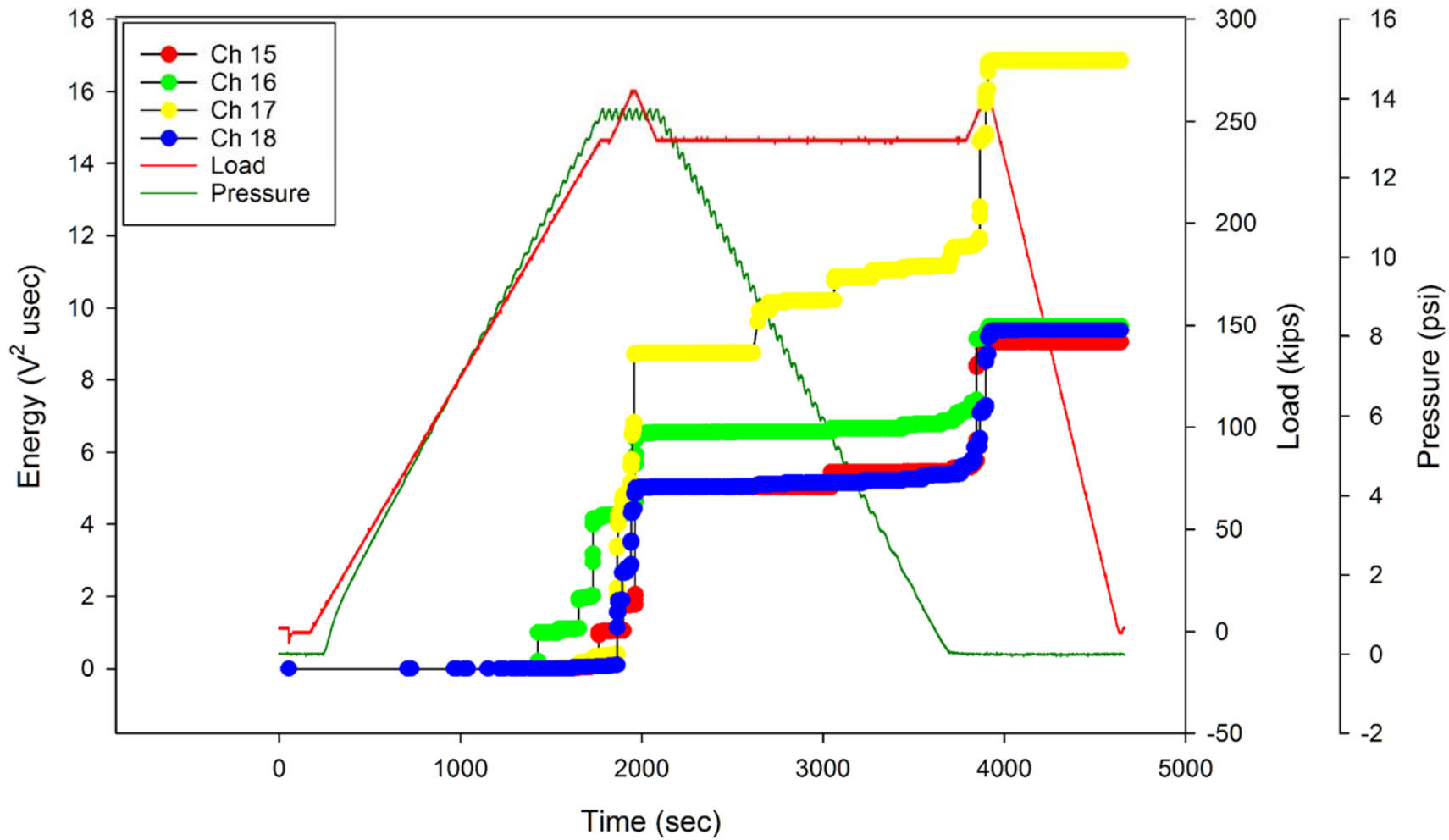


Figure G-2. Bulkheads AE Cumulative Energy by Channel: Phase VII, PICL Failure.

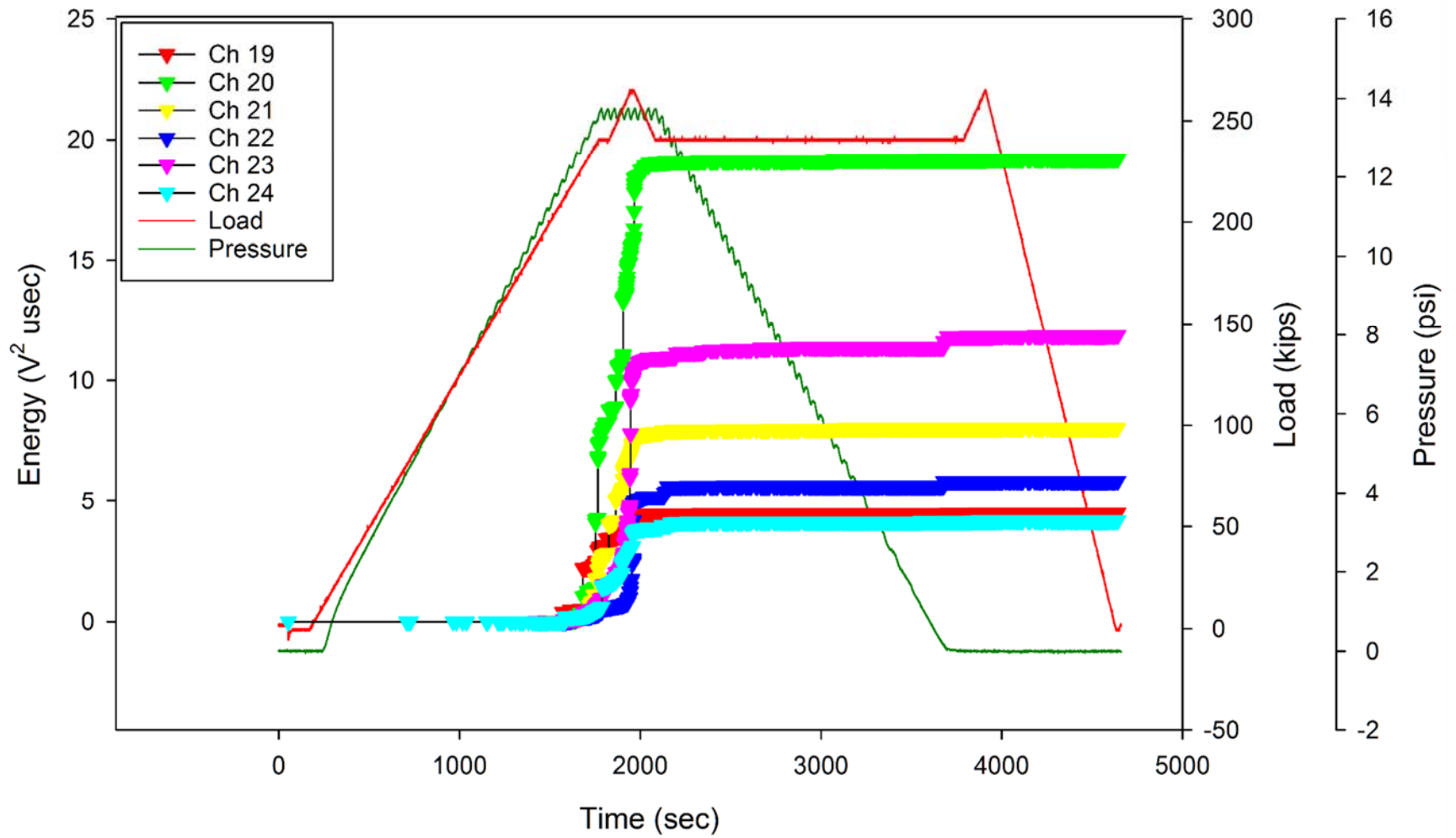


Figure G-3. Keel AE Cumulative Energy by Channel: Phase VII, PICL Failure.

Appendix H: Phase VIII Post-Sawcut Final Failure Test

Table of Figures

Figure H-1. Crown AE Cumulative Energy by Channel: Phase VIII, Post-sawcut Final Failure.	H3
Figure H-2. Bulkheads AE Cumulative Energy by Channel: Phase VIII, Post-sawcut Final Failure.	H4
Figure H-3. Keel AE Cumulative Energy by Channel: Phase VIII, Post-sawcut Final Failure.....	H5

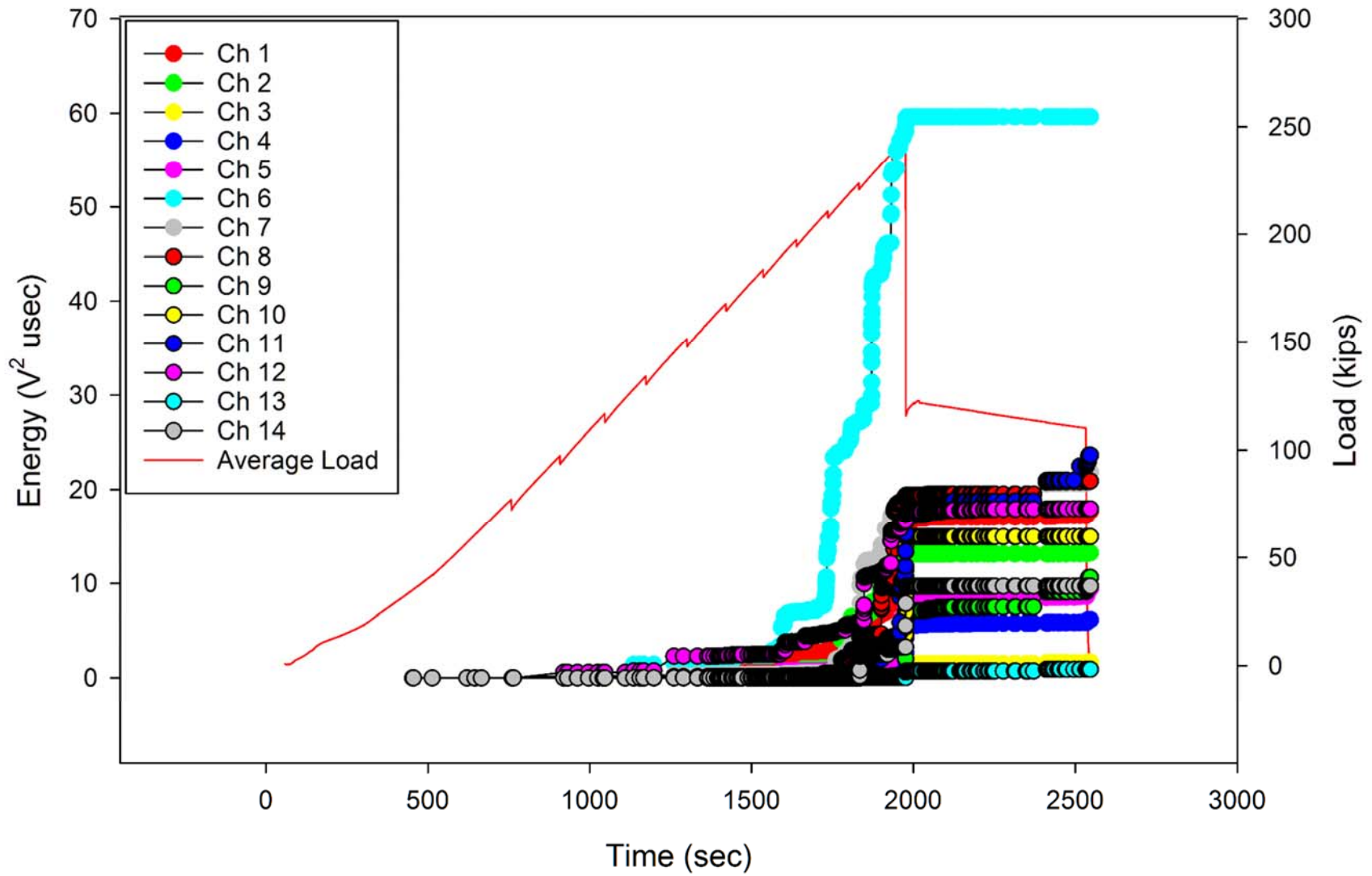


Figure H-1. Crown AE Cumulative Energy by Channel: Phase VIII, Post-sawcut Final Failure.

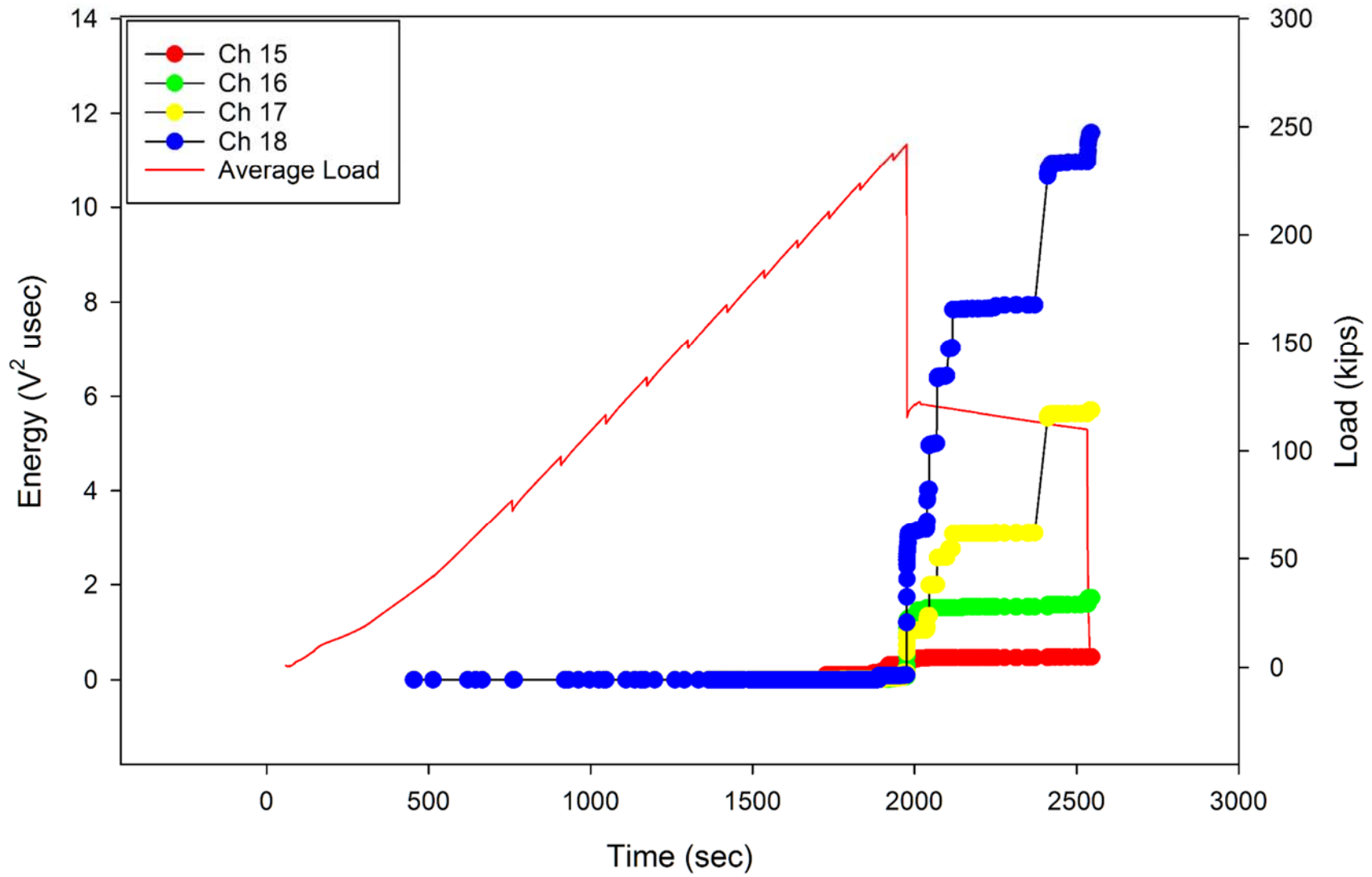


Figure H-2. Bulkheads AE Cumulative Energy by Channel: Phase VIII, Post-sawcut Final Failure.

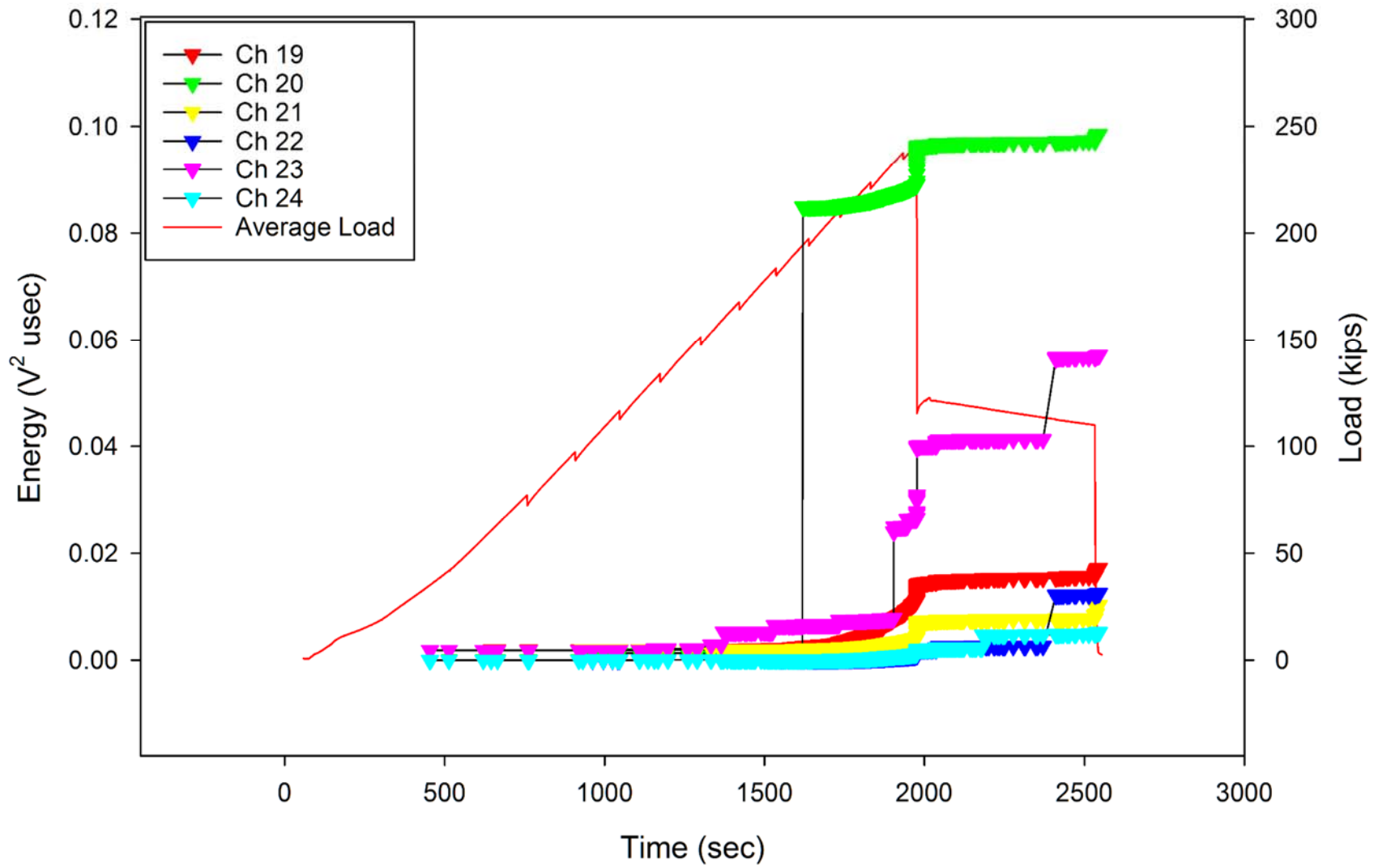


Figure H-3. Keel AE Cumulative Energy by Channel: Phase VIII, Post-sawcut Final Failure.

Appendix I: Test Matrix

Table 1: Test Matrix

Test Date	Test Description	CoLTs run #	External Preamp	Amplifier Gain Settings			Amplifier Filter Settings		Total Gains (dB)	
				Preamp	Signal	Trigger	Signal	Trigger	Signal	Trigger
4/9/2015	Pressure check 2 psi	1	PA0 (0 dB)	24	12	29	20	50-750	36	53
Phase I Checkout:										
4/13/2015	No test, collected noise		PA0 (0 dB)	24	12	29	20	50-750	36	53
4/14/2015	31.8 kips downbend (-0.5g)	2	PA0 (0 dB)	24	12	15	20	50-750	36	39
4/14/2015	79.5 kips upbend (1.25g)	3	PA0 (0 dB)	24	12	15	20	50-750	36	39
4/14/2015	31.8 kips down + 4.6 psi (-0.5g + 0.5P)	4	PA0 (0 dB)	24	12	15	20	50-750	36	39
4/14/2015	79.5 kips up + 4.6 psi (1.25g + 0.5P)	5	PA0 (0 dB)	24	12	15	20	50-750	36	39
Phase II DLL:										
4/14/2015	12.2 psi (1.33P)	6	PA0 (0 dB)	24	12	15	20	50-750	36	39
4/15/2015	63.6 kips down (-1g)	7	PA0 (0 dB)	24	0	12	20	50-750	24	36
4/15/2015	63.6 kips down + 9.2 psi (-1g + 1P)	8	PA0 (0 dB)	24	0	12	20	50-750	24	36
4/15/2015	159 kips up (2.5g)	9	PA0 (0 dB)	24	0	12	20	50-750	24	36
4/15/2015	159 kips up + 9.2 psi (2.5g + 1P)	10	PA0 (0 dB)	24	0	12	20	50-750	24	36
Phase III DUL:										
4/15/2015	95.4 kips down (-1.5g)	11	PA0 (0 dB)	24	0	12	20	50-750	24	36
4/16/2015	95.4 kips down + 13.8 psi (-1.5g + 1.5P)	12	PA0 (0 dB)	24	0	12	20	50-750	24	36
4/16/2015	238.5 kips up (3.75g): trial 1	13	PA0 (0 dB)	24	0	12	20	50-750	24	36
4/16/2015	238.5 kips up (3.75g): success	14	PA0 (0 dB)	24	0	12	20	50-750	24	36
4/16/2015	238.5 kips up + 13.8 psi (3.75g + 1.5P)	15	PA0 (0 dB)	24	0	12	20	50-750	24	36
4/16/2015	18.4 psi (2P): trial 1	16	PA0 (0 dB)	24	0	12	20	50-750	24	36
4/16/2015	18.4 psi (2P): success	17	PA0 (0 dB)	24	0	12	20	50-750	24	36
4/24/2015	Impacts: Collected AE part-time		PA0 (0 dB)	24	0	12	20	50-750	24	36
Phase IV Checkout:										
4/30/2015	4.6 psi (0.5P)	18	PA0 (0 dB)	24	0	12	20	50-750	24	36
4/30/2015	31.8 kips (-0.5g)	19	PA0 (0 dB)	24	0	12	20	50-750	24	36
4/30/2015	79.5 kips up (1.25g)	20	PA0 (0 dB)	24	0	12	20	50-750	24	36
4/30/2015	31.8 kips down + 4.6 psi (-0.5g + 0.5P)	21	PA0 (0 dB)	24	0	12	20	50-750	24	36
4/30/2015	79.5 kips + 4.6 psi (1.25g up + 0.5P)	22	PA0 (0 dB)	24	0	12	20	50-750	24	36
Phase V DLL:										
5/1/2015	63.6 kips down (-1g)	23	PA0 (0 dB)	24	0	12	20	50-750	24	36
5/1/2015	63.6 kips down + 9.2 psi (-1g + 1P)	24	PA0 (0 dB)	24	0	12	20	50-750	24	36
5/1/2015	12.2 psi (1.33P)	25	PA0 (0 dB)	24	0	12	20	50-750	24	36
5/1/2015	159 kips up (2.5g)	26	PA0 (0 dB)	24	0	12	20	50-750	24	36
5/1/2015	159 kips up + 9.2 psi (2.5g + 1P)	27	PA0 (0 dB)	24	0	12	20	50-750	24	36
Phase VI DUL:										
5/7/2015	95.4 kips down (-1.5g)	28	PA0 (0 dB)	24	0	12	20	50-750	24	36
5/7/2015	95.4 kips down + 13.8 psi (-1.5g+1.5P): trial 1-4	29-32	PA0 (0 dB)	24	0	12	20	50-750	24	36
5/7/2015	95.4 kips down + 13.8 psi (-1.5g+1.5P): success	33	PA0 (0 dB)	24	0	12	20	50-750	24	36
5/7/2015	18.4 psi (2P)	34	PA0 (0 dB)	24	0	12	20	50-750	24	36
5/7/2015	238.5 kips up (3.75g)	35	PA0 (0 dB)	24	0	12	20	50-750	24	36
Ph VII Combined loads:										
5/8/2015	Trial 1-3	36-38	PA0 (0 dB)	24	0	12	20	50-750	24	36
5/8/2015	Trial 4: success	39	PA0 (0 dB)	24	0	12	20	50-750	24	36
Post-sawcut failure:										
6/3/2015	Trial 1-3	40-42	PA0 (0 dB)	24	0	12	20	50-750	24	36
6/3/2015	Trial 4: success	43	PA0 (0 dB)	24	0	12	20	50-750	24	36

REPORT DOCUMENTATION PAGE

Form Approved
OMB No. 0704-0188

The public reporting burden for this collection of information is estimated to average 1 hour per response, including the time for reviewing instructions, searching existing data sources, gathering and maintaining the data needed, and completing and reviewing the collection of information. Send comments regarding this burden estimate or any other aspect of this collection of information, including suggestions for reducing the burden, to Department of Defense, Washington Headquarters Services, Directorate for Information Operations and Reports (0704-0188), 1215 Jefferson Davis Highway, Suite 1204, Arlington, VA 22202-4302. Respondents should be aware that notwithstanding any other provision of law, no person shall be subject to any penalty for failing to comply with a collection of information if it does not display a currently valid OMB control number.
PLEASE DO NOT RETURN YOUR FORM TO THE ABOVE ADDRESS.

1. REPORT DATE (DD-MM-YYYY) 01-08-2016	2. REPORT TYPE Technical Memorandum	3. DATES COVERED (From - To)
--	---	-------------------------------------

4. TITLE AND SUBTITLE Initial Evaluation of Acoustic Emission SHM of PRSEUS Multi-Bay Box Tests	5a. CONTRACT NUMBER
	5b. GRANT NUMBER
	5c. PROGRAM ELEMENT NUMBER

6. AUTHOR(S) Horne, Michael R.; Madaras, Eric I.	5d. PROJECT NUMBER
	5e. TASK NUMBER
	5f. WORK UNIT NUMBER 338881.02.22.07.01.01

7. PERFORMING ORGANIZATION NAME(S) AND ADDRESS(ES) NASA Langley Research Center Hampton, VA 23681-2199	8. PERFORMING ORGANIZATION REPORT NUMBER L-20731
---	--

9. SPONSORING/MONITORING AGENCY NAME(S) AND ADDRESS(ES) National Aeronautics and Space Administration Washington, DC 20546-0001	10. SPONSOR/MONITOR'S ACRONYM(S) NASA
	11. SPONSOR/MONITOR'S REPORT NUMBER(S) NASA-TM-2016-218976

12. DISTRIBUTION/AVAILABILITY STATEMENT
Unclassified - Unlimited
Subject Category 05
Availability: NASA STI Program (757) 864-9658

13. SUPPLEMENTARY NOTES

14. ABSTRACT

A series of tests of the Pultruded Rod Stitched Efficient Unitized Structure (PRSEUS) HWB Multi-Bay Test Article were conducted during second quarter 2015 at NASA Langley Research Center (LaRC) in the Combined Loads Test facility (COLTS). This report documents the Acoustic Emission (AE) data collected during those tests.

15. SUBJECT TERMS

Acoustic Emission; PRSEUS; composite structures

16. SECURITY CLASSIFICATION OF:			17. LIMITATION OF ABSTRACT	18. NUMBER OF PAGES	19a. NAME OF RESPONSIBLE PERSON
a. REPORT	b. ABSTRACT	c. THIS PAGE			STI Help Desk (email: help@sti.nasa.gov)
U	U	U	UU	199	19b. TELEPHONE NUMBER (Include area code) (757) 864-864-9658